

DESIGN AND EVALUATION OF OPEN-CIRCUIT RESPIRATION CHAMBERS FOR BEEF
CATTLE

BY

BRETT CARLOS RAMIREZ

THESIS

Submitted in partial fulfillment of the requirements
for the degree of Master of Science in Agricultural and Biological Engineering
in the Graduate College of the
University of Illinois at Urbana-Champaign, 2014

Urbana, Illinois

Advisers:

Associate Professor Luis F. Rodríguez
Assistant Professor Angela R. Green

Abstract

Methane (CH₄) generated by cattle is a major source of greenhouse gas emissions and an indicator of feed efficiency; thus, accurate and confident quantification of CH₄ production is required for addressing future global agricultural requirements without the neglect of environmental impacts. One of the most common techniques for quantifying CH₄ emissions from cattle is the chamber technique, known as the respiration chamber or indirect calorimeter, which houses the head or the whole body of the animal in a chamber. Psychrometric properties and gas concentration measurements at the inlet and exhaust of the chamber, in conjunction with fresh air flowrate, are used to calculate the Emission Rate (ER) of CH₄ produced by the animal inside the chamber.

Reliability and accuracy of estimated ERs with the chamber technique is a concern and often only verified through release-recovery methods, but should also include documentation and quantification of measurement uncertainty. Research with the chamber technique is primarily focused on the application for understanding relationships between ruminant CH₄ emissions and nutrition, genetics, and rumen biology. There is limited work regarding estimates of confidence in computed CH₄ emissions that goes into understanding these relationships. Individual measurements as well as the integrity of the system introduce uncertainty that affects the computed ER; therefore, confidence in the results obtained by the chamber technique can be described through an evaluation of each source of uncertainty and the release-recovery test. Identifying and quantifying the uncertainty from each source and its contribution to the overall uncertainty associated with ER will lead to greater confidence in the results of CH₄ emission research and provide insight to which measurements are most critical. The overall aim of this work was to document the design, including construction and uncertainty analysis, and evaluate

performance through bias significance testing for a version of the chamber technique named the Ruminant Emission Measurement System (REMS).

The REMS was developed to quantify eructated CH₄ emissions from beef cattle and consists of six positively pressured, ventilated hood-type, open-circuit respiration chambers installed at the University of Illinois Urbana-Champaign Beef and Sheep Field Research Unit. The design and construction documentation for each chamber included specifications for the thermal environmental control subsystem, fresh air supply and measurement subsystem, and gas sampling subsystem. Measurement standard uncertainty was quantified and propagated through the computation of ER, which was derived from mass flow balances on CH₄ and air. A sensitivity analysis simulated the normal operation of the REMS and variations in gas analyzer and ventilation measurement uncertainties to assess the relative contributions of each source of uncertainty to the combined ER standard uncertainty. Expanded uncertainty (~95% confidence level) associated with ER was approximately 5.9% for CH₄ emission rates between 3.5 to 17.2 g h⁻¹. Ventilation rate and concentration measurements contributed approximately 69% and 29% to the ER standard uncertainty, respectively. The ER standard uncertainty provides insight to the sensitivity required to detect differences between computed ERs.

The fresh air supply measurement was separately evaluated and consisted of six orifice meters designed and fabricated for accurate measurement fresh airflow to each chamber. Calibration of each orifice meter was completed using a reference comprised of two chambers with a precision nozzle for flowrates from 279 to 510 lpm (9.9 to 18 cfm). Regression analysis showed a linear relationship with slope significantly different from unity ($P < 0.05$) between the calibration reference and orifice meter, demonstrating that each orifice meter required an individual calibration for best accuracy. At a nominal 500 lpm (17.65 cfm), the relative expanded

uncertainty ranged from 3.6% to 4.9%. Custom designed, constructed, and calibrated orifice meters are accurate and cost effective (approximately \$250 for materials plus 5 h of labor each) for volumetric ventilation rate measurement in animal emission studies.

The commissioning of the REMS included incorporating the propagation of measurement uncertainties, systematic errors, and the variability in repeated release-recovery tests. In addition, each subsystem was evaluated to ensure design criteria were met. A whole system verification experiment (mass recovery test) compared the mass flow recovered by the REMS to the total mass flow injected by a reference integrated over the steady-state regime. An uncertainty analysis was applied to the mass recovery test, including eight replications of the test over time, to establish the confidence in the release-recovery method. Mean mass recovery percent for the six chambers ranged from 92.0% to 96.6%, with SSMRP absolute expanded uncertainties (~95% confidence interval) ranging from 10.4% to 13%. Mass recovered uncertainty contributed from 70.1% to 90.7% to SSMRP uncertainty, mass injected uncertainty contributed from 2.5% to 4.0%, and reproducibility contributed from 5.6% to 27.3%. Significant ($P < 0.05$) SSMRP systematic error was detected for five of the six chambers; therefore, emissions measured with these chambers should be corrected for bias following the methods and guidelines presented here. Mass recovery rates should include a documented stated standard uncertainty to establish a confidence level for whole system verification and subsequent emission rate measurements, as demonstrated in the discussed commissioning results.

The documented methodology for the design and evaluation of the REMS fulfills the need for establishing the best estimate of confidence in accumulated emissions reported from the chamber technique. The analysis described here, although specific to the REMS, can be applied to quantify confidence and performance of other respiration systems or indirect calorimeter.

Reliable estimates of uncertainty associated with the chamber technique will lead to development of improved understanding of the relationships between CH₄ production and nutrition, genetics, and different management strategies.

Acknowledgements

I would like to thank everyone who has aided in developing my success as not only a student and a researcher but also a person during my undergraduate and graduate career at the University of Illinois at Urbana-Champaign. Through their support, guidance, and inspiration I was able to achieve goals beyond my expectations and accomplish many great achievements. The direction, feedback and encouragement from my passionate and enthusiastic committee members Drs. Luis Rodriguez, Angela Green, Daniel Shike, and Richard Gates, allowed me to further enhance my skills and succeed in my efforts. I had the privilege to be mentored by post-doctoral research associate Dr. Guilherme Del Nero Maia who provided me with invaluable experience, feedback, and support on this project.

Words cannot express my gratitude to the endless list of people in the BioMASS and AWES Laboratories, Department of Animal Sciences, Department of Agricultural and Biological Engineering, and at the Beef and Sheep Field Research Unit. Everyone has contributed to the success of this project in many ways, by donating time, effort, and assistance.

To close, I would like to thank my family and friends for their unconditional support and inspiration in all aspects of my life.

Table of Contents

Chapter 1: Introduction	1
1.1 Objectives	3
1.2 Organization of the Thesis	4
Chapter 2: Literature Review	5
2.1 Overview and Application of the Chamber Technique.....	5
2.2 Classification.....	6
2.3 Design and Components.....	8
2.4 Calculation Methods	14
2.5 Instrumentation	17
2.6 Whole System Validation.....	21
2.7 Performance Evaluation and Limitations	34
2.8 Conclusions	35
2.9 References	36
Chapter 3: Design and Validation of a Precision Orifice Meter for Ventilation Rate Control in Open-Circuit Respiration Chambers	43
3.1 Abstract	44
3.2 Introduction	45
3.3 Materials and Methods	49
3.4 Results and Discussion	57
3.5 Summary and Conclusions	59
3.6 Acknowledgements	60
3.7 References	60
Chapter 4: A Novel Ruminant Emission Measurement System: Part I – Design Evaluation and Description	64
4.1 Abstract	66
4.2 Introduction	67
4.3 Materials and Methods	70
4.4 Results and Discussion	87
4.5 Summary and Conclusions	94
4.6 Acknowledgments.....	95
4.7 References	95
Chapter 5: A Novel Ruminant Emission Measurement System: Part II - Commissioning	101
5.1 Abstract	103
5.2 Introduction	104
5.3 Materials and Methods	106
5.4 Results and Discussion	123
5.5 Summary and Conclusions	135
5.6 Acknowledgments.....	137
5.7 References	138
Chapter 6: Conclusions and Future Work	141
Appendix A: Orifice Meter Construction, Calibration, and Standard Uncertainty	146
A.1 Orifice Construction.....	146
A.2 Calibration curves	147
A.3 Orifice Meter Flowrate Standard Uncertainty Pseudo Code	150

Appendix B: Emission Rate Equation Derivation	151
B.1 Introduction.....	151
B.2 Moist Air Mass Flow Balance	151
B.3 Gas Component Mass Flow Balance	152
B.4 Volumetric Concentration Conversion	153
B.5 Combining for Emission Rate.....	156
Appendix C: Emission Rate Sensitivity Analysis Code	158
C.1 REMS_ER_STD_UNCERTAINTY.m	159
C.2 air_density_std_uncertainty.m	162
C.3 REMS_ER_SA_PLOT.m.....	164
Appendix D: Steady-State Mass Recovery Percent Derivation	166
D.1 Introduction	166
D.2 Moist Air Mass Flow Balance.....	166
D.3 Tracer Gas Component Mass Flow Balance	168
D.4 Mass Flow Injected.....	169
Appendix E: Steady-State Mass Recovery Test SOP	171
E.1 Scope and Applicability	171
E.2 Personnel Qualifications.....	171
E.3 Equipment and Supplies	171
E.4 Procedures	172
E.5 Data Management.....	182
Appendix F: Steady-State Mass Recovery Test Data	184
Appendix G: Steady-State Mass Recovery Percent Analysis and Standard Uncertainty	
Code.....	209
G.1 MR_std_uncertainty.m	209
G.2 std_uncertainty_rho_inj.m	218
G.3 std_uncertainty_om.m.....	219
G.4 MR_importfile.m.....	221
Appendix H: Animal Daily Emission Program.....	223
H.1 REMS_ER_calc_28.m.....	223
H.2 daily_E_std_uncertainty.m.....	230
H.3 subsamp_ER_integration.m	231
H.4 P_diff_func.m.....	232
H.5 std_uncertainty_om_ER.m.....	232
H.6 leftsum.m	234
H.7 ER_plot.m	235
H.8 importfile2.m.....	236
Appendix I: Testing for Chamber Bias.....	238

CHAPTER 1: INTRODUCTION

Methane (CH₄) production from cattle has significant implications to the environment as a greenhouse gas contributing to climate change (Cubasch et al., 2013) and to animal productivity as an indicator of feed efficiency. Further, with the rising global population expected to double from 2013 by the year 2050, the demand for cattle as a protein source will continue to increase, requiring more animals in production (Skoet & Stamoulis, 2006; United Nations, Department of Economic and Social Affairs, Population Division, 2013). Enteric microbial fermentation of hydrolyzed dietary carbohydrates in cattle generates CH₄ and can represent a loss of energy between 2% and 12% of the gross intake of the animal; thus, it is an important parameter to evaluate ruminant production efficiency (K. A. Johnson & Johnson, 1995). Environmentally, enteric fermentation, primarily from beef and dairy cattle, accounted for an estimated 23% of the total CH₄ emissions in the agricultural sector in 2011 (EPA, 2013). Methane production from cattle requires accurate quantification for development of mitigation and management strategies that are both economically and environmentally advantageous (McGinn, 2006).

Methods such as the open-circuit indirect calorimeter and the open-circuit respiration chamber, classified under the chamber technique, have been the most common method for animal energetics and metabolism research (Bhatta, Enishi, & Kurihara, 2007; Storm, Hellwing, Nielsen, & Madsen, 2012). The chamber technique measures environmental conditions, fresh air supply rate to the chamber, and respiratory gas exchange (including eructated CH₄), to compute an Emission Rate (ER). There are numerous applications of the chamber technique, each complex and with a unique construction and design, providing an extensive range of measurement capabilities. Although the chamber technique is considered the reference for ruminant CH₄ emissions research, there is limited documentation regarding the confidence in

CH₄ production rates using this method (McGinn, 2006). Further, to estimate uncertainty associated with CH₄ production rates, a well-documented and comprehensive error analysis must be derived for each application. An error analysis is a significant part of validating the measurement system because it provides an estimate of the computed ER uncertainty and subsequently establishes a level of confidence with data from the chamber technique (Gates, Casey, Xin, & Burns, 2009). The accuracy of CH₄ production estimates from ruminants for development of management strategies can be improved through determining and quantifying the confidence in the chamber technique. Improved beef and dairy cattle production will be required to meet the future global agricultural demand (Skoet & Stamoulis, 2006); thus, accurate estimates of CH₄ emission will be critical to management and mitigation strategies that are environmentally and economically beneficial (McGinn, 2006; Schmidhuber & Tubiello, 2007). Applying a well-documented systematic design, validation, and evaluation process to livestock energetics and metabolism research will enhance the understanding of the accuracy and improve the quality of data generated by these complex measurement systems. The approaches applied to describe the uncertainty and validation of newly constructed open-circuit respiration chambers should enable the identification of details and methodologies lacking in the literature and provide avenues for further improvement of metabolism and energetics research (McGinn, 2006). A more comprehensive understanding of the validation of the chamber technique is necessary for future applications of the chamber technique and will be a key component in the advancement of this technology.

An open-circuit respiration system, named the Ruminant Emission Measurement System (REMS) was used to establish the documented methodology for determining the uncertainty associated with emission rate and the whole system validation. The REMS consists of six

identical, ventilated-hood type chambers located at University of Illinois at Urbana-Champaign Beef and Sheep Field Research Lab. The operational goal of the REMS is to study relationships between CH₄ production and nutrition, genetics, and different management strategies. Housed in an environmentally controlled barn, chambers are constructed with an aluminum frame and clear polycarbonate walls with an internal volume of 1.2 m³. Each chamber has an individual Thermal Environmental Control Subsystem (TECS) to supply conditioned air for comfort and humidity control. A Fresh Air Supply and Measurement Subsystem (FASMS) to provide animal ventilation requirements featured custom designed and calibrated orifice meters to accurately measure and control ventilation rates at flowrates less than 550 lpm (Ramirez et al., 2013). A Gas Sampling System (GSS) collects background gas concentrations and environmental conditions (temperature and relative humidity) at the FASMS inlet and inside each chamber. In addition, a seven-way solenoid manifold controls sampling selection and routes gas to an infrared photo-acoustic gas analyzer capable of measuring methane (CH₄), carbon dioxide (CO₂), sulfur hexafluoride (SF₆), nitrous oxide (NO₂), and water vapor.

1.1 Objectives

The overall goal of this research was to determine and document the methodology to quantify standard uncertainty associated with calculated eructated CH₄ emissions from beef cattle and the whole system validation of the REMS. Specific objectives of this work were to:

- 1) Design, construct, and validate an orifice meter for accurate volumetric flow measurement for the REMS as a part of the fresh air supply and measurement subsystem

- 2) Construct and perform design analysis of the REMS to derive the calculation for the best estimate of accumulated eructated CH₄ emissions and its associated standard uncertainty.
- 3) Commission the REMS by verifying subsystem performance relative to design criteria and evaluate significant systematic bias based standard uncertainty for each chamber through repeated tests, and when applicable apply a correction factor.

1.2 Organization of the Thesis

Chapter 1 provides an overview of the research problem and objectives with each following chapter supporting the aforementioned objectives. Chapter 2 presents a literature review covering the design, operation, and whole system validation methodology of the chamber technique. Chapter 3 is a manuscript describing the calibration and uncertainty analysis for ventilation rate measurement by a custom designed and constructed orifice meter. The following two chapters, Chapters 4 and 5, are a two-part series that describes the unique design and evaluation of the Ruminant Emission Measurement System (REMS). These manuscripts also document the methodology to establish confidence with accumulated CH₄ emission estimates from open-circuit respiration chambers by quantifying the uncertainty associated with the whole system validation and the integration of emission rate. My specific contributions to Chapters 3, 4, and 5 are highlighted at the beginning of each chapter. Lastly, Chapter 6 discusses the conclusions and future work. Appendices A through I contain data and programs used to support the methods and results in Chapters 3, 4, and 5.

CHAPTER 2: LITERATURE REVIEW

To aid in the understanding and validation of the chamber technique for measuring methane production from ruminants, this literature review focuses on (1) overview and applications, (2) classification, (3) design and components, (4) emission calculation methods, (5) instrumentation, (6) system validation methods, and (7) the performance evaluation of the chamber technique.

2.1 Overview and Application of the Chamber Technique

Accurate quantification of methane (CH₄) emissions from cattle is required for the design of the most effective management strategies that have both environmental influence and economic benefit (McGinn, 2006; Storm et al., 2012). Many different factors affect CH₄ production such as the type of animal, body weight, climate, and feed. Methane is produced in the rumen as a result of the microbial fermentation of hydrolyzed starches and is released through flatulence and exhaled through the nose and mouth of the animal from eructations (Makkar & Vercoe, 2007). Approximately 88% of all enterically produced CH₄ is released through the respiratory tract (D. Johnson, Johnson, Ward, & Branine, 2000). Therefore, collecting only respiratory gases (including eructated CH₄) can provide an estimate for CH₄ emissions from ruminants. Measurement systems capturing only eructated gases are less expensive and simpler to construct but fail to collect the remaining hindgut CH₄ production (Bhatta et al., 2007; K. A. Johnson & Johnson, 1995; Storm et al., 2012).

Historically, the chamber technique has been the primary method for animal energetics and metabolism research. It was originally developed for use as a calorimeter to study heat production from animals (McLean & Tobin, 1987). Estimations of livestock heat production influence the design of housing and its thermal environments, as well as management strategies (Hillman, 2009). Thermal environment has a significant impact on animal physiology, which in

turn affects production parameters (Brown-Brandl, Nienaber, & Eigenberg, 2011). Further, digestible, metabolizable, gross, and net energy (frequently used by animal nutrition researchers) can be determined from heat production estimates coupled with measurement of the animal's inputs (i.e. amount and composition of feed) and outputs (i.e. amount and composition of feces, urine, and respiration gases (Nienaber et al., 2009).

Renewed interest in Greenhouse Gas (GHG) mitigation strategies has led to application of the chamber technique to quantify GHG emissions produced from production agriculture animals, mainly ruminants (Pinares-Patiño & Waghorn, 2012). The chamber technique has been utilized to investigate CH₄ loss in energy metabolism for improved production and to develop CH₄ reduction techniques. Many aspects of feeding and nutrition such as level of feeding, effect of feedstuffs, effect of chemical and physical composition, restricted versus ad libitum feeding, feeding schedules, different additives etc. can all be explored with the chamber technique (Sejian, Lal, Lakritz, & Ezeji, 2011). Hence, the chamber technique, when properly validated, is suitable for studying and understanding CH₄ production from cattle and other ruminants in a non-grazing setting.

2.2 Classification

The chamber technique includes respiration chambers and calorimeters for measurement of respiratory gas exchange (including eructated CH₄) for both energetics and emissions research (Figure 2.1). Respiration chambers may be used to solely measure GHG emissions or as an indirect calorimeter when Oxygen (O₂) measurement is incorporated. Calorimeters are subdivided into direct and indirect, the latter being more prevalent. Direct calorimeters quantify total heat dissipation by measuring sensible heat loss to the environment and evaporative losses, while the indirect calorimeter quantifies heat production from quantitative measurements of

materials consumed and produced (including respired gases) during metabolism (Nienaber et al., 2009).

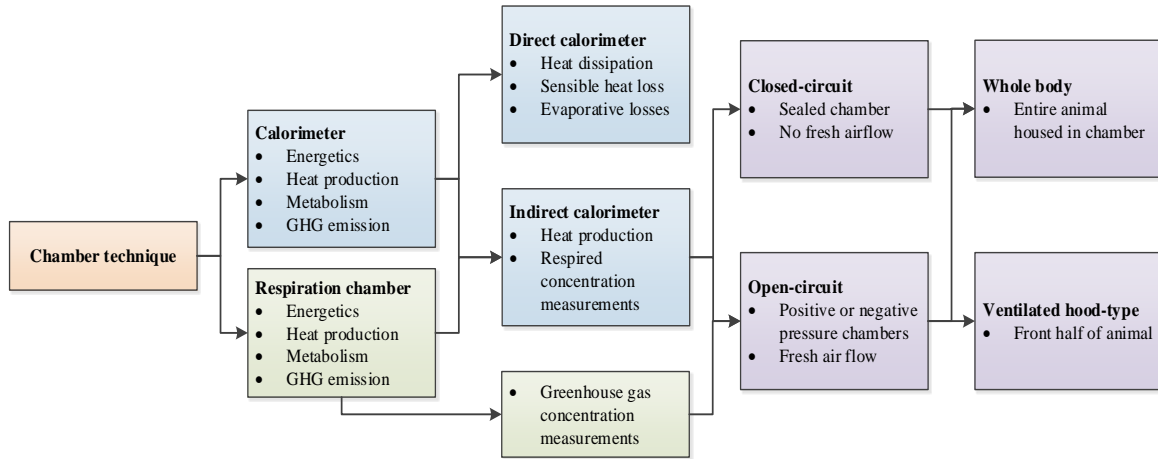


Figure 2.1. Classification of respiration chambers and calorimeters. Respiration chambers can be configured as indirect calorimeters or can be used solely to measure greenhouse gas production.

Both respiration chambers and indirect calorimeters are then classified by their operational design: closed-circuit and open-circuit. Although uncommon, a closed-circuit design measures water vapor and carbon dioxide (CO₂) produced by the animal housed in a completely sealed chamber. Oxygen (O₂) consumption is then measured by the amount of O₂ required to maintain a constant O₂ concentration in the sealed system (Suzuki, McCrabb, Nishida, Indramanee, & Kurihara, 2007). Conversely, open-circuit systems determine emission rate or heat production, from the flowrate of fresh air through the chamber and net gas concentration at the inlet and outlet. The chamber technique is further sub-categorized by physical design. Whole body chambers house the entire animal but restrict animal movement and are often expensive to construct. The alternative, the ventilated hood-type chamber, encloses the animal's head and secures its shoulders, while a hood is used seal the opening of the chamber to the animal's body. Ventilated hood-type chamber designs are less expensive (fewer materials) than whole body but

the animal requires restraining/training and hindgut CH₄ production cannot be captured (Storm et al., 2012). Due to their popularity, open-circuit indirect calorimeters and respiration chambers will be the focus of the remainder of this chapter.

2.3 Design and Components

Open-circuit respiration chambers and indirect calorimeters of the ventilated hood-type or whole body have an inherently similar design and operation. They consist of a chamber to collect gas produced by the animal, a ventilation supply for fresh air, thermal environmental control, and a gas sampling system (Figure 2.2). Currently, there is no single approach to designing these systems but researchers have reported the advantages and disadvantages of their unique system. The important design concepts and essential components acquired from the literature will be presented here.

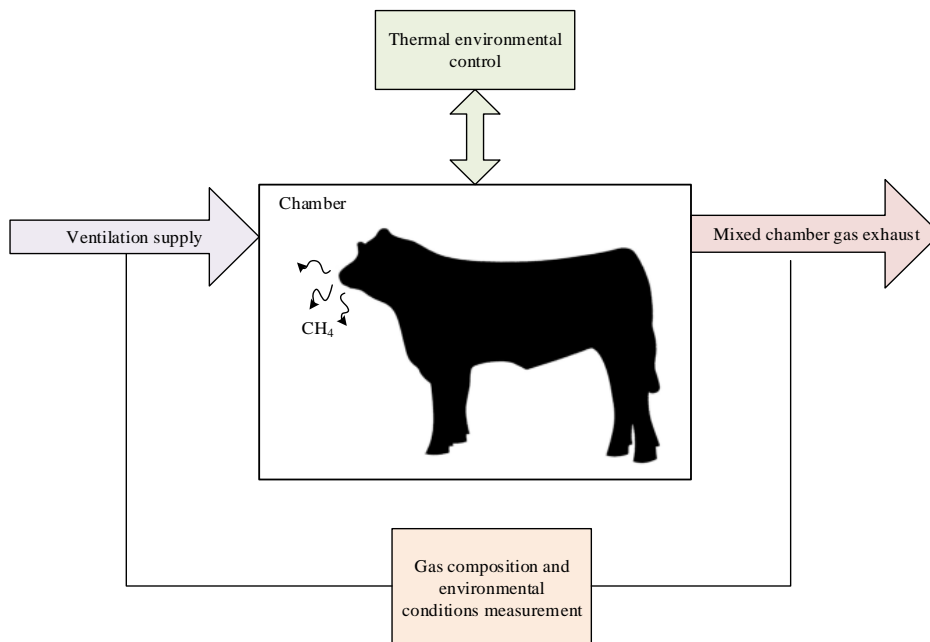


Figure 2.2. Simple diagram of a whole body open-circuit respiration chamber. Features include a chamber for the animal, fresh air ventilation supply, gas concentration measurements at the inlet and exhaust, and a method for thermal environmental control.

One of the most important functions, common to all systems, is the collection of representative data. Integrity of data generated from animal metabolism and energetics studies may be impacted by the responses of the animal to the measurement process (McGinn, 2006; Storm et al., 2012). A safe environment must be provided for the animal and operator with safeguards in the event of a system failure. Placing animals inside a chamber introduces a new environment, which the animal must cope with in order to survive. The possible resultant state of being of the animal can have negative effects on energy metabolism; thus, poor data quality (Hillman, 2009). The environmental conditions inside the chamber as well as the construction of the chamber can be controlled to best suit the animal's needs and minimize potential stressors.

2.3.1 Chamber

Chamber designs have incorporated methods to reduce animal stress and minimally change natural metabolism (Storm et al., 2012). Placement of the animal inside the chamber or other housing, and removal for normal activities creates an “artificial” environment that may have an effect on metabolism such as increased or decreased feed consumption or respiration rate (Gooding, Duncan, Atkinson, & Shoveller, 2012; Hellwing, Lund, Weisbjerg, Brask, & Hvelplund, 2012; Lobeck, Endres, Shane, Godden, & Fetrow, 2011). Many chambers are constructed of clear polycarbonate walls (Place, Pan, Zhao, & Mitloehner, 2011; Storm et al., 2012; Suzuki et al., 2007). There are two advantages of using this material as it is (1) extremely durable and (2) the animal can see its surroundings. For large animals, such as beef cattle that can weigh in excess of 900 kg (1984 lb.) can easily destroy weaker materials posing harm to themselves, the equipment, and operators. Clear chamber walls and ceiling allow light to enter and the animal to see both approaching people and animals in other chambers, in order to decrease stress (National Research Council, 2011). Consequently, placing the animal inside a

chamber will restrict their movement and constrain the animal to some degree. The subsequent effect on data quality is relatively unknown.

These systems are often constrained by the physical and environmental limitations of the barn, stall, or room in which they are housed. Chamber systems are often housed in a controlled environment, such as a barn or building, but can also be mobile units (Hellwing et al., 2012; Storm et al., 2012). The location of the chamber system within a barn can reduce materials and energy in the operation of the system and may promote a more natural environment for the animal. Rows of chambers in close proximity with each other, allows the animals to all view one another (Hellwing et al., 2012; Pinares-Patiño & Waghorn, 2012). The configuration of the barn also plays an important role in the size, mobility, and features of the system. Systems can also be designed to integrate into the barn such as a ventilated hood chamber that can be easily move in and out of a metabolism stall (Kelly, Kerrigan, Milligan, & McBride, 1994; Place et al., 2011; Suzuki et al., 2007).

2.3.2 Ventilation

For the open-circuit chamber systems, a continuous supply of fresh air must be provided to the chamber. Ventilation rate is measured at either the inlet or the outlet of the system. The classical design of the open-circuit chamber technique uses a blower to pull fresh air into the chamber, pass the respiring animal, and out of the chamber through a flow meter; thus, creates a negative pressure inside the chamber (Nienaber et al., 2009; Storm et al., 2012). The alternative design measures ventilation rate at the inlet, with the blower pushing air into the chamber; thus, creates a positive pressure inside the chamber (Brown, Cole, Dauncey, Marrs, & Murgatroyd, 1984). Air is then distributed around the respiring animal and exhausts out through cracks in the chamber. It is important to discuss the spatial distribution of internal chamber pressure for each

ventilation method as the result can affect the integrity of the collected gas samples from the chamber. A negatively pressurized chamber relies significantly on the chamber being completely sealed (McLean & Tobin, 1987). In addition, all incoming air must come through a single location where environmental parameters and gas concentrations can be measured. Any infiltration of gas not quantified at the inlet may dilute the gas sample in the chamber. Conversely, a positively pressurized chamber does not require complete sealing, as the supplied air must leave the chamber through outward leakage. The positive pressurized chamber is advantageous because no background gases can potentially dilute concentrations inside the chamber and any “leaks” will not cause infiltration. Similar approaches using positive pressure have been implemented in gas sampling systems used for broiler housing emissions research (Moody et al., 2008). All components within the positive pressure system must be positively pressurized or infiltration may occur.

The most critical risk to animal safety is the potential loss of ventilation or under ventilating. Reduced or no fresh air without operator response may result in asphyxiation. In the event of a failure, several systems have employed automatic messaging systems to alert the operator of equipment failure, gas concentrations, and ventilation rates (Pinares-Patiño & Waghorn, 2012). Ventilation blowers have been installed in parallel such that if one fails, the other blower continues to operate. For power failure situations, automatic opening of the chamber doors have been installed (Pinares-Patiño & Waghorn, 2012). Several systems activate gas concentration alarms when CO₂ concentration reaches 5000-9000 ppm_v or when oxygen concentration falling below 18% (Pinares-Patiño & Waghorn, 2012; Place et al., 2011). Understanding level and length of exposure to CO₂ for cattle is relatively unknown. These alarm systems provide baseline

methods for future chamber systems to include for the reduction of hazards to the animal and the operator.

2.3.3 Mixing

The quality of the gas sampled from the chamber depends significantly on the capture of a well-mixed gas. Gas samples collected from a poorly mixed chamber may misrepresent the gas produced by the animal due to high concentration pockets or “dead” zones that may occur within areas of the chamber. Poor mixing may also result in a separation of gases in the chamber. CO₂ (1.977 g L⁻¹) is more dense than air (~1.2 g L⁻¹), it can fall to the bottom of the chamber while CH₄ (0.6556 g L⁻¹) can rise to the top because it is less dense than air (Pinares-Patiño & Waghorn, 2012). The location of the animal’s head in the chamber affects where the gases will be released; hence, higher concentrations will be at the point of release. Ideally, respired gases are mixed rapidly with the incoming fresh air but this is difficult to achieve. Knowledge of the time it takes released gases to mix is critical. Several methods for achieving a well-mixed gas sample include location of the ventilation inlet and outlets, small rotational fans inside the chamber, and the ventilation flow rate (Pinares-Patiño & Waghorn, 2012). Evaluation of mixing can be potentially characterized through continuous injection of a tracer gas in a mass recovery test (Zhang, 2005) or with the visual characterization of smoke released from a smoke stick (Sales, Green, & Gates, 2013). Inability to achieve the predicted steady concentration may be due to poor mixing or a combination of mixing and fresh air exchange rate. Determination of the time constant provides insight to the time required to reach steady state.

2.3.4 Thermal Environment

A well-designed chamber with good mixing, properly sized ventilation system, and thermal environmental control (TEC) can significantly improve data quality using the chamber

technique. Heating and air conditioning systems are utilized to provide a stable thermal environment inside the chamber. A controlled thermal environment is not only beneficial to the animal but also the gas sampling system (Bhatta et al., 2007; Nienaber et al., 2009; Storm et al., 2012). Humidity interference with several gas analyzers can negatively affect the quality of gas composition measurement (Maia, 2010). Estimations of latent and sensible heat production from the animal can be used to calculate heating and cooling loads specific to the type and size of the animal (Albright, 1990).

Typically, each chamber has an individual TEC unit to maintain environmental conditions specific to that chamber as the animal requirements may vary (Storm et al., 2012). A heat source is used to dry the air and add sensible heat. In addition, a cooling coil reduces sensible heat until condensation where latent heat is then reduced. In order to facilitate mixing inside the chamber and move air past the TEC components, an air recirculation system with a blower is incorporated into the design for mixing. Other methods for TEC include using a fresh air source inside the building in which the chambers are housed rather than outside. This method provides fresh air to the chambers that has been conditioned by the building and can be used to reduce heating and cooling loads needed to maintain animal comfort (Storm et al., 2012).

Thermal environmental control is used to maintain the environment inside the chamber such that it is within the animal's thermoneutral zone to avoid thermal stress. The thermoneutral zone is defined as the range of temperatures the animal can maintain a constant core body temperature with minimal metabolic heat production (Hillman, 2009). This range is not fixed but a dynamic function of acclimation, air movement, relative humidity, time of day, degree of exposure to sunlight, and other factors. If conditions go beyond the upper and lower critical temperatures, heat and cold stress can be induced, respectively. Behavioral and physiological responses to

thermal stress may alter energetics and metabolism, compromising data generated within the chambers (Hillman, 2009).

2.4 Calculation Methods

The principle of the chamber technique is that any gaseous mass generated by the animal in the chamber can be determined by the difference in mass flow at the inlet and outlet (Gates et al., 2009). Development of emission rate calculation (mass flow generated by the animal) will be the primary focus of this section.

2.4.1 Mass Balance Approach

The Law of Mass Conservation (mass cannot be created or destroyed, only changed in form) can be applied to entire REMS to yield a mass balance. That is, the mass that enters a system must either leave the system or accumulate within the system. The general mass balance formula (Equation 2.1) can be simplified through several assumptions and modified to be in terms of measureable parameters.

$$IN + GENERATION - OUT - CONSUMPTION = ACCUMULATION \quad (\text{Equation 2.1})$$

where

<i>IN</i>	= mass that enters the system (g)
<i>GENERATION</i>	= mass generated within the system (g)
<i>OUT</i>	= mass that exits the system (g)
<i>CONSUMPTION</i>	= mass that consumed within the system (g)
<i>ACCUMULATION</i>	= mass that accumulates within the system (g)

The boundaries or the “control volume” of the system must be well defined before a mass balance can be applied, in this case the chamber with the animal inside. Further, the mass balance can be modified to a mass flow balance (divide Equation 2.1 by time), which can be used to determine the Emission Rate (ER) of a gas from an animal. When the mass balance is represented in terms of measurable parameters, the mass balance becomes a mass flow balance.

Since the animal is inside the control volume, the mass flow of gas produced by the animal is the *GENERATION*. While *IN* can be represented by airflow coming into the system and *OUT* as the airflow leaving the system. Gases such as CH₄, N₂O, CO₂, and O₂ can be converted from a concentration to a mass basis to fulfill the mass balance. For CH₄ emissions studies, the *CONSUMPTION* term is assumed negligible. Even though the animal is breathing, inhaled gas is then also exhaled. This is not the case when O₂ is being monitored for energetics studies, as the animal is respiring and consuming the O₂ in the air. In addition, the *ACCUMULATION* term is assumed zero as the gas is well mixed inside the chamber, non-reactive with materials in the system, and the gas can leave the system through exhaust. The assumptions of the mass balance are only as good as the design and the measurements of the chamber system, i.e. mass is not lost through unquantified measurements. For heat production and energetics calculations, the Law of Energy Conservation can be applied in a similar manner (McLean & Tobin, 1987).

2.4.2 Fresh Air Exchange Steady-State Consideration

Assuming the accumulation term is zero indicates the system is at steady state or the fresh air exchange rate equals the generation of gas inside the chamber. This implies that gaseous mass created inside the chamber (from an animal or quantified injection) reaches a constant rate and change in mass over time is zero (Zhang, 2005). Rearranging Equation 2.1 in terms of assumptions shows:

$$\frac{d\dot{m}^{gas}}{dt} = 0 = IN - OUT + GENERATION \quad (\text{Equation 2.2})$$

$$GENERATION = OUT - IN \quad (\text{Equation 2.3})$$

where

$$\frac{d\dot{m}^{gas}}{dt} = \text{assumption that the system is at steady state (i.e. accumulation is zero)}$$

Achievement of the steady-state regime is dependent of the design and internal mixing of the chamber as discussed in Section 2.3.3. Analysis of the gas mass flow at the outlet requires steady-state regime because the approach to steady-state is often exponential. This exponential approach is difficult to analyze and to determine the actual mass generated inside the chamber, which will be discussed more in Section 2.6.

The time required to reach steady-state can be mathematically approximated by a linear homogeneous first-order differential equation (Zhang, 2005). Applying the regression to experimentally generated data from the continuous injection of a gas into the chamber yields the time constant of the system. One time constant represents the time it takes the system to reach ~63.2% of the steady state. Greater confidence in the time to reach steady state can be approximated by five time constants, which is ~99% to reach steady state (Zhang, 2005). System characterization is important for operation with animals and for understanding system biases and accuracy. When an animal is present in the chamber, gas sampling cannot begin until eructated gas has completely mixed and allowed to reach steady-state.

Alternatively, the time required to reach steady state can be determined by estimating the chamber residence time based on the chamber volume and ventilation rate (Place et al., 2011). Three times the chamber residence time yields chamber turnover rate or the time it takes all the air in the chamber to be replaced. Not only does this require accurate measurement of volumetric flow rate but also chamber volume. Empty chamber volume can be estimated with relatively low error if there are no objects inside the chamber such as a drinker or a feed bin. The chamber volume also changes considerably when the animal and feed are present inside the chamber as they occupy space. The empty chamber volume no longer becomes a reasonable estimate.

2.4.3 Emission Calculation

Chamber systems combine numerous measurements to evaluate the parameters of the mass balance. The resultant equation, commonly referred to as the Emission Rate (ER), flux, or production rate equation, is often unique to the system as each application of the chamber technique uses different units and instruments. The emission rate equation is often reported as mass of a gas per unit time e.g. $\text{kg}^{\text{CH}_4} \text{s}^{-1}$. However, the objective of the study has a significant impact on the unit. The denominator will often change, e.g. a feed efficiency trial may characterize emission rate as $\text{kg}^{\text{CH}_4} \text{s}^{-1} \text{DMI}^{-1}$, where DMI is dry matter intake. Conversely, an energy metabolism study may seek $\text{kg}^{\text{CH}_4} \text{s}^{-1} \text{KJ feed}^{-1}$ (Storm et al., 2012). ER can also be reported in volumetric units rather than mass such as $\text{L}^{\text{CH}_4} \text{min}^{-1}$. Using 1 g of CH_4 equals 1.3962 L CH_4 , mass and volumetric units can be interchanged (Pinares-Patiño & Waghorn, 2012). For comparison, data obtain from animal monitoring in the chamber may be normalized to one day. This is achieved by summing the total number of ER calculations and multiplying by the time between ER calculations (sampling frequency).

2.5 Instrumentation

The parameters in the Emission Rate (ER) equation are determined from either a single instrument or a combination of multiple instruments. Instruments commonly found in chamber systems are gas analyzers, flow meters, and environmental condition indicators. Instrument technology is important for system design but it is more critical to understand the accuracy, precision, drift, and calibration associated with each instrument. Comprehensive knowledge of the parameters that contribute to the uncertainty associated each measurement or computation is required to determine the ER standard uncertainty (Gates et al., 2009). The accuracy of the chamber technique cannot exceed the standard uncertainty of measuring instruments in the

system. It is equally true that accurate instruments cannot improve upon imprecise data (McLean & Tobin, 1987). A whole system validation to quantify mass conservation is needed in addition to an uncertainty analysis.

2.5.1 Technology

Selection of a gas analyzer technology is a function of time to process a sample, accuracy, integration with the system, and the gases to be studied. Currently, technologies used in the chamber technique include gas chromatography, infrared photo acoustic spectrometer, Fourier transform infrared, absorption spectroscopy, semiconductor chip sensor, and tunable diode laser absorption spectroscopy (Bhatta et al., 2007). The units of the gas concentration measurement are important for correct evaluation of the ER equation. More information can be found in Appendix B.3 regarding the use of gas concentration units in the ER equation.

Flow meters measure ventilation rate at either the inlet or outlet of the chamber, depending on the chamber design for either positive or negative pressure. Volumetric flowrate is often the parameter used in the ER equation and is measured with one of the following types of technology: mechanical or differential pressure. Other technologies do exist but they are often too expensive for the instrumentation of multiple chambers (Ramirez et al., 2013). Differential pressure flow meters take advantage of the pressure and velocity of a fluid based on Bernoulli's principle. A restriction in a pipe causes the fluid velocity to increase and a measureable pressure drop occurs (Rhinehart, Gebreyohannes, Sridhar, Patrachari, & Rahaman, 2011). Liptak and Lomas (2010) describe a variety of differential pressure class flow meters such as orifice meters, Venturi meters, V-cones, and nozzles that use this principle to quantify volumetric or mass flow. Differential pressure class flow meters have been used extensively in research applications for livestock emission studies (Derno, Elsner, Paetow, Scholze, & Schweigel, 2009; Powers,

Zamzow, & Kerr, 2007), cattle manure emission studies (Sun et al., 2008), and air quality studies (Wang & Zhang, 1999). Multiple anemometers and pitot tube have been used to determine air velocity to compute volumetric flow rate. Alternatively, mass flowrate can be used to evaluate the ER equation and mass airflow meters such as those used in animal calorimetry studies (Xin & Harmon, 1996) or open-circuit respiration studies (Hellwing et al., 2012) directly measure ventilation air mass flow. High accuracy measurement of mass flow rate is expensive, especially when numerous instruments are required (Purswell, Adams, Montross, & Davis, 2011).

The remaining measurements required to determine emission rate are from temperature sensors, relative humidity sensors, and barometers. Temperature and relative humidity sensors come coupled together or separate in a variety of technologies. Barometric pressure is measured on-site, or calculated with ASHRAE Handbook of Fundamentals (2013).

2.5.2 Characterizing Instrument Error

An uncertainty analysis can be used to characterize random or systematic errors (ISO/IEC, 2008). Error is the difference between the measured value and the actual; however, it often difficult to know the true value. Systematic errors, when correctly identified, should be eliminated or minimized by applying appropriate corrections. The uncertainty associated with correction must be expressed in the overall uncertainty of the measurement (Hasselbarth, 2006). This type of error can be quantified from manufacturer's specifications, calibration reports, previous data and known uncertainties of reference data (Taylor & Kuyatt, 1994). In addition, systematic error includes drift or offset in which the measurement system does not read zero when the quantity measured should be zero and multiplier types in which the measurement system consistently reads greater or less than the measured quantity. Conversely, random error represents unpredictable random effects, such as imperfect repeatability of instrument or

measurement and slight changes in experimental conditions (ISO/IEC, 2008). Random error can be characterized by repeated measurements and the precision of those measurements; hence, is described by uncertainty. Accuracy characterizes both trueness and precision, where trueness describes how close the mean of the measured values is to the true value and precision accounts for nearness amongst discrete measurements (Hasselbarth, 2006). Understanding and reducing random error is accomplished with increasing the number of repeated measurements and quantifying the uncertainty (Taylor & Kuyatt, 1994). Identification and quantification of both random and systematic errors is essential for confident and accurate measurements. A schematic of the categories for measurement uncertainty is describe in Figure 2.3.

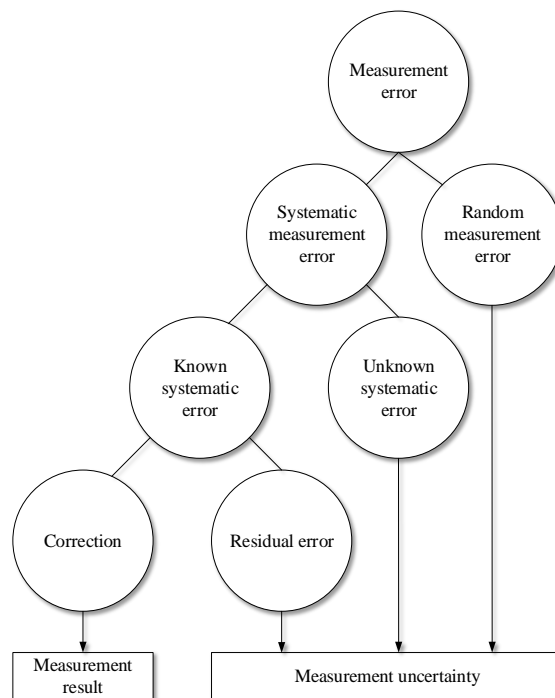


Figure 2.3. Categories of measurement error and their input to find the measurement resulted and its associated uncertainty (Hasselbarth, 2006). Systematic errors can be corrected if the associated uncertainty is included with the random errors in the measurement uncertainty.

2.6 Whole System Validation

It is necessary to calibrate individual components of the measurement system but the most critical calibration must be in terms of the whole system performance (McLean & Tobin, 1987). A Mass Recovery Test (MRT) is an evaluation of whole system performance and assesses the conservation of mass via a release-recovery method. The four major types of release-recovery methods are alcohol combustion, alcohol evaporation, point volume gas injection, and continuous gas injection. MRTs are performed by releasing a known amount of a substance within the chambers and measuring the mass estimated by the chamber system (McLean & Tobin, 1987). Not only does a MRT validate the instruments in the measurement system but also serves to test that the system has negligible infiltration. Any discrepancy in the MRT identifies potential losses of mass in the system, which needs to be addressed before implementation (Pinares-Patiño & Waghorn, 2012). The procedures to conduct these various MRTs have often been neglected in the literature or methods poorly described. Knowledge of the chamber system accuracy is significant to understanding the quality of measurement and validity of the collected data.

The accuracy of ER computed by the chamber technique is a function of the system's ability to measure mass generated within the chamber and uncertainty propagation of the ER calculation. These complex and often custom-constructed systems involve many pumps, fittings, tubes, seals, and the chamber itself, which are potential sources of unintended leaks. In addition, the ER equation is calculated from several measurements from gas analyzers, temperature and relative humidity sensors, and flow meters, each with their individual uncertainties. Understanding and quantifying the uncertainty in respiration chamber or calorimeter provides confidence with the measured results.

2.6.1 Emission Rate Uncertainty

Prior to conducting a validation experiment, analysis of the propagation of measurement error provides understanding into which measurements are the most critical (Gates et al., 2009). For the computed quantity such as an ER or heat production, there are many individual measurements and computations in conjunction with the entire chamber system functioning properly. An uncertainty analysis is performed by considering the contribution of each individual measurement's uncertainty (assuming they are independent), using a truncated first-order Taylor series approximation (ISO/IEC, 2008). Estimates of animal ERs conducted in chamber systems should include a documented analysis of uncertainty in published results, but such analyses are lacking in the literature. Few estimates of CH₄ emissions using the chamber technique (either indirect calorimeter or respiration chamber) have included a statement of uncertainty in published results (McGinn, 2006). ER uncertainty analysis identifies parameter measurement error, such as incoming and effluent concentration or ventilation rate, contribution to calculated ER uncertainty. Nienaber and Maddy (1985) provided detailed method of component calibration and used the results for evaluation of system total error, which ranged from 3.45 to 5.58% for an open-circuit indirect calorimeter. In addition, McGinn et al. (2004) determined overall error was estimated to be 7% for emission calculations using the sensitivity of ventilation and gas concentration measurement. In other fields, Price and Lacey (2003) performed an uncertainty analysis for gravimetric sampling of particulate matter and Gates et al. (2009) determined the uncertainty associated with ERs from field-scale broiler houses.

For a MRT validation method, there are additional instruments involved beyond the chamber system to generate the reference amount of mass. Confidence in the validation method must be established for correct interpretation of the whole system validation. These additional

inputs contribute to the overall uncertainty associated with the MRT. The standard uncertainty for the injected mass should be small because it is used as the reference to calibrate the chamber technique. The confidence interval established from coupling a MRT with an uncertainty analysis is significant to understanding sources of uncertainty and the magnitude of the mass recovered.

2.6.2 Alcohol Combustion

One of the earliest methods for validating calorimeters was using the stoichiometric relationship from the combustion of any alcohol to determine mass generation rate of CO₂ and mass consumption rate of O₂, which could be subsequently measured by the system (Carpenter & Fox, 1923). For example, the combustion of ethyl alcohol yields, for every gram of alcohol burned, the mass O₂ consumed is 1.461 g (STP), the mass CO₂ produced is 0.974 g, and the respiratory quotient of 0.667 (Brown-Brandl et al., 2011). Applying the mass balance relationship of the chamber, the known mass generation of CO₂ and O₂ can be compared to the ER calculated by the measurement system. Different alcohols have been used, such as ethyl alcohol (Brown-Brandl et al., 2011; McLean & Tobin, 1987), methanol (Takahashi, Chaudhry, Beneke, & Young, 1999), and ethanol (Nienaber & Maddy, 1985). However, the methodology is the same. Several variations of this test have been conducted to improve its accuracy such as altering burner designs to reduce evaporation (Nienaber & Maddy, 1985) and using other hydrocarbons (Young, Fenton, & McLean, 1984).

The alcohol combustion method is dependent on the assumption that the alcohol was completely combusted; however, there is no technique to determine actual amount combustion (if not 100% combusted) and that there was no additional losses through vaporization. This will introduce some unquantifiable error in the MRT and lead to a lack of confidence in

measurements. Several studies have observed the respiratory quotient (regardless of burner or fuel) to always be 0.667 (Brown-Brandl et al., 2011; McLean & Tobin, 1987; Nienaber & Maddy, 1985). This is a useful check for CO₂ and O₂ analyzers and the respiratory quotient is comparable to a resting animal (McLean & Tobin, 1987). The alcohol combustion method is generally not applicable to respiration chambers just measuring greenhouse gas production because O₂ is not measured.

2.6.3 Alcohol Evaporation

As alcohol evaporates, the change in mass can be measured over time and used to verify the system. Aqueous alcohol is placed on a microbalance inside the chamber and the change in mass is recorded for specified time intervals (Stackhouse, Pan, Zhao, & Mitloehner, 2011). The alternative is to place a known mass of alcohol inside the chamber and wait until complete evaporation (Place et al., 2011). Both methods yield a mass flow rate determined empirically as average flow rate over the time evaporation was taking place that can be compared to the mass flow rate measured by the system. The evaporation rate of ethanol (Smith, 2000) has been determined and could be used to predict the result of the MRT. Methanol and ethanol have been employed for verification of volatile organic compound (VOC) emission measurements.

The accuracy of this method is highly dependent on the complete evaporation of alcohol and delicate experimental procedures. The change in mass of the alcohol must also be able to be measured by the scale, which requires knowledge of the accuracy associated with the scale and purity of the alcohol. For best results, the scale would require connection to data logger for precise changes in mass over time. The gas must not be allowed to evaporate prior to entering the chamber or an unquantified mass of alcohol will not be captured by the measurement system. Another consideration is whether the system needs to reach or ever reaches the steady-state

before the change in mass can be recorded. This method is advantageous because it allows for verification of VOC measurement instruments, which may be more difficult than verifying CO₂ and O₂. This test is also inexpensive to conduct and of relatively short duration.

2.6.4 Point Volume Gas Injection

An alternative to using alcohol to verify mass recovery rates is the injection of a known volume of a gas that can be measured by the system's gas analyzer. This is essentially a time-decay test where the decay curve generated from diluting the gas is used to determine the mass injected. Several greenhouse gases such as CO₂ and H₂S, have been used as tracer gas. Methane is the primary gas measured for GHG emission and metabolism studies and may serve as an indicator to errors with the gas analyzer. Carbon dioxide is an indicator of adequate ventilation and used for calorimetry studies so it is most likely used for the same reason as CH₄. Whichever gas is used, ultra high purity concentration of the gas (i.e. > 99.9% analytical accuracy from the supplier) is stored in a vessel with a known volume. The canister is then placed completely inside the chamber or gas is injected via a tube. The chamber must be completely sealed, the gas allowed to mix, and the concentration allowed to reach steady-state. The corresponding decrease in gas concentration caused by the released gas follows a logarithmic decline i.e. $[CH_4]_t = ae^{-kt}$. Goopy et al. (2011) and Pinares-Patiño and Waghorn (2012) determined recovery percent by fitting a linear relationship between the natural log of CH₄ concentration verses the time and multiplying area under the linear regression by flow rate. This test also verifies the target CH₄ concentration by taking the antilog of the linear regression intercept at the instant the exhaust and intakes were opened. The known CH₄ concentration was determined by dividing the volume of the CH₄ injected by the volume of the chamber. This can be used to validate the measurement of the gas analyzer.

The single injection method has several advantages such as it is applicable to systems not measuring VOCs or O₂. Not only does it quantify the degree of mass conservation but also concentration measurement. This method can also be beneficial from a time standpoint (only takes about 25 min) but is highly dependent on the accurate fit of the logarithmic regression and integration. Pinares-Patiño and Waghorn (2012) report an R² of greater than 0.99 but do not discuss the standard error regression, which provides insight to uncertainty of the regression. The chamber must be completely sealed in this method and may be very difficult for some systems to achieve if there are many ports and holes. Further, the gas is assumed to have reached steady state when the sealed chamber is opened and sampling begins. This could be determined by trial and error because if sampling begins prior or after steady-state a logarithmic decline may not be observed. In addition, the accuracy of the known volume, purity of the gas, and environmental conditions (volume of a gas is a function of temperature and pressure) must be quantified. It would be very difficult to obtain an accurate volume measurement inside the chamber due to the presence of feed bins, drinkers, and other items. For comparison of known to measured mass flow rate requires complete release of the gas and sufficient change in concentration. Another assumption is the complete release of CH₄ from the canister and resultant steady-state concentration of CH₄ is greater than ambient which implies background monitoring before and after the MRT is required.

2.6.5 Continuous Gas Injection

There are two approaches to achieve continuous injection of gas into the chamber: gravimetrically or by a Mass Flow Controller (MFC). Rather than inject a single volume of gas, the gas is continuously injected into the chamber. The gravimetric method is accomplished by placing a primary certified gas cylinder on a scale and recording the change in mass once the

cylinder is opened and gas is injected into the chamber (Hellwing et al., 2012; Murray, Moss, Lockyer, & Jarvis, 1999; Suzuki et al., 2007). The change in mass of the cylinder from start to end of the injection is measured; therefore, the amount of mass injected can be determined. The gravimetric method can be extremely lengthy procedure lasting up to 24 h for CH₄ and 4 h for CO₂. Shorter tests have been conducted by using pure gas and potentially higher gas injection flow rate. Alternatively, a MFC can be used to control a constant volumetric flowrate from primary certified gas (mixed or pure) cylinder. The analysis of conservation of mass and the system time constant can be determined from this method. The gas is injected into the chamber via a tube and the system is allowed to reach steady state (Grainger et al., 2007; Pinares-Patiño et al., 2011; Stackhouse et al., 2011). The system operates as if an animal was present; thus, an accurate representation of the system's function can be described. Once numerous measurements at the mathematically determined steady-state have been recorded, the mass recovered and mass injected can be determined by integrating the mass flow over the steady-state regime.

Without the use of a MFC, it is very important to ensure the flow is continuous and not dynamic because increases or decreases of mass injected will not be captured if the sampling of the chamber is slower than the fluctuations. As gas is released from a compressed cylinder, over time there is a loss of pressure in the regulator and subsequently a loss of flow. Careful use of the two-stage regulator connected to the gas cylinder is required to ensure continuous and stable flow. Unless the scale is connected to a datalogger, a dynamic flow rate would negatively affect the recovery percent. The gravimetric method also requires a scale that can support a heavier compressed gas cylinder with sufficient accuracy. The MFC method requires assumption of the density of the gas inside the cylinder to calculate mass flow. Gas immediately expands upon release from the cylinder causing a change in the temperature and pressure. This has an effect on

density and the computed mass flow. A MFC is significantly more expensive than a gravimetric balance but is more accurate (typically less than 2% error). The continuous gas injection is advantageous because it does not require altering of the system (i.e. sealing), can be used with a variety of gases, and can be used to characterize the system time constant. This method can be more expensive and slightly more time consuming but it does not introduce manipulations to the system or assumptions with substantial impact on the mass recovery.

2.6.6 Results and Comparison Discussion

The chamber technique has been primarily validated through a single mass recovery test method or combination of several. There is still a need to incorporate uncertainty analysis for the calculating of the known mass injected. For the MRT, it is desirable to achieve 100% of the mass recovered for all methods. The percent recovered provides important system performance information and identification of problems with the gas sampling system or chamber design. There is limited literature regarding a detailed analysis of methods and results of recovery tests (McGinn, 2006). Further, for studies that do provide sufficient information on the performance of their system, replication of their work would be challenging.

For indirect calorimeters or respiration chambers that did report recovery test methods and results, a comprehensive summary is summarized in Table 2.1. No published recovery percent included a statement of standard uncertainty for any chamber tested. An included standard uncertainty associated with recovery percent provides insight to the level of confidence in the validation. This standard uncertainty should contain the measurement uncertainty of the system, the reference mass, and the standard deviation (SD) from repeated recovery tests over time. Further, each chamber should be reported and evaluated individually. For those that did report a SD with the recovery percent, it was often difficult to discern the source of the data used to

determine that SD. Calculation of SD may have been from performing a recovery test on a single chamber multiple times; thus, a mean and SD were obtained for each chamber. Alternatively, the results from one recovery test completed for each chamber in the system could have been averaged with that SD reported. The two previous methods for possibly calculating SD could have also been combined such that a mean recovery percent for all chambers over all replicates of the tests. No significance testing was reported to statistically show differences from the obtained recovery percent and the target of 100%.

In general, recovery tests show results from 90% to 105% for all the methods. Potential explanation from the few groups that have reported less than 90% and some greater than 105% may be due to mixing, leakage, errors in calculations or correction factors, instrument precision, background gas concentration measurement, and instrument calibration. Pinares-Patiño and Waghorn (2012) acknowledged problems with the background level can explain the fact that the recovery of gasses is not always 100%. If the background level of CO₂ is ± 50 ppm of the measured value it can explain 1 to 2 percentage points of the difference in the recovery rate. The use of gases found in the atmosphere or in a barn such as CO₂, CH₄, O₂, and H₂S requires frequent background measurement so the net concentration is accurately determined. Further, the recovery of gas is dependent on an accurate estimation of the ventilation flow rate. If the flow meter accuracy changes as flow rate changes, the recovery percent is only applicable at that result (Hellwing et al., 2012). This is further support that the MRT should be conducted just before or after an animal study. Direct comparison of recovery percent for different gases and alcohol is difficult due to the different types of errors the methods introduce, limited information on number of chambers evaluated, and replication size. Additionally, with incomplete knowledge

on overall system uncertainty, it is difficult to tell whether a recovery percent is acceptable i.e. reported recovery percent within the relative uncertainty of 100%.

Table 2.1. Summary of reported Mass Recovery Tests (MRTs) methods and results for alcohol combustion, alcohol evaporation, point gas injection, and continuous injection. Systems were classified by type of animals studied and authors' description. The number of tests was determined from the author's report, with prior to the experiment describing a MRT conducted before animals were placed in the chamber. Percent of mass recovered typically ranged from 90% to 105% with the majority reporting no corrections to data. Limited information was available on the source of the reported variance in recovery percent i.e. standard deviation of chambers or MRTs or standard uncertainty.

Validation method	Control type	Author	System classification	Primary animals studied	Number of tests	Recovery percent (mean \pm standard deviation, if reported)				
						CO ₂	O ₂	CH ₄	Alcohol	H ₂ S
Alcohol combustion	Ethyl alcohol lamp	Foth et al. (2013)	Indirect calorimeter chamber	Cattle	4	100.8% \pm 0.19%	101.19% \pm 2.17%	-	-	-
					4	103.1% \pm 3.32%	104.1% \pm 0.57%	-	-	-
					4	97.6% \pm 4.81%	99.6% \pm 2.1%	-	-	-
		Nienaber et al. (1985)	Chamber indirect calorimeter	Swine, sheep, and calves	46	100.9% \pm 0.7%	103.5% \pm 0.4%	-	-	-
					47	100.4% \pm 0.9%	102.4% \pm 0.5%	-	-	-
Alcohol evaporation	Gravimetric	Takahasi et al. (1998)	Open-circuit hood system	Small ruminants	5	-	102.0% \pm 1.1%	-	-	-
					49	98.0% \pm 0.8%	100.9% \pm 0.3%	-	-	-
		Place et al. (2011)	Ventilated hood system	Cattle	prior to experiment	-	-	-	98.50%	-
					prior to experiment	-	-	-	97.60%	-
					prior to experiment	-	-	-	methanol: 90% ethanol: 98%	-
Sun et al. (2008)	Environmental chamber	Dairy Cows	prior to experiment	-	-	-	methanol: 90% ethanol: 98%	-		
			prior to experiment	-	-	-	methanol: 90% ethanol: 98%	-		
Point gas injection	Known volume cylinder	Derno et al. (2009)	Open-circuit indirect calorimetry	Dairy Cows	prior to experiment	99.9%	-	-	-	-
					prior to experiment	-	-	95% - 103%	-	-
		Goopy et al. (2011)	Open-circuit chambers	Sheep	2	99.25% \pm 0.75%	-	-	-	-
					1	94.30%	-	-	-	-
					2	100.0% \pm 0.50%	-	-	-	-
Miller and Koes (1988)	Open-circuit indirect calorimetry	Small ruminants	2	97.0% \pm 0.45%	-	-	-	-		
			2	97.0% \pm 0.45%	-	-	-	-		
Munoz et al. (2012)	Known quantity	Indirect open-circuit respiration chambers	Dairy Cows	8	almost 100%	-	-	-	-	

Table 2.1 (cont.). Summary of reported mass recovery test methods and results.

Validation method	Control type	Author	System classification	Primary animal studied	Number of tests	Recovery percent (mean ± standard deviation, if reported)								
						CO ₂	O ₂	CH ₄	Alcohol	H ₂ S				
Continuous gas injection	Analytical regulator	Klien and Wright (2006)	Open-circuit methane chambers	Sheep	6	-	-	101.1% ± 1.82% (4.1%)	-	-				
	Controlled amount	McGinn et al. (2004)	Whole body chamber	Cattle	3 times during experiment prior to experiment	A correction factor 1.01, 1.14, 1.13, and 1.00 were applied to four chambers (CH ₄)								
		Pinares-Patino et al. (2011)	Respiration chamber	Sheep		-	-	98.2% ± 0.60%	-	100.5% ± 4.0%				
	Flow meter	Place et al. (2011)	Ventilated hood system	Cattle	prior to experiment	97.60%	-	-	-	-				
						99.30%	-	-	-	-				
	Gravimetric	Hellwing et al. (2012)	Open-circuit indirect calorimetry	Dairy cows	CH ₄ : 13 CO ₂ : 26	101.4% ± 4.0%	-	98.5% ± 6.6%	-	-				
		Suzuki et al. (2007)	Ventilated hood-type respiration calorimeter	Ruminants		prior to experiment	96.5% ± 1.0%	-	-	-	-			
	Mass flow controller	Cattle Respiration Facility, Aarhus University, Denmark	Respiration chambers	Cattle	35	95% - 108%	-	90% - 110%	-	-				
						Murray et al. (1999)	Open-circuit respiration chamber	Sheep	prior to experiment	-	-	92.6% ± 1.55%	-	-
						Grainger et al. (2007)	Open-circuit respiration chamber	Dairy cows	8	-	-	99% - 101%	-	-
						Pinares-Patino et al. (2011) b	Respiration chamber	Sheep	prior to experiment	-	-	98.9% - 100.2%,	-	-
						Sun et al. (2008)	Environmental chamber	Cattle	prior to experiment	-	-	90%	-	-
						AgResearch, Palmerston North	Respiration chamber system	Sheep	3 month interval	-	-	98.2% ± 0.60%	-	100.5% ± 4.01%
	Stackhouse et al. (2011)	Environmental chamber	Cattle	prior to experiment	-	-	101% 90%	-	102%, -					

Attaining exactly 100% mass recovered is often unachievable due to the combined measurement uncertainty of the calculated mass recovered and mass injected. A 100% mass recovery percent would indicate the system is unbiased and leak free. A recovery percent may be less than 100% and still be acceptable because it is within the measurement uncertainty of the system. Although the mass recovery test can indicate potential problems with sample lines (leaks or bad seals) and poor mixing, instrument accuracy and the propagation of uncertainty must be completed prior to the recovery test.

A recovery percent different than 100% may be attributed to the design of the system or continuous use that has caused instruments to drift, seals to loosen, piping to leak, etc. At what value different from 100% should action be taken? This question can be answered through a quantification of the uncertainty analysis and a detailed approach to the recovery test. Suzuki et al. (2007) recommends a newly constructed chamber system should achieve between 95% to 105% recovery values. A possible explanation of this range may be as an estimate that these systems have an assumed 5% uncertainty in mass recovered but methodology for this conclusion is lacking. In addition, the Cattle Respiration Facility, Armidale, NSW, Australia (Pinares-Patiño & Waghorn, 2012) declare 98% to 102% as the acceptable recovery percent range. There is a need for what is an acceptable recovery percent and what subsequent actions should be taken if the recovery percent is different from 100%. An example of an established protocol for quality assurance was reported by Moody et al. (2008) for U.S. broiler house emission studies. In this plan, data quality objectives (DQO) were established for verification tests of various system instruments. As a result, the DQOs were used to establish the degree of confidence required for measurements and the subsequent action if the error was too large. A systematic process was

used to evaluate the measurement system and the computed emission rate had an attached uncertainty.

2.6.7 Zero Offset

The entire system should be run with no gas injection (i.e. mass recovery test) and no animal inside the chamber to ensure the calculated emission rate is in fact zero (Grainger et al., 2007). This evaluation will provide insight to any system bias that may need to be corrected or issues with the gas sampling system. Incoming air from the ventilation system is distributed into the chambers. Gas composition measured at the ventilation inlet (background) should be the same as the gas composition inside the chambers. Thus, the computed emission rate should be zero.

2.7 Performance Evaluation and Limitations

After the completion of the design, construction, and successful validation of a chamber system, a performance evaluation of temperature control, moisture removal, gas sampling system integrity, and fresh air supply measurement and control with and without animals is conducted prior to animal studies. The significance of performance evaluation is it can lead to improved experimental design and operating procedures. A systematic approach to assessing the chamber system operation with animals will increase data quality through established protocols.

Whole body or ventilated hood-type chambers are a new environment for animals to cope with. Their response to the chamber system should be closely monitored and analyzed. Storm et al. (2012) reported there was no difference in amount of feed consumed in chamber versus out. An increase or decrease in feeding behavior may negatively affect CH₄ emissions. Physiological responses to heat stress such as sweating or panting may indicate exceeding the thermoneutral zone for that animal (Hillman, 2009). Animal comfort and interaction with the chamber should be assessed in case there is need for design and operation improvements. Ventilation rate

assessment ensues that there no accumulation of gases to uncomfortable levels. CO₂ levels should be analyzed and verified not to be above upper limits for animal safety.

An acclimation period may be used to improve adaptation to the chamber. Allowing the animal to acclimate to the chamber prior to a study will familiarize the animal with being restrained and the housing. The length of the acclimation period varies amongst sources, but some acclimation periods have replicated the intended experimental protocol or allowed for just an hour prior to data collection (Hellwing et al., 2012; Williams, Klein, & Wright, 2007). Only qualitative results have been reported and the general result has been a positive effect on data quality and animal behavior. Placing the animal in the chamber with no feed may help with acclimation and provide insight to the impact of feed on CH₄ emissions.

2.8 Conclusions

The chamber technique encompasses a wide range of application from measuring greenhouse gas generation to heat production. Each implementation of the chamber technique results in a complex, unique system that varies design, instrumentation, and validation. The uncertainty associated with the calculation of emission rate should be included in published results to indicate the level of confidence in the results. Uncertainty can be evaluated through the propagation of instrument error, while the validation of the system is performed by a mass recovery test.

The work that has been reported here has highlighted the advantages and disadvantages of many aspects of the chamber technique. The documentation of this knowledge has been beneficial for the development of these systems and identified area for future improvement. From these studies, it is clear that a systematic approach to evaluate component measurement errors is needed to determine the standard uncertainty of complex emission measurement

systems and confidently report animal emissions with a stated standard uncertainty. In addition, there is a need for establishing a mass recovery test that includes well-documented methods and accompanying uncertainty analysis.

2.9 References

- Albright, L. D. (1990). *Environment control for animals and plants*. American Society of Agricultural Engineers.
- Bhatta, R., Enishi, O., & Kurihara, M. (2007). Measurement of methane production from ruminants. *Asian-Australasian Journal of Animal Sciences*, 20(8), 1305-1318.
- Brown, D., Cole, T. J., Dauncey, M. J., Marrs, R. W., & Murgatroyd, P. R. (1984). *Analysis of gaseous exchange in open-circuit indirect calorimetry*
- Brown-Brandl, T. M., Nienaber, J. A., & Eigenberg, R. A. (2011). Temperature and humidity control in indirect calorimeter chambers. *Transactions of the ASABE*, 54(2), 685-692.
- Carpenter, T. M., & Fox, E. L. (1923). Alcohol check experiments with portable respiration apparatus. *The Boston Medical and Surgical Journal*, 189(16), 551-561.
- Cubasch, U., Wuebbles, D., Chen, D., Facchini, M. C., Frame, D., Mahowald, N., & Winther, J. (2013). *Introduction. in: Climate change 2013: The physical science basis. contribution of working group I to the fifth assessment report of the intergovernmental panel on climate change*. United Kingdom and New York, NY: Cambridge University Press, Cambridge.
- Derno, M., Elsner, H. G., Paetow, E. A., Scholze, H., & Schweigel, M. (2009). Technical note: A new facility for continuous respiration measurements in lactating cows. *Journal of Dairy Science*, 92(6), 2804-2808. doi:10.3168/jds.2008-1839
- EPA. (2013). *Inventory of US greenhouse gas emissions and sinks: 1990-2011*. (No. EPA 430-R-13-001).EPA 430-R-11-005.

- Foth, A., Brown Brandl, T., Freetly, H., Hayes, M., & Kononoff, P. (2013). Validation and recovery rates of an indirect calorimetry headbox system used to measure heat production of cattle. *Journal of Animal Science*, *91*, 262.
- Gates, R. S., Casey, K. D., Xin, H., & Burns, R. T. (2009). Building emissions uncertainty estimates. *Transactions of the ASABE*, *52*(4), 1345-1351.
- Gooding, M. A., Duncan, I. J. H., Atkinson, J. L., & Shoveller, A. K. (2012). Development and validation of a behavioral acclimation protocol for cats to respiration chambers used for indirect calorimetry studies. *Journal of Applied Animal Welfare Science*, *15*(2), 144-162. doi:10.1080/10888705.2012.658332
- Goopy, J. P., Woodgate, R., Donaldson, A., Robinson, D. L., & Hegarty, R. S. (2011). Validation of a short-term methane measurement using portable static chambers to estimate daily methane production in sheep. *Animal Feed Science & Technology*, *166-167*, 219-226. doi:10.1016/j.anifeedsci.2011.04.012
- Grainger, C., Clarke, T., McGinn, S. M., Auldist, M. J., Beauchemin, K. A., Hannah, M. C., . . . Eckard, R. J. (2007). Methane emissions from dairy cows measured using the sulfur hexafluoride (SF₆) tracer and chamber techniques. *Journal of Dairy Science*, *90*(6), 2755-2766. doi:10.3168/jds.2006-697
- Hasselbarth, W. (2006). *Guide to the evaluation of measurement uncertainty for quantitative test results*. (No. 1/2006).
- Hellwing, A. L. F., Lund, P., Weisbjerg, M. R., Brask, M., & Hvelplund, T. (2012). Technical note: Test of a low-cost and animal-friendly system for measuring methane emissions from dairy cows. *Journal of Dairy Science*, *95*(10), 6077-6085.

- Hillman, P. E. (2009). Thermoregulatory physiology. In J. DeShazer (Ed.), *Livestock energetics and thermal environmental management* (pp. 23-48) American Society of Agricultural and Biological Engineers.
- ISO/IEC. (2008). *Uncertainty of measurement: Part 3. guide to the expression of uncertainty in measurement (GUM:1995)* (ISO Guide 9803:2008(E). ed.). Geneva, Switzerland: International Standards Organization.
- Johnson, D., Johnson, K., Ward, G., & Branine, M. (2000). Ruminants and other animals. *Atmospheric methane* (pp. 112-133) Springer.
- Johnson, K. A., & Johnson, D. E. (1995). Methane emissions from cattle. *Journal of Animal Science*, 73(8), 2483-2492.
- Kelly, J. M., Kerrigan, B., Milligan, L. P., & McBride, B. W. (1994). Development of a mobile, open-circuit indirect calorimetry system. *Canadian Journal of Animal Science*, 74(1), 65-71.
- Lipták, B. G. (2010). *Instrument engineers' handbook, volume two: Process control and optimization* CRC press.
- Lobeck, K. M., Endres, M. I., Shane, E. M., Godden, S. M., & Fetrow, J. (2011). Animal welfare in cross-ventilated, compost-bedded pack, and naturally ventilated dairy barns in the upper midwest. *Journal of Dairy Science*, 94(11), 5469-5479. doi:10.3168/jds.2011-4363
- Maia, G. D. N. (2010). *Ammonia Biofiltration and Nitrous Oxide Generation as Affected by Media Moisture Content*,
- Makkar, H. P. S., & Vercoe, P. E. (2007). *Measuring methane production from ruminants*. Dordrecht, The Netherlands: Springer.
- McGinn, S. M. (2006). Measuring greenhouse gas emissions from point sources in agriculture. *Canadian Journal of Soil Science*, 86(3), 355-371.

- McGinn, S. M., Beauchemin, K. A., Coates, T., & Colombatto, D. (2004). Methane emissions from beef cattle: Effects of monensin, sunflower oil, enzymes, yeast, and fumaric acid. *Journal of Animal Science*, 82(11), 3346-3356.
- McLean, J., & Tobin, G. (1987). *Animal and human calorimetry* Cambridge University Press.
- Moody, L. B., Li, H., Burns, R. T., Xin, H., Gates, R. S., Hoff, S. J., . . . Overhults, D. (2008). *A quality assurance project plan for monitoring gaseous and particulate matter emissions from broiler housing (sections 1-6)* (ASABE Special Publication ed.). St. Joseph, Mich.: ASABE.
- Murray, P. J., Moss, A., Lockyer, D. R., & Jarvis, S. C. (1999). A comparison of systems for measuring methane emissions from sheep. *Journal of Agricultural Science*, 133(4), 439-444.
- National Research Council. (2011). *Guide for the care and use of laboratory animals* National Academies Press.
- Nienaber, J. A., DeShazer, J., Xin, H., Hillman, P. E., Yen, J. T., & Ferrell, F. F. (2009). Measuring energetics of biological processes. In J. DeShazer (Ed.), *Livestock energetics and thermal environmental management* (pp. 73-112) American Society of Agricultural and Biological Engineers.
- Nienaber, J. A., & Maddy, A. L. (1985). Temperature controlled multiple chamber indirect calorimeter-design and operation. *Transactions of the American Society of Agricultural Engineers*, 28(2), 555-560.
- Pinares-Patiño, C. S., McEwan, J. C., Dodds, K. G., Cárdenas, E. A., Hegarty, R. S., Koolgaard, J. P., & Clark, H. (2011). Repeatability of methane emissions from sheep. *Animal Feed Science & Technology*, 166-167, 210-218. doi:10.1016/j.anifeedsci.2011.04.068

- Pinares-Patiño, C. S., & Waghorn, G. C. (Eds.). (2012). *Technical manual on respiration chamber designs*. Wellington, New Zealand: Ministry of Agriculture and Forestry.
- Place, S. E., Pan, Y., Zhao, Y., & Mitloehner, F. M. (2011). Construction and operation of a ventilated hood system for measuring greenhouse gas and volatile organic compound emissions from cattle. *Animals (2076-2615)*, *1*(4), 433-446. doi:10.3390/ani1040433
- Powers, W. J., Zamzow, S. B., & Kerr, B. J. (2007). Reduced crude protein effects on aerial emissions from swine. *Applied Engineering in Agriculture*, *23*(4), 539-546.
- Price, J. E., & Lacey, R. E. (2003). Uncertainty associated with the gravimetric sampling of particulate matter. *American Society of Agricultural Engineers Annual International Meeting 2003*, ASAE Paper No. 034116.
- Purswell, J. L., Adams, W. C., Montross, M. D., & Davis, J. D. (2011). Evaluation of automotive mass airflow sensors for animal environment research and control applications. *American Society of Agricultural and Biological Engineers Annual International Meeting 2011*, ASABE Paper No: 1110839.
- Ramirez, C. B., Maia, G. D. N., Green, A. R., Shike, D. W., Gates, R. S., & Rodriguez, L. F. (2013). *Design and validation of a calibrated orifice meter for sub-500 liter per minute flow rate applications*
- Rhinehart, R. R., Gebreyohannes, S., Sridhar, U. M., Patrachari, A., & Rahaman, M. S. (2011). A power law approach to orifice flow rate calibration. *ISA Transactions*, *50*(2), 329-341. doi:10.1016/j.isatra.2011.01.005
- Sales, G. T., Green, A. R., & Gates, R. S. (2013). Commissioning an animal preference chamber for behavioral studies with laying hens exposed to atmospheric ammonia. *Computers and Electronics in Agriculture*, *95*, 48-57.

- Schmidhuber, J., & Tubiello, F. N. (2007). Global food security under climate change. *Proceedings of the National Academy of Sciences of the United States of America*, 104(50), 19703-19708. doi:10.1073/pnas.0701976104
- Sejian, V., Lal, R., Lakritz, J., & Ezeji, T. (2011). Measurement and prediction of enteric methane emission. *International Journal of Biometeorology*, 55(1), 1-16. doi:10.1007/s00484-010-0356-7
- Skoet, J., & Stamoulis, K. (2006). *The state of Food insecurity in the world 2006*. (). Rome, Italy: Food and Agriculture Organization of the United Nations.
- Smith, R. L. (2000). Predicting evaporation rates and times for spills of chemical mixtures. *Annals of Occupational Hygiene*, 45(6), 437-445.
- Stackhouse, K. R., Pan, Y., Zhao, Y., & Mitloehner, F. M. (2011). Greenhouse gas and alcohol emissions from feedlot steers and calves. *Journal of Environmental Quality*, 40(3), 899-906.
- Storm, I. M., Hellwing, A. L. F., Nielsen, N. I., & Madsen, J. (2012). Methods for measuring and estimating methane emission from ruminants. *Animals*, 2(2), 160-183.
- Sun, H., Trabue, S. L., Scoggin, K., Jackson, W. A., Pan, Y., Zhao, Y., . . . Mitloehner, F. M. (2008). Alcohol, volatile fatty acid, phenol, and methane emissions from dairy cows and fresh manure. *Journal of Environmental Quality*, 37(2), 615-622.
- Suzuki, T., McCrabb, G., Nishida, T., Indramanee, S., & Kurihara, M. (2007). Construction and operation of ventilated hood-type respiration calorimeters for in vivo measurement of methane production and energy partition in ruminants. *Measuring methane production from ruminants* (pp. 125-135) Springer.

- Takahashi, J., Chaudhry, A. S., Beneke, R. G., & Young, B. A. (1999). An open-circuit hood system for gaseous exchange measurements in small ruminants. *Small Ruminant Research*, 32(1), 31-36.
- Taylor, B. N., & Kuyatt, C. E. (1994). *Guidelines for evaluating and expressing the uncertainty of NIST measurement results* (NIST Tech Note 1297 ed.). Gaithersburg, Md: National Institute for Standards and Technology.
- United Nations, Department of Economic and Social Affairs, Population Division. (2013). *World population prospects: The 2012 revision, highlights and advance tables*. (No. ESA/P/WP.228).
- Wang, X., & Zhang, Y. (1999). Development of a critical airflow venturi for air sampling. *Journal of Agricultural Engineering Research*, 73(3), 257-264.
- Williams, Y. J., Klein, L., & Wright, A. -. G. (2007). In Makkar H. V.,PE (Ed.), *A protocol for the operation of open-circuit chambers for measuring methane output in sheep*
doi:10.1007/978-1-4020-6133-2_7
- Xin, H., & Harmon, J. D. (1996). Responses of group-housed neonatal chicks to posthatch holding environment. *Transactions of the American Society of Agricultural Engineers*, 39(6), 2249-2254.
- Young, B. A., Fenton, T. W., & McLean, J. A. (1984). Calibration methods in respiratory calorimetry. *Journal of Applied Physiology Respiratory Environmental and Exercise Physiology*, 56(4), 1120-1125.
- Zhang, Y. (2005). *Indoor air quality engineering* CRC press Baco Raton, FL.

CHAPTER 3: DESIGN AND VALIDATION OF A PRECISION ORIFICE METER FOR VENTILATION RATE CONTROL IN OPEN-CIRCUIT RESPIRATION CHAMBERS

B.C. Ramirez, G.D.N. Maia, A.R. Green, D.W. Shike, L.F. Rodríguez, and R.S. Gates

A manuscript submitted to *Transactions of ASABE*

This chapter describes the design, construction, and validation of six orifice meters for volumetric flowrate measurement used in the Ruminant Emission Measurement System (REMS) as a part of the fresh air supply and measurement subsystem (Chapter 4). The orifice meters were developed to accurately measure ventilation rate between 279 to 510 lpm (9.9 to 18 cfm). The validation methodology including the calibration and propagation of measurement uncertainty was documented for future applications. The individual calibration curves for each orifice meter are presented in Appendix A.1 and the program to assess the uncertainty with volumetric flowrate is reported in Appendix A.2. The precision orifice meters provide a reliable measurement of volumetric flowrate with a reasonable and stated source of accuracy for a low cost.

This chapter owes its success to the teamwork of Brett Ramirez, Guilherme Maia, Angela Green, Daniel Shike, Luis Rodríguez, and Richard Gates. I led the overall research, designed and constructed the orifice meters, collected and analyzed calibration data, and drafted the manuscript. Dr. Maia developed the uncertainty analysis of volumetric flowrate measurement and Drs. Green, Shike, Rodríguez, and Gates contributed to the research design and the draft revision.

3.1 Abstract

Accurate and reliable control of ventilation rate is an essential input and can be a major source of uncertainty in animal emission studies. Open-circuit respiration chambers and calorimeters requiring low ventilation rate operated at low static pressure present a unique and potentially costly challenge for volumetric flowrate measurement. Orifice meters, when properly calibrated, are differential pressure flowmeters providing accurate, economical, and reliable volumetric flow measurement and are found in many industrial processes and engineering applications. Orifice meters were designed and fabricated following ASHRAE and ASME guidelines for flow measurement to accurately provide ventilation to six environmentally controlled respiration chambers. Orifice meters were constructed with a 50.8 mm (2 in.) diameter PVC pipe for the entry and exit sections, a 3.175 mm (1/8 in.) thick acrylic orifice plate with a 20.6 mm (13/16 in.) diameter concentric beveled orifice, and four pressure flange taps on both upstream and downstream sides of the orifice plate. Individual calibration of each orifice meter was completed using a reference system comprised of two chambers with a nozzle for flowrates from 279 to 510 lpm (9.9 to 18 cfm). The calibration procedure described here is unique because it was conducted under the low static pressure operation used in the respirations chambers. Concurrent differential pressure measurements across the calibration reference and the orifice meter were recorded and the corresponding flowrates were calculated using the differential pressures and orifice flow theory. A unique method of calibration was developed. Analysis showed a linear relationship with slope different from unity between the calibration reference and orifice meter, demonstrating that each orifice meter required an individual calibration for best accuracy. Linear regression coefficients (standard error of coefficient, \pm SE) varied from 0.9244 (\pm 2.48 E-03) to 1.0699 (\pm 2.50 E-03) for the six orifice meters calibrations. At a nominal

500 lpm (17.65 cfm), the relative standard uncertainty with an applied coverage factor of two (approximately 95% C.I.) ranged from 3.6% to 4.9% across the six orifice meters. Custom designed, constructed, and calibrated orifice meters can be accurate and cost effective (approximately \$250 and 5 h of labor each) for volumetric ventilation rate measurement in individual animal emission measurement systems.

Keywords. Calorimetry, Emissions, Flowmeter, and Uncertainty.

3.2 Introduction

Uncertainty in ventilation rate measurement largely contributes to emission uncertainty quantified from housed animal systems (Calvet et al., 2013; Gates, Casey, Xin, & Burns, 2009; Nienaber & Maddy, 1985). Therefore, flowmeters with well-documented design, calibration, and uncertainty analysis are essential to improve the reliability of emission estimates. While some literature is available for quantifying volumetric flowrate uncertainty in gravimetric sampling of particulate matter (Price & Lacey, 2003), this work provides key supplemental information for including the design and calibration of an orifice meter for respiration chambers. Flowmeter applications for respiration chambers and calorimeters typically require low ventilation rates (defined as less than 550 lpm) with ventilation supplies operating at low static pressures, resulting in unique cost-related challenges and technical constraints. This work describes the selection, design, construction, and uncertainty analysis of an orifice meter that provides the requisite critical control of ventilation to six respiration chambers in the Ruminant Emission Measurement System (REMS). The REMS was designed to support research on the relationships between nutrition, genetics, and management strategies with methane emissions from ruminal activity. The parameters presented in the uncertainty analysis of this work are a significant

component for determining the uncertainty associated with emissions of methane from animals placed in the REMS. Further details of the REMS are provided in Maia et al. (2014; 2014).

Volumetric flowrate measurement using differential pressure flowmeters is advantageous because it is relatively inexpensive, and with proper fabrication and calibration, can be as accurate as higher-cost devices and other technologies. Several livestock emissions studies have used differential pressure flowmeters, such as a V-cone flowmeter capable of 500 lpm (17.6 cfm) (Derno, Elsner, Paetow, Scholze, & Schweigel, 2009), a Venturi tube operating between 100 to 400 lpm (3.5 to 14.1 cfm) (Pinares-Patiño & Waghorn, 2012), and a 125.4 mm orifice plate (Powers, Zamzow, & Kerr, 2007) with $\pm 0.14\%$ full-scale precision. Alternatively, mass flowmeters have been implemented in animal calorimetry studies (Xin & Harmon, 1996) and cattle emission studies with 3000 lpm flow capacity (Hellwing, Lund, Weisbjerg, Brask, & Hvelplund, 2012). Commercially available, high accuracy measurement of mass and/or volumetric flow is expensive, especially when numerous instruments are required (Purswell, Adams, Montross, & Davis, 2011).

Some key challenges for integrating flowmeters into low static pressure systems such as respiration chambers are summarized Table 3.1. Typical high-flow centrifugal blowers operate at static pressures less than about 1.74 kPa (7 in. H₂O), thereby excluding most of the available commercial flowmeters including rotameters, turbine, thermal mass, and vortex meters. Additionally, these devices are rather complex for custom-design and fabrication. The Venturi meter is a good technical option for low supply static pressures, and is able to recover a high percent of pressure loss (compared to orifice meters); however, challenges during handling, installation, and maintenance limit its use. Furthermore, commercial Venturi meters are costly when multiple devices are required; if customized and purchased with a traceable calibration, the

construction process is more complex than orifice meters and the price per unit greatly increases. Nozzles are less costly than Venturi meters and have similar advantages, but also similar challenges regarding installation and maintenance, especially if nozzles need to be replaced. In comparison to orifices, nozzles have significantly more energy recovery because the fluid passes through the more gradual restriction (ASHRAE, 2013c). Automotive mass airflow sensors are a promising alternative for energetics and metabolism research and control applications (Purswell et al., 2011); however, the technology is not suited for lower-range flows.

Table 3.1. Application limitations for commercially and non-commercially available sub-550 lpm flow measurement instruments include cost (especially when multiple devices are required), and lack of calibration certification and traceability. Custom orifice meters were less accurate than other flowmeters but featured a traceable, statistical approach to quantifying the accuracy and lower cost than most other options.

Flowmeter (gas)	Model	Range (lpm)	Operating pressure (kPa)	Approximate cost (USD)	Stated accuracy
Orifice meter (UIUC)	Custom	279 - 510	0 - 0.65	250 ^[1]	< ±5% FS
Variable area rotameter ^[2]	VFC-121	113 - 708	< 689	80	±2% FS
Automotive mass airflow sensor ^[3]	Hot wire	> 833	0	< 200	±1% FS
Orifice plate ^[2]	PE-F-1	< 592	0	250	±0.6% FS
Venturi meter ^[2]	VFLO w/ gauge	0 - 566	0 - 2.49	538	±2.5% FS
Thermal mass flowmeter ^[2]	GFC-1144	< 500	34.4 - 413.7	1805	±1.5% FS
Vortex shedding ^[4]	FV-520C-F-D	115 - 803	4.6	2897	±1% RS

^[1] Cost includes materials and approximate labor cost of a student

^[2] Dwyer Instruments, Inc., Michigan City, IN, USA

^[3] Purswell et al., 2011

^[4] Omega Engineering, Inc., Stamford, CT, USA

Custom-designed orifice meters are a viable option when supply static pressure, accuracy, cost, installation, and maintenance are considered together. They can be sensitive to downstream and upstream system pressure variations, but this problem can be overcome by calibrating with a similar supply static pressure and replicating the ventilation system. Material cost and availability are critical design and construction constraints, with procurement time reduced by using available or local materials. Final cost of materials including labor (estimated at \$20 h⁻¹)

was approximately \$250 and took about 5 h to construct per orifice meter. Limitations of orifice meters include the irrecoverable energy loss from the fluid when passing through the orifice and the previously mentioned sensitivity to installation conditions. Additionally, fluid composition and corrosiveness may wear or damage the edge of the orifice over time, degrading the accuracy of measurement (ASHRAE, 2013a). None of these factors presents a serious concern in low flow and low operating pressure applications such as indirect calorimeters or respiration chambers for animals, and these meters can be useful as a primary measurement device.

Owing to their simplicity and relatively low cost, orifice meters are widely used in industries and applied to a wide range of liquids and gases. A variety of instruments such as a manometer or pressure transducer can be used to measure differential pressure across the orifice plate. Flow range is dependent on the pipe, orifice diameter, and the type of fluid, with a typical accuracy of 1% to 5% at maximum flow (ASHRAE, 2013c). Materials for custom orifice meters not adhering to certified standards are readily available, inexpensive, and their application to animal emission studies are often overlooked. Calibration coupled with uncertainty analysis is essential, and the procedures for design, construction, calibration, and application of the custom flowmeter must be documented.

The objectives of this paper are to:

1. Design an economic orifice meter applicable to low ventilation (< 550 lpm) and low static pressure (< 1.742 kPa) systems
2. Document a novel orifice meter calibration procedure that replicates operating conditions of the application
3. Quantify combined and expanded standard uncertainty associated with volumetric flowrate measurements

3.3 Materials and Methods

Six orifice meters were designed, constructed, and calibrated to measure and control ventilation rate at the inlet of each chamber in an open-circuit respiration system. The combination of low static pressure of the blower and total ventilation system pressure loss prevented the use of flowmeters that require a minimum backpressure to operate (i.e. rotameters) as elaborated in the previous sections. High retail cost of alternative flowmeters with sufficient accuracy was also a critical factor in selecting this approach. More details regarding the design, construction, and calibration of these orifice meters can be found elsewhere (Ramirez et al., 2013; Ramirez, 2014).

3.3.1 Ventilation System Description

Air was supplied to the orifice meters by a common radial blade blower (1.12 kW (1½ hp); Model PW11, Peerless Blowers, Hot Springs, NC, USA). Maximum static pressure of the blower was 1.742 kPa (7 in. H₂O); therefore, differential pressure across any in-line flowmeter could not equal or exceed 1.742 kPa (7 in. H₂O). A manifold distributed air from the blower to each of the six orifice meters.

3.3.2 Orifice Meter Design

Orifice meters were designed to accurately provide a controlled ventilation rate to each of the six open-circuit ventilated hood-type chambers, as estimated based on minimum animal ventilation requirements (Maia et al., 2014). This design flow range of 279 to 510 lpm was used to calculate orifice meter dimensions and parameters. Theoretical flow through an orifice is a function of orifice diameter, pipe diameter, moist air density, and static pressure drop across the orifice plate (Equation 38; ASHRAE, 2013c). A 51 mm (2 in.) diameter PVC pipe was selected for low-cost and availability and a 20.6 mm (13/16 in.) orifice diameter was selected to ensure

existence of a fully developed turbulent flow regime with constant discharge coefficient throughout the intended operating flow range (ASHRAE, 2013b). Entrance section of the pipe was specified as 10 times the pipe diameter, or 508 mm (20 in.) to ensure fully developed flow entering the orifice (ASME, 2004). Similarly, the minimum allowable exit section length was 5 times the pipe diameter, or 254 mm (10 in.) (Figure 3.1; Table 3.2).

Table 3.2. Orifice meter design dimensions label correspond to the selected orifice meter design (Figure 3.1). Design flowrate dictated the parameters and dimensions of the orifice meter. A constant discharge coefficient (0.6806) was obtained by optimizing pipe diameter, orifice diameter, and flowrate.

Dimensions			
Label	Design	Value	Unit
A	Orifice diameter	20.6 (13/16)	mm (in)
B	Pipe diameter	50.8 (2)	mm (in)
C	Entry pipe length	508 (20)	mm (in)
D	Exit pipe length	254 (10)	mm (in)
E	Flange tap diameter	1.588 (1/16)	mm (in)
F	Orifice plate thickness	3.175 (1/8)	mm (in)
Parameters			
	Flowrate	279 - 510 (9.9 - 18)	lpm (cfm)
	Reynolds number	7301 - 13142	-
	Discharge coefficient	0.6806	-
	Differential pressure	0.12 - 0.36 (0.5-1.47)	kPa (in. H ₂ O)
	Beta ratio	0.40625	-

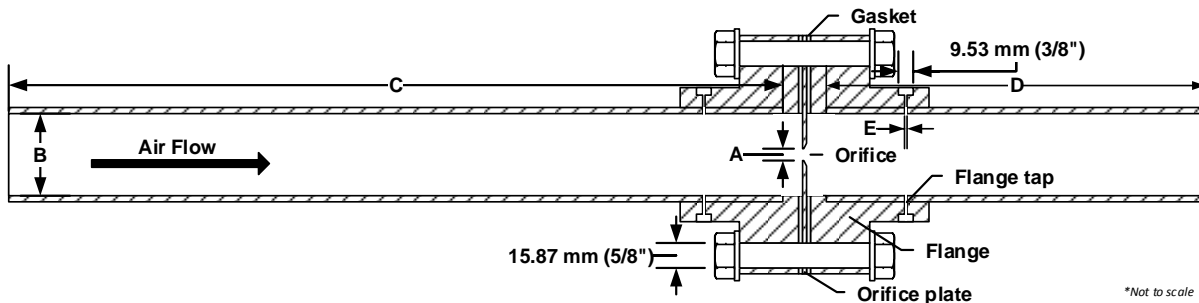


Figure 3.1. Orifice meter construction with labels A-F previously defined (Table 3.2). Flange taps were spaced evenly around the flange neck on the upstream and downstream sides of the orifice plate, four in each side for composite differential pressure measurement. Barbed fittings were secured in each tap for pressure measurement.

3.3.3 Orifice Meter Construction

A 3.175 mm (1/8 in.) acrylic orifice plate was sealed with a rubber gasket and silicone between two thick-walled easy align Schedule-80 PVC flanges (4881K236, McMaster-Carr Supply Company, Elmhurst, IL, USA). A 20.6 mm (13/16 in.) diameter concentric orifice with a 45-degree bevel was partially bored into the one side (downstream) of each of the six orifice plates. Orifice plates were mounted between flanges with the flat edge of the orifice facing upstream. The entrance pipe section was glued into the upstream flange while the exit pipe section was glued to the downstream flange. Four flange taps distributed uniformly around the flange circumference were placed on the upstream side and another four on the downstream side to measure pressure differential across the orifice plate (Figure 3.1) per design requirements (ASME, 2004) and were connected simultaneously to obtain a single composite measurement. Composite static pressures on the upstream and downstream sides of the orifice plate were measured with an inclined-vertical oil manometer (resolution = 0.1 in. H₂O (24.9 Pa), Series Mark II, Dwyer Instruments, Inc., Michigan City, IN, USA). A 50.8 mm (2 in.) PVC ball valve was installed on the upstream side and used for flow control through the orifice. Further details of the orifice meter construction can be found in Ramirez (2014).

3.3.4 Calibration Reference Chamber-Nozzle Airflow System

The Chamber-Nozzle Airflow System (CNAS, Figure 3.2) used as the reference standard in this work consisted of an entry chamber with internal dimensions (LxWxH) of 1210 mm x 610 mm x 610 mm (48 in. x 24 in. x 24 in.) and an exit chamber 910 mm x 610 mm x 610 mm (36 in. x 24 in. x 24 in.) with a conical reduction for attachment to the orifice meter. The entry chamber included a 101.6 mm (4 in.) diameter iris valve for flow regulation. A 19.05 mm (3/4 in.)

diameter nozzle (Helander Metal Spinning Company, Lombard, IL, USA) was sealed between the entry and exit sections (Figure 3.2).

Fittings and hoses used to integrate the orifice meter into the REMS ventilation system were also used during calibration to replicate similar pressure and flow conditions. Three metal grates in the entry section of the well-sealed calibration chamber served as flow straighteners to form fully developed flow and stabilize pressure measurements during calibration data collection (ASME, 2004). The nozzle was mounted in the center of a 19.05 mm (3/4 in.) piece of plywood and secured between the entry and exit chambers by 12 C-clamps (three on each side) to reduce leaks on both upstream and downstream side. Four pressure taps (one on each side) were placed on the upstream entry chamber and four on the exit chamber downstream of the nozzle. The inclined-vertical oil manometer was connected to the four taps at each section to measure the composite pressure drop (Figure 3.2). Air is a compressible fluid, so a conic reduction from the 14630 mm² (576 in.²) exit chamber to the 506.7 mm² (0.785 in.²) rubber hose to minimized pressure build up at the nozzle. Backpressure upstream of the hose may potentially cause error in flowrate calculation by affecting the pressure differential at both the nozzle and orifice plate.

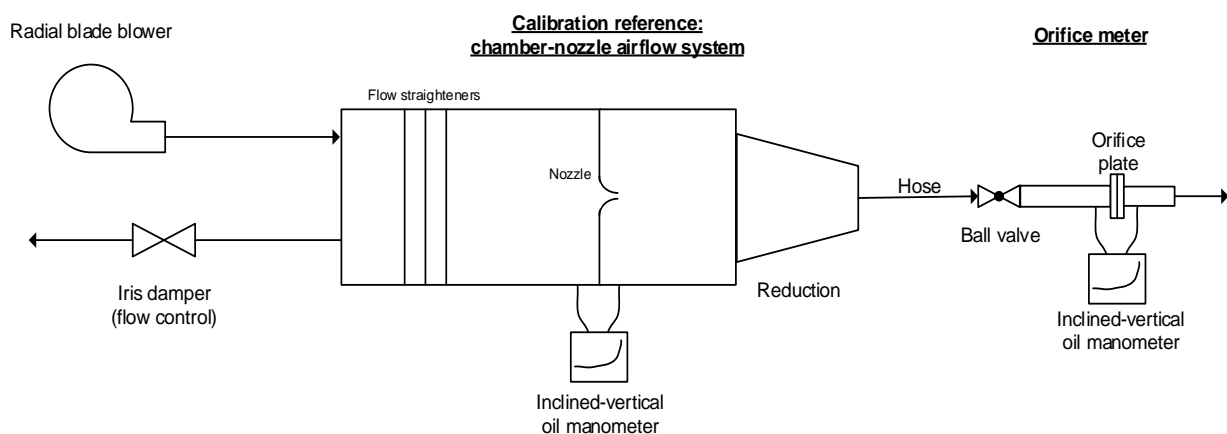


Figure 3.2. Orifice meter calibration was performed using Chamber-Nozzle Airflow System (CNAS) set-up as shown above. Air from a blower was conditioned through mesh grate flow straighteners in the entry section and flowrate is regulated with iris damper. Flowrate was calculated based on air density and differential pressure across the nozzle.

3.3.5 Orifice Meter Calibration

Calibration of the orifice meters was performed using the CNAS calibration reference described in the previous section to provide a flowrate range of approximately (mean \pm standard deviation) 299.2 ± 13.9 to 506.4 ± 2.5 lpm (10.6 ± 0.5 to 17.9 ± 0.1 cfm). Temperature and relative humidity (Hygropalm 23, Rotronic Instrument Corp., Hauppauge, NY, USA) were recorded before and after calibration to calculate air density (Albright, 1990). Barometric pressure was determined as a function of altitude (ASHRAE, 2013a). Pressure differentials across the nozzle and the orifice meter were recorded for 21 different flowrates in the following order: ten increasing flowrates [min = 279.2 lpm (9.8 cfm); max = 505.4 lpm (17.8 cfm)], ten decreasing flowrates [min = 279.2 lpm (9.6 cfm); max = 505.4 lpm (17.8 cfm)], and one maximum flowrate overall [min = 501.7 lpm (17.7 cfm); max = 509.5 lpm (17.9 cfm)], to account for hysteresis.

Data were analyzed using the statistical and regression fitting procedures of OriginPro 9.0 (OriginLab, Northampton, MA, USA). Calibration curves were generated from the calibration reference flow (independent variable) and the theoretical orifice meter flow (ASHRAE, 2013b). Calibration reference flowrate was calculated as a function of the discharge coefficient for the nozzle, expansion factor, nozzle diameter, moist air density, and differential pressure (AMCA/ASHRAE, 2007). A linear regression was fit to each calibration curve shown by Equation 3.1.

$$Q_{theoretical} = c Q_{ref} \quad (\text{Equation 3.1})$$

where

- $Q_{theoretical}$ = orifice meter theoretical flowrate ($\text{m}^3 \text{s}^{-1}$; ASHRAE, 2013c)
- c = regression coefficient (slope) specific to individual orifice meter (dimensionless)
- Q_{ref} = calibration reference flowrate at calibration conditions ($\text{m}^3 \text{s}^{-1}$; AMCA/ASHRAE, 2007)

A unique slope was determined for each orifice meter (Equation 3.1). This approach of linear regression between theoretical and reference flowrates, rather than a nonlinear regression of parameters in the theoretical flow calculations, allows for a means of quantifying measurement precision using linear regression statistics, and removal of systematic bias by using the slope of the regression.

To apply the calibration to subsequent flow measurements, Equation 3.1 was inverted (Equation 3.2). The best estimate of flowrate ($Q_{predicted}$) corresponding to any theoretical orifice meter flowrate can be determined from Equation 3.2:

$$Q_{predicted} = c^{-1} Q_{theoretical} \quad (\text{Equation 3.2})$$

where

$Q_{predicted}$ = predicted (actual) moist air ventilation rate at field conditions for future measurements ($\text{m}^3 \text{s}^{-1}$)

A measure of uncertainty in the resultant predicted ventilation rate measurement ($Q_{predicted}$) is defined as the standard error of inverse prediction SE(IP) and is the standard error (SE) of Equation 3.2, which in turn is the SE of $Q_{theoretical}$ (Equation 3.1) divided by the slope, c as shown in Equation 3.3 (Doebelin, 1968):

$$SE(IP) = SE(Q_{theoretical}|Q_{ref}) = c^{-1} SE(Q_{ref}|Q_{theoretical}) \quad (\text{Equation 3.3})$$

where

$SE(IP)$ = standard error of inverse prediction for predicted moist air ventilation rate ($\text{m}^3 \text{s}^{-1}$)

This novel calibration approach directly quantifies measurement uncertainty and removes system bias; further, since calibration is not performed at standard conditions (e.g. 273.15 K and 101.325 kPa), when the orifice meter is used at conditions other than those at calibration, the effects of temperature and pressure are captured by the orifice meter theoretical flow equation. This method incorporates changes in air density at operating conditions and relates them to the actual flowrate at those conditions.

3.3.6 Orifice Meter Flowrate Standard Uncertainty

To quantify the overall uncertainty associated with the ventilation rate measurements ($\Delta Q_{predicted}$), the standard uncertainty of key input measurements must be determined (ISO/IEC, 2008). The standard uncertainty (denoted by Δ) is a statistically based approximation of measurement error (Taylor & Kuyatt, 1994). In order to develop a method for estimating the standard uncertainty of a flow “measurement” which is itself also dependent on differential pressure and moist air density, these other measurements’ standard uncertainties are needed. Dry-bulb temperature standard uncertainty and relative humidity standard uncertainty (Equation 3.4) were determined from the manufacturer’s Non-Traceable Accuracy (NTA):

$$\Delta T, \Delta RH = \frac{NTA_j}{d} \quad (\text{Equation 3.4})$$

where

- j = temperature, relative humidity
- ΔT = dry-bulb temperature standard uncertainty (K or °C)
- ΔRH = relative humidity standard uncertainty (%)
- $NTA_{\Delta T}$ = temperature non-traceable accuracy (± 0.5 ; K or °C; normal distribution)
- $NTA_{\Delta RH}$ = relative humidity non-traceable accuracy (± 1 ; %; normal distribution)
- d = probability distribution (rectangular = $\sqrt{3}$; normal = 1)

The standard uncertainty of moist air density ($\Delta\rho_{ma}$) was calculated (Equation 3.5) by propagating the uncertainty of temperature and relative humidity measurement in the psychrometric equations (Albright, 1990). Barometric pressure was a negligible source of error when compared to the uncertainty associated with temperature and relative humidity.

$$\Delta\rho_{ma} = \sqrt{\left(\frac{\partial\rho_{ma}}{\partial T}\Delta T\right)^2 + \left(\frac{\partial\rho_{ma}}{\partial RH}\Delta RH\right)^2} \quad (\text{Equation 3.5})$$

where

- $\Delta\rho_{ma}$ = moist air (ma) density combined standard uncertainty ($\text{kg}_{ma} \text{m}^{-3}$)

Differential pressure standard uncertainty [$\Delta(\delta P_{OM})$] was determined (Equation 3.6) from the manufacturer’s NTA and the reading scale resolution of the instrument. A rectangular

distribution (divisor of $\sqrt{3}$) was associated with the NTA and reading scale resolution because probability is assumed constant over the given range and zero elsewhere (Taylor & Kuyatt, 1994).

$$\Delta(\delta P_{OM}) = \sqrt{\left(\frac{NTA}{d}\right)^2 + \left(\frac{Res}{d}\right)^2} \quad (\text{Equation 3.6})$$

where

- $\Delta(\delta P_{OM})$ = differential pressure combined standard uncertainty (Pa)
- NTA = manufacturer's non-traceable accuracy ($\pm 3\%$ of FS, FS = 747.5 Pa; rectangular distribution)
- Res = reading scale resolution of the manometer (half of the smallest reading scale division = 12.6 Pa; rectangular distribution)
- d = probability distribution (rectangular = $\sqrt{3}$; normal = 1)

Orifice meter combined standard uncertainty (Equation 3.7) was determined from the root-sum square of the following terms: SE of inverse prediction [$SE(IP)$] and slope SE (Δc) from the linear regression analysis, the differential pressure measurement standard uncertainty, and moist air density standard uncertainty at experiment conditions. Propagation of these terms from the theoretical orifice meter flow equation (Equation 38; ASHRAE, 2013c) combines according to:

$$\Delta Q_{predicted} = \sqrt{[SE(IP)]^2 + \left(\frac{\partial Q_{predicted}}{\partial \rho_{ma}} \Delta \rho_{ma}\right)^2 + \left(\frac{\partial Q_{predicted}}{\partial \delta P_{OM}} \Delta(\delta P_{OM})\right)^2 + \left(\frac{\partial Q_{predicted}}{\partial c} \Delta c\right)^2} \quad (\text{Equation 3.7})$$

where

- $\Delta Q_{predicted}$ = moist air ventilation rate combined standard uncertainty ($\text{m}^3 \text{s}^{-1}$)
- Δc = slope SE from calibration (dimensionless; normal distribution)

Partial derivatives represent the sensitivity coefficients for each input parameters and quantify how ventilation rate combined standard uncertainty changes with variations of its inputs (ISO/IEC, 2008). To provide an approximately 95% level of confidence, a coverage factor (k) of two, was applied to moist air ventilation rate combined standard uncertainty (Taylor & Kuyatt, 1994).

3.4 Results and Discussion

A unique calibration curve was generated for each orifice meter (Table 3.3; Figure 3.3). Calibration was performed once for each of the six orifice meters, as calibration does not require replicates (AMCA/ASHRAE, 2007). No hysteresis was observed in any of the orifice meter calibrations. Linear regression slope (\pm SE) varied from 0.9244 (\pm 2.48 E-03) to 1.0699 (\pm 2.50 E-03). Coefficients of determination (R^2) from the linear regression were greater than 0.99 for each calibration curve. The SE(IP) provided an idea of the overall uncertainty over the range of calibration, and the slope SE provided insight into whether it is different from unity. At the 95% confidence level, the slope was found to be significantly different from unity for each orifice meter, suggesting that individual calibration was justified and required. At a nominal 500 lpm (17.6 cfm), absolute measurement standard uncertainty ranged from 9.22 to 12.32 lpm (0.32 to 0.43 cfm) for all orifice meters, and when expressed on a relative basis, with an applied coverage factor of two, standard uncertainty ranged from 3.6% to 4.9%. Thus, the orifice meters performed consistently well.

Differential pressure measurement standard uncertainty contributed from 98% to > 99% of the total combined standard uncertainty (Equation 3.6) associated with flowrate measurement. The slope SE contributed less than 2% while the moist air density and SE(IP) each contributed less than 1% to combined standard uncertainty for all orifice meters. The combined standard uncertainty can be substantially decreased if a more accurate instrument was used to measure the differential pressure during calibration. When using commercial or custom flowmeters, it is important to check and include the contribution of the standard uncertainty from the measurement device, (i.e. manometer, pressure transducer, gages, etc.) associated with the flowmeter.

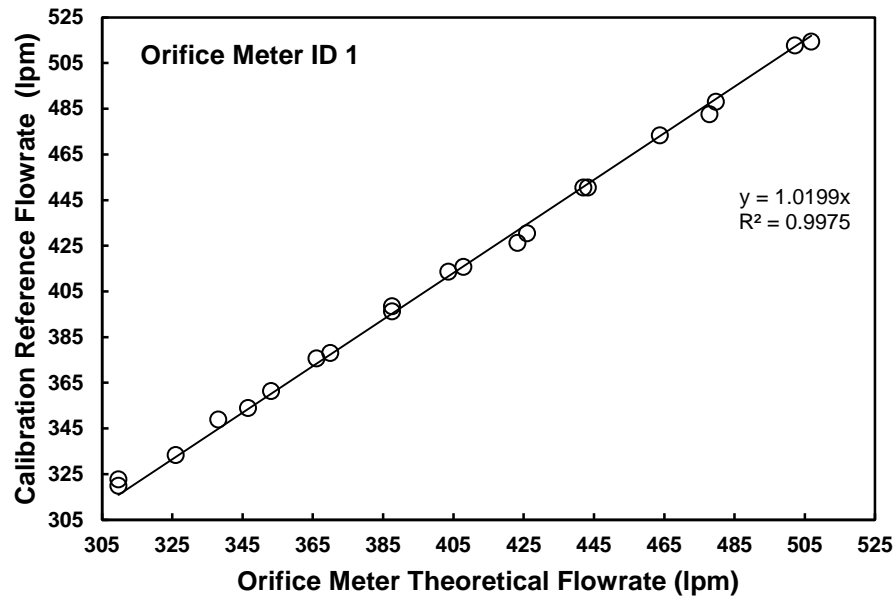


Figure 3.3. Example of Orifice Meter ID 1 calibration curve with linear regression between the theoretical orifice meter flowrate (x) and calibration reference flowrate (y). Linear regression was forced through zero as no flow at the calibration reference should result in zero flow at the orifice meter. The calibration curve is inverted to obtain the predicted ventilation rate (x) using the calculated theoretical flowrate at the predicted operating conditions.

Table 3.3. Summary of ventilation rate measurement uncertainty analysis and calibration linear regressions for each orifice meter. Results showed each one performed differently; thus, each one required individual calibration. Relative error at 500 lpm (17.65 cfm) was very small and indicated an accurate calibration. At the 0.05 confidence level, the slope is significantly different from one for all individually-tested orifices.

Orifice meter ID	Calibration regression parameters			Absolute standard uncertainty		$Q_{predicted}$ combined standard uncertainty (Equation 3.7) at nominal 500 lpm (17.65 cfm)		
	Slope, $c^{[1]}$	SE of c (Δc) ^[1]	SE(IP) (lpm)	$\Delta\rho_{ma}$ (kg m^{-3})	$\Delta(\delta P_{OM})$ (Pa)	Absolute (lpm)	Relative (%)	Expanded ^[2] (%)
1	1.0199	1.62E-03	0.1068	2.68E-03	14.85082	10.11	2.02	4.05
2	0.9650	1.59E-03	0.1035	2.57E-03	14.85082	11.27	2.25	4.50
3	0.9735	1.57E-03	0.1024	2.68E-03	14.85082	11.08	2.22	4.43
4	0.9244	2.48E-03	0.1604	2.68E-03	14.85082	12.32	2.46	4.92
5	0.9865	2.71E-03	0.1730	2.69E-03	14.85082	10.84	2.17	4.33
6	1.0699	2.50E-03	0.1629	2.69E-03	14.85082	9.22	1.84	3.68

^[1] Dimensionless unit

^[2] Relative expanded uncertainty assumes a coverage factor (k) of 2 (approximately 95% C.I.)

Direct use of the theoretical orifice meter flowrate (ASHRAE, 2013b) without calibration is valid when it precisely follows design and construction procedures (ASME, 2004); nevertheless, it does not account for the independent assessment of flowrate uncertainty for each device, the role of temperature and humidity measurements, nor the contribution of the differential pressure measurement. Construction materials, dimensions, and fabrication methods for each orifice

meter were similar, but they were individually calibrated to account for variations among them. For example, the drilling and beveling of the orifice in the orifice plate is a task difficult to replicate identically.

3.5 Summary and Conclusions

Custom orifice meters were successfully designed, fabricated, and calibrated for use with an operating flow range of 279 to 510 lpm (9.9 to 18 cfm) as needed in livestock energetics or emissions studies. Six orifice meters were fabricated from acrylic plates with a 20.6 mm (13/16 in.) concentric orifice and mounted between flanges with two PVC pipe sections. This assembly is a key component in an open-circuit respiration chamber system to measure inlet ventilation rate and can be removed for calibration or replacement. Construction costs were reduced using commonly available and inexpensive materials; consequently, this approach introduced some variability between orifice meters.

A reference system was constructed for calibration purposes by using a reliable and stable flow nozzle upstream of the custom designed and constructed orifice meters. All orifice meters exhibited a significant linear relation between theoretical flowrate and actual flowrate. Each orifice meter was found to require an individual calibration curve for best accuracy. Linear regression slope (\pm SE) varied from 0.9244 (\pm 2.48 E-03) to 1.0699 (\pm 2.50 E-03) for all six orifice meters. The SE of inverse prediction from each regression provides an idea of the overall uncertainty over the range of calibration. At a nominal 500 lpm (17.65 cfm), the absolute standard uncertainty ranged from 9.22 to 12.32 lpm (0.32 to 0.43 cfm). Relative flowrate standard uncertainty with an applied coverage factor of two (approximately 95% C.I.) ranged from 3.6% to 4.9% at the nominal 500 lpm (17.65 cfm). The oil manometer used for the differential pressure measurement was found to contribute from 98% to >99% of the combined

standard uncertainty associated with ventilation rate measurement. A comprehensive error analysis of these flowmeters and associated instruments was shown to be useful for quantifying the measurement uncertainty. Custom designed, constructed, and calibrated orifice meters can provide a cost effective method of measuring volumetric flowrate in low flow and low upstream static pressure research applications such as calorimeters and respiration chambers.

3.6 Acknowledgements

This research was supported with funding provided by the Dudley Smith Initiative, University of Illinois College of ACES and the Office of Research, University of Illinois College of ACES. The authors would like to acknowledge the contributions of graduate students Jacob Segers and Yi Sun, and undergraduate student Kellie Kroscher during the preparation and completion of this work.

3.7 References

- Albright, L. D. (1990). *Environment control for animals and plants*. American Society of Agricultural Engineers.
- AMCA/ASHRAE. (2007). *ANSI/AMCA standard 210-07/ANSI/ASHRAE standard 51-07, laboratory methods of testing fans for certified aerodynamic performance rating*. Arlington Heights, IL: Air Movement and Control Association/American Society of Heating, Refrigerating and Air-Conditioning Engineers.
- ASHRAE. (2013a). Chapter 1: Psychrometrics. In M. S. Owen (Ed.), *Handbook of fundamentals*. Atlanta, GA: American Society of Heating, Refrigerating and Air-Conditioning Engineers.
- ASHRAE. (2013b). Chapter 3: Fluid flow. In M. S. Owen (Ed.), *Handbook of fundamentals*. Atlanta, GA: American Society of Heating, Refrigerating and Air-Conditioning Engineers.

- ASHRAE. (2013c). Chapter 36: Measurement and instruments. In M. S. Owen (Ed.), *Handbook of fundamentals*. Atlanta, GA: American Society of Heating, Refrigerating and Air-Conditioning Engineers.
- ASME. (2004). Section 4: Orifice meters. *ASME flow measurement standard PTC 19.5*. New York, NY: American Society of Mechanical Engineers.
- Calvet, S., Gates, R. S., Zhang, G., Estellés, F., Ogink, N. W. M., Pedersen, S., & Berckmans, D. (2013). Measuring gas emissions from livestock buildings: A review on uncertainty analysis and error sources. *Biosystems Engineering*, *116*(3), 221-231. doi:10.1016/j.biosystemseng.2012.11.004.
- Derno, M., Elsner, H. G., Paetow, E. A., Scholze, H., & Schweigel, M. (2009). Technical note: A new facility for continuous respiration measurements in lactating cows. *Journal of Dairy Science*, *92*(6), 2804-2808. doi:10.3168/jds.2008-1839.
- Doebelin, E. O. (1968). *Measurement systems*. McGraw-Hill Education.
- Gates, R. S., Casey, K. D., Xin, H., & Burns, R. T. (2009). Building emissions uncertainty estimates. *Transactions of the ASABE*, *52*(4), 1345-1351.
- Hellwing, A. L. F., Lund, P., Weisbjerg, M. R., Brask, M., & Hvelplund, T. (2012). Technical note: Test of a low-cost and animal-friendly system for measuring methane emissions from dairy cows. *Journal of Dairy Science*, *95*(10), 6077-6085.
- ISO/IEC. (2008). *Uncertainty of measurement: Part 3. guide to the expression of uncertainty in measurement (GUM:1995) (ISO Guide 9803:2008(E). ed.)*. Geneva, Switzerland: International Standards Organization.

- Maia, G. D. N., Ramirez, B. C., Green, A. R., Rodriguez, L. F., Segers, J. R., Shike, D. W., & Gates, R. S. (2014). A novel ruminant emission measurement system: Part I-design evaluation and description. *Submitted to Transactions of ASABE*.
- Maia, G. D. N., Ramirez, B. C., Green, A. R., Sun, Y., Rodriguez, L. F., Shike, D. W., & Gates, R. S. (2014). A novel ruminant emission measurement system: Part II-commissioning. *Submitted to Transactions of ASABE*.
- Nienaber, J. A., & Maddy, A. L. (1985). Temperature controlled multiple chamber indirect calorimeter-design and operation. *Transactions of the American Society of Agricultural Engineers*, 28(2), 555-560.
- Pinares-Patiño, C. S., & Waghorn, G. C. (Eds.). (2012). *Technical manual on respiration chamber designs*. Wellington, New Zealand: Ministry of Agriculture and Forestry.
- Powers, W. J., Zamzow, S. B., & Kerr, B. J. (2007). Reduced crude protein effects on aerial emissions from swine. *Applied Engineering in Agriculture*, 23(4), 539-546.
- Price, J. E., & Lacey, R. E. (2003). Uncertainty associated with the gravimetric sampling of particulate matter. *American Society of Agricultural Engineers Annual International Meeting 2003*, ASAE Paper No. 034116.
- Purswell, J. L., Adams, W. C., Montross, M. D., & Davis, J. D. (2011). Evaluation of automotive mass airflow sensors for animal environment research and control applications. *American Society of Agricultural and Biological Engineers Annual International Meeting 2011*, ASABE Paper No: 1110839.
- Ramirez, B. C., Maia, G. D. N., Green, A. R., Shike, D. W., Gates, R. S., & Rodríguez, L. F. (2013). Design and validation of a calibrated orifice meter for sub-500 liter per minute flow

rate applications. *American Society of Agricultural and Biological Engineers Annual International Meeting 2013*, ASABE Paper No. 1618475.

Ramirez, B. C. (2014). *Design and evaluation of open-circuit respiration chambers for beef cattle*. (Masters, University of Illinois at Urbana-Champaign, Department of Agricultural and Biological Engineering).

Taylor, B. N., & Kuyatt, C. E. (1994). *Guidelines for evaluating and expressing the uncertainty of NIST measurement results* (NIST Tech Note 1297 ed.). Gaithersburg, Md: National Institute for Standards and Technology.

Xin, H., & Harmon, J. D. (1996). Responses of group-housed neonatal chicks to posthatch holding environment. *Transactions of the American Society of Agricultural Engineers*, 39(6), 2249-2254.

CHAPTER 4: A NOVEL RUMINANT EMISSION

MEASUREMENT SYSTEM: PART I – DESIGN

EVALUATION AND DESCRIPTION

G.D.N. Maia, B.C. Ramirez, A.R. Green, J.R. Segers, D.W. Shike, L.F. Rodríguez, and R.S.

Gates

A manuscript submitted to *Transactions of ASABE*

This chapter describes the design and uncertainty analysis for six open-circuit, positively pressurized, ventilated hood-type respiration chambers named the Ruminant Emission Measurement System (REMS). The REMS was designed to quantify eructated methane emission from beef cattle and study relationships between methane emissions and nutrition, genetics, and management strategies. The detailed documentation of the design is critical for understanding the sources of uncertainty and reference for future systems. The measurement uncertainty for incoming ventilation rate measurement presented in Chapter 3 combined with the remaining sources in the REMS and propagated through the Emission Rate equation. The standard uncertainty associated with ER is the best estimate of the confidence in a measured ER. This work is critical for establishing uncertainty and confidence in emission rates estimated by the chamber technique.

This chapter owes its success to the combined efforts of Brett Ramirez, Guilherme Maia, Angela Green, Jacob Segers, Daniel Shike, Luis Rodríguez, and Richard Gates. Dr. Maia led the research and developed the uncertainty analysis for the parameters in the emission rate equation.

Mr. Segers aided in the research design, construction and implementation. Drs. Green, Shike, Rodríguez, and Gates contributed to the research design and the draft revision.

My direct contribution to this work included the derivation of the moist air mass flow balance and subsequent gas component mass flow balance to determine the ER quantified by the REMS presented in Section 2.2. A detailed derivation of these equations can be found in Appendix B. The ER equation and mass balance approach are a significant contribution to establishing a documented methodology for open-circuit respiration chambers. In addition, using the equations developed for determining ER standard uncertainty, I designed and executed the sensitivity analysis scenarios outlined in Section 2.5, Section 3.1, and Section 3.2 while providing the analysis. The program used to simulate these scenarios can be found in Appendix C. The sensitivity analysis has several key impacts: (i) provides a holistic approach to understanding critical sources of measurement error propagated through the ER equation, (ii) quantifies anticipated ER standard uncertainty over a range of commonly measured ER values, and (iii) identifies which instruments contribute the greatest to ER standard uncertainty and their subsequent impact on ER standard uncertainty if their uncertainty increases.

4.1 Abstract

Methane (CH₄) generated by cattle is both a major source of greenhouse gas emissions and a powerful indicator of feed conversion efficiency; thus, accurate quantification of CH₄ production is required for addressing future global food security without neglecting environmental impacts. A newly developed Ruminant Emission Measurement System (REMS) supports research on the relationships between bovine nutrition, genetics, and management strategies by measuring eructated CH₄ emissions from ruminal activity. REMS is a substantial improvement and extension of the “chamber technique”, considered the standard method to quantify ruminant CH₄ generation. Part I of this series describes the design of REMS and its design evaluation. An uncertainty analysis of chamber Emissions Rate (ER) was conducted to identify critical measurement component contributions to overall ER uncertainty and guide component selection. In Part II, REMS commissioning was performed and a method for system validation including overall emission uncertainty is reported. REMS consists of six positive pressure ventilated hood-type chambers individually equipped with a thermal environmental control subsystem, fresh air supply control subsystem, and gas sampling subsystem. Estimates of the standard uncertainty for each measurement parameter were quantified and propagated through the ER equation derived from CH₄ and air mass flow balances. A sensitivity analysis was conducted to assess the contribution of each parameter to the combined ER uncertainty under predicted normal operation, by varying gas analyzer and ventilation measurement uncertainties as anticipated with REMS use. Results showed that the expanded uncertainty (~95% confidence interval) associated with the methane ER computation were approximately 5.9% for ERs between 3.5 to 17.2 g h⁻¹. Ventilation rate and gas concentration measurements were the major sources of uncertainty, contributing about 69% and 29% to the uncertainty associated with methane ERs, respectively.

This work provides the foundation for future studies using respiration chambers to include a stated standard uncertainty associated with animal emission measurements.

Keywords: Climate Change, Feeding, Food Security, Methane Production, and Uncertainty.

4.2 Introduction

In 2011, the agricultural sector in the United States contributed to approximately 8.1% of total greenhouse gas emissions (EPA, 2013). Methane (CH₄) produced from enteric fermentation, primarily from beef and dairy cattle, was estimated to account for 23.4% of the total CH₄ emissions in the US (EPA, 2013). Accurate CH₄ emissions quantification has serious implications to ruminant livestock production, to food security, and to the environment (Schmidhuber & Tubiello, 2007; Skoet & Stamoulis, 2006). It is also a critical requirement for evaluating possible mitigation strategies (Makkar & Vercoe, 2007; McGinn, 2006). Process-based CH₄ emission evaluations (Tier 3 methods) using a variety of diets can substantially increase the quality of inventories used to estimate CH₄ global emissions, by providing new variables and information that will affect emission factor estimates currently used in Tier 1 and 2 methods (IPCC, 2006).

Methane is a key parameter to evaluate animal production efficiency (McGinn, 2006). As the global demand for enhanced animal productivity without adversely affecting the environment becomes more prevalent, there is an urgent need to maximize ruminant feed conversion efficiency while accurately quantifying and understanding CH₄ emissions. Cattle enteric and rumen CH₄ production is a result of anaerobic microbial fermentation of hydrolyzed dietary carbohydrates, representing a loss of between 2% and 12% of the gross metabolic energy intake of the animal (Johnson & Johnson, 1995).

The “gold standard” method for animal energetics and metabolism research has been the open-circuit indirect calorimeter and respiration chamber (Bhatta, Enishi, & Kurihara, 2007; Storm, Hellwing, Nielsen, & Madsen, 2012). Chamber techniques measure respiratory gas exchange including the CH₄ production from enteric fermentation, and have better accuracy and precision over alternative methods such as the sulfur hexafluoride (SF₆) tracer gas technique (Grainger et al., 2007; Muñoz, Yan, Wills, Murray, & Gordon, 2012; Pinares-Patiño et al., 2011). Mathematical models are necessary to assess national or global emissions, but accurate extrapolations are limited by accuracy and experimental data from which they are derived (Ellis et al., 2009; Gates, Casey, Wheeler, Xin, & Pescatore, 2008; Storm et al., 2012). Micrometeorological methods for determining grazing animal emissions and CH₄ generation models of ruminal fermentation of feed and feed additives measured by the *in vitro* gas production technique provide reasonable accuracy compared to the chamber technique, but often are difficult to validate and extrapolate (Bhatta et al., 2006; Murray, Moss, Lockyer, & Jarvis, 1999; Tomkins, McGinn, Turner, & Charmley, 2011). Although the chamber technique is considered the reference for ruminant CH₄ emissions measurements, a documented comprehensive error analysis is required for understanding the confidence in this technique (McGinn, 2006).

Few estimates of CH₄ emissions using the chamber technique (either indirect calorimeter or respiration chamber) have included a statement of uncertainty in published results (McGinn, 2006). For a computed quantity based on multiple measurements, such as animal Emission Rate (ER), there are many individual sources of errors often unique to each monitoring system. Methods for instrument calibration combined with total system error evaluation have been documented for the chamber technique. For example, a study provided measurement uncertainty

estimates ranging from 3.45% to 5.58% for an open-circuit indirect calorimeter study (Nienaber & Maddy, 1985), and approximately 7% uncertainty for ER determined from the analysis of ventilation and gas concentration measurement sensitivities (McGinn, Beauchemin, Coates, & Colombatto, 2004). Comprehensive uncertainty analyses are available for other applications, such as gravimetric sampling of particulate matter (Price & Lacey, 2003) and for other animal production systems, including ammonia emissions from field-scale broiler houses (Casey, 2005; Gates, Casey, Xin, & Burns, 2009). A systematic documentation and integrated methodology to assess system uncertainties is needed, especially in animal studies with the chamber technique.

Emission rate uncertainty is a critical design parameter; hence, it should be an integral part of the design analysis of any measurement system used in energetics or metabolism research. A detailed methodology with a worked example to quantify uncertainties associated with the chamber technique is provided here. The goal of this work is to introduce and describe a systematic approach to evaluate the Ruminant Emission Measurement System (REMS), which is an improvement and extension of the chamber technique design methodology. The design phase evaluation applies mathematical relationships and derivations to the system computations and measurements, in turn, guiding subsystem development. In addition, this analysis estimates the combined standard uncertainty associated with ER determined by REMS. To achieve these goals, the objectives of this paper were to:

1. Document REMS design and key REMS subsystems, including characterizing and quantifying instrument standard uncertainty.
2. Derive REMS emission rate equation and its associated combined standard uncertainty.
3. Perform a sensitivity analysis to assess measurement uncertainty contributions relative to ER combined standard uncertainty.

This analysis establishes a well-documented procedure to quantify ER combined uncertainty determined by REMS, and by extension, to the instruments and operation of other respiration chambers and indirect calorimeters. This study precedes part two of this series, in which the system commissioning and performance using measured data were conducted to validate uncertainty estimates and to assess potential systematic errors (Maia, Ramirez, Green, Sun et al., 2014). Separation of design evaluation and commissioning emphasizes the need to first utilize uncertainty analysis to guide the system design and focus methodological assumptions used in the analysis. When applicable, adjustments to the design and analysis using collected empirical information were performed during the commissioning phase.

4.3 Materials and Methods

A detailed description of REMS design was arranged into subsystems and used to identify potential sources of measurement uncertainty. A comprehensive instrument error analysis described the best estimate of standard uncertainties for each measurement used to compute ER. Finally, the measurement uncertainties were propagated to obtain the standard uncertainty associated with ER calculation and utilized in a three-scenario sensitivity analysis with varied (but typical) gas analyzer and ventilation measurement accuracies.

4.3.1 Design and Subsystems

4.3.1.1 Overview

REMS was installed in six of twelve metabolism stalls at the University of Illinois at Urbana-Champaign Beef and Sheep Field Facility, and consisted of four major subsystems: (1) six identical positive pressure Ventilated Hood Chambers (VHC) with an internal volume of approximately 1100 L, capable of enclosing the head and neck of 230 kg to 1000 kg beef

animals, (2) individual Thermal Environmental Control Subsystem (TECS) units used to condition recirculated air for comfort and humidity control for each VHC, (3) Fresh Air Supply and Measurement Subsystem (FASMS) to provide animal fresh air requirements and deliver precisely metered ventilation, and (4) Gas Sampling Subsystem (GSS) to collect gas samples from chambers and the ventilation supply air (background), and to record gas concentrations used in gas emission calculations

A detailed schematic of the instrument and equipment for each component is provided (Figure 4.1) with isometric views of the VHCs with TECS and FASMS components (Figure 4.2). The VHCs, FASMS, GSS collection lines, and pumps are housed in a controlled environment, while personal computer and gas analyzer are in an adjacent room (Figure 4.3). REMS also features an alarm system to alert operators in the event of high CO₂ levels (> 9000 ppm_v) in order to protect operators, maintain animal welfare, and ensure data integrity.

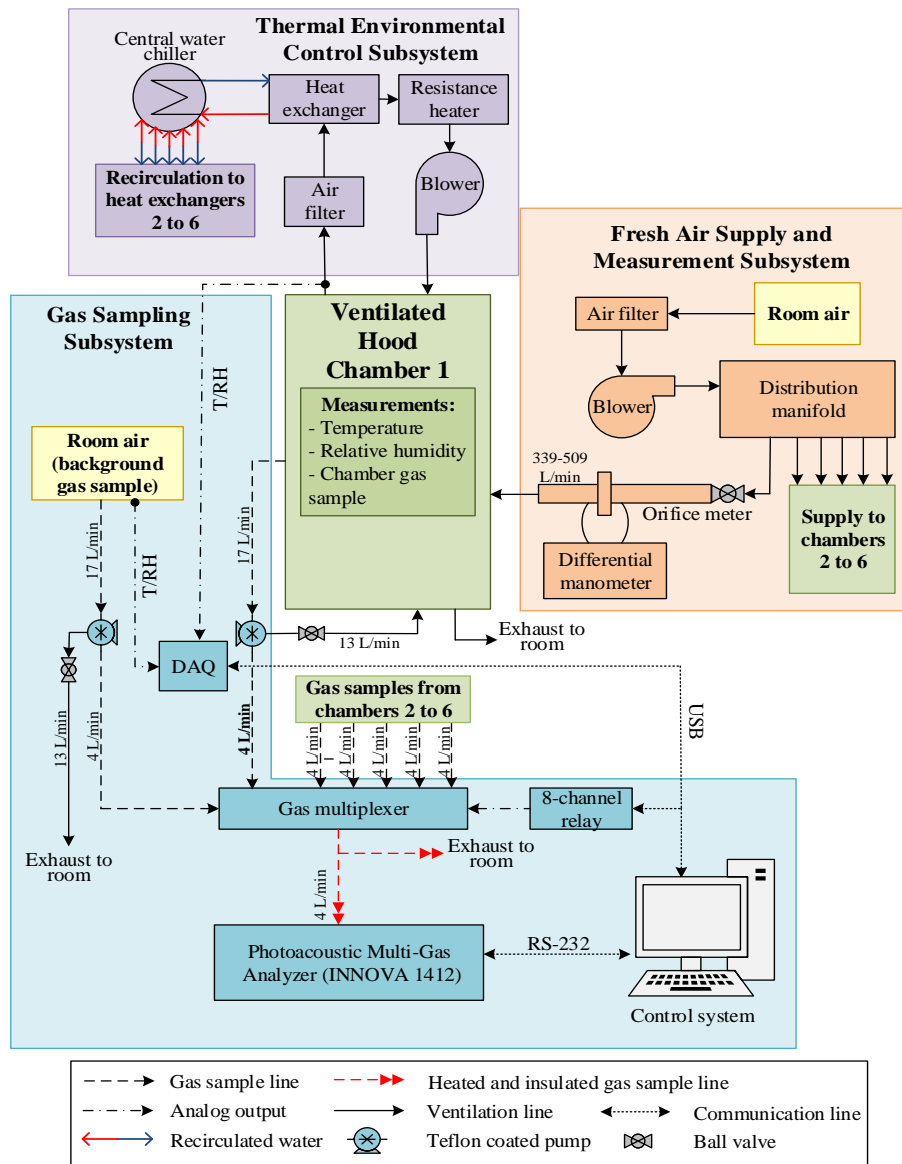


Figure 4.1. Schematic of the ruminant emission measurement system with a detailed subsystem breakdown for one ventilated hood chamber. Six identical chambers are part of the system and each has individual thermal environmental control subsystems (TECS) and fresh air supply and measurement subsystems (FASMS). The central water chiller in the TECS, blower in the FASMS, and gas sampling subsystem (GSS) is connected and integrated with the six chambers.

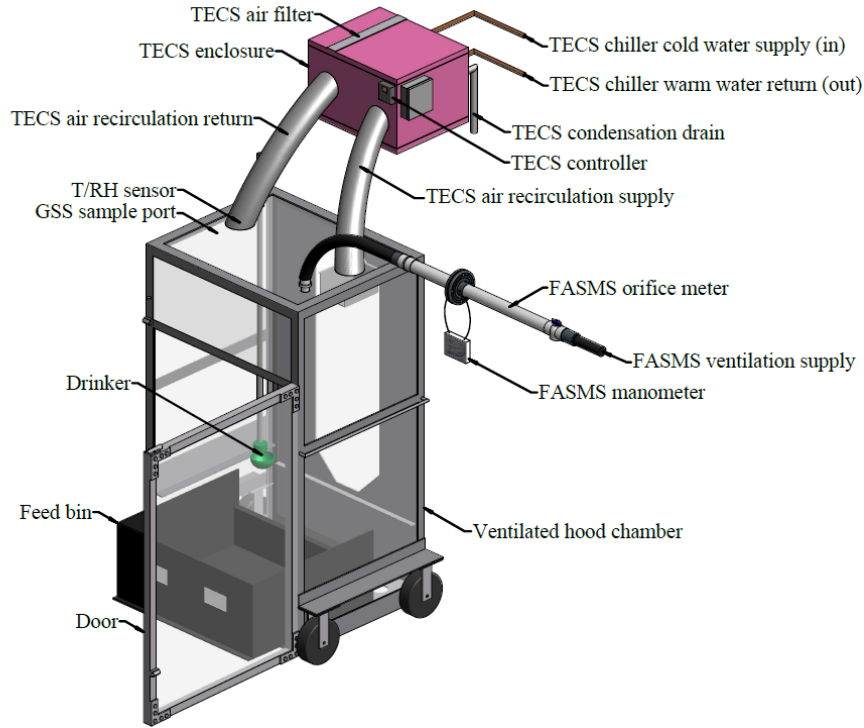


Figure 4.2. Isometric drawing of one ventilated hood chamber with thermal environmental control subsystem (TECS) and fresh air supply and measurement subsystem (FASMS) components. The gas sampling subsystem (GSS) is connected to the gas multiplexer and integrated with the other six ventilated hood chambers (Figure 4.1).

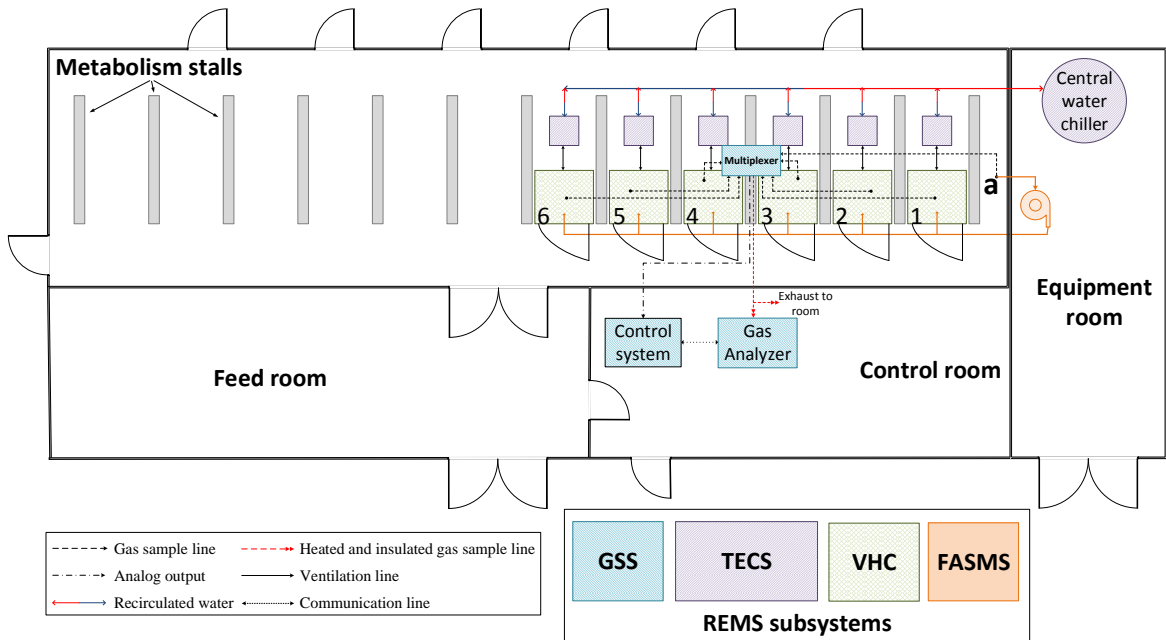


Figure 4.3. Layout of the ruminant emission measurement system with four major subsystems highlighted. (a) Denotes the location of the background gas concentrations, temperature, and relative humidity measurement that is supplied through the fresh air supply and measurement subsystem (FASMS).

4.3.1.2 Ventilated Hood Chambers

The six positively pressurized VHCs were custom assembled to design specifications by ShapeMasters Inc. (Ogden, IL, USA; Figure 4.4). Each VHC featured transparent polycarbonate panels on the sides, top, and bottom, except the back (animal entrance) where aluminum was used (Figure 4.2). Polycarbonate panels were secured in an aluminum frame (80/20, Columbia City, IN, USA) for durability, reduced weight, animal comfort, and safety. Similar chamber design and construction have been reported elsewhere (Kelly, Kerrigan, Milligan, & McBride, 1994; Place, Pan, Zhao, & Mitloehner, 2011; Suzuki, McCrabb, Nishida, Indramanee, & Kurihara, 2007). Openings at the top were added for ventilation and gas sampling ports (Figure 4.2). On the front, a door with a foam tape seal allowed easy access to the removable feed bin (Figure 4.2). The inside of the chamber included a drinker (C20103N, Nasco Inc., Fort Atkinson, WI, USA). Two larger circular holes (0.152 m) on top of the chamber accommodated the TECS recirculation supply and return connected via flexible, insulated 0.1016 m (4 in.) ducts. The FASMS inlet, GSS chamber gas sampling port, a hole for the drinker hose, and excess gas sample return were drilled in the top of the chamber (Figure 4.4-b). Placement of the FASMS inlet and TECS recirculation return promoted the mixing of fresh air by entraining it into the recirculation supply air and using the recirculation return to pull air back to the top. Each chamber was mounted on four casters with wheels for moving into and out of the metabolism stall.

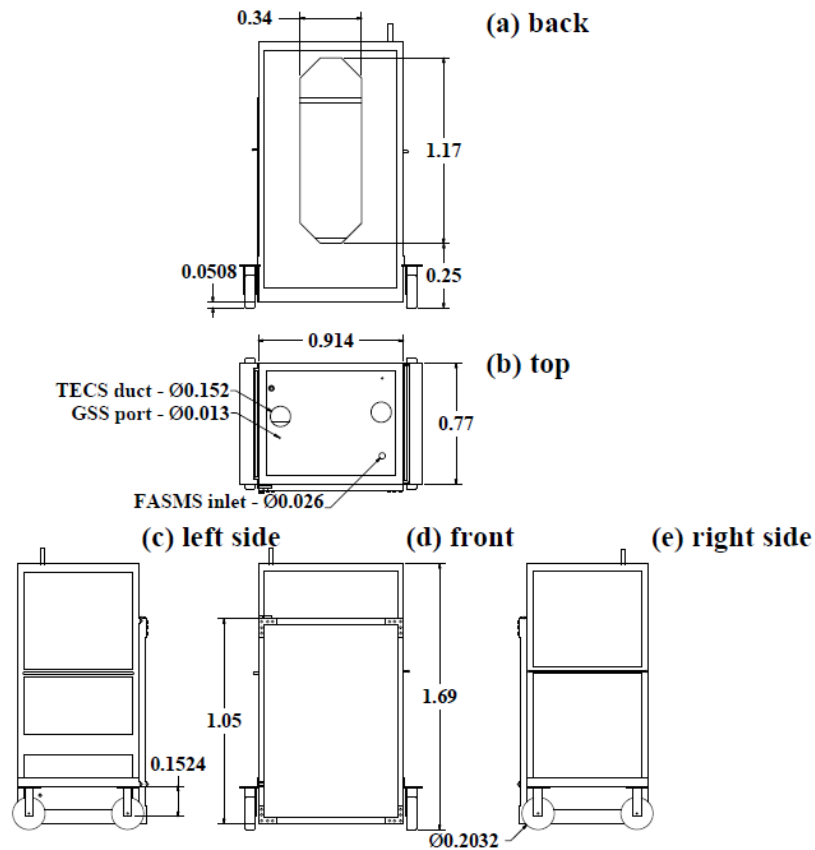


Figure 4.4. Ventilated hood chamber dimensions. Plan views of back (a), top (b), left side (c), front (d), and right side (e) are provided (all units in meters). The animal head and neck accesses the chamber through the back (a). Key inlets and outlets with dimensions for the Fresh Air Supply and Measurement Subsystem (FASMS), Thermal Environmental Control Subsystem (TECS), and Gas Sampling Subsystem (GSS) (b).

The neck stanchion in the existing metabolism stalls was used to restrain the animal and a zippered canvas hood with drawstring was secured around the animal's neck to enclose the space between the chamber opening and the animal's body. The hood was attached to the octagonal opening on the back of chamber (Figure 4.4-a) to minimize potential infiltration into the chamber, which could affect emission calculations. The design allows the animal to stand or lie down for comfort while its head and neck remained inside the chamber.

4.3.1.3 Thermal Environmental Control Subsystem

The thermal environment inside the chamber was regulated by the TECS (Figure 4.1, 4.2, and 4.3). Located above each chamber, a carefully sealed enclosure was made from 2.54 cm (1 in.) rigid foam polystyrene insulation. The enclosure housed a pleated air filter for dust removal, a 750 W electric resistance heater (Model CSF00232, TEMPCO Electric Heater Corp., Wood Dale, IL, USA), a blower (Model 1TDR3, Dayton, USA) for air recirculation and to promote thorough gas mixing, and a 1 kW capacity (750 W sensible and 250 W latent heat) heat exchanger (cooling coil). The blower inside the enclosure recirculated air at a constant rate from the chamber through the filter, heat exchanger, and heater. Water vapor generated by the animal was continuously removed from the airstream by condensation at the heat exchanger. The six heat exchangers utilized supply and return manifolds to circulate chilled water from a central unit with a set-point of 7.2°C (10.6 kW, Koolant Kooler SV3000-W, Dimplex Thermal Solutions, Kalamazoo, MI, USA). The TECS was custom fabricated and installed by Polar Refrigeration, Heating, and Cooling Inc. (Urbana, IL, USA). Capacities for cooling and water vapor removal were estimated slightly beyond the anticipated maximum total heat production of a 1000 kg steer (Albright, 1990). A proportional temperature controller (C450CPN-1C, Johnson Control Inc., Milwaukee, WI, USA) connected to the heat source was programmed to operate between the temperature range of 26°C (heater off) and 16°C (heater on) within the heat exchange enclosure, in order to maintain the desired temperature within the chamber. The programmed temperature range ensured thermoneutral conditions. Thermal control capacity requirements for the TECS were substantially reduced by supplying the chambers with air from the environmentally controlled barn (Figures 4.1 and 4.3).

4.3.1.4 Fresh Air Supply and Measurement Subsystem

The Fresh Air Supply and Measurement Subsystem (FASMS) was uniquely designed to supply continuous fresh air and to positively pressurize the VHCs (Figure 4.1, 4.2, and 4.3), independent of the TECS operation. Many reported applications of the chamber technique as either whole body or ventilated hood-type used negatively pressurized chambers (Bhatta et al., 2007; Hellwing, Lund, Weisbjerg, Brask, & Hvelplund, 2012; McLean & Tobin, 1987; Pinares-Patiño & Waghorn, 2012; Place et al., 2011; Storm et al., 2012). The disadvantages of negatively pressurized chambers include potential unquantified infiltration of gases entering the chamber. By contrast, a positive pressure system has some advantages for gas sampling because chamber leaks occur outwards (from chamber to the room) and pose no risk of unmeasured outside air infiltration, which could result in gas sample dilution (Moody et al., 2008). This configuration prevents gas sample dilution even for high flowrate leakages, and avoids potential uncertainty (primarily as a bias) in emission calculations due to unquantifiable leakage or infiltration. A key requirement is to maintain positive pressure in the VHC to achieve these advantages.

Fresh air was supplied by a radial centrifugal blower (Model PW11, Peerless Blowers, Hot Springs, NC, USA) and distributed to all six chambers by a 7.62 cm (3 in.) PVC pipe manifold. A filter upstream of the blower removed dust and other particles from contaminating the flow meters. The ventilation and recirculation rates were selected to maintain detectable gas concentrations while sustaining acceptable equilibrium CO₂ levels in the chamber. Background gas samples (incoming ventilation air) for gas concentration, temperature, and relative humidity measurement were monitored at the inlet of the blower (in the room; Figure 4.3). The incoming volumetric flow rate for each chamber was measured with custom-made, individually calibrated orifice meters, for which a detailed description of the design, construction, calibration, and

uncertainty analysis was documented elsewhere (Ramirez et al., 2013; Ramirez, 2014; Ramirez et al., 2014).

4.3.1.5 Gas Sampling Subsystem

The Gas Sampling Subsystem (GSS; Figure 4.1, 4.2, and 4.3) of REMS applied similar monitoring practices to those established for U.S. air emissions from feeding operations (Maia, Day V, Gates, & Taraba, 2012; Moody et al., 2008). The GSS was positively pressurized except from the gas sampling port in the chamber to the inlet on the vacuum side of pump; thus, reducing any potential leakage between the VHC and the gas analyzer. A custom gas distribution multiplexer made of a solenoid array and relays controlled the switching of gas samples taken from each chamber and background sampling ports (Sun, 2013). Samples were routed to an infrared photoacoustic spectroscopy multi-gas analyzer (Model 1412, INNOVA, LumaSense Technologies, Inc., Santa Clara, CA, USA) configured with CH₄, CO₂, N₂O, NH₃, and SF₆ optical filters. A Polytetrafluoroethylene coated pump (model EW-79200-30, Cole-Parmer, Inc., Vernon Hills, IL, USA) extracted gas samples at approximately 17 L min⁻¹, with 4 L min⁻¹ routed to the gas analyzer and the remaining 13 L min⁻¹ recirculated to the chamber. After passing through the gas analyzer, samples were exhausted to the room. Custom control system software developed in LabVIEW™ (Version 8.2.1., National Instruments Inc., Austin, TX, USA) interfaced the multiplexer and gas analyzer for real time monitoring of concentration and environmental conditions. Once the control system received a serial input (RS-232) from the gas analyzer, a command to a USB 8-channel relay (USB-ERB08, Measurement Computing Corporation, Norton, MA, USA) sequentially opened each of the seven solenoid valves to direct flow from sampling locations to the gas analyzer. Environmental parameters were also monitored and recorded by the control system with temperature and relative humidity sensors

(HMP60-L, Vaisala, Helsinki, Finland) connected to a data acquisition card (USB-1608G Series, Measurement Computing Corporation, Norton, MA, USA).

For each gas sampling location (chambers and background), ten gas concentration measurements were taken for each of the five gases (CH₄, CO₂, N₂O, NH₃, and SF₆), at a customizable sampling interval dependent upon the Sample Integration Time (SIT) of each gas analyzer optical filter. For the aforementioned configuration, the SITs were 5 s (CH₄), 1 s (CO₂), 1 s (N₂O), 5 s (NH₃), and 1 s (SF₆); thus, taking approximately 43 s per sample to complete (gas analyzer sampling cycle when the five gases are monitored). From the ten gas samples, the first five were discarded (flushing), and the last five were used for analysis. This procedure followed gas sampling protocols developed to guarantee that the response time for each gas was reached (Maia et al., 2012; Sun, 2013).

4.3.2 Emission Rate Calculation

The REMS integrates measurements from numerous instruments to compute animal emission rate. The parameters from these measurements were incorporated into the mass flow balances of the system to derive ER. Moist air (total) and gas component mass flow balances were performed using the chamber as the control volume and assuming steady-state conditions prevailed.

4.3.2.1 Moist Air Mass Flow Balance

In the moist air mass flow balance (Equation 4.1), net animal moist air generation was assumed negligible; thus, the mass flow of incoming air equaled the mass flow leaving the chamber. Moist air density of the mixed air inside the chamber was derived from the measurable parameters of temperature, relative humidity and barometric pressure using psychrometric equations (Albright, 1990). The moist air mass balance resulted in:

$$\dot{V}_{ex} = \dot{V}_{in} \times \left(\frac{\rho_{in}^{ma}}{\rho_{ex}^{ma}} \right) \quad (\text{Equation 4.1})$$

where

- \dot{V}_{ex} = exhaust volumetric flowrate leaking out of the chamber ($\text{m}^3 \text{s}^{-1}$)
- \dot{V}_{in} = incoming moist air ventilation volumetric flowrate ($\text{m}^3 \text{s}^{-1}$)
- ρ_{in}^{ma} = incoming moist air density ($\text{kg}_{da} \text{m}^{-3}$)
- ρ_{ex}^{ma} = exhaust moist air density ($\text{kg}_{da} \text{m}^{-3}$)

4.3.2.2 Gas Mass Flow Balance

The steady-state gas balance was obtained from the difference between the chamber exhaust gas mass flow (\dot{m}_{ex}^{gas}) and incoming gas mass flow (\dot{m}_{in}^{gas}) (Figure 4.5; Equation 4.2). The result of this difference provided gas generation rate \dot{m}_{gen}^{gas} .

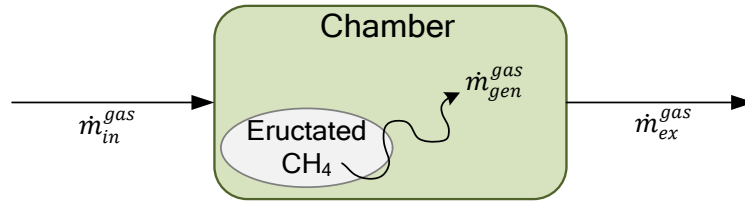


Figure 4.5. Simplified gas component mass balance diagram. The gas represented was methane, but any gas can be used, accordingly.

Isolating for mass flow generated and incorporating measurement parameters yields:

$$\dot{m}_{gen}^{gas} = \underbrace{\left(\dot{V}_{ex} \times C_{ch} \times \frac{M \cdot p_b}{R \cdot T_{ch}} \times 10^{-6} \right)}_{\dot{m}_{ex}^{gas}} - \underbrace{\left(\dot{V}_{in} \times C_{in} \times \frac{M \cdot p_b}{R \cdot T_{in}} \times 10^{-6} \right)}_{\dot{m}_{in}^{gas}} \quad (\text{Equation 4.2})$$

where

- \dot{m}_{gen}^{gas} = generated gas mass flow (g s^{-1})
- C_{ch} = chamber gas concentration (ppm_v)
- C_{in} = incoming background gas concentration (ppm_v)
- T_{ch} = chamber dry-bulb temperature (K)
- T_{in} = incoming background dry-bulb temperature (K)
- M = molecular mass of gas (g mol^{-1})
- p_b = local barometric pressure (98.639 kPa; ASHRAE, 2013)
- R = universal ideal gas constant (8.314; $\text{m}^3 \text{Pa K}^{-1} \text{mol}^{-1}$)

The terms $\frac{M \cdot p_b}{R \cdot T_{ch}} \times 10^{-6}$ and $\frac{M \cdot p_b}{R \cdot T_{in}} \times 10^{-6}$ convert ppm_v (volumetric concentration) into g m⁻³ (absolute units) at the measured conditions. Exhaust gas mass flow is comprised of the exhaust ventilation rate and the concentration of the mixed chamber gas; however, exhaust ventilation rates cannot be measured directly because positive pressure leakages occur in several parts of the chamber (outward direction). Exhaust ventilation rate was determined from other direct measurements after manipulation of measurable parameters. The result of the gas mass flow balance expressed in terms of measurable parameters was obtained with the substitution of Equation 4.1 into Equation 4.2 and simplifying:

$$ER = \dot{m}_{gen}^{gas} = \dot{V}_{in} \left(\frac{\rho_{in}^{ma} C_{ch}}{\rho_{ch}^{ma} T_{ch}} - \frac{C_{in}}{T_{in}} \right) \cdot 10^{-6} \frac{M \cdot P_b}{R} \quad (\text{Equation 4.3})$$

where

ER = animal emission rate derived from the mass balance (g s⁻¹)

The accumulated emission (E , g) is obtained from the integration of the emission rates (Equation 4.3) over the length of the experiment:

$$E = \sum_{i=1}^{n-1} \frac{1}{2} (t_{i+1} - t_i) \times (ER_i + ER_{i+1}) \quad (\text{Equation 4.4})$$

where

E = accumulated emission while the animal is monitored in the chamber (g)
 n = number of emission rate measurements
 t = elapsed time (s)

4.3.3 Emission Standard Uncertainty

The standard uncertainty (denoted by Δ) associated with the computed ER (Equation 4.4) is a statistically based approximation of measurement error obtained from Root-Sum-Square (RSS) of measurement uncertainty sources, which are represented by the parameters in Equation 4.3 (ISO/IEC, 2008; Taylor & Kuyatt, 1994). Barometric pressure, molecular mass, and the universal ideal gas constant were determined to have negligible standard uncertainty; thus,

excluded from the analysis. The physical relationships between measurements and ER (sensitivity coefficients) are signified by the partial derivatives (Taylor & Kuyatt, 1994). A truncated first-order Taylor series approximation, applied to Equation 4.3, assuming independent measurements, was used to determine ΔER (Gates et al., 2009; ISO/IEC, 2008).

$$\Delta ER = \sqrt{\left(\frac{\partial ER}{\partial \dot{V}_{in}} \Delta \dot{V}_{in}\right)^2 + \left(\frac{\partial ER}{\partial T_{in}} \Delta T_{in}\right)^2 + \left(\frac{\partial ER}{\partial T_{ch}} \Delta T_{ch}\right)^2 + \left(\frac{\partial ER}{\partial \rho_{in}^{ma}} \Delta \rho_{in}^{ma}\right)^2 + \left(\frac{\partial ER}{\partial \rho_{ch}^{ma}} \Delta \rho_{ch}^{ma}\right)^2 + \left(\frac{\partial ER}{\partial C_{in}} \Delta C_{in}\right)^2 + \left(\frac{\partial ER}{\partial C_{ch}} \Delta C_{ch}\right)^2} \quad (\text{Equation 4.5})$$

where

ΔER	= expected root-sum-square error of the combined standard uncertainties (g s^{-1})
$\Delta \dot{V}_{in}$	= incoming moist air ventilation standard uncertainty ($\text{m}^3 \text{s}^{-1}$)
ΔT_{in}	= incoming dry-bulb temperature standard uncertainty (K)
ΔT_{ch}	= chamber dry-bulb temperature standard uncertainty (K)
$\Delta \rho_{in}^{ma}$	= incoming moist air density standard uncertainty ($\text{kg}_{\text{da}} \text{m}^{-3}$)
$\Delta \rho_{ch}^{ma}$	= chamber moist air density standard uncertainty ($\text{kg}_{\text{da}} \text{m}^{-3}$)
ΔC_{in}	= incoming gas concentration standard uncertainty (ppm_v)
ΔC_{ch}	= chamber gas concentration standard uncertainty (ppm_v)

Relative standard uncertainty was expressed as $\Delta ER / ER$.

The standard uncertainty (ΔE , g) associated with the accumulated emission (Equation 4.6), is the standard uncertainty associated with each ER computation, integrated over the length of the experiment.

$$\Delta E = \sqrt{\sum_{i=1}^{n-1} \left(\frac{1}{2} (t_{i+1} - t_i) \times (\Delta ER_i + \Delta ER_{i+1})\right)^2} \quad (\text{Equation 4.6})$$

where

ΔE	= standard uncertainty of accumulated emission while the animal is monitored in the chamber (g)
------------	---

4.3.3.1 Parameter Standard Uncertainty

Uncertainty sources considered for each parameter were associated with the instrumentation involved in the measurement, including instrument resolution, repeatability, calibration reference standard error, other calibration parameters, and the manufacturer's traceable and non-traceable

accuracy. A normal error distribution (divisor = 1; C.I. = 68%) and rectangular error distribution (divisor = $\sqrt{3}$; C.I. = 68%) were applied accordingly (Taylor & Kuyatt, 1994). The following sections describe the methods used to determine parameter uncertainties from Equation 4.4 and are summarized in Table 4.1.

A detailed uncertainty analysis for the parameters and instruments in the FASMS was provided in previous work (Ramirez, 2014; Ramirez et al., 2014). The standard uncertainties of temperature and relative humidity were determined from the manufacturer's non-traceable accuracy and moist air density standard uncertainty was quantified from the partial derivative of density with respect to temperature and relative humidity. Incoming ventilation rate standard uncertainty was dependent on differential pressure measurement standard uncertainty, moist air density standard uncertainty, linear regression slope standard error, and standard error of inverse prediction (Ramirez et al., 2014).

4.3.3.2 Gas Concentration

Incoming and exhaust concentration standard uncertainties measured with the gas analyzer were estimated from five sources (Equation 4.7). The first source was obtained from a post-calibration repeatability test using a primary certified CH₄ gas cylinder (500 ppm_v). Instrument repeatability was checked after calibration at ideal instrument operation conditions, and was obtained from the standard deviation of 13 readings. The second source was from the Primary Certified Tolerance (*PCT*), which is the CH₄ primary certified reference used to calibrate the gas analyzer ($\pm 1\%$ of the certified value). The remaining three uncertainty sources were based on manufacturer's information. These included repeatability (*REP*), range drift (*RD*), and resolution (*Res*). Resolution was assumed to be half of the practical CH₄ optical filter detection limit. The practical detection limit followed manufacturer's recommendations, taken as 10-fold greater than

the theoretical detection limit provided in the specifications for a sample integration time of 5 s. The detection limit of other gases were SF₆ = 0.006 ppm_v, CO₂ = 5 ppm_v, N₂O = 0.03 ppm_v, and NH₃ = 0.2 ppm_v. The five sources of standard uncertainties combined produced:

$$\Delta C_i = \sqrt{\left(\frac{0.005 \cdot SDPC}{1}\right)^2 + \left(\frac{REPI \cdot C_i}{\sqrt{3}}\right)^2 + \left(\frac{PCT \cdot AC}{\sqrt{3}}\right)^2 + \left(\frac{RD \cdot C_i}{\sqrt{3}}\right)^2 + \left(\frac{(10 \cdot DL)/2}{\sqrt{3}}\right)^2} \quad (\text{Equation 4.7})$$

where

- i = { *in* = incoming air, *ch* = chamber }
- ΔC_i = gas concentration combined standard uncertainty (ppm_v)
- $SDPC$ = standard deviation (n=13) of post-calibration repeatability (±1%; ppm_v; normal distribution)
- $REPI$ = instrument repeatability measured value (±1%; ppm_v; normal distribution)
- AC = actual concentration from manufacturer of primary certified tank (499.9; ppm_v)
- PCT = primary certified tolerance (±1% of AC ; ppm_v; rectangular distribution)
- RD = range drift for measured gas concentration (±2.5% for three months; rectangular distribution)
- DL = detection limit for CH₄ (0.4; ppm_v; rectangular distribution)

Table 4.1. Summary of parameters from instrument error analysis contributing to Equation 4.4 used to determine standard uncertainty associated with animal emissions. Sources of uncertainty from each measurement were unique, thus requiring an individual characterization.

Parameter symbol	Unit	Description	Source of uncertainty	Manufacturer	Source
$\Delta T_{in}, \Delta T_{ch}$	K	Dry-bulb temperature	T/RH sensor	Vaisala, HMP60-L, Helsinki, Finland	Ramirez et al., 2014
$\Delta RH_{in}, \Delta RH_{ch}$	%	Relative humidity	T/RH sensor	Vaisala, HMP60-L, Helsinki, Finland	Ramirez et al., 2014
$\Delta \dot{V}_{in}$	m ³ s ⁻¹	Incoming flowrate	Orifice meter	Custom	Ramirez et al., 2014
$\Delta \rho_{in}^{ma}, \Delta \rho_{ch}^{ma}$	kg m ⁻³	Moist air density	Equation 2-16 (Albright 1990)	-	Ramirez et al., 2014
$\Delta C_{in}, \Delta C_{ch}$	ppm _v	Gas concentration	Infrared photoacoustic multi-gas analyzer	INNOVA 1412, LumaSense Technologies, Inc., Santa Clara, CA, USA	Equation 4.6

4.3.3.3 Expanded Standard Uncertainty

The contribution of each parameter in Equation 4.5 to ΔER was expressed as the product of the sensitivity coefficient and the standard uncertainty of the input quantity (Equation 4.8). The expanded uncertainty for ER was determined by applying a coverage factor (k) derived from the combined degrees of freedom (effective, df_{eff}) of parameters with the largest contribution to the

total uncertainty (Equation 4.9). Measurements with normal error distribution were candidates in the analysis. For degrees of freedom > 30, a coverage factor of two (k = 2) was used, which corresponds to approximately 95% C.I. (Taylor, 2009).

$$C_a = \frac{\left(\frac{\partial ER}{\partial a} \Delta a\right)^2}{(\Delta ER)^2} \quad \text{(Equation 4.8)}$$

where

$$\begin{aligned} C_a &= \text{contribution of an individual parameter } a, \text{ decimal} \\ \left(\frac{\partial ER}{\partial a} \Delta a\right)^2 &= \text{absolute standard uncertainty associated with an individual parameter} \end{aligned}$$

$$df_{eff} = \frac{(\Delta ER)^4}{\sum_{i=1}^N \frac{\left(\frac{\partial ER}{\partial a_i} \Delta a_i\right)^4}{df_{a_i}}} \quad \text{(Equation 4.9)}$$

where

$$\begin{aligned} df_{eff} &= \text{effective degrees of freedom} \\ i &= \text{index for each parameter of Equation 4.4 for } i = \{1, \dots, 7\} \end{aligned}$$

Degrees of freedom of rectangular error distributions were assumed to be large (Type B error, $df_{eff} \rightarrow \infty$); hence, these parameters were not included in the analysis because they force

denominator terms to zero: $\lim_{df_{a_i} \rightarrow \infty} \frac{\left(\frac{\partial RMSE}{\partial a_i} \Delta a_i\right)^4}{df_{a_i}} = 0$.

4.3.4 Sensitivity Analysis with Three Scenarios

A sensitivity analysis was performed to determine the standard uncertainty (Equation 4.5) expanded (k = 2) associated with ER (Equation 4.3) and to assess the effects of each ER input parameter (Table 4.1) and their associated standard uncertainties on ER relative expanded uncertainty. Three different scenarios were considered and for all three scenarios, eleven levels of CH₄ concentrations were used (50, 75, 100, 200, 300, 400, 500, 600, 700, 800, and 900 ppm_v) encompassing an ER range of 0.6 to 17.2 g h⁻¹, which follows a baseline range found in the literature (Place et al., 2011) for cattle.

In scenario 1, only CH₄ concentrations were varied while ventilation rate and associated uncertainties remained constant. In scenario 2, incoming and chamber gas concentration relative uncertainties were tested for five levels (1%, 2.5%, 5%, 7.5%, and 10%). Finally, in scenario 3, ventilation rate relative uncertainty was tested for five levels (1%, 2.5%, 5%, 7.5%, and 10%). This represents a worst-case scenario where the ventilation rate remained constant, but ventilation rate standard uncertainty varied (Table 4.2).

For all the scenarios, ventilation rate and associated uncertainty were set as constants (500 ± 12.32 L min⁻¹) (Ramirez et al., 2014). In addition, incoming CH₄ concentration (20 ppm_v), incoming temperature (20°C), chamber temperature (22°C), incoming moist air density (1.17 kg m⁻³), and chamber moist air density (1.16 kg m⁻³) were held constant (Table 4.2). For scenario 2, the five gas concentration relative uncertainties were fixed for the simulation.

Table 4.2. Parameter values and associated absolute (Abs.) and relative (Rel.) standard uncertainties used in sensitivity analysis. Scenario 1 simulated expected operation of the REMS while Scenarios 2 and 3 simulated relative gas concentration and ventilation measurements uncertainty, respectively at 1%, 2.5%, 5%, 7.5%, and 10%

Input	Value ^[a]	Unit	Parameter standard uncertainty					
			Scenario 1		Scenario 2		Scenario 3	
			Abs.	Rel. (%)	Abs.	Rel. (%)	Abs.	Rel. (%)
CH ₄ Concentration	In: 20	ppm _v	0.4	1.9	0.4	Varied ^[d]	0.4	1.9
	Out: ^[b]		Varied ^[c]	Varied ^[b]	Varied ^[c]	Varied ^[d]	Varied ^[b]	Varied ^[b]
Ventilation	In: 500	L min ⁻¹	12.32	2.46	12.32	2.46	Varied ^[c]	Varied ^[d]
Temperature	In: 20	°C	0.5	2.5	0.5	2.5	0.5	2.5
	Out: 22		0.5	2.3	0.5	2.3	0.5	2.3
Moist air density	In: 1.17	kg m ⁻³	0.003	0.2	0.003	0.2	0.003	0.2
	Out: 1.16		0.003	0.2	0.003	0.2	0.003	0.2
Constants:								
Barometric pressure	98,639.31	Pa						
Gas constant	8.31462	m ³ Pa K ⁻¹ mol ⁻¹						
CH ₄ molar mass	16.04	g mol ⁻¹						

^[a] In = background and out = mixed chamber gas

^[b] State point range was 50, 75, 100, 200, 300, 400, 500, 600, 700, 800, and 900 ppm_v for expected animal CH₄ generation

^[c] Absolute and relative uncertainty is a function of input value

^[d] Absolute uncertainty determined from simulated relative uncertainty^[d]

^[e] Simulated relative uncertainties: 1%, 2.5%, 5%, 7.5%, and 10%

4.4 Results and Discussion

Results of the ER sensitivity analysis for three scenarios (Table 4.2) are summarized below. Unless otherwise stated, all uncertainties associated with ER are expressed as the expanded combined standard uncertainty with a coverage factor of two ($k = 2$), corresponding to an approximate 95% Confidence Interval (CI).

4.4.1 Scenario 1

In scenario 1 (Figure 4.6, 4.7, and Table 4.3), ER expanded uncertainties linearly increased with CH_4 emissions, and ER relative uncertainties exponentially decreased to a constant value (Figure 4.6). Methane ER uncertainties were lowest ($\cong 5.9\%$) for higher CH_4 emission rates ($\text{ER} > 3.5 \text{ g h}^{-1}$; CH_4 concentrations $> 200 \text{ ppm}_v$). ER uncertainties were greater (6% to 13%) for lower CH_4 concentrations ($\text{ER} < 3.5 \text{ g h}^{-1}$; concentration $< 200 \text{ ppm}_v$), which can be explained by the increase in the contribution of the background concentration measurement when the chamber concentration was in the lower range (Figure 4.7). The ER relative uncertainty was stable ($5.9\% \pm 0.1\% \text{ SD}$) for CH_4 emission rates $> 3.5 \text{ g h}^{-1}$ (CH_4 concentrations $> 200 \text{ ppm}_v$).

Methane concentration and ventilation rate measurements had the largest role in ER uncertainty, and are plotted in Figure 4.7. The combination of incoming and chamber moist air density and temperature contributed less than 2% of the ER uncertainty for all ER values (Table 4.3). Temperature and moist air density standard uncertainties were $< 3\%$ and $< 1\%$, respectively. Ventilation rate contribution to ER uncertainty increased from 14% to 70% as ER increased and CH_4 concentration increased. Conversely, the contribution of the chamber concentration to ER uncertainty decreased from 49% to 29% as ER increased. Similarly, background concentration contribution to uncertainty decreased from 36% to $< 1\%$ as ER increased. Scenario 1 provides insights on the effect of primary parameters (gas analyzer and

ventilation rate) on ER expanded uncertainty. Because the uncertainty of these two parameters will affect the ER uncertainty the greatest, carefully controlling them can substantially improve ER estimates.

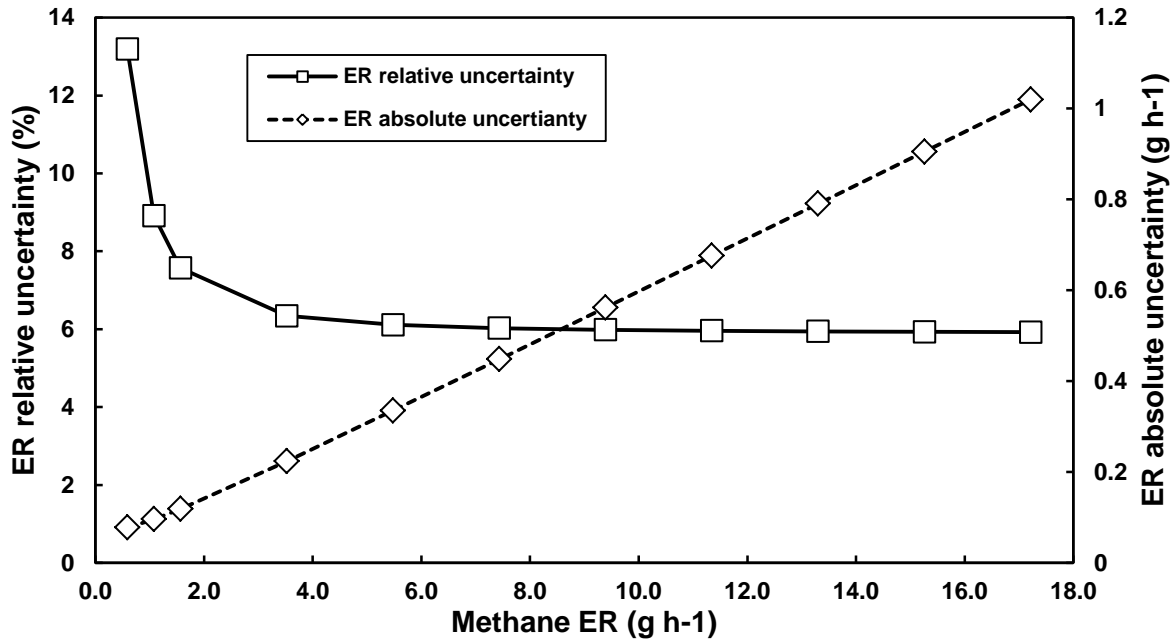


Figure 4.6. Methane ER relative and absolute expanded uncertainties ($k = 2$; $\sim 95\%$ C.I.) for 11 levels of ER. Emission rate range of 0.6 to 17.2 g h^{-1} corresponds to a CH_4 concentration range of 50 to 900 ppm_v .

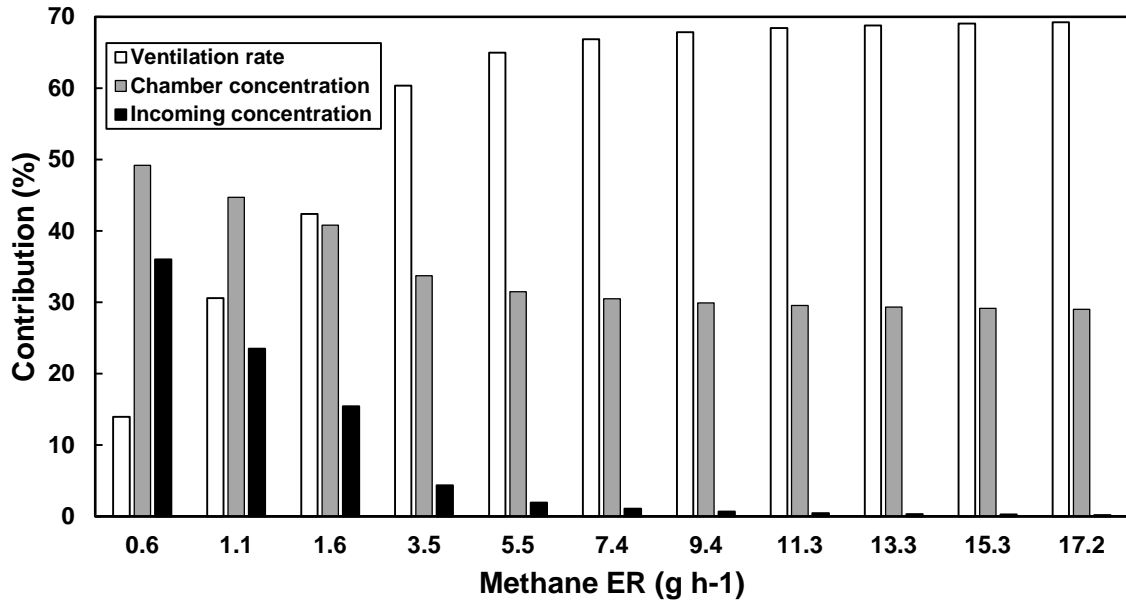


Figure 4.7. Contribution for three major sources to ER expanded uncertainty. Other sources were omitted for clarity but are summarized in Table 4.3.

Table 4.3. Summary of absolute (Abs.) and relative (Rel.) standard uncertainties of the parameters contributing to ER expanded uncertainty for two simulation levels of a CH₄ concentration of 50 and 500 ppm_v.

Parameter symbol	Value	Unit	Scenario 1		
			Uncertainty		$\Delta ER/ER$ Contribution (%)
			Abs.	Rel. (%)	
$ER^{[a]}$	0.6	g h ⁻¹	0.1 ^[b]	13.2	
C_{ch}	50.0	ppm _v	1.4	2.8	49.2
C_{in}	20.0	ppm _v	1.2	6.0	36.0
\dot{V}_{in}	500.0	L min ⁻¹	12.3	2.5	14.0
T_{ch}	22.0	°C	0.5	2.3	0.2
T_{in}	20.0	°C	0.5	2.5	2.9E-02
ρ_{ch}^{ma}	1.16	kg m ⁻³	2.7E-03	0.2	0.3
ρ_{in}^{ma}	1.17	kg m ⁻³	2.5E-03	0.2	0.3
$ER^{[a]}$	9.4	g h ⁻¹	0.6 ^[b]	6.0	
C_{ch}	500.0	ppm _v	7.9	1.6	29.9
C_{in}	20.0	ppm _v	1.2	6.0	0.7
\dot{V}_{in}	500.0	L min ⁻¹	12.3	2.5	67.8
T_{ch}	22.0	°C	0.6	2.7	0.3
T_{in}	20.0	°C	0.6	3.0	3.0E-02
ρ_{ch}^{ma}	1.16	kg m ⁻³	2.6E-03	0.2	0.6
ρ_{in}^{ma}	1.17	kg m ⁻³	2.6E-03	0.2	0.6

^[a] ER is defined in Equation 4.3

^[b] expanded standard uncertainty with applied coverage factor of $k = 2$ (95% CI)

4.4.2 Scenario 2

In scenario 2, as CH₄ emission rate increased, the ER relative uncertainty decreased until it became constant for $ER > 3.5 \text{ g h}^{-1}$ (CH₄ concentration $> 200 \text{ ppm}_v$) (Figure 4.8 and Table 4.4). For CH₄ emission rates $< 3.5 \text{ g h}^{-1}$ (CH₄ concentrations $< 200 \text{ ppm}_v$) and gas analyzer uncertainty $> 1\%$, the ER relative uncertainties were variable until they reached a plateau (Figure 4.8). In the plateau phase (CH₄ emission rate $> 3.5 \text{ g h}^{-1}$ and CH₄ concentrations $> 200 \text{ ppm}_v$), gas analyzer uncertainties were 1%, 2.5%, 5%, 7.5% and 10%, which corresponded to ER relative uncertainties of 5.4%, 7.1%, 11.4%, 16.1%, and 21.1%, respectively.

The contribution of the ventilation rate uncertainty to the ER relative uncertainty (Table 4.4) decreased as the gas analyzer uncertainty increased. For concentrations $> 200 \text{ ppm}_v$, the gas analyzer contribution lower and upper limits were 16% and 94%, respectively, which

corresponds to a ventilation contribution with upper and lower limits of 84% and 5%, respectively. When gas analyzer uncertainty was the lowest (1%), gas analyzer contribution was about 16% and ventilation rate contribution was about 84% to the ER relative uncertainty. Conversely, when gas analyzer uncertainty was the highest (10%), ventilation rate contribution was about 5% while exhaust concentration measurement was 94%. The combination of incoming and exhaust moist air density and temperature contributed less than 2% to the ER relative uncertainty for all ER values and the range of gas analyzer uncertainty values.

4.4.3 Scenario 3

In scenario 3, as methane ER increased, the ER relative expanded uncertainty decreased for all simulated ventilation rate uncertainties, until they reached a plateau for $ER > 3.5 \text{ g h}^{-1}$ (Figure 4.9). In addition, as ventilation rate uncertainty was increased, the ER relative uncertainty increased. For low CH_4 emission rates $< 3.5 \text{ g h}^{-1}$ (concentrations $< 200 \text{ ppm}_v$), the ER relative uncertainties were variable until they reached a plateau, for all simulated ventilation rate uncertainties (Figure 4.9). In the plateau phase, where CH_4 emission rates were $> 3.5 \text{ g h}^{-1}$ (concentration $> 200 \text{ ppm}_v$), ER relative uncertainties increased (3.8%, 5.9%, 10.5%, 15.4%, and 20.3%) with the increased in the simulated ventilation rate uncertainties (1%, 2.5%, 5%, 7.5%, and 10%, respectively).

In terms of individual instrument uncertainty contributions, the gas analyzer uncertainty contribution (Equation 4.5) decreased as ventilation rate uncertainty increased. At CH_4 emission rates $> 3.5 \text{ g h}^{-1}$ (concentrations $> 200 \text{ ppm}_v$), the highest and lowest values of the gas analyzer contribution to the ER relative uncertainty were 98% to 2.5%, respectively, which corresponds to a ventilation contribution of 2.6% and 97%, respectively. For the lowest ventilation rate uncertainty (1%), the gas analyzer contribution was about 95% and ventilation rate contribution

was 4.2%. Conversely, for the highest ventilation rate uncertainty (10%), the gas analyzer contribution was about 2.5% and ventilation rate contribution was about 97%. The combination of incoming and chamber moist air density and temperature contributed less than 2% of the ER relative uncertainty for all state points and gas analyzer scenarios.

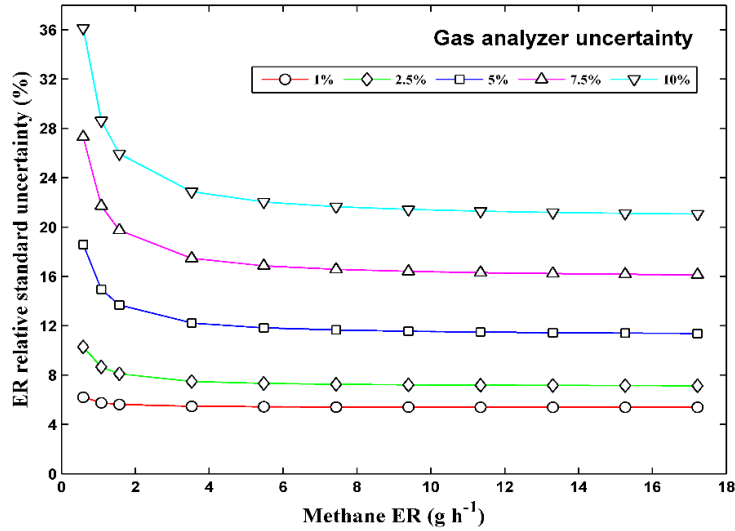


Figure 4.8. Methane concentration measurement uncertainties were held constant at 1%, 2.5%, 5%, 7.5%, and 10%. All other values are listed in Table 4.4. The plot shows that gas analyzer relative expanded uncertainty increased as ER relative expanded uncertainty increased (Scenario 2).

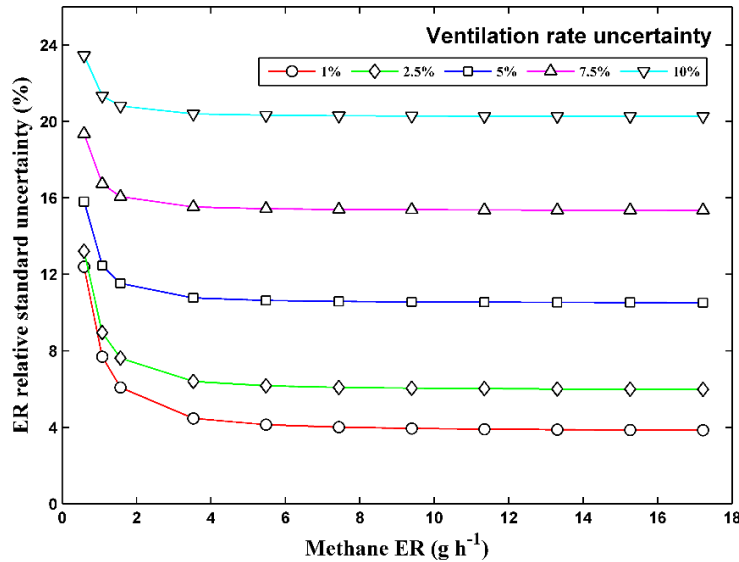


Figure 4.9. Ventilation rate uncertainty was held constant at 1%, 2.5%, 5%, 7.5%, and 10%. All other values as listed in Table 4.4. The plot shows that ventilation relative uncertainty increased as and ER relative expanded uncertainty increased (Scenario 3).

Table 4.4. Absolute (Abs.) and relative (rel.) standard uncertainties for the three major measurements and contribution to ER expanded uncertainty. In Scenario 2, gas analyzer uncertainty was 1% or 5%. For Scenario 3, ventilation uncertainty was 1% or 5%. Two levels for CH₄ concentrations of 50 and 500 ppm_v were chosen as an example.

Parameter symbol	Value	Unit	Scenario 2			Scenario 3		
			Uncertainty		$\Delta ER/ER$ Contribution (%)	Uncertainty		$\Delta ER/ER$ Contribution (%)
			Abs.	Rel. (%)		Abs.	Rel. (%)	
$ER^{[a]}$	0.6	g h ⁻¹	0.04 ^[b]	6.2		0.07 ^[b]	12.4	
C_{ch}	50.0	ppm _v	0.5	1.0	28.6	1.4	2.8	55.7
C_{in}	20.0	ppm _v	0.2	1.0	4.5	1.2	6.0	40.7
\dot{V}_{in}	500.0	L min ⁻¹	12.3 ^[b]	2.5	63.0	5.0	1.0	2.6
$ER^{[a]}$	9.4	g h ⁻¹	0.5	5.4		0.4 ^[b]	3.9	
C_{ch}	500.0	ppm _v	5.0	1.0	14.9	7.9	1.6	69.0
C_{in}	20.0	ppm _v	0.2	1.0	0.0	1.2	6.0	1.6
\dot{V}_{in}	500.0	L min ⁻¹	12.3 ^[b]	2.5	83.2	5.0	1.0	25.8
$ER^{[a]}$	0.6	g h ⁻¹	0.1	18.6		0.09 ^[b]	15.8	
C_{ch}	50.0	ppm _v	2.5	5.0	79.9	1.4	2.8	34.3
C_{in}	20.0	ppm _v	1.0	5.0	12.7	1.2	6.0	25.1
\dot{V}_{in}	500.0	L min ⁻¹	12.3 ^[b]	2.5	7.0	25.0	5.0	40.0
$ER^{[a]}$	9.4	g h ⁻¹	1.1	11.6		1.0 ^[b]	10.6	
C_{ch}	500.0	ppm _v	25.0	5.0	81.3	7.9	1.6	9.6
C_{in}	20.0	ppm _v	1.0	5.0	0.1	1.2	6.0	0.2
\dot{V}_{in}	500.0	L min ⁻¹	12.3 ^[b]	2.5	18.2	25.0	5.0	89.7

^[a] ER is defined in Equation 4.3

^[b] expanded standard uncertainty with applied coverage factor of $k = 2$ (95% CI)

Scenarios 2 and 3 provide insight on the effects of concentration and ventilation rate measurement uncertainty on the ER relative uncertainty. Uncertainty may increase from uncalibrated instrument drift or from using a less accurate calibrated instrument. Several factors will affect instrument uncertainty. For instance, the fresh air source can have a significant impact on instrumentation uncertainty, such as unfiltered air degrading the orifice of pressure differential flowmeters. In addition, this analysis also assumes a nonzero background CH₄ concentration in the ventilation. This is important because many chamber systems are housed in barns or other buildings holding additional animals that may cause variations in CH₄ concentration present in the chamber air supply. Similarly, the use of positive pressure systems helps eliminate background CH₄ from entering the chamber or gas sampling system. Neglecting

background concentration may over-predict animal emissions, which is dependent on the relative magnitude of background and chamber concentrations. Neglecting air density, including fluctuations changes from the ventilation to the chamber, can also result in emission over-predictions.

The identification of the individual contributions relative to the combined uncertainty (ER expanded uncertainty) is also important for instrument selection and maintenance. An increase in ventilation rate uncertainty can cause substantial impacts in the ER combined uncertainty. Instruments with low drift, easy to calibrate, and not affected by frequent changes in environmental conditions will reduce potential increases in the combined uncertainty. Awareness of these factors can lead to improved experimental design and measurement system implementation. Frequent verification of accuracy of key instrumentation (i.e. gas analyzer and flowmeter) can reduce uncertainty increases over time.

Knowledge of the ER combined uncertainty provides insight to the amount of confidence in the measurement system. Quantifying the combined uncertainty is essential for all respiration chambers and indirect calorimeters because reported values will carry standard uncertainties associated with each measurement. In addition, quantifying combined uncertainty is imperative for determining the level of sensitivity needed to detect differences between experimental treatments i.e. diets, mitigation strategies, etc. Two computed values of CH₄ emission rate are significantly different if that difference lies outside the combined uncertainty of each CH₄ emission rate computation – assuming other random sources of error are assessed and systematic errors are estimated. Thus, combined uncertainty must be determined and reported. The determined combined uncertainty from design analysis should be subsequently applied to the system commissioning along with the assessment of systematic errors. Although the results

presented here are applied to REMS, the presented methodology can, and should, be applied to other systems designed to quantify gas emissions.

4.5 Summary and Conclusions

REMS is an open-circuit respiration system comprising six positive pressure ventilated hood-type chambers for measuring beef cattle CH₄ emissions. The design features a unique positive pressure ventilation system for minimizing infiltration and subsequent gas measurement error by dilution. Uncertainties in REMS are shown to depend on instrument type and resolution, measurement reproducibility, calibration reference standard error, other calibration parameters, traceable and non-traceable manufacturer's accuracy, and assumption regarding instrument error distributions. Emission rate standard uncertainty was determined by propagating the standard uncertainty derived for each instrument into the ER root-sum square error.

Methane ER expanded uncertainty ($k=2$, ~95% CI) was approximately constant at $\cong 5.9\%$ for chamber ERs $> 3.5 \text{ g h}^{-1}$ (for concentration $>200 \text{ ppm}_v$). In addition, contribution to ER expanded uncertainty was 29% from the gas analyzer and 69% from the ventilation rate. Other input measurements had negligible contributions to the combined uncertainty. Gas analyzer and ventilation rate uncertainties, independently, increased as ER standard uncertainty increased. Increases in uncertainty associated with ventilation rate and gas concentration measurement have significant impact on ER standard uncertainty; thus, these instruments should have the lowest reasonable standard uncertainty, and emphasis should be given to calibration and accuracy verification.

REMS provides a lower cost alternative to the whole body chamber technique. Its application can potentially increase knowledge of what drives CH₄ production and ER in ruminates, particularly if REMS capabilities are used to investigate CH₄ production factors.

REMS is uniquely qualified to accurately measure gas production from cattle, which is a key first step in understanding metabolic activity in cattle production and establishing possible mitigation strategies for environmental emissions.

A systematic approach to evaluate component measurement errors such as conducted in this work provide an estimate of the standard uncertainty of complex emission measurement systems and allow researchers to report animal emissions with a stated standard uncertainty. The analysis presented in this study can be extended to other systems, because it applies equally to any other open-circuit respiration chambers or indirect calorimeters computing quantities from several measurement inputs. In conclusion, a comprehensive uncertainty analysis should be a requirement in any gas measurement system design, and the present study is a major step in that direction.

4.6 Acknowledgments

This research was supported with funding provided by the Dudley Smith Initiative, University of Illinois College of ACES and the Office of Research, University of Illinois College of ACES. The authors would like to acknowledge the contributions of research specialist Jingwei Su, graduate student Yi Sun, and undergraduate students Kellie Kroscher and Patricia Paulausky during the preparation and completion of this work.

4.7 References

Albright, L. D. (1990). *Environment control for animals and plants*. American Society of Agricultural Engineers.

ASHRAE. (2013). Chapter 1: Psychrometrics. In M. S. Owen (Ed.), *Handbook of fundamentals*.

Atlanta, GA: American Society of Heating, Refrigerating and Air-Conditioning Engineers.

- Bhatta, R., Enishi, O., & Kurihara, M. (2007). Measurement of methane production from ruminants. *Asian-Australasian Journal of Animal Sciences*, 20(8), 1305-1318.
- Bhatta, R., Tajima, K., Takusari, N., Higuchi, K., Enishi, O., & Kurihara, M. (2006). Comparison of sulfur hexafluoride tracer technique, rumen simulation technique and in vitro gas production techniques for methane production from ruminant feeds. *International Congress Series*, 1293, 58-61. doi:10.1016/j.ics.2006.03.075.
- Casey, K. D. (2005). *The determination of ammonia emissions from mechanically ventilated poultry houses: An examination of the issues involved*. (Doctorate, University of Kentucky, Biosystems and Agricultural Engineering).
- Ellis, J. L., Kebreab, E., Odongo, N. E., Beauchemin, K., McGinn, S., Nkrumah, J. D., . . . France, J. (2009). Modeling methane production from beef cattle using linear and nonlinear approaches. *Journal of Animal Science*, 87(4), 1334-1345. doi:10.2527/jas.2007-072.
- EPA. (2013). *Inventory of US greenhouse gas emissions and sinks: 1990-2011*. (No. EPA 430-R-13-001).EPA 430-R-11-005.
- Gates, R. S., Casey, K. D., Wheeler, E. F., Xin, H., & Pescatore, A. J. (2008). U.S. broiler housing ammonia emissions inventory. *Atmospheric Environment*, 42(14), 3342-3350. doi:10.1016/j.atmosenv.2007.06.057.
- Gates, R. S., Casey, K. D., Xin, H., & Burns, R. T. (2009). Building emissions uncertainty estimates. *Transactions of the ASABE*, 52(4), 1345-1351.
- Grainger, C., Clarke, T., McGinn, S. M., Auldist, M. J., Beauchemin, K. A., Hannah, M. C., . . . Eckard, R. J. (2007). Methane emissions from dairy cows measured using the sulfur hexafluoride (SF₆) tracer and chamber techniques. *Journal of Dairy Science*, 90(6), 2755-2766. doi:10.3168/jds.2006-697.

- Hellwing, A. L. F., Lund, P., Weisbjerg, M. R., Brask, M., & Hvelplund, T. (2012). Technical note: Test of a low-cost and animal-friendly system for measuring methane emissions from dairy cows. *Journal of Dairy Science*, 95(10), 6077-6085.
- IPCC. (2006). *IPCC guidelines for national greenhouse gas inventories, prepared by the national greenhouse gas inventories program*.
- ISO/IEC. (2008). *Uncertainty of measurement: Part 3. guide to the expression of uncertainty in measurement (GUM:1995) (ISO Guide 9803:2008(E). ed.)*. Geneva, Switzerland: International Standards Organization.
- Johnson, K. A., & Johnson, D. E. (1995). Methane emissions from cattle. *Journal of Animal Science*, 73(8), 2483-2492.
- Kelly, J. M., Kerrigan, B., Milligan, L. P., & McBride, B. W. (1994). Development of a mobile, open-circuit indirect calorimetry system. *Canadian Journal of Animal Science*, 74(1), 65-71.
- Maia, G. D. N., Ramirez, B. C., Green, A. R., Sun, Y., Rodriguez, L. F., Shike, D. W., & Gates, R. S. (2014). A novel ruminant emission measurement system: Part II-commissioning. *Submitted to Transactions of ASABE*.
- Maia, G. D. N., Day V, G. B., Gates, R. S., & Taraba, J. L. (2012). Ammonia biofiltration and nitrous oxide generation during the start-up of gas-phase compost biofilters. *Atmospheric Environment*, 46(0), 659-664.
- Makkar, H. P. S., & Vercoe, P. E. (2007). *Measuring methane production from ruminants*. Dordrecht, The Netherlands: Springer.
- McGinn, S. M. (2006). Measuring greenhouse gas emissions from point sources in agriculture. *Canadian Journal of Soil Science*, 86(3), 355-371.

- McGinn, S. M., Beauchemin, K. A., Coates, T., & Colombatto, D. (2004). Methane emissions from beef cattle: Effects of monensin, sunflower oil, enzymes, yeast, and fumaric acid. *Journal of Animal Science*, 82(11), 3346-3356.
- McLean, J., & Tobin, G. (1987). *Animal and human calorimetry* Cambridge University Press.
- Moody, L. B., Li, H., Burns, R. T., Xin, H., Gates, R. S., Hoff, S. J., . . . Overhults, D. (2008). *A quality assurance project plan for monitoring gaseous and particulate matter emissions from broiler housing (sections 1-6)* (ASABE Special Publication ed.). St. Joseph, Mich.: ASABE.
- Muñoz, C., Yan, T., Wills, D. A., Murray, S., & Gordon, A. W. (2012). Comparison of the sulfur hexafluoride tracer and respiration chamber techniques for estimating methane emissions and correction for rectum methane output from dairy cows. *Journal of Dairy Science*, 95(6), 3139-3148.
- Murray, P. J., Moss, A., Lockyer, D. R., & Jarvis, S. C. (1999). A comparison of systems for measuring methane emissions from sheep. *Journal of Agricultural Science*, 133(4), 439-444.
- Nienaber, J. A., & Maddy, A. L. (1985). Temperature controlled multiple chamber indirect calorimeter-design and operation. *Transactions of the American Society of Agricultural Engineers*, 28(2), 555-560.
- Pinares-Patiño, C. S., Lasey, K. R., Martin, R. J., Molano, G., Fernandez, M., MacLean, S., . . . Clark, H. (2011). Assessment of the sulphur hexafluoride (SF₆) tracer technique using respiration chambers for estimation of methane emissions from sheep. *Animal Feed Science & Technology*, 166-167, 201-209. doi:10.1016/j.anifeedsci.2011.04.067.
- Pinares-Patiño, C. S., & Waghorn, G. C. (Eds.). (2012). *Technical manual on respiration chamber designs*. Wellington, New Zealand: Ministry of Agriculture and Forestry.

- Place, S. E., Pan, Y., Zhao, Y., & Mitloehner, F. M. (2011). Construction and operation of a ventilated hood system for measuring greenhouse gas and volatile organic compound emissions from cattle. *Animals (2076-2615)*, *1*(4), 433-446. doi:10.3390/ani1040433.
- Price, J. E., & Lacey, R. E. (2003). Uncertainty associated with the gravimetric sampling of particulate matter. *American Society of Agricultural Engineers Annual International Meeting 2003*, ASAE Paper No. 034116.
- Ramirez, B. C., Maia, G. D. N., Green, A. R., Shike, D. W., Gates, R. S., & Rodríguez, L. F. (2013). Design and validation of a calibrated orifice meter for sub-500 liter per minute flow rate applications. *American Society of Agricultural and Biological Engineers Annual International Meeting 2013*, ASABE Paper No. 1618475.
- Ramirez, B. C. (2014). *Design and evaluation of open-circuit respiration chambers for beef cattle*. (Masters, University of Illinois at Urbana-Champaign, Department of Agricultural and Biological Engineering).
- Ramirez, B. C., Maia, G. D. N., Green, A. R., Shike, D. W., Rodríguez, L. F., & Gates, R. S. (2014). Design and validation of a precision orifice meter for ventilation rate measurement in open-circuit respiration chambers. *Submitted to Transactions of ASABE*.
- Schmidhuber, J., & Tubiello, F. N. (2007). Global food security under climate change. *Proceedings of the National Academy of Sciences of the United States of America*, *104*(50), 19703-19708. doi:10.1073/pnas.0701976104.
- Skoet, J., & Stamoulis, K. (2006). *The state of Food insecurity in the world 2006*. (). Rome, Italy: Food and Agriculture Organization of the United Nations.
- Storm, I. M., Hellwing, A. L. F., Nielsen, N. I., & Madsen, J. (2012). Methods for measuring and estimating methane emission from ruminants. *Animals*, *2*(2), 160-183.

- Sun, Y. (2013). *Quality assurance project plan for a ruminant emission measurement system*. (Masters, University of Illinois at Urbana-Champaign, Department of Agricultural and Biological Engineering).
- Suzuki, T., McCrabb, G., Nishida, T., Indramanee, S., & Kurihara, M. (2007). Construction and operation of ventilated hood-type respiration calorimeters for in vivo measurement of methane production and energy partition in ruminants. *Measuring methane production from ruminants* (pp. 125-135) Springer.
- Taylor, B. N., & Kuyatt, C. E. (1994). *Guidelines for evaluating and expressing the uncertainty of NIST measurement results* (NIST Tech Note 1297 ed.). Gaithersburg, Md: National Institute for Standards and Technology.
- Tomkins, N. W., McGinn, S. M., Turner, D. A., & Charmley, E. (2011). Comparison of open-circuit respiration chambers with a micrometeorological method for determining methane emissions from beef cattle grazing a tropical pasture. *Animal Feed Science and Technology*, 166-167, 240-247.

CHAPTER 5: A NOVEL RUMINANT EMISSION MEASUREMENT SYSTEM: PART II - COMISSIONING

**Maia, G. D. N., B. C. Ramirez, A. R. Green, Y. Sun, L. F. Rodriguez, D.W. Shike, and R. S.
Gates**

A manuscript submitted to *Transactions of ASABE*

This chapter describes the methodology to evaluate the REMS subsystem performance, characterize the integrity of the whole system, and quantify the standard uncertainty associated with the mass recovery percent. The detailed documentation of the commissioning is critical for establishing the procedures needed to obtain reliable and accurate estimations of the methane production. The experimental methods and, steady-state analysis of the mass recovery test provide insight to the integrity of the system and when coupled with an uncertainty analysis, confidence in the measured results can be established. Current literature presenting results of mass recovery tests have limited information regarding the confidence in the results; thus, a well-documented and comprehensive analysis is required prior to implementing the system.

This chapter owes its success to the combined efforts of Brett Ramirez, Guilherme Maia, Angela Green, Yi Sun, Daniel Shike, Luis Rodríguez, and Richard Gates. Mr. Sun helped with conducting the subsystem performance evaluation and documentation of the mass recovery test. Dr. Maia led the research and developed the uncertainty analysis for the parameters in the steady-state mass recovery percent. Drs. Green, Shike, Rodríguez, and Gates participated in the research design and the draft revision.

My direct contributions to this work included the thermal environment performance (Section 2.2.2 and Section 3.1.2) and gas subsampling system integrity (Section 2.2.3 and

Section 3.1.3) evaluation. Mean humidity ratio, temperature, and dew point temperature were calculated using psychrometric equations to assess the thermal conditions and moisture removal from the chambers. I conducted the experimental procedure described in Section 2.2.3 and analyzed the results to show the sampling lines had minimal leakage between the chamber and the gas analyzer. Both the performance and integrity evaluations were significant to ensuring the system performed to design specifications prior to implementation. In addition, my efforts conceptualized the design of the steady-state mass recovery test described in Section 2.3.1, implemented the procedure, and analyzed results. Pictures, operating procedures, and data for all replicates of the recovery test can be found in Appendix E. I also performed the analytical approach to determining the mass injected by the reference (Section 2.4.1) and to creating and solving the mass balance used to calculate the mass recovered (Section 2.4.2). Derivations of both can be found in Appendix D. I contributed largely to the final analysis of the steady-state mass recovery percent standard uncertainty and contributions of its parameters. The data collected from the six replicates of the mass recovery test are summarized in Appendix F. Using the previously developed equations, I wrote and analyzed the results from the program presented in Appendix G to determine the mass flow recovered and injected standard uncertainty for all steady-state measurements obtained from the mass recovery tests. A detailed and expansion of the chamber bias testing with alternative methods is presented in Appendix I.

5.1 Abstract

Part I of this series provided the description and design evaluation of a newly developed Ruminant Emission Measurement System (REMS) using uncertainty analysis tools. Part II of this series describes REMS commissioning, and documents the whole system and subsystem performance. Subsystem assessments verified chambers positive pressurization, thermal environmental control performance, and the integrity of the gas sampling system. The integrity of the entire system was verified through a Steady-State Mass Recovery Percent (SSMRP) analysis, which compared the total mass measured by REMS (mass recovered) to the total mass injected from a certified reference (mass injected) during the steady-state regime. Uncertainty analysis conducted with commissioning included propagation of instrument uncertainties, quantification of the variability in repeated tests, and identification of systematic errors. Results from the subsystem evaluation verified that chambers were positively pressurized, maintained thermal environmental comfort, and resulted in minimal leakage along the sampling path from the chamber to the gas analyzer. The mean SSMRP for the six chambers ranged from 92.0% to 96.6% with SSMRP absolute expanded uncertainties (~95% confidence interval) ranging from 10.4% to 13%. Mass recovered uncertainty contributed from 70.1% to 90.7% to SSMRP uncertainty, mass injected uncertainty contributed from 2.5% to 4.0%, and reproducibility contributed from 5.6% to 27.3%. Significant ($P < 0.05$) SSMRP systematic bias was found for most chambers; therefore, correction for bias following the methods developed here is recommended. Example measurements from REMS research were presented to demonstrate how to incorporate a documented standard uncertainty for emissions. Methods presented are useful for improving respiration system or indirect calorimeter design and implementation.

Keywords: Climate Change, Feeding, Food Security, Methane Production, and Uncertainty.

5.2 Introduction

Part one of this series (Maia et al., 2014) introduced the design evaluation and description of the Ruminant Emission Measurement System (REMS), which consists of six positive-pressure ventilated hood-type respiration chambers. This evaluation documented a systematic methodology to estimate combined standard uncertainty associated with calculated methane (CH₄) emissions from ruminant eructation. An analytical approach to the design analysis was critical to assess the contributions of measurement parameters and the effects of these parameters on the Emission Rate (ER) uncertainty. Knowledge of uncertainty is useful to compare ruminant emission measurement techniques (i.e. SF₆ tracer or *in vitro* gas production technique) or amongst different chamber systems to provide expected confidence levels for the measurements reported.

In addition to the analytical approach, REMS design also required commissioning to verify performance and compare that to the design assumptions and analysis, as well as to evaluate integrity of the physical system. Commissioning is the final step before full implementation, and incorporates information that includes uncertainties associated with REMS operation, identification of systematic errors, and quantification of variability over repeated tests. A mass recovery analysis serves as a “whole system calibration”, or as a check on operation integrity. These are crucial steps in the evolution of open-circuit systems for livestock emissions measurement.

The mass recovery test compares a known amount of mass injected (reference) into the chamber to the total mass measured by the system, and it has been the primary method to

validate the chamber technique (McLean & Tobin, 1987). Several approaches have been used to evaluate system recovery. The alcohol combustion method (Carpenter & Fox, 1923) utilizes stoichiometric relations of the combustion of alcohols to determine mass generated, but it is often difficult to determine whether the full combustion of the alcohol actually occurred (McLean & Tobin, 1987). Recently, more accurate mass recovery tests used pulse injections of a known volume of gas and by continuous or step injection of a known mass flow (Hellwing, Lund, Weisbjerg, Brask, & Hvelplund, 2012; Klein & Wright, 2006; Pinares-Patiño et al., 2011; Suzuki, McCrabb, Nishida, Indramanee, & Kurihara, 2007). A number of precise measurements are required to accurately quantify the known mass entering the system; for example, input gas (e.g. CH₄, CO₂, and H₂S) mass flow controlled by a mass flow controller, or determined gravimetrically as the change in weight of an open gas cylinder on a scale. Errors during the determination of the injected mass may lead to incorrect estimates of mass recovered, and should be included in the final stated uncertainty. A mass recovery test provides insights about the dynamics of the chamber and integrity of the sampling system. Limited work is available on error analysis and methodology of the injected mass, along with an analytical approach to determine system time constant applied to the chamber technique (McGinn, 2006). More descriptive calibration procedures are available in other disciplines, i.e., for soil carbon flux measurement chambers (McGinn, 2006). A mass recovery test reported without quantification of the injected and recovered masses standard uncertainties will substantially reduce confidence in emissions measurement.

The main goal for this work was to introduce and describe a systematic methodology of REMS commissioning building upon the design analysis (Maia et al., 2014). In the commissioning phase, REMS subsystems operations were assessed (subsystems full description

is available in Part I), followed by a mass recovery whole system validation. In addition, this analysis determined the systematic error and combined individual instrument measurement uncertainties related to a reference mass of tracer gas injected into the system, which was a new input, not assessed in Part I. To achieve these goals, the following objectives were completed:

1. Subsystem performance validation prior to whole system evaluation.
2. Whole system evaluation, subdivided into four procedures:
 - a. Determination of the time required to reach the exchange rate of fresh air steady-state condition for five time constants.
 - b. Quantification of mass recovered of a reference tracer gas (SF_6) during the aforementioned steady-state.
 - c. Determination of the combined standard uncertainty associated with the mass recovery percent and assessment of individual parameter uncertainty contributions to the mass recovery percent uncertainty.
 - d. Identification of systematic errors during whole system evaluation to determine system repeatable offsets and the applicability of correction factors.

This commissioning analysis fulfilled a need to establish and document a procedure to quantify uncertainty of emissions measured with REMS, but it also applies to other respiration chamber and indirect calorimeter systems in operation, or to future designs.

5.3 Materials and Methods

5.3.1 REMS Overview

REMS was installed in six metabolism stalls at the University of Illinois at Urbana-Champaign Beef and Sheep Field Facility and consists of four major subsystems: (1) six identical positive pressure Ventilated Hood Chambers (VHC), (2) individual Thermal

Environmental Control Subsystem (TECS), (3) Fresh Air Supply and Measurement Subsystem (FASMS), and (4) Gas Sampling Subsystem (GSS). Orifice meter (in the FASMS) design, construction, and validation can be found elsewhere (Ramirez et al., 2013; Ramirez, 2014; Ramirez et al., 2014). A description of the operation and a set of schematics of REMS are provided in Part I of this series (Maia et al., 2014).

5.3.2 Subsystem Validation

Individual subsystems were assessed for proper function and to guide future troubleshooting after whole system commissioning. Detailed protocols for system maintenance and testing are documented in a system standard operating procedure (Sun, 2013). All experiments using animals were approved by the University of Illinois at Urbana-Champaign Institutional Animal Care and Use Committee (IACUC) under the protocol # 11214.

5.3.2.1 Ventilated Hood Chamber Pressure Distribution

Positive pressurization is required over the entire internal volume of the VHCs to ensure no background gas infiltration that could dilute the sample. Fifteen static pressure readings were taken inside each of the six VHCs, five locations at three heights (Figure 5.1). A fresh air ventilation rate of $481 \text{ L min}^{-1} \pm 0.1 \text{ L min}^{-1}$ ($17 \text{ cfm} \pm 0.2 \text{ cfm}$), was selected as the expected flow during experiments and was used during all tests. The canvas hood was cinched during the test to create a similar situation as observed during preliminary animal testing. An electronic differential manometer (Model 260-MS4, SETRA, Boxborough, MA, USA) was used to map chamber static pressure rise above room conditions. A pressure buffer was attached to the end of the high-pressure port tube to reduce disturbances from turbulent air in the chamber. In order to replicate the process of an animal shifting position (i.e. smaller animals), half the area of the hood cinch was left open. Results were reported from the average of each sample location across

the three heights, and the average of the five cross-section sample locations for each of the three heights (Figure 5.2). A smoke test was performed to visually confirm positive pressurization, flow patterns, and gas mixing. A smoke stick (S102, Regin HVAC Products, Inc., Oxford, Connecticut, USA) with 45 s burn-time and volume generation capacity of 4.25 m³ (150 ft³) was initially placed inside the feeding bin (bottom of the chamber), then around the outside of the chamber, and lastly in the canvas hood.

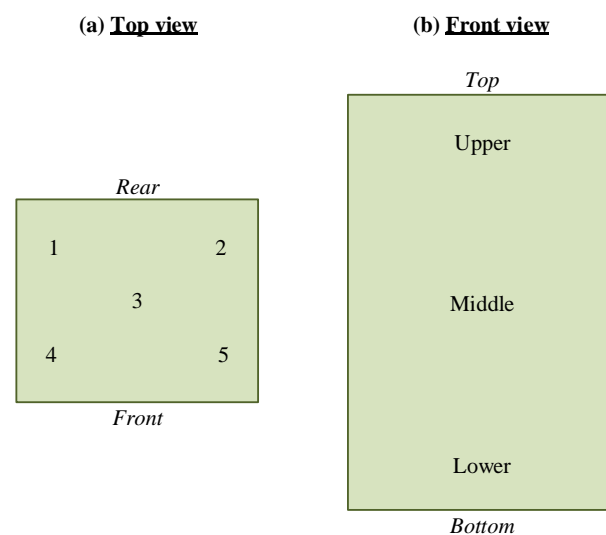


Figure 5.1. Static pressure sampling locations and regions. (a) Chamber plan view (top) displays the five locations of pressure sample collection; (b) Chamber plan view (front) displays cross-section regions (upper, middle, and lower) of pressure samples collected.

5.3.2.2 Thermal Environment Performance

A 23 h test with six steers (826 kg \pm 64 kg; one steer per chamber) was conducted to evaluate the ability of TECS to maintain set-point temperature, remove moisture, and assess potential chamber internal condensation. Humidity ratio and dew point temperature (Albright, 1990) were used as the thermal environment assessment parameters, and were calculated for temperature and relative humidity measurement recorded every 43 s over the duration of the test. Animals were provided *ad libitum* food and water.

5.3.2.3 Gas Sampling Subsystem Integrity

Leakage along the gas sampling path (which contains multiple connections that are subject to potential leakage) from the sampling port can provide false, diluted, readings. The GSS integrity was evaluated by applying a flow of SF₆ at a known concentration to the gas sampling port of each VHC, and noting the concentration recorded at the gas analyzer (Figure 5.2; Equation 5.1). The supplied SF₆ concentration was 6.235 ppm_v ± 0.004 ppm_v (mean ± SD), which was the actual concentration measured by the gas analyzer when the primary certified tank of SF₆ was directly connected to the gas analyzer (flow of approximately 4 L min⁻¹) using a single connection free of leakage. Gas analyzer optical filter configuration and sampling integration time followed the same setup reported in Maia et al. (2014). The solenoid array in the gas multiplexer was independently tested and found to have no leaks prior to the GSS integrity test (Sun, 2013).

$$GSSR = 100 \times \frac{C_{measured} (full\ sampling\ line)}{C_{target} (calibration)} \quad (\text{Equation 5.1})$$

where

- $GSSR$ = gas sampling subsystem recovery (%)
- $C_{measured}$ = measured gas concentration (ppm_v)
- C_{target} = target gas concentration determined from post-calibration check (6.235 ppm_v)

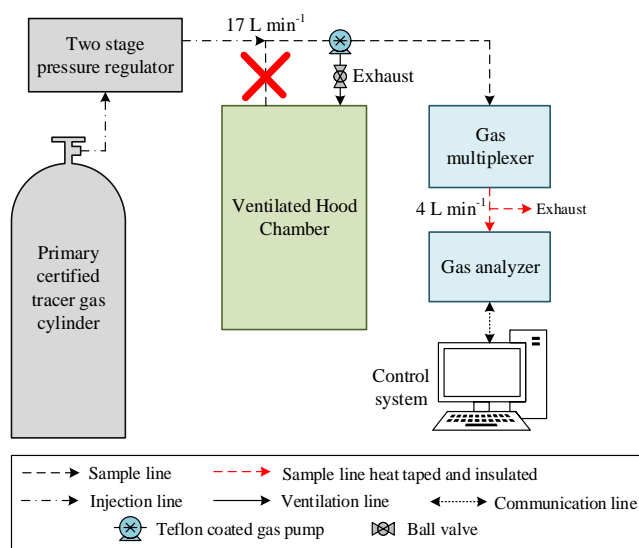


Figure 5.2. Configuration of gas sampling subsystem integrity test for one chamber. Sampling line was disconnected from the sampling port located through the top of the chamber and connected to the outlet of a tracer gas cylinder. FASMS, TECS, and other GSS components omitted for clarity. Same procedure and configuration was applied for each of the six chambers.

5.3.3 Steady-State Mass Recovery Test

A Steady-State Mass Recovery Test (SSMRT) was developed to provide a whole system evaluation for one chamber at a time. The SSMRT consisted of the injection of a known quantity mass (reference) and comparing it to the mass measured by REMS. This approach is useful to verify system performance and identify potential problems that might have developed such as leaks or failed components (McLean & Tobin, 1987).

5.3.3.1 Experimental Setup

Mass flow injected (reference): A SSMRT was performed individually in each of the six chambers with eight replicates ($n = 8$) in time for each chamber. The mass flow injected into the system (reference) was supplied by a primary certified tank containing 3929 ppm_v (first four replicates) and 3947 ppm_v (last four replicates) of SF₆ (tracer gas) balanced with N₂ (Airgas Inc., Bowling Green, KY, USA) connected to a Mass Flow Controller (MFC) (Series 4040,

Environics, Tolland, CT, USA) and set to inject a constant flowrate of 4 L min^{-1} (Figure 5.3; Figure 5.4).

Mass flow recovered: REMS was set to operation as if an animal were present in the chamber, with the TECS and FASMS operating and the feed bin in place (Figure 5.3). Dry-bulb temperature and relative humidity from the background (incoming ventilation) and mixed chamber gas were recorded at each gas concentration measurement during steady-state conditions. Fresh air ventilation rate was set at a constant rate for each SSMRT and ranged from 479.1 to 525.1 lpm (16.9 to 18.6 cfm) for all chambers and replicates, which was the calculated ventilation rate required for control of moisture, temperature, and CO_2 with one animal in the chamber for a cattle weight range of 230 to 1000 kg. Gas analyzer optical filter configuration and sampling integration time was set as reported in Maia et al. (2014). The outlet tube from the MFC was placed where the TECS recirculation supply and FASMS supply mixed. This ensured thorough mixing of the injected gas upon release. The canvas hood located in the back of the chamber was cinched around a 38.1 cm (15 in.) diameter plastic pipe. The inside area of the pipe was sealed and a 103 cm^2 (16 in.²) section was removed to create a small opening serving as a conservative representation of the leakage around the animal's neck. This procedure was verified to not affect positive pressurization of the chamber (Sun, 2013). Prior to gas injection, five background gas concentrations were measured at the ventilation inlet, followed by five additional background measurements inside the chamber (Figure 5.4). During tracer gas injection, 12 consecutive measurements collected at steady-state were used to determine REMS mass flow recovered. Finally, after all chamber samples were collected, 10 additional background concentrations were recorded and averaged with the first ten recorded background concentrations (prior to injection), to establish a mean background concentration.

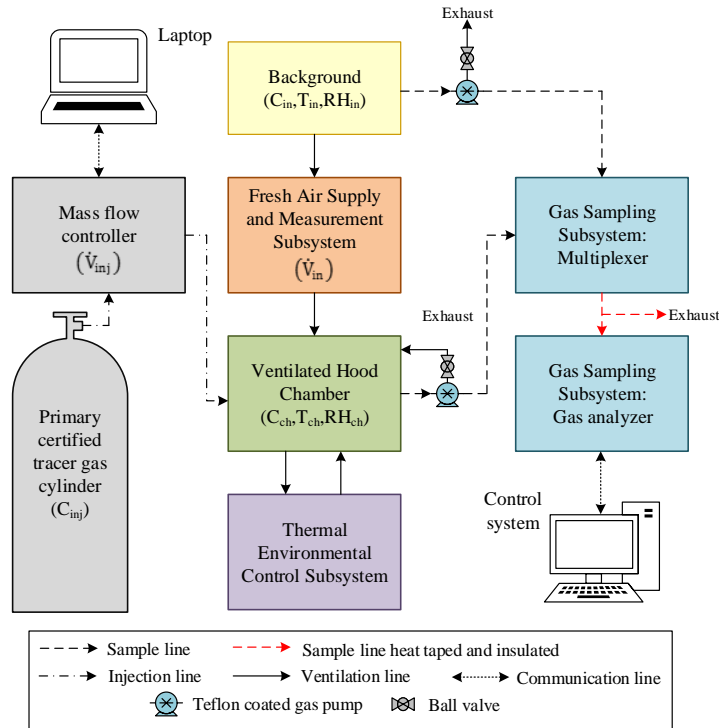


Figure 5.3. Experimental setup for steady-state mass recovery test in one chamber. Tracer gas (C_{inj}) was supplied at a constant volumetric flow (\dot{V}_{inj}) from a mass flow controller. Mass recovered was determined from temperature (T_{in} , T_{ch}), relative humidity (RH_{in} , RH_{ch}), gas concentration (C_{in} , C_{ch}), and ventilation rate (\dot{V}_{in}) measurements in REMS.

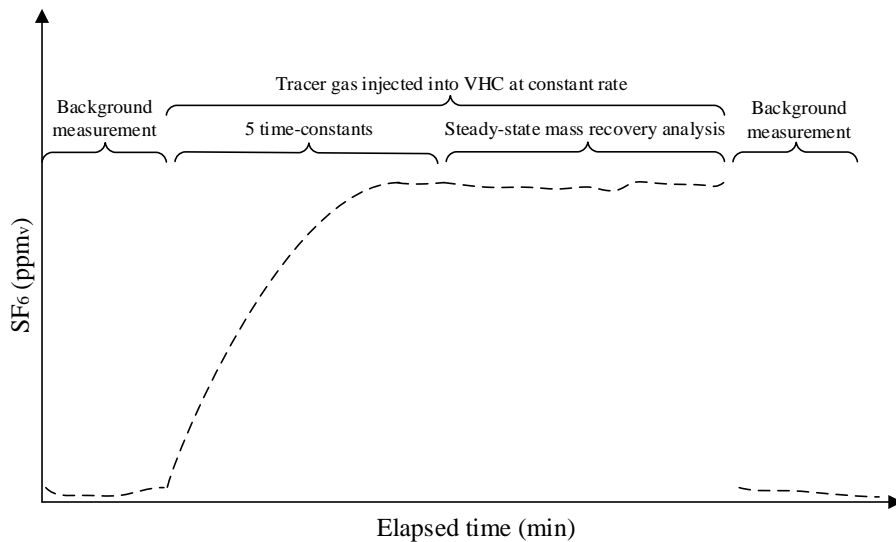


Figure 5.4. The system was considered to be at the steady-state after five system time constants. Recovery test procedure measured background first, allowed the chamber to reach steady-state, and concluded with background measurement.

5.3.3.2 Steady-State Determination

The system time constant was determined for each VHC from the time series recording of tracer gas injection. The time constants then served as a metric to determine the time to reach the chamber steady-state for an elapsed time of five time-constants ($\cong 99\%$ of the steady-state; Figure 5.5). The time constant was determined assuming gas concentrations in each VHC acted as a first order system (Zhang, 2005). Thus, this initial value problem (Equation 5.2) can be written as:

$$C(t) = C_s + (C_0 - C_s)e^{-\frac{t}{\tau}} \quad (\text{Equation 5.2})$$

where

- $C(t)$ = tracer gas concentration as a function of time (ppm_v)
- C_s = steady-state tracer gas concentration (ppm_v)
- C_0 = incoming tracer gas concentration (ppm_v)
- t = time (min)
- τ = system time-constant (min⁻¹)

The regression parameters C_s , C_0 , and τ were estimated from a non-linear regression of tracer gas concentrations versus elapsed time using the software package Origin-Pro 9 (OriginLab, Northampton, MA, USA).

5.3.4 Steady-State Mass Recovery Analysis

The measurement parameters described in the experimental setup were used in the analysis of the ratio between mass recovered and mass injected. When expressed on a percent basis, this ratio determines the Steady-State Mass Recovery Percent (SSMRP). Mass flow injected and recovered were obtained for each steady-state measurement prior to their integration over the steady-state period, which subsequently determines total mass injected and total mass recovered, respectively. The mass flow recovery equation was obtained from a derivation of a tracer gas component mass balance (with VHC chamber as the control volume) at steady-state, while the

mass flow injected equation was a function of the volumetric flow and tracer gas cylinder concentration.

5.3.4.1 Reference Mass Injected

Total mass injected during steady-state was determined by the constant mass flow injected (Equation 5.3) integrated over the steady-state period (Equation 5.4). Further, the mass flow injected was calculated from the volumetric flowrate at standard conditions and the concentration of the tracer gas. The mass injected was obtained as follows:

$$\dot{m}^{inj} = \dot{V}_{inj} \times C_{inj} \times \frac{M \cdot p_{std}}{R \cdot T_{std}} \times 10^{-6} \quad (\text{Equation 5.3})$$

where

\dot{m}^{inj}	= mass flow injected (g h ⁻¹)
\dot{V}_{inj}	= injected volumetric flowrate (m ³ s ⁻¹)
C_{inj}	= injected gas concentration (ppm _v)
M	= molecular mass of gas (146.06 kg mol ⁻¹)
R	= universal constant of ideal gases (8.314 m ³ Pa K ⁻¹ mol ⁻¹)
T_{std}	= standard temperature (273.15 K)
p_{std}	= standard pressure (101325 Pa)

$$m^{inj} = (t_n - t_1) \times \dot{m}^{inj} \quad (\text{Equation 5.4})$$

where

n	= number of steady-state measurements
m^{inj}	= total tracer gas mass injected by the reference (g)
t_n	= time at last steady-state measurement (h)

Because the tracer gas injection rate was constant, the area under the curve (mass flow rate versus time) was obtained straightforwardly from the multiplication of the mass flow rate injected times the duration of the steady-state duration.

5.3.4.2 Mass Recovered

The moist air mass flow balance previously presented in Maia et al. (2014; Equation 5.1) requires an additional input due to the non-negligible mass contribution of the injected tracer gas

mixture. Including the injected tracer gas flowrate, the moist air mass flow balance (Equation 5.5) becomes:

$$\dot{V}_{ex}^{rec} = \dot{V}_{in} \times \left(\frac{\rho_{in}^{ma}}{\rho_{ex}^{ma}} \right) + \dot{V}_{inj} \times \left(\frac{\rho_{inj}^{cyl}}{\rho_{ex}^{ma}} \right) \quad (\text{Equation 5.5})$$

where

$$\begin{aligned} \dot{V}_{ex}^{rec} &= \text{exhaust volumetric flowrate (m}^3 \text{ s}^{-1}\text{)} \\ \dot{V}_{in} &= \text{incoming air flowrate (m}^3 \text{ s}^{-1}\text{)} \\ \rho_{in}^{ma} &= \text{incoming moist air density (kg}_{\text{da}} \text{ m}^{-3}\text{)} \\ \rho_{ex}^{ma} &= \text{exhaust moist air density (kg}_{\text{da}} \text{ m}^{-3}\text{)} \\ \dot{V}_{inj} &= \text{the injected tracer gas flowrate (m}^3 \text{ h}^{-1}\text{)} \\ \rho_{inj}^{cyl} &= \text{dry density of the injected tracer gas at standard conditions (273.15 K and} \\ &\quad \text{101325 Pa; 6.52 kg}_{\text{dry mixture}} \text{ m}_{\text{dry volume mixture}}^{-3}\text{)}. \end{aligned}$$

Thus, the second term on the right hand side of Equation 5.5 accounts for tracer gas injection. Density of the tracer gas mixture (Equation 5.6) was determined as follows:

$$\rho_{inj}^{cyl} = y_{N_2} \times \rho_{N_2}^{std} + y_{SF_6} \times \rho_{SF_6}^{std} \quad (\text{Equation 5.6})$$

where

$$\begin{aligned} y_{N_2} &= \text{mole fraction of N}_2 \text{ in the cylinder (dimensionless)} \\ \rho_{N_2}^{std} &= \text{dry densities of N}_2 \text{ at standard conditions (1.25 kg}_{\text{dry mixture}} \text{ m}_{\text{dry volume mixture}}^{-3}\text{)}. \\ y_{SF_6} &= \text{mole fraction of SF}_6 \text{ in the cylinder (dimensionless)} \\ \rho_{SF_6}^{std} &= \text{dry densities of SF}_6 \text{ at standard conditions (6.17 kg}_{\text{dry mixture}} \text{ m}_{\text{dry volume mixture}}^{-3}\text{)}. \end{aligned}$$

A similar gas mass flow balance derived in Maia et al. (2014; Equation 4.2) was used in the SSMRP analysis with one modification: substitution of the exhaust volumetric flow rate \dot{V}_{ex}^{rec} from Equation 5.5, which accounts for the addition of the injected mass flow of the tracer gas into the chamber. The difference between the exhaust mass flow rate (\dot{m}_{ex}^{gas}) and the incoming mass flowrate (\dot{m}_{in}^{gas}) produces the following mass recovery rate equation (Equation 5.7):

$$\dot{m}^{rec} = \left[\left(\dot{V}_{in} \frac{\rho_{in}^{ma}}{\rho_{ex}^{ma}} + \dot{V}_{inj} \frac{\rho_{inj}^{cyl}}{\rho_{ex}^{ma}} \right) \cdot \frac{C_{ch}}{T_{ch}} - \left(\dot{V}_{in} \frac{C_{in}}{T_{in}} \right) \right] \cdot 10^{-6} \frac{M \cdot P_b}{R} \quad (\text{Equation 5.7})$$

where

$$\begin{aligned} \dot{m}^{rec} &= \text{recovered gas mass flow (g h}^{-1}\text{)} \\ C_{ch} &= \text{chamber gas concentration (ppm}_v\text{)} \\ C_{in} &= \text{incoming background gas concentration (ppm}_v\text{)} \\ T_{in} &= \text{chamber dry-bulb temperature (K)} \end{aligned}$$

T_{ch} = incoming background dry-bulb temperature (K)
 M = molecular mass of gas (g mol⁻¹)
 p_b = local barometric pressure (98.639 kPa; ASHRAE, 2013)

In Maia et al. (2014; Equations 4.2 and 4.3), the difference between the exhaust gas mass flow and incoming gas mass flow was equal to the generated gas mass flow, which provided the animal emission rate ($\dot{m}_{ex}^{gas} - \dot{m}_{in}^{gas} = \dot{m}_{gen}^{gas} = ER$). Here, the difference produces the mass flow recovered ($\dot{m}_{ex}^{gas} - \dot{m}_{in}^{gas} = \dot{m}^{rec}$) instead (Equation 5.7). This is an important distinction because the emission rate equation (Maia et al., 2014) does not account for systematic uncertainties (bias) that can only be verified through assessment of system operation and performance.

The total mass recovered (Equation 5.8) was determined by a trapezoidal integration of the mass flow over the steady-state period:

$$m^{rec} = \sum_{i=1}^{n-1} \frac{1}{2} (t_{i+1} - t_i) \times (\dot{m}_i^{rec} + \dot{m}_{i+1}^{rec}) \quad (\text{Equation 5.8})$$

where

n = number of steady-state measurements
 m^{rec} = total tracer gas mass recovered by REMS (g)
 t = time at steady-state measurement i (h)

The input parameters for this test included incoming and chamber temperatures, moist air densities, and tracer gas concentrations.

5.3.4.3 Steady-State Mass Recovery

The ratio of the mass recovered by REMS (Equation 5.8) to the mass injected by the reference (Equation 5.4) was defined as the SSMRP (Equation 5.9):

$$SSMRP = 100 \times \left(\frac{m^{rec}}{m^{inj}} \right) \quad (\text{Equation 5.9})$$

where

$SSMRP$ = steady-state mass recovery percent (%)

5.3.5 Steady-State Mass Recovery Uncertainty Analysis

The steady-state mass recovery percent standard uncertainty is determined from the propagation of standard uncertainties (ISO/IEC, 2008; Taylor & Kuyatt, 1994) from input measurements to mass recovered (Equation 5.8) and mass injected (Equation 5.4). The standard uncertainties (Δ) are the associated best estimate of combined measurement error of each parameter obtained with a truncated first-order Taylor series approximation applied to Equation 5.3 and Equation 5.7 assuming independent measurements (Jordan, 1991; Gates, 1994; and Gates et al., 2009). The following sections characterize additional uncertainties associated with the commissioning of the system, and include uncertainty analyses for the reference mass injected (mass flow and total mass), mass recovered (total mass), and SSMRP reproducibility. Parameter standard uncertainties associated with mass flow recovered temperature, relative humidity, moist air density, ventilation rate and gas concentration) are described elsewhere (Maia et al., 2014; Ramirez et al., 2014). A normal error distribution (divisor = 1; C.I. = 68%) and rectangular error distribution (divisor = $\sqrt{3}$; C.I. = 68%) were applied accordingly (Taylor & Kuyatt, 1994).

5.3.5.1 Reference Mass Injected

The tracer gas mass flow injected uncertainty (Equation 5.10) was the combination of three primary sources of uncertainty, including tracer gas concentration, flowrate of injection, and tracer gas density:

$$\Delta \dot{m}^{inj} = \sqrt{\left(\frac{\partial \dot{m}^{inj}}{\partial C_{inj}} \Delta C_{inj}\right)^2 + \left(\frac{\partial \dot{m}^{inj}}{\partial \dot{V}_{inj}} \Delta \dot{V}_{inj}\right)^2 + \left(\frac{\partial \dot{m}^{inj}}{\partial \rho_{inj}^{cyl}} \Delta \rho_{inj}^{cyl}\right)^2} \quad (\text{Equation 5.10})$$

where

- $\Delta \dot{m}^{inj}$ = mass flow injected standard uncertainty (g h^{-1})
- ΔC_{inj} = tracer gas concentration standard uncertainty (ppm_v)
- $\Delta \dot{V}_{inj}$ = injected flowrate standard uncertainty ($\text{m}^3 \text{s}^{-1}$)
- $\Delta \rho_{inj}^{cyl}$ = injected tracer gas mixture density standard uncertainty (kg m^{-3})

Tracer gas concentration standard uncertainty (Equation 5.11) was based on the primary certified tolerance specified by the manufacturer (Airgas Inc., Bowling Green, KY, USA) and the concentration uncertainty of the MFC accuracy. A rectangular distribution was assumed for the two sources of uncertainty:

$$\Delta C_{inj} = \sqrt{\left(\frac{MFCA \times SP}{\sqrt{3}}\right)^2 + \left(\frac{PCT \times CV}{\sqrt{3}}\right)^2} \quad (\text{Equation 5.11})$$

where

- PCT* = primary certified tolerance ($\pm 1\%$ of the certified value)
- CV* = certified value (ppm_v)
- MFCA* = mass flow controller accuracy ($\pm 1\%$ of the set-point)
- SP* = set point for *CV* (ppm_v).

The injected flow rate had three major sources of uncertainty (Equation 5.12): calibration reference standard error obtained from the manufacturer's NIST traceable calibration (normal distribution), repeatability of the measurements, and reading resolution (rectangular distributions):

$$\Delta \dot{V}_{inj} = \sqrt{\left(\frac{CRSE_x}{1}\right)^2 + \left(\frac{Rep}{\sqrt{3}}\right)^2 + \left(\frac{Res}{\sqrt{3}}\right)^2} \quad (\text{Equation 5.12})$$

where

- CRSE_x* = calibration reference standard error (3.63E-07 m³ s⁻¹; normal distribution)
- Rep* = repeatability (0.0005·*SP* m³ s⁻¹; rectangular distribution)
- Res* = resolution (1.67E-11 m³ s⁻¹; rectangular distribution)

Tracer gas mixture density standard uncertainty (Equation 5.13) was defined from the combined contribution of uncertainty in molar fraction of constituents in the mixture:

$$\Delta \rho_{inj}^{cyl} = \sqrt{\left(\frac{\partial \rho_{inj}^{cyl}}{\partial y_{N_2}} \Delta y_{N_2}\right)^2 + \left(\frac{\partial \rho_{inj}^{cyl}}{\partial y_{SF_6}} \Delta y_{SF_6}\right)^2} \quad (\text{Equation 5.13})$$

where

- Δy_{N_2} = molar fraction of nitrogen (dimensionless; $\pm 1\%$ relative; rectangular distribution)
- Δy_{SF_6} = molar fraction of sulfur hexafluoride (dimensionless; $\pm 1\%$ relative; rectangular distribution)

distribution)

The mass injected standard uncertainty (Equation 5.14) was determined as follows:

$$\Delta m^{inj} = \sqrt{((t_n - t_1) \times \Delta \dot{m}^{inj})^2} \quad (\text{Equation 5.14})$$

where

- n = number of steady-state measurements
- Δm^{inj} = tracer gas mass injected by the reference standard uncertainty (g)
- $\Delta \dot{V}_{inj}$ = injected flowrate standard uncertainty ($\text{m}^3 \text{s}^{-1}$)
- ΔC_{inj} = injected tracer gas concentration standard uncertainty (ppm_v)

5.3.5.2 Mass Recovered

The standard uncertainty of mass recovered (Equation 5.15) can be written as:

$$\Delta m^{rec} = \sqrt{\sum_{i=1}^{n-1} \left(\frac{1}{2} (t_{i+1} - t_i) \times (\Delta \dot{m}_i^{rec} + \Delta \dot{m}_{i+1}^{rec}) \right)^2} \quad (\text{Equation 5.15})$$

where

- n = number of steady-state measurements
- Δm^{rec} = total tracer gas mass recovered by REMS standard uncertainty (g)
- $\Delta \dot{m}_i^{rec}$ = mass flow recovered standard uncertainty (g h^{-1})

5.3.5.3 Reproducibility

Reproducibility (Equation 5.16; Taylor & Kuyatt, 1994) of SSMRP was the variability of the replicated measurements in time ($n = 8$) obtained over a one-year period:

$$Rep_c = \sqrt{\frac{1}{n-1} \sum_{r=1}^n (SSMRP_{c,r} - \overline{SSMRP}_c)^2} \quad (\text{Equation 5.16})$$

where

- Rep_c = reproducibility of SSMRP for c^{th} chamber (%)
- n = number of replicates ($n = 8$)
- c = chamber {1,...,6}
- r = replicate {1,...,n}
- $SSMRP_{c,r}$ = steady-state mass recovery percent for c^{th} chamber and r^{th} replicate (%)
- \overline{SSMRP}_c = mean ($n = 8$) steady-state mass recovery percent for c^{th} chamber (%)

Changes in conditions for the reproducibility test included personnel taking the measurements, time and day of the measurements, and changes in indoor and outdoor environmental conditions.

5.3.5.4 Steady-State Mass Recovery Percent

Finally, the SSMRP uncertainty (Equation 5.17) was obtained from the combined uncertainties associated with the mass injected, mass recovered, and SSMRP analysis reproducibility:

$$\Delta SSMRP_{c,r} = \sqrt{\left(\frac{\partial SSMRP_{c,r}}{\partial m_{c,r}^{inj}} m_{c,r}^{inj}\right)^2 + \left(\frac{\partial SSMRP_{c,r}}{\partial m_{c,r}^{rec}} \Delta m_{c,r}^{rec}\right)^2 + (Rep_c)^2} \quad (\text{Equation 5.17})$$

where

$\Delta SSMRP$ = steady-state mass recovery percent standard uncertainty (%)

A coverage factor of two ($k = 2$) was applied to the SSMRP standard uncertainty in order to expand the confidence interval to 95% (Maia et al., 2014; Taylor & Kuyatt, 1994). Relative standard uncertainty was also expanded following the same coverage factor. Table 5.1 summarizes the sources of uncertainties used to calculate $\Delta SSMRP$.

Table 5.1. Summary from instrument and parameter error analysis used to determine standard uncertainty associated with mass flow recovered, mass flow injected, and steady-state mass recovery percent.

Parameter symbol	Unit	Description	Source of uncertainty	Manufacturer	Source
$\Delta T_{in}, \Delta T_{ch}$	K	Dry-bulb temperature	T/RH sensor	Vaisala, HMP60-L, Helsinki, Finland	Ramirez et al., 2014
$\Delta RH_{in}, \Delta RH_{ch}$	%	Relative humidity	T/RH sensor	Vaisala, HMP60-L, Helsinki, Finland	Ramirez et al., 2014
$\Delta \dot{V}_{in}$	$m^3 s^{-1}$	Incoming flowrate	Orifice meter	Custom	Ramirez et al., 2014
$\Delta \rho_{in}^{ma}, \Delta \rho_{ch}^{ma}$	$kg m^{-3}$	Moist air density	Equation 2-16 (Albright 1990)	-	Ramirez et al., 2014
$\Delta C_{in}, \Delta C_{ch}$	ppm _v	Gas concentration	Infrared photoacoustic multi-gas analyzer	INNOVA 1412, LumaSense Technologies, Inc., Santa Clara, CA, USA	Maia et al., 2014
$\Delta \dot{V}_{inj}$	$kg m^{-3}$	Injected flowrate	Mass flow controller	Series 4040, Environics, Tolland, CT, USA	Equation 5.11
ΔC_{inj}	ppm _v	Tracer gas concentration	Primary certified cylinder	Airgas, Inc., Bowling Green, KY, USA	Equation 5.12
$\Delta \rho_{inj}^{cyl}$	$kg m^{-3}$	Tracer gas mixture density	Primary certified cylinder	-	Equation 5.13
Rep_c	%	Replications of SSMRT	Standard deviation of mean SSMRP	-	Equation 5.16

5.3.6 Systematic Error Analysis

5.3.6.1 Test for Significance

For each chamber, the SSMRPs and their standard uncertainties calculated from the replicated ($n = 8$) SSMRT, were used to determine if the mean SSMRP was significantly different from the hypothetical mean of 100% mass recovered. If so, this would indicate that a bias existed in the mass recovered measurement for each chamber.

Let the mean SSMRP for each chamber be independent normal random variable with an unknown population mean and let the best estimate of population variance be the mean standard uncertainty of SSMRP. The mean standard uncertainty of SSMRP was calculated as follows:

$$\overline{\Delta SSMRP}_c = \frac{1}{n} \sqrt{\sum_{r=1}^n (\Delta SSMRP_{c,r})^2} \quad (\text{Equation 5.18})$$

where

$$\overline{\Delta SSMRP}_c = \text{mean standard uncertainty of SSMRP (\%)}$$

Equation 5.19 provides the basis for a hypothesis test for whether a significant systematic bias exists. For no bias, \overline{SSMRP}_c for each chamber would be 100%. Assuming that \overline{SSMRP}_c is distributed according to the Student t-distribution with standard error given by Equation 5.18.

$$t_c^{calc} = \frac{\overline{SSMRP}_c - 100}{\Delta \overline{SSMRP}_c} \quad (\text{Equation 5.19})$$

Is distributed according to the Student t-distribution with mean zero and variance unity, where t_c^{calc} = calculated t value for each chamber c

For this work, there were 8 repetitions of SSMRT for each chamber (n=8); thus; 7 degrees of freedom (n-1), and significance was assumed at the two-sided 5% level ($t_{\frac{(1-\alpha)}{2}, v} = 2.365$, for two-tailed test with $\alpha = 0.05$, $v = 7$).

5.3.6.2 Bias Correction

For systematic errors that are found to be significant ($p < 0.05$), a correction factor can be applied to the accumulated emission (Equation 5.20). The effective accumulated emission was obtained from the multiplication of a correction factor (mean SSMRP fraction) by the computed accumulated emission (Maia et al., 2014):

$$E_c^{eff} = E_c \times \left(\frac{100}{\overline{SSMRP}_c} \right) \quad (\text{Equation 5.20})$$

where

E_c^{eff} = effective accumulated emission per chamber c (g)

E_c = accumulated emission per chamber c (g; Maia et al., 2014; Equation 4.4)

The standard uncertainty associated with effective accumulated emission (Equation 5.21) combined the accumulated emission standard uncertainty (Maia et al., 2014; Equation 4.6) and $\Delta \overline{SSMRP}_c$ (Equation 5.18), yielding the following equation:

$$\Delta E_c^{eff} = \sqrt{\left(\frac{\partial E_c^{eff}}{\partial E_c} \Delta E_c \right)^2 + \left(\frac{\partial E_c^{eff}}{\partial \overline{SSMRP}_c} \Delta \overline{SSMRP}_c \right)^2} \quad (\text{Equation 5.21})$$

where

ΔE_c^{eff} = standard uncertainty of effective accumulated emission per chamber c (g)

If a significance test rejects the hypothesis of a system bias, the correction (Equations 5.20 and 5.21) does not apply.

5.4 Results and Discussion

5.4.1 Subsystem Validation

The spatial distribution of static pressure inside the chambers verified chamber positive pressurization. The thermal environment performance verified the thermal environmental control system removal of moisture and maintenance of set-point temperature in the presence of an animal. The gas sampling subsystem evaluation assessed discrepancies between the known reference gas concentration and the concentration measured with the gas analyzer. Each validation is summarized below.

5.4.2 Ventilated Hood Chamber Pressure Distribution

The six chambers were found to be positively pressurized for all scenarios tested (Figure 5.1) with values ranging from 14.5 to 37.8 Pa. The minimum value of 14.5 Pa is approximately 60 times greater than the resolution of the pressure transducer (0.25 Pa). The average and standard deviation for each sample location across the three regions and average and standard deviation for all sample locations in each region are summarized in Table 5.2. Visual observation of chamber flow patterns with the smoke test also confirmed chamber positive internal pressurization. The smoke moved outwards from chamber to the room when smoke was released inside each chamber. No smoke entered the chamber when released outside of each chamber.

Table 5.2. Pressure distribution for the six chambers at five sample locations and three chamber regions corresponding to Figure 5.1. Results are the average of each sample location across the three regions, and the average of the five cross-section sample locations for each of the three regions.

Chamber ID	Pressure (Pa) = (mean ± standard deviation)							
	Cross section location (n ^[1] = 3)					Height (n ^[1] = 5)		
	1	2	3	4	5	Upper	Middle	Lower
1	25 ± 2.1	25 ± 0.9	23 ± 1.7	24 ± 1.4	24 ± 1.1	23 ± 1.5	25 ± 1.4	24 ± 1.1
2	23 ± 3.1	22 ± 3.7	22 ± 3.4	20 ± 1.5	19 ± 0.4	22 ± 3.0	23 ± 2.4	18 ± 0.9
3	23 ± 0.9	22 ± 4.1	21 ± 0.4	24 ± 2.7	21 ± 1.2	24 ± 2.2	21 ± 1.1	22 ± 2.6
4	20 ± 2.0	21 ± 3.6	22 ± 6.5	20 ± 2.2	17 ± 2.3	17 ± 1.7	22 ± 3.0	21 ± 3.2
5	33 ± 6.7	35 ± 2.0	35 ± 1.6	35 ± 0.6	33 ± 2.2	35 ± 1.8	35 ± 1.2	32 ± 4.3
6	19 ± 0.5	19 ± 2.7	17 ± 1.9	17 ± 2.5	20 ± 0.8	17 ± 2.5	19 ± 1.1	19 ± 1.1

^[1] n = number of samples

5.4.2.1 Thermal Environment Performance

Temperature for each chamber was maintained within the desired temperature range (15°C to 25°C) for adult cattle (Federation of Animal Science Societies, 2010). Chamber and background temperatures ranged from 20.5°C to 24.1°C and 21.9°C to 26.2°C, respectively (Figure 5.5; Table 5.3). Chamber temperatures were influenced by diurnal patterns of background temperature. The TECS was also effective for moisture removal shown by no significant increase in the humidity ratio (accumulation of moisture) of chambers using the background humidity ratio as the reference; thus, moisture was constantly removed and kept below the humidity ratio saturation (Figure 5.6; Table 5.3). Humidity ratio ranged from 8.1 to 12.6 g_{H2O} kg_{da}⁻¹ for chambers and 9.5 to 12.6 g_{H2O} kg_{da}⁻¹ for the background. The background temperature for the duration of the test remained above the dew point temperatures (13.7°C to 15.9°C) inside the chambers; therefore, no internal condensation was formed. Condensation or excessive moisture has substantial negative impacts on gas concentration measurements because of potential gas sample dilution and gas compromised analyzer operation.

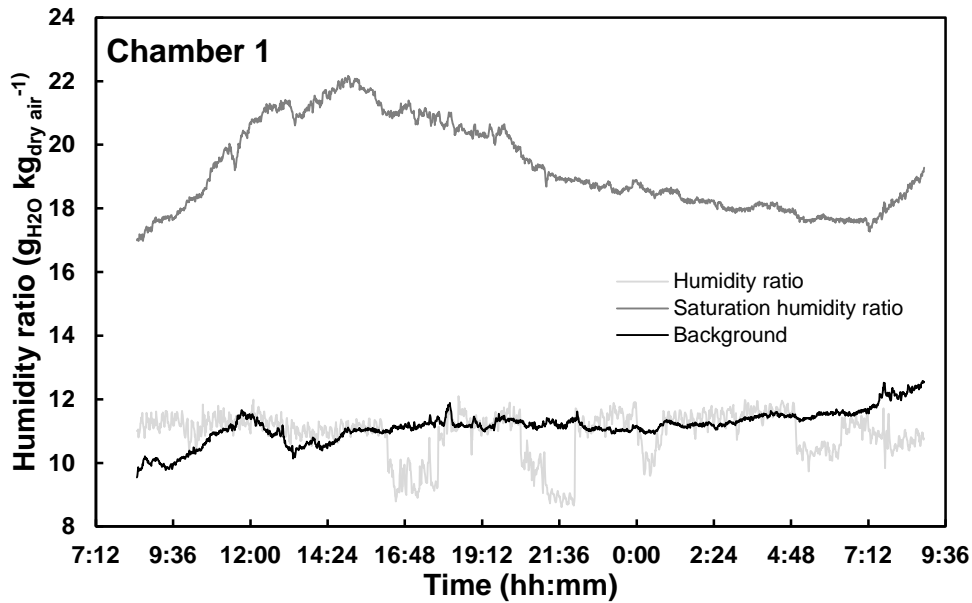


Figure 5.5. Example of temperature measurement over approximately 23 h for chamber 1 and the background. All chambers were maintained within the desired temperature range (upper limit of 25°C shown in figure) despite exceeding background conditions and no condensation formed inside the chambers.

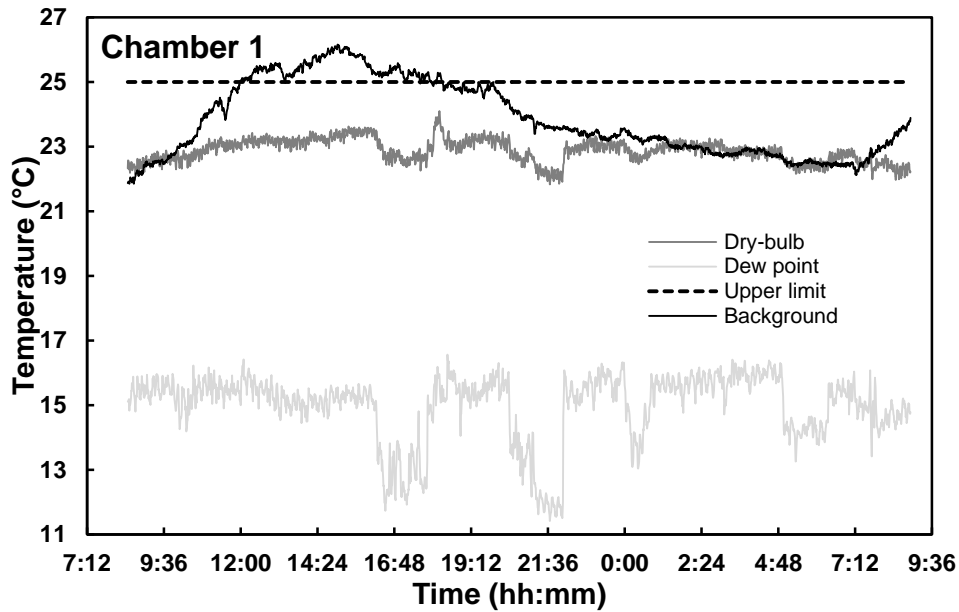


Figure 5.6. Example of humidity ratio from temperature and relative humidity measurement over approximately 23 h for chamber 1 and the background. All chambers adequately removed moisture generated by the animal.

Table 5.3. Summary of dry-bulb temperatures, dew point temperatures, and humidity ratios inside the chambers with animals present for approximately 23 h.

Parameter		Chamber ID						Background
		1	2	3	4	5	6	
Temperature (°C)	Mean ± SD ¹	22.9 ± 0.4	22.9 ± 0.4	22.5 ± 0.3	22.7 ± 0.3	22.4 ± 0.4	22.2 ± 0.4	23.8 ± 1.2
	Maximum	24.1	23.7	23.2	23.5	23.1	23	26.2
	Minimum	21.83	22	21.62	21.4	20.72	20.51	21.85
Dew point Temperature (°C)	Mean ± SD ¹	15.7 ± 0.8	14.8 ± 0.9	15.9 ± 0.7	15.4 ± 0.6	14.6 ± 0.7	15.3 ± 0.7	15 ± 1.1
	Maximum	17.2	17	17.2	16.8	15.9	17.2	16.6
	Minimum	13.7	12.4	13.2	12	10.6	13	11.4
Humidity ratio (g H ₂ O kg _{dry air} ⁻¹)	Mean ± SD ¹	10.9 ± 0.7	11.4 ± 0.6	10.8 ± 0.6	11.6 ± 0.5	11.3 ± 0.5	10.6 ± 0.5	11.1 ± 0.5
	Maximum	12.1	12.6	12.4	12.6	12.3	11.6	12.6
	Minimum	8.6	10	9.2	9.7	8.9	8.1	9.5

¹SD = standard deviation

5.4.2.2 Gas Sampling Subsystem Integrity

The six gas sampling paths (from each of the six chambers through the multiplexer to the gas analyzer) evaluated in the gas sampling subsystem integrity test achieved a recovery within the uncertainty of the gas analyzer ($\leq \pm 2\%$). Gas sampling subsystem recoveries ranged from 100.0% to 101.4% of the expected value. Results indicated that there was no leakage into the gas sampling path, which would have been identifiable by a diluted sample.

5.4.3 Steady-State Determination

The time constant for the exchange rate of fresh air in each chamber (four replicates) ranged from 2.31 to 2.5 min⁻¹ and the time for each chamber to reach steady-state (5τ) ranged from 11.57 to 12.48 min (Table 5.4). A regression plot for a chamber is shown as an example (Figure 5.7). This information established that gas concentration measurements used to calculate mass flow recovered or ER are made after 14 min (a conservative estimate that ensured steady-state for all chambers) after the start of injection or disturbance in the system.

Table 5.4. Summary of non-linear regression for four replicates (n=4) to determine the exchange rate of fresh air time constant (τ) and time to reach steady-state (5τ). Each chamber had a unique time to reach steady-state ranging from 12.99 to 13.92 min; therefore, SSMRT analysis was conducted with gas concentration measurements after 14 min.

Chamber ID	Parameter (minimum - maximum)			Maximum time to reach steady-state ^[1] (min)
	R ²	Regression SE (ppm _v)	τ (min ⁻¹)	
1	0.98 - 1.00	0.19 - 1.16	2.17 - 2.71	13.54
2	0.98 - 1.00	0.15 - 1.15	2.13 - 2.78	13.92
3	0.99 - 1.00	0.21 - 0.88	2.18 - 2.60	12.99
4	0.98 - 1.00	0.12 - 1.30	2.09 - 2.69	13.45
5	0.98 - 1.00	0.25 - 1.02	2.30 - 2.61	13.07
6	0.99 - 1.00	0.13 - 1.00	2.36 - 2.75	13.74

^[1] five time constants (5τ)

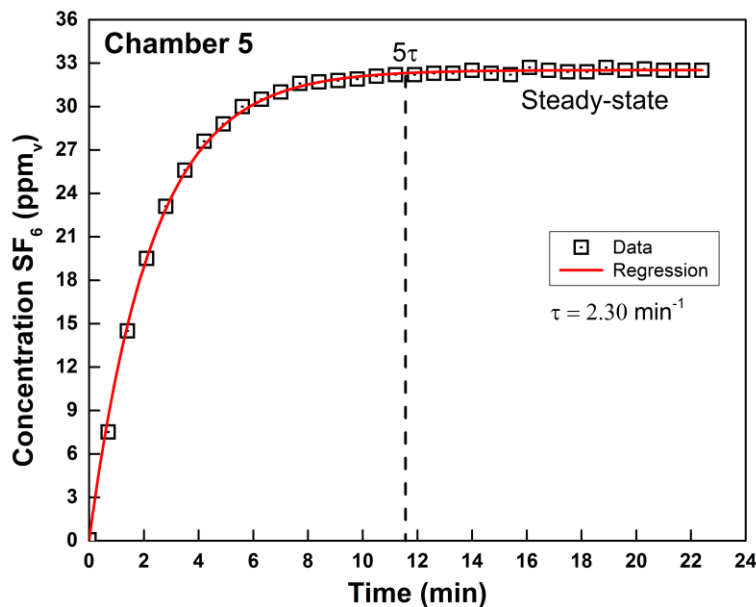


Figure 5.7. Example of the nonlinear regression steady-state analysis for one chamber. The full line is the nonlinear regression (Equation 5.2) fitted to the measured concentrations(data). Five time constants (τ) were used as a conservative estimate for determining the time to steady-state (< 14 min for all chambers).

Overall uncertainty for the regression was quantified with the regression Standard Error (SE). The SE of each coefficient (i.e. τ) provides information about the overall uncertainty associated with the computation of the time constant. In addition, the average coefficients of determination (R^2) were greater than 0.99 for the nonlinear regression applied to Equation 5.2.

The time to reach steady-state was used to improve experiment and operation protocols. For example, gas sampling should not begin until chamber conditions reach steady-state (i.e. after 14 min). Once gas concentration profile patterns are stable at a steady-state, changes in CH₄

generation can be estimated. For REMS, injected gas should be allowed to mix undisturbed for at least 14 min prior to using gas concentration measurements for analysis. In addition, if the chamber is opened during an experiment, gas concentration measurements must be discarded until the gas inside the chamber has returned to steady state.

This methodology for conducting a mass recovery test can potentially reduce labor costs and quantity of materials needed for each test. Four hours were required to perform a complete steady-state recovery analysis for the six chambers. In addition, one SF₆ primary certified tank can be used to complete 24 mass recovery tests. Alternative methods of mass recovery tests such as gas release from a cylinder on a balance or single volume gas injection from a canister can take upwards of four to 24 hours to complete (Hellwing et al., 2012; Williams, Klein, & Wright, 2007), and have greater costs due to the quantity of gas required.

5.4.4 Steady-State Mass Recovery Analysis

The mean SSMRP for the six chambers ranged from 92.0% (Chamber 3) to 96.6% (Chamber 6; Table 5.5). Reproducibility (standard deviation of the SSMRP mean) for each chamber ranged from 1.3% (Chamber 5) to 3.2% (Chamber 4). The technical literature has recommended recoveries from 95% to 105% for newly constructed respiration chambers (Suzuki et al., 2007), or an extensive evaluation should be conducted to attain 100% recovery (McLean & Tobin, 1987). Equally important is the systematic quantification and documentation of the uncertainties and bias associated with the recovery. Lower recovery, such as measured here, can be attributed to several factors including gas sampling system leakage, measurement errors, and non-ideal mixing inside the chamber. GSS leakage and infiltration in the chamber were excluded as a cause of lower recovery, because the GSS underwent a comprehensive and systematic evaluation of leaks and the chamber was verified as a positively pressurized low-leak system.

Second, instrument measurement error has been exhaustively covered (Maia et al., 2014). Non-ideal mixing patterns could occur from short-circuiting of the injected gas inside the chamber. While that might be a cause for recoveries lower than 95% in this work, the high reproducibility of the recoveries also indicated consistent bias. For these cases, systematic errors can be corrected following the previously described methods.

A correction factor may be applied in the event that recovery percent is not improved and different from 100% (McLean and Tobin 1987). McGinn et al. (2004) created correction factors accounting for between-chamber differences in order to increase treatment sensitivity. Using three replicated mass recovery tests during the course of an experiment, a correction factor for each chamber was obtained from the ratio of the maximum recovery to the other chambers recovery (McGinn, Beauchemin, Coates, & Colombatto, 2004). However, the development, validity, and consequence of these correction factors are scarcely documented, and what is reported does not include the detailed experimental and analytical procedures to determine mass recovery percent and its associated standard deviation (i.e. standard deviation of replicates or of the set of chambers; (Ramirez, 2014). An approach to correct for consistently lower recoveries (such as encountered here) was implemented to include reproducibility into the calculation of the mean SSMRP standard uncertainty (Equations 5.17 and 5.18).

Table 5.5. Summary of mass recovered by each chamber, mass injected by the reference, and the mean Steady-State Mass Recovery Percent (SSMRP) for eight replicates.

Chamber ID	Parameter (minimum - maximum)		
	Mass recovered (g)	Mass injected (g)	$\overline{SSMRP} \pm \text{Rep}^{[1]}$ (%)
1	0.7 - 1.0	0.8 - 1.1	93.2 ± 1.7
2	0.8 - 1.0	0.8 - 1.1	94.9 ± 1.6
3	0.7 - 1.0	0.8 - 1.1	92.0 ± 2.2
4	0.7 - 1.0	0.8 - 1.1	92.8 ± 3.2
5	0.8 - 1.1	0.8 - 1.1	94.3 ± 1.3
6	0.8 - 1.1	0.8 - 1.1	96.6 ± 1.4

^[1] Reproducibility; Equation 5.6

5.4.5 Steady-State Mass Recovery Standard Uncertainty

Standard uncertainty associated with the mass of recovered and injected tracer gas, and their ratio (SSMRP) were reported (Table 5.6). All six chambers exhibited a standard uncertainty of mass recovered < 0.06 g SF₆ (Table 5.6). Relative standard uncertainties of mass recovered was $< 6\%$ for all chambers and all replicates. Prior to integration over the steady-state test period, mass flow recovered standard uncertainty was similar to that reported for emission rate standard uncertainty (Maia et al., 2014). This was expected because the individual sources of uncertainty in the mass flow recovery and the uncertainties associated with these sources, were equivalent to those used to determine the uncertainties associated with emission rates. Mass injected standard uncertainty was the same for all six chambers (< 0.01 g of SF₆) with a relative standard uncertainty of 1.1% for all chambers and all replicates.

Table 5.6. Absolute (Abs.) and relative (Rel.) standard uncertainties for mass recovered and mass injected. The range of absolute standard uncertainties for SSMRP was also reported.

Chamber ID	Combined standard uncertainty (minimum – maximum)				
	Mass recovered		Mass injected		$\Delta SSMRP$ (%)
	Abs. (g)	Rel. (%)	Abs. (g)	Rel. (%)	
1	< 0.06	5.2 - 5.3	< 0.01	1.1	5.2 - 5.4
2	< 0.06	5.5 - 5.5	< 0.01	1.1	5.4 - 5.7
3	< 0.06	5.3 - 5.3	< 0.01	1.1	5.4 - 5.7
4	< 0.06	5.7 - 5.7	< 0.01	1.1	6.2 - 6.5
5	< 0.06	5.3 - 5.5	< 0.01	1.1	5.2 - 5.4
6	< 0.06	5.2 - 5.2	< 0.01	1.1	5.2 - 5.5

5.4.5.1 Mass Flow Recovered Contributions

For all six chambers, ventilation rate contributed the most to the mass flow recovered standard uncertainty, with contributions ranging from 48.3% (Chamber 1) to 60.3% (Chamber 4; Figure 5.8). Concentration measurement during the steady-state was the second highest contributor ranging from 32.8% (Chamber 4) to 42.1% (Chamber 1), followed by background concentration measurement ranging from 5.5% (Chamber 4) to 8% (Chamber 3; Figure 5.8). Absolute standard uncertainties of ventilation rate measurement (Ramirez, 2014; Ramirez et al.,

2014) and concentration measurement (Maia et al., 2014) are discussed elsewhere. Remaining sources (chamber and background temperature, density, and injected flow) totaled less than 3% for all chambers and all replicates. Although the background mass of SF₆ was not neglected in this analysis, it had a minimal effect on the overall standard uncertainty because SF₆ background concentrations were close to zero. The decision to maintain SF₆ background concentrations in the recovery model was retained so that this methodology may be extended to other candidate gases, where background concentrations are substantially present and variable (i.e., CO₂ and CH₄).

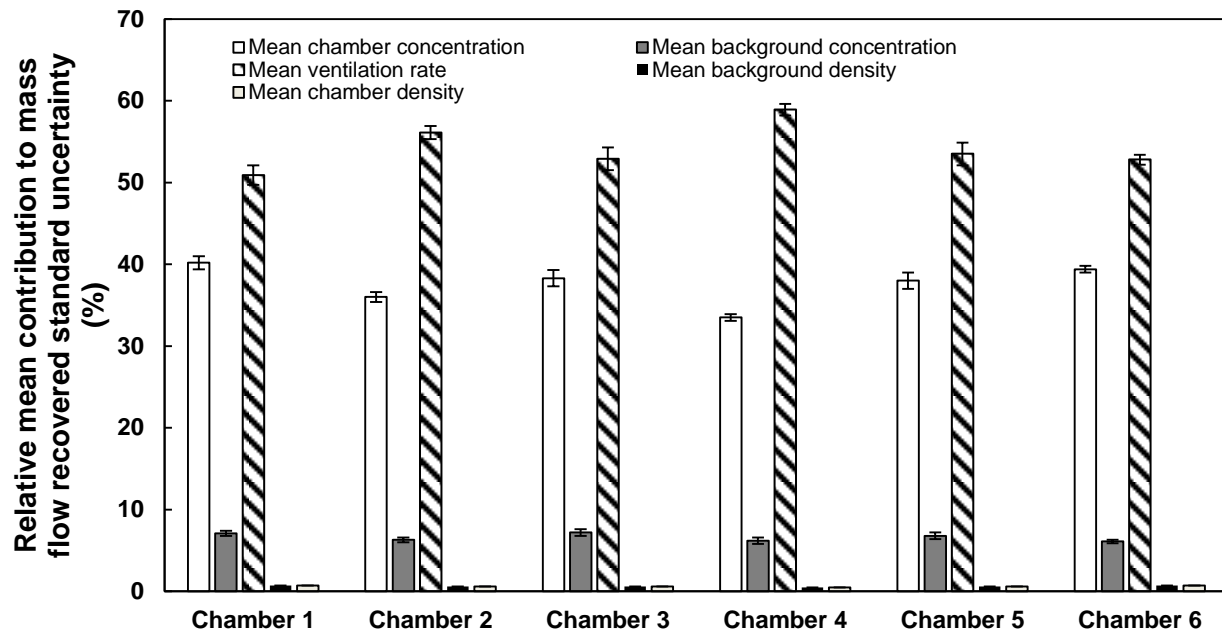


Figure 5.8. Relative mean contribution to mass flow recovered standard uncertainty averaged for all replicates. Error bars represent standard deviation obtained by replicates. Other parameters omitted for clarity and had < 3% contribution. Major contributions from ventilation rate and concentration measurement were consistent across all the six chambers.

5.4.5.2 Mass Flow Injected Contributions

For all six chambers, injected tracer gas flow uncertainty contributed the most to the mass flow injected standard uncertainty (91%, Figure 5.9). The remaining 9% contributing to mass flow injected standard uncertainty was uncertainty related to injected concentration. This illustrates the importance of having an accurate and stable mass flow controller or other source

of constant gas injection. Relative mass injected standard uncertainty using the method reported here was low (~1.1%); thus, not a source for the low mean SSRMPs nor an important component to

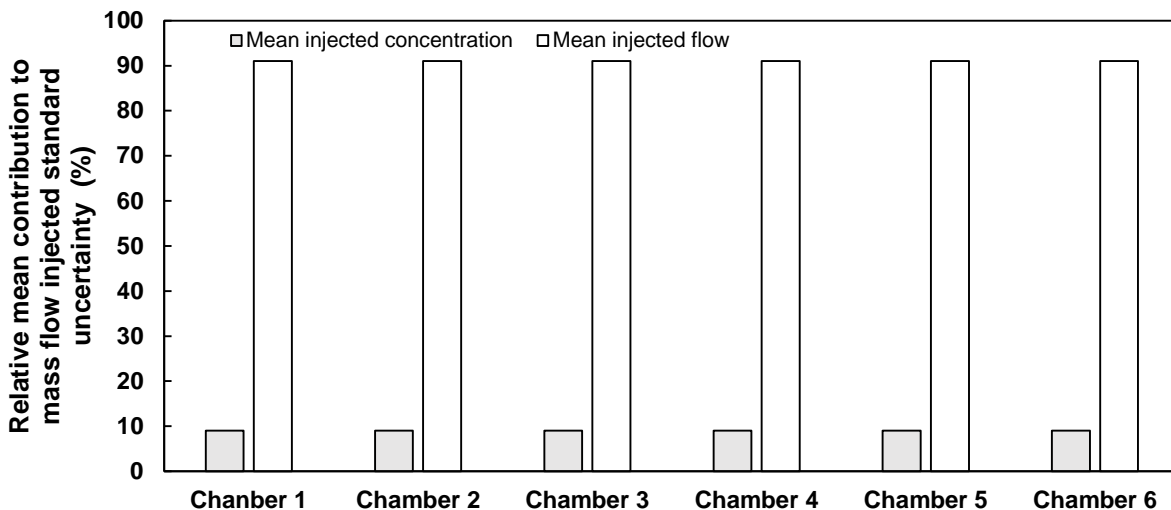


Figure 5.9. Relative mean contribution to mass flow injected standard uncertainty averaged for all replicates. Error bars represent standard deviation obtained by replicates and were much less than 1%. Injected flow contributed approximately 91% to mass flow injected standard uncertainty.

5.4.5.3 Steady-State Mass Recovery Percent Contributions

The three major sources of uncertainty in SSMRP for each chamber (mass injected, mass recovered, and reproducibility) were assessed in terms of their relative contribution to overall SSMRP uncertainty. Mass recovered uncertainty contributed from 70.1% (Chamber 4) to 90.7% (Chamber 5) to SSMRP standard uncertainty while mass injected uncertainty contributed from 2.5% (Chamber 4) to 4.0% (Chamber 6; Figure 5.10). The small contribution of the reference mass injected was due to the use of accurate instrumentation and gas certification, which highlights the importance in providing detailed uncertainty information for the reference mass to improve confidence in recovery results. Reproducibility had a small but substantial contribution ranging from 5.6% (Chamber 5) to 27.3% (Chamber 4) to the SSMRP standard uncertainty (Figure 5.10), which reflects qualified personnel operating the system combined with regular

instrument drift checks and calibration. By reducing the uncertainty in the major sources identified here, such as ventilation rate and gas concentration measurement, the SSMRP standard uncertainty can also be decreased.

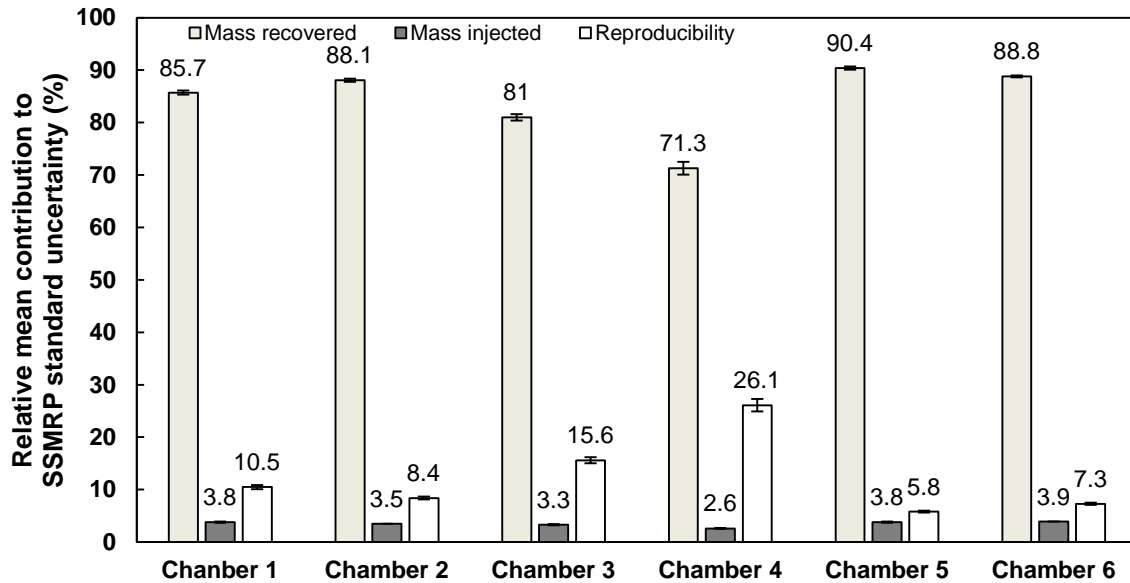


Figure 5.10. Mean relative contribution to Steady-State Mass Recovery Percent (SSMRP) standard uncertainty for all replicates. Error bars represent standard deviation for replicates (n=8). Mass recovered contributed the greatest while the contribution of reproducibility was positively correlated with its magnitude.

5.4.6 Systematic Bias Evaluation for Accumulated Emission

Systematic errors (bias) were significant ($p < 0.05$) for chambers 1 through 5 as summarized in Table 5.7. Bias correction is recommended for chambers 1 through 5 (Equations 5.21 and 5.22) and not needed for chamber 6. Note that as new experiments are performed, correction factors used to calculate the effective accumulated emission should be updated, pending the results of new SSMRTs.

Table 5.7. Summary of parameters for inference testing to determine a systematic bias for the six chambers using eight replicates of the SSMRT over one year. Bias correction is recommended for chambers 1-5 using equations 5.21 and 5.22 and not recommended for chamber 6.

Parameter	Chamber ID					
	1	2	3	4	5	6
\overline{SSMRP}_c (%)	93.2	94.9	92.0	92.8	94.3	96.6
$\Delta\overline{SSMRP}_c$ (%)	1.9	2.0	2.0	2.2	1.9	1.9
t_{calc}	3.6	2.6	4.1	3.2	3.0	1.8
<i>P</i> value	0.009	0.037	0.005	0.015	0.019	0.113
Outcome	Reject H ₀	Reject H ₀	Reject H ₀	Reject H ₀	Reject H ₀	Cannot reject H ₀
Systematic bias	Yes	Yes	Yes	Yes	Yes	No

An example of the calculated accumulated emissions and its associated standard uncertainty is presented in Table 5.8 for the six chambers. The data provided in Table 5.8 were obtained from six steers placed in the chambers for approximately 24 h. Values from chambers 1-5 were corrected for systematic errors and their corresponding effective emissions were determined.

Table 5.8. Sample accumulated CH₄ emissions and associated standard uncertainty calculation for six steers fed grain and forage diets. Correction factors and their associated standard uncertainty were applied to accumulated emissions data for chambers one through five.

Chamber ID	Animal ID	Body weight (kg)	Diet	E ± ΔE (g d ⁻¹) ^[1]	Relative ΔE (%)	Correction factor	E ^{eff} ± ΔE ^{eff} (g d ⁻¹) ^[2]	Relative ΔE ^{eff} (%)
1	A	922.6	forage	75.59 ± 8.72	11.53	1.07	81.07 ± 9.49	11.71
		982.0	grain	43.56 ± 5.80	13.31		46.71 ± 6.29	13.46
2	B	740.3	forage	112.36 ± 9.85	8.77	1.05	118.34 ± 10.66	9.01
		793.8	grain	110.22 ± 9.19	8.34		116.10 ± 9.98	8.59
3	C	787.0	forage	109.09 ± 8.38	7.68	1.09	118.56 ± 9.44	7.96
		862.3	grain	105.31 ± 7.34	6.97		114.46 ± 8.33	7.28
4	D	782.9	forage	69.69 ± 7.34	10.54	1.08	75.07 ± 8.11	10.81
		771.1	grain	74.06 ± 6.65	8.97		79.79 ± 7.41	9.29
5	E	904.0	forage	74.79 ± 5.81	7.77	1.06	79.32 ± 6.36	8.02
		879.5	grain	106.37 ± 8.66	8.14		112.80 ± 9.46	8.38
6	F	882.7	forage	119.26 ± 7.65	6.42	-	-	-
		843.2	grain	123.22 ± 8.14	6.6	-	-	-

^[1] accumulated emissions with standard uncertainty reported (Equation 4.4)

^[2] effective accumulated emissions from application of correction factor (Equation 5.20) with standard uncertainty reported (Equation 5.21)

For all six chambers, as the accumulated emissions increased, the relative standard uncertainty decreased. This result was similar to the result found in the ER sensitivity analysis documented in Part I (Maia et al., 2014). The effective accumulated emissions and associated

standard uncertainty increased after application of the systematic error correction (Equations 5.20 and 5.21) for chambers 1-5.

Analysis of the effects of different treatments on CH₄ emissions is beyond the scope of this work; however, there are important implications relative to using the methods presented here. For example, the sources of measurement errors combined into the emission standard uncertainty (corrected or uncorrected) are rarely used in a means comparison to evaluate the effects of e.g. diet, management, or genetics, on CH₄ production. Consequently, treatment effects are often found to be significant because measurement errors are not accounted for. Alternatively, treatment effects detected by REMS have a high probability to represent real effects. REMS is a major contribution towards the integration of the measurement system uncertainty analysis into the statistical design.

5.5 Summary and Conclusions

REMS subsystems were individually evaluated, followed by a whole system evaluation via SSMRT analysis. The SSMRT analysis included REMS steady-state determination, the steady-state mass recovery ratio expressed in a percent basis (SSMRP), and the relative contributions of individual sources of uncertainty to the SSMRP uncertainty.

Subsystem evaluation: Results of the subsystem evaluation showed the six chambers were positively pressurized, maintained a comfortable thermal environment, and minimal leakage along the sampling path from the chamber to the gas analyzer. No obvious errors or malfunctions were found; therefore, any loss of mass indicated by the SSMRT was due to other sources of errors than the ones found in the subsystem assessment.

Steady-State Mass Recovery Test: The SSMRT analysis quantified the degree of mass conservation detected by REMS. It served as a whole system verification, identified random and

systematic errors, and determined the time constant for the exchange rate of fresh air in each chamber.

Steady-State determination: Steady-state operation was quantified and was achieved within 14 min for all six chambers (five time constants). A mathematically determined time constant provides insight about chamber mixing patterns, which improves the development of experimental and operational procedures and protocols. Changes in the time constants over time are a useful metric to identify system drift or other problems.

Steady-State Mass Recovery Percent: REMS mass conservation was assessed as the ratio between the total mass recovered by REMS and a precisely metered amount of mass injected by the reference. Mean SSMRP for the six chambers ranged from 92.0% (Chamber 3) to 96.6% (Chamber 6) with a reproducibility ranging from 1.3% (Chamber 5) to 3.2% (Chamber 4). The SSMRP absolute expanded uncertainty ($k=2$, ~95% C.I.) ranged from 10.4% (Chambers 1, 5, and 6) to 13% (Chamber 4), and accounted for individual instrument measurement uncertainties, mass recovered uncertainty, mass injected uncertainty, and reproducibility.

Individual uncertainty relative contributions: SSMRP uncertainty relative contributions ranged from 70.1% (Chamber 4) to 90.7% (Chamber 5) for the mass recovered, 2.5% (Chamber 4) to 4.0% (Chamber 6) for mass injected, and 5.6% (Chamber 5) to 27.3% (Chamber 4) for recovery test reproducibility. Uncertainty related to the orifice meter and gas analyzer were the two major sources of uncertainty for the mass recovered, with the orifice meter being the highest. These two uncertainty sources were analyzed in detail for REMS emission rates in Maia et al. (2014). The mass flow controller was the major source of uncertainty for the injected reference mass.

Systematic error: Significant systematic errors were detected in the SSMRT analysis for chambers 1 through 5. A correction (Equation 5.20) is recommended for accumulated emissions calculated from these chambers.

While this analysis was applied to REMS, it applies equally to any open-circuit respiration chamber or indirect calorimeter. Confidence in a measurement system is strongly dependent upon the quality of the information obtained from instrument resolution, reproducibility, calibration reference standard error, other calibration parameters, and traceable and non-traceable manufacturer's accuracy. The integration of these sources of uncertainty and development of an expanded standard uncertainty using coverage factors provides confidence intervals on operation and emission measurements. In addition, the analysis of the relative contribution of individual uncertainty sources to the overall system uncertainty should be performed, along with the assessment and correction (if applicable) of system systematic errors. In conclusion, a comprehensive analysis of measurement uncertainty should be integral part of the experimental design of any open-circuit respiration system constructed to study the effects of different treatments on ruminant emissions.

5.6 Acknowledgments

This research was supported with funding provided by the Dudley Smith Initiative, University of Illinois College of ACES and the Office of Research, University of Illinois College of ACES. The authors would like to acknowledge the contributions of research specialist Jingwei Su, graduate students Jacob Segers and Blake Lehman, and undergraduate students Kellie Kroscher and Patricia Paulausky during the preparation and completion of this work.

5.7 References

- Albright, L. D. (1990). *Environment control for animals and plants*. American Society of Agricultural Engineers.
- ASHRAE. (2013). Chapter 1: Psychrometrics. In M. S. Owen (Ed.), *Handbook of fundamentals*. Atlanta, GA: American Society of Heating, Refrigerating and Air-Conditioning Engineers.
- Carpenter, T. M., & Fox, E. L. (1923). Alcohol check experiments with portable respiration apparatus. *The Boston Medical and Surgical Journal*, 189(16), 551-561.
- Federation of Animal Science Societies. (2010). *Guide for the care and use of agricultural animals in research and teaching*. Champaign, IL: Federation of Animal Science Societies.
- Hellwing, A. L. F., Lund, P., Weisbjerg, M. R., Brask, M., & Hvelplund, T. (2012). Technical note: Test of a low-cost and animal-friendly system for measuring methane emissions from dairy cows. *Journal of Dairy Science*, 95(10), 6077-6085.
- ISO/IEC. (2008). *Uncertainty of measurement: Part 3. guide to the expression of uncertainty in measurement (GUM:1995) (ISO Guide 9803:2008(E). ed.)*. Geneva, Switzerland: International Standards Organization.
- Klein, L., & Wright, A. G. (2006). Construction and operation of open-circuit methane chambers for small ruminants. *Australian Journal of Experimental Agriculture*, 46(10), 1257-1262.
- Maia, G. D. N., Ramirez, B. C., Green, A. R., Rodriguez, L. F., Segers, J. R., Shike, D. W., & Gates, R. S. (2014). A novel ruminant emission measurement system: Part I-design evaluation and description. *Submitted to Transactions of ASABE*.
- McGinn, S. M. (2006). Measuring greenhouse gas emissions from point sources in agriculture. *Canadian Journal of Soil Science*, 86(3), 355-371.

- McGinn, S. M., Beauchemin, K. A., Coates, T., & Colombatto, D. (2004). Methane emissions from beef cattle: Effects of monensin, sunflower oil, enzymes, yeast, and fumaric acid. *Journal of Animal Science*, 82(11), 3346-3356.
- McLean, J., & Tobin, G. (1987). *Animal and human calorimetry* Cambridge University Press.
- Pinares-Patiño, C. S., Lassey, K. R., Martin, R. J., Molano, G., Fernandez, M., MacLean, S., . . . Clark, H. (2011). Assessment of the sulphur hexafluoride (SF₆) tracer technique using respiration chambers for estimation of methane emissions from sheep. *Animal Feed Science & Technology*, 166-167, 201-209. doi:10.1016/j.anifeedsci.2011.04.067.
- Ramirez, B. C., Maia, G. D. N., Green, A. R., Shike, D. W., Gates, R. S., & Rodríguez, L. F. (2013). Design and validation of a calibrated orifice meter for sub-500 liter per minute flow rate applications. *American Society of Agricultural and Biological Engineers Annual International Meeting 2013*, ASABE Paper No. 1618475.
- Ramirez, B. C. (2014). *Design and evaluation of open-circuit respiration chambers for beef cattle*. (Masters, University of Illinois at Urbana-Champaign, Department of Agricultural and Biological Engineering).
- Ramirez, B. C., Maia, G. D. N., Green, A. R., Shike, D. W., Rodríguez, L. F., & Gates, R. S. (2014). Design and validation of a precision orifice meter for ventilation rate measurement in open-circuit respiration chambers. *Submitted to Transactions of ASABE*.
- Sun, Y. (2013). *Quality assurance project plan for a ruminant emission measurement system*. (Masters, University of Illinois at Urbana-Champaign, Department of Agricultural and Biological Engineering).
- Suzuki, T., McCrabb, G., Nishida, T., Indramanee, S., & Kurihara, M. (2007). Construction and operation of ventilated hood-type respiration calorimeters for in vivo measurement of

methane production and energy partition in ruminants. *Measuring methane production from ruminants* (pp. 125-135) Springer.

Taylor, B. N., & Kuyatt, C. E. (1994). *Guidelines for evaluating and expressing the uncertainty of NIST measurement results* (NIST Tech Note 1297 ed.). Gaithersburg, Md: National Institute for Standards and Technology.

Williams, Y. J., Klein, L., & Wright, A. G. (2007). In Makkar H. V., PE (Ed.), *A protocol for the operation of open-circuit chambers for measuring methane output in sheep*
doi:10.1007/978-1-4020-6133-2_7

Zhang, Y. (2005). *Indoor air quality engineering*. CRC press Boca Raton, FL.

CHAPTER 6: CONCLUSIONS AND FUTURE WORK

With a better understanding and quantification of the sources of uncertainty in one specific application of the chamber technique, we will be able to provide the best estimate of confidence in accumulated CH₄ emissions from beef cattle; thus, allowing for the improvement management strategies and an enhanced knowledge of rumen biology.

While the accuracy of chamber technique research is commonly focused on the mass recovery test, the work presented here outlines a framework for fully describing the uncertainty of emissions estimates. The goals of this research were to design, construct, and validate an orifice meter for accurate flow measurement for the REMS as a part of the fresh air supply and measurement subsystem, derive the calculation for estimating methane production, and determine the sensitivity of input measurements on the standard uncertainty associated with emission rate, and perform a mass recovery test to evaluate whole REMS integrity.

The ventilation rate uncertainty determined from the calibration of the orifice meter was a key input to finding standard uncertainty associated with the animal emission rate. The subsystems and the whole REMS were evaluated for performance and integrity to determine the uncertainty associated with the mass recovery test. The documented methodology provides a foundation for future validation and design of the chamber technique.

The custom designed, constructed, and validated orifice meter was found to be a cost-effective method for accurately measuring volumetric flowrate in low flow (sub-550 lpm) and low supply static pressure applications. The concept, design, and methodology can be applied in numerous research applications requiring low flow and low static pressure or in any situation requiring a low-cost, high-accuracy ventilation rate measurement. The comprehensive documentation of the uncertainty analysis is critical if the orifice meter is to be replicated or it

can be applied to quantify uncertainty in commercial instruments. The quantified uncertainty, in conjunction with the manufacturer calibration certificate and stated accuracy (if known), can be a powerful tool for establishing confidence in volumetric flowrate measurement.

In addition to the design performance and analysis evaluation described earlier to commission the REMS and quantify standard uncertainty associated with CH₄ emissions and the mass recovery test, several experiments and data analysis methods to further explore the chamber technique are recommended. Preliminary work showed the damper controlling the recirculation flowrate inside the chamber has an impact on the mass recovery percent. For all mass recovery tests described here, the damper was set to fully open. An experiment is needed to quantify the impact of the damper position (i.e. the range from closed to open) on the chamber's internal static pressure and the mass recovery percent. A mass recovery test following the methods presented earlier would be performed with damper set to different positions ranging from fully closed to fully opened. By closing the damper, the recirculation of air is decreased; thus, the mixing has also changed. The time constant for the ventilation exchange must be determined and compared to the previously established ventilation exchange time constant. This should provide some indication on the impact of the recirculation on mixing. One additional possibility may include adding a fan to facilitate mixing and isolate the effects of the damper position on the mass recovery percent.

Another recommended experiment would explore the distribution of injected tracer gas inside the chamber to identify any potential bias in the mass recovery percent due to poor mixing from the injection location. Currently, the mass recovery test is performed with the injection point where the fresh air supply and recirculation return meet. I believe this location should be tested in various locations inside the chamber and the subsequent effect on mass recovery

percent quantified. In addition to a single point release, a diffuser placed inside the chamber could be used to distribute the injected gas more evenly throughout the chamber. Further, since the sampling inside the chamber occurs from one location, the purpose for the aforementioned diffuser could be reversed, such that it was a sampling tube. If connected to the negative pressure side of the pump and placed inside the chamber it would capture a more even distribution of the air. If the results of using multiple sampling locations inside the chamber match the results achieved with the current single sampling point, it could be concluded that the single sampling point is collecting a sample of air that is representative of the well-mixed air throughout the chamber.

The standard uncertainty was quantified for each ER calculation corresponding to a composite CH₄ concentration measurement. Approximately 28 ERs are computed while the animal is being monitored in the REMS for a 24 h period. Daily emissions are then calculated by taking the sum of all the computed ERs multiplied by the sampling frequency and then normalized to 24 h. In order to determine the standard uncertainty of the daily emissions, the standard uncertainty associated with each ER must be propagated. This topic has been currently unexplored for this application and is essential for determining the confidence in the chamber technique. Further, a rectangular integration is used in the calculation of daily emissions. The impact of this method on the daily emissions is relatively unknown and the exploration of other methods, such as a trapezoidal integration is limited. I propose calculating daily emissions standard uncertainty by using a root-sum square of the ER standard uncertainty.

Standard uncertainty associated with ER could be reduced in the REMS by targeting the major sources of uncertainty, ventilation rate and gas concentration measurement. The method for ventilation rate measurement, the custom orifice meter, may be replaced with a flowmeter

with greater accuracy and a traceable calibration. Due to the unique installation of the flowmeters, a calibration should be conducted using the blower, manifold, and hoses in the FASMS. The addition of an electronic pressure transducer to constantly monitor the differential pressure across the orifice plate should be considered. The Venturi meter would be a good commercial alternative to the orifice meter, as it has similar operating requirements and is only several hundred dollars more than the orifice meter. Flowmeters and the gas analyzer should be calibrated or minimally, verified prior to the start of animal data collection. Gas analyzer uncertainty could be decreased by improving the detection limit of the optical filter or using a gas analyzer specifically for the gas of interest. This serves several purposes: (1) it may lower the response time; thus, less time between gas samples and more ER per day, (2) it may be less expensive allowing for the purchase of two, in which they could run in parallel and decrease sampling interval, and (3) the gas analyzer may be more sensitive or have a lower detection limit allowing for greater detection in concentration differences.

The methods and results documented in this thesis have contributed to the development of improving the reliability and establishing the confidence in the chamber technique. The standard uncertainty associated with the calculation of eructated methane ER from beef cattle and the mass recovery test used to assess whole system validation provides the tools to evaluate ER measurements from the chamber technique while creating the foundation for future analysis of the chamber technique. The quantified standard uncertainty will be used to develop the level of sensitivity needed to detect differences in diet or management strategy in future emission studies. When comparing accumulated emissions with a standard uncertainty, a difference can only be detected if the difference is greater than the standard uncertainty of each accumulated emission. The standard uncertainty represents the width of the confidence that the measured accumulated

emission lies within due to the random error in the measurements and their propagation through the ER and accumulated emissions equations. It is required for attempting to compare small differences. Correct evaluation of the relationships between CH₄ emissions and diet, genetics, and management strategies will be dependent on knowledge of the standard uncertainty associated with accumulated emissions. Having a documented methodology and better understanding of the sources of uncertainty will ultimately allow other existing and future systems to estimate uncertainty and improve estimates of CH₄ emissions.

APPENDIX A: ORIFICE METER CONSTRUCTION, CALIBRATION, AND STANDARD UNCERTAINTY

A.1 Orifice Construction

A detailed schematic of the orifice drilled into the orifice plate used in the orifice meter in Section 3.2 is shown in Figure A.1.

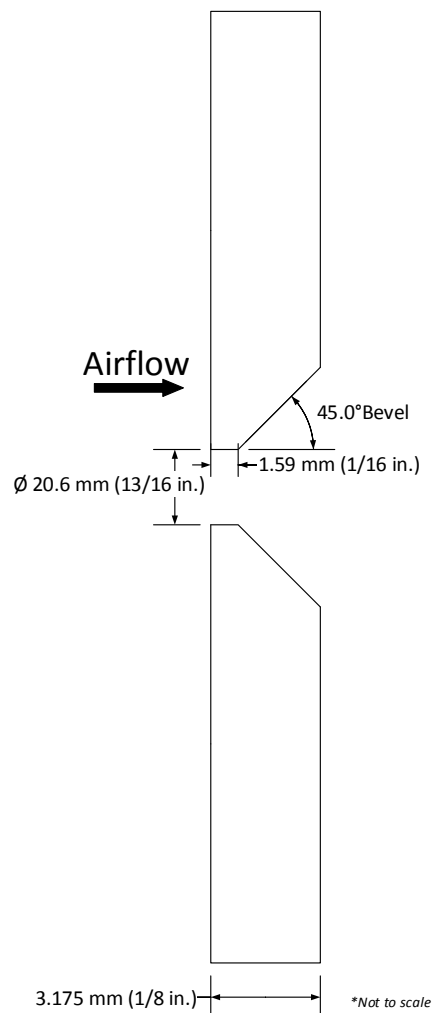


Figure A.1 Detailed schematic of orifice with dimensions for the downstream bevel.

A.2 Calibration curves

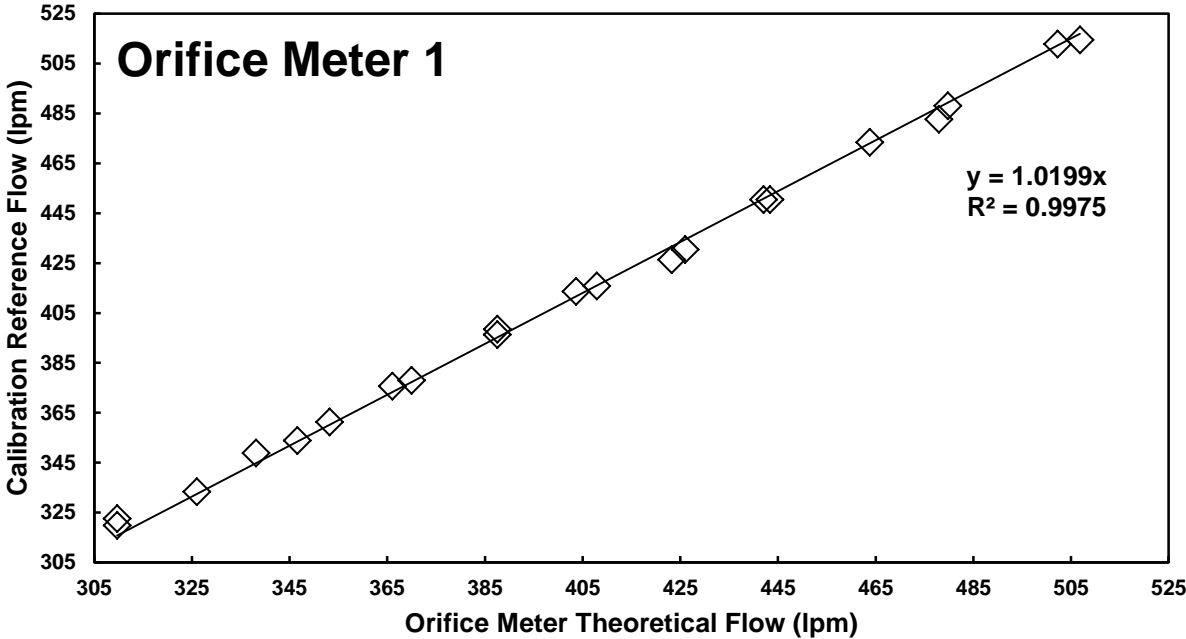


Figure A.2. Linear regression from orifice meter calibration.

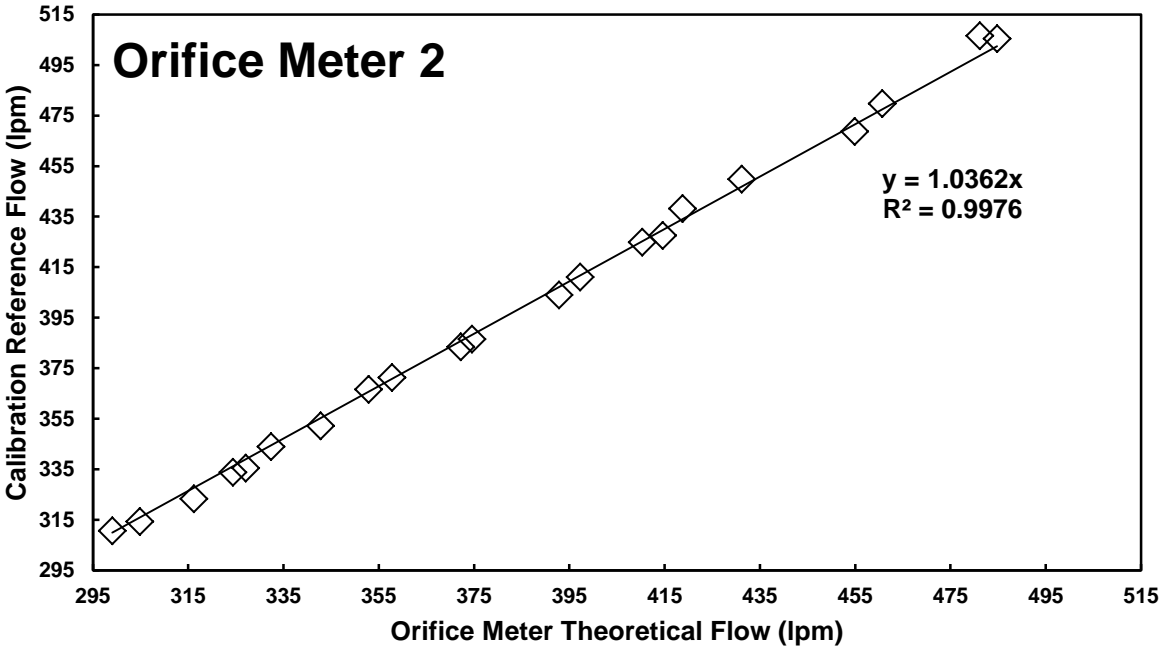


Figure A.3. Linear regression from orifice meter calibration.

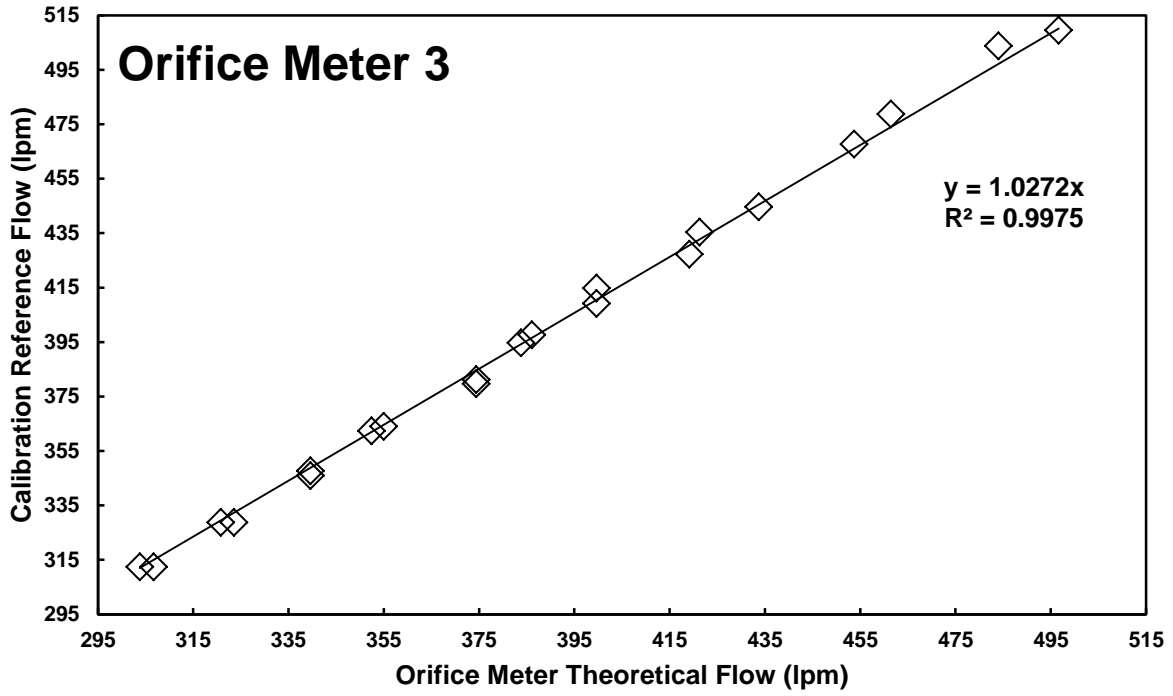


Figure A.4. Linear regression from orifice meter calibration.

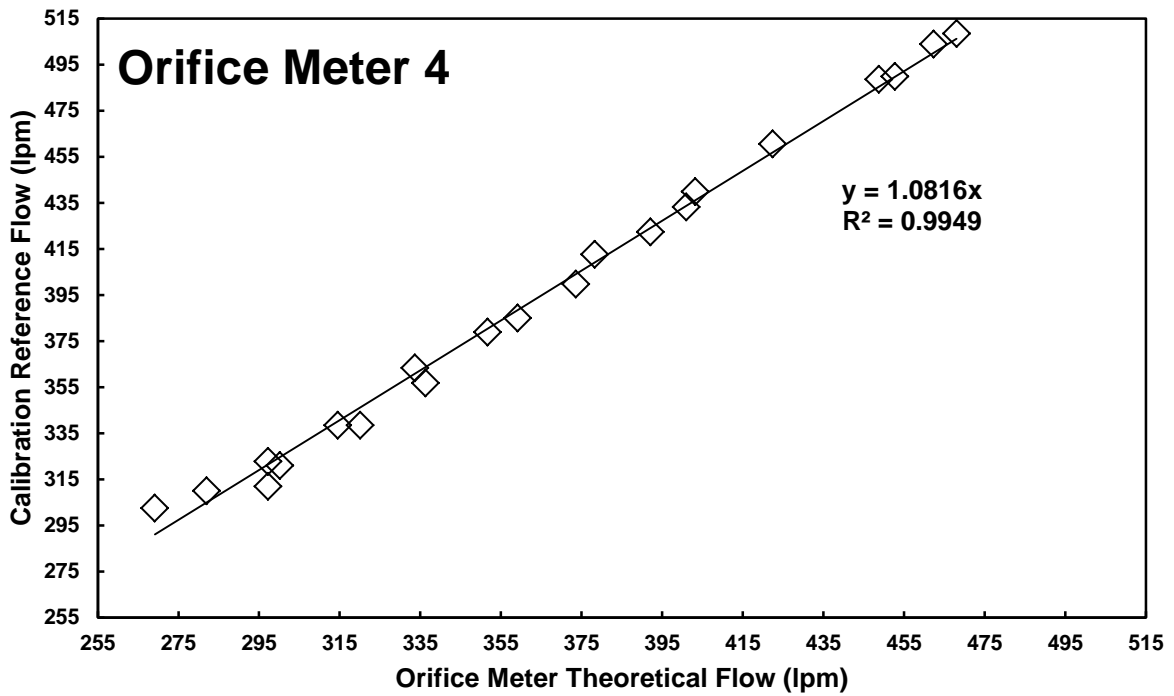


Figure A.5. Linear regression from orifice meter calibration.

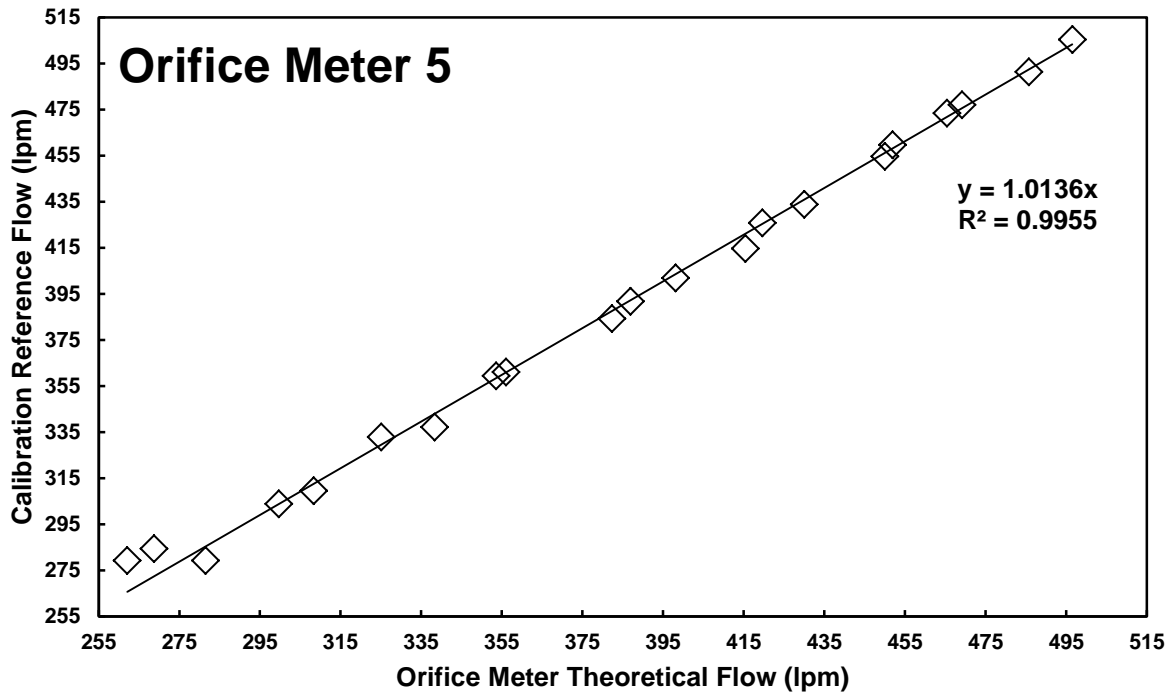


Figure A.6. Linear regression from orifice meter calibration.

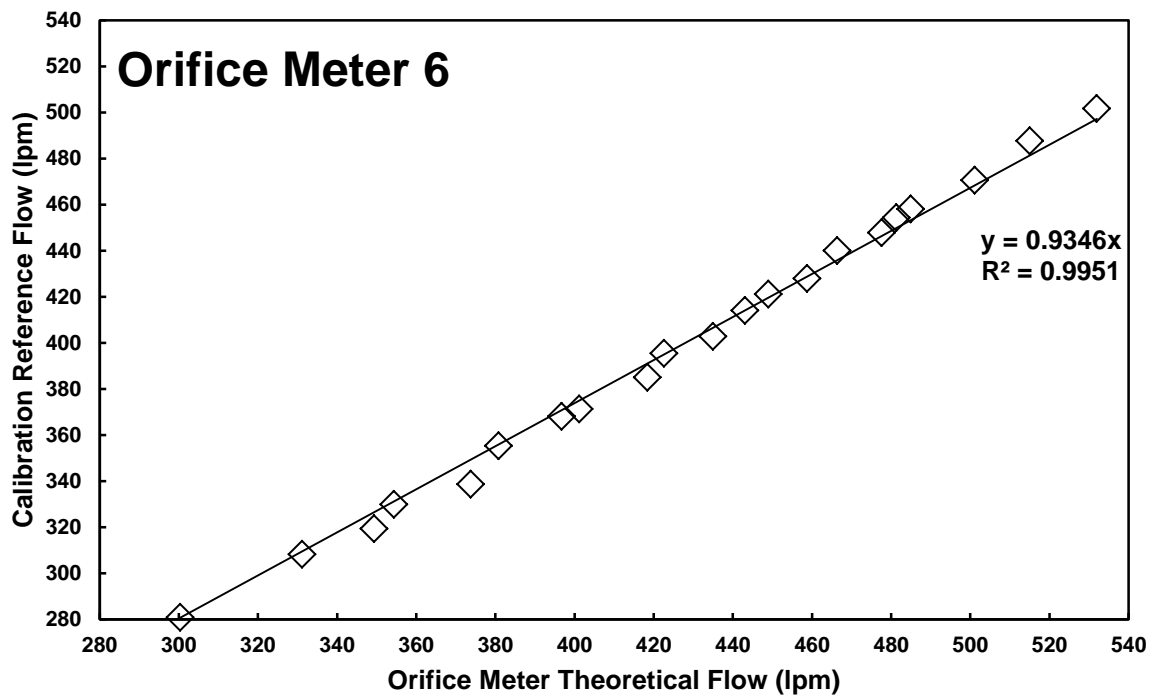


Figure A.7. Linear regression from orifice meter calibration.

A.3 Orifice Meter Flowrate Standard Uncertainty Pseudo Code

The program used to determine the standard uncertainty associated with ventilation rate measurement by the custom orifice meter was written in MATLAB R2013a. The code is not provided, as a slightly modified version of the program is supplied in Appendix G.3. The pseudo code is provided below:

1. Define calibration parameters (slope, slope SE, SE of inverse prediction)
2. Define simulated differential pressure measurement range from 0.4 to 2.5 in H₂O.
3. Loop through all six orifice meters and then through the simulated differential pressure measurements
4. Declare symbolic representation for variables in the orifice meter flowrate equation
5. Create the orifice meter flowrate equation and its associated standard uncertainty equation
6. Create the contributions of the each parameter to orifice meter flowrate standard uncertainty
7. Call function to find the moist density and its associated standard uncertainty, it is available in Appendix C.2
8. For each orifice meter in the loop, use the parameters defined in Step 1, the moist air density in Step 7, the differential pressure measurement in the loop, evaluate the orifice meter flowrate and its associated standard uncertainty
9. Write output to an Excel file

APPENDIX B: EMISSION RATE EQUATION DERIVATION

B.1 Introduction

The two mass flow balances described below were applied to the REMS following the general mass balance depicted in Section 2.4.1. The following is a continuation of the where Section 2.4.1 concludes with addition parameters specific to the REMS.

B.2 Moist Air Mass Flow Balance

The moist air mass flow balance shows the incoming moist air mass flow must be equal to the exhaust moist air mass flow (Equation B.1). Moist air mass flow was determined by the measured volumetric flowrate and moist air density, which is derived from the measurable parameters of temperature, relative humidity and barometric pressure using psychrometric equations (Equation B.2). In the moist air (ma) mass flow balance, animal moist air net generation was assumed negligible due to respiration.

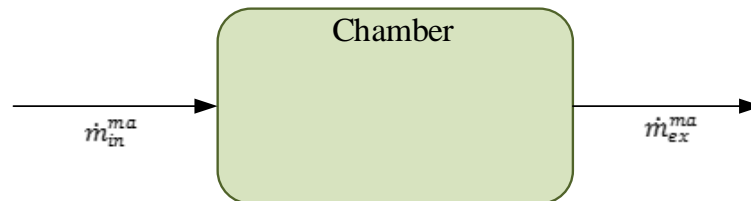


Figure B.1. Simplified moist air (ma) mass flow balance diagram. Total mass entering the chamber (control volume) must also exit the chamber.

$$\dot{m}_{in}^{ma} = \dot{m}_{ex}^{ma} \quad \text{(Equation B.1)}$$

$$\dot{V}_{in} \times \rho_{in}^{ma} = \dot{V}_{ex} \times \rho_{ex}^{ma} \quad \text{(Equation B.2)}$$

where

\dot{m}_{in}^{ma} = incoming moist air mass flow (e.g. g s⁻¹)

\dot{m}_{ex}^{ma} = exhaust moist air mass flow (e.g. g s⁻¹)

\dot{V}_{ex} = exhaust moist air flowrate leaking out of the chamber (m_{ma}³ s⁻¹)

\dot{V}_{in} = incoming moist air ventilation volumetric flowrate (m_{ma}³ s⁻¹)

ρ_{in}^{ma} = incoming moist air density (g_{da} m_{ma}⁻³)

ρ_{ex}^{ma} = exhaust moist air density (g_{da} m_{ma}⁻³)

Exhaust moist air flowrate is not quantified in the REMS as the ventilated hood-type chambers were specifically designed to be hyperbaric. Fresh air is supplied to each chamber to provide positive pressurization over the internal volume of the chamber; hence, the volumetric flowrate of fresh air entering the chamber must be quantified (Equation B.3). Simplifying yields and arranging in terms of measureable parameters:

$$\dot{V}_{ex} = \dot{V}_{in} \times \left(\frac{\rho_{in}^{ma}}{\rho_{ex}^{ma}} \right) \quad (\text{Equation B.3})$$

B.3 Gas Component Mass Flow Balance

The same methodology as the moist air mass flow balance was applied to the gas component mass flow balance (Equation B.4). The difference between the chamber exhaust gas mass flow and incoming gas mass flow yields the gas generation rate.

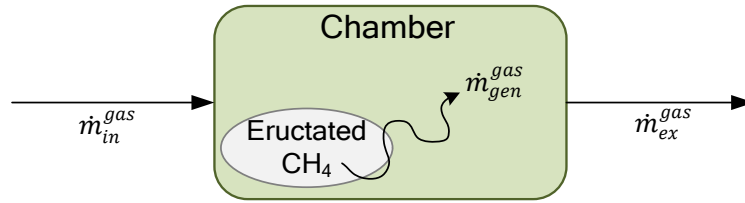


Figure B.2. Simplified gas component mass flow balance diagram corresponding to Equation B.5. The gas represented was methane, but any gas can be used, accordingly.

$$ER = \dot{m}_{gen}^{gas} = \dot{m}_{out}^{gas} - \dot{m}_{in}^{gas} \quad (\text{Equation B.4})$$

where

- ER = emission rate of gas produced by the animal (g h^{-1})
- \dot{m}_{gen}^{gas} = mass flow of a gas generated inside the control volume (g h^{-1})
- \dot{m}_{in}^{gas} = incoming gas mass flow (g h^{-1})
- \dot{m}_{out}^{gas} = gas mass flow determined from the chamber (g h^{-1})

The mass flow of a gas in terms of measureable parameters is simply the volumetric flowrate of moist air multiplied by the mass concentration (Equation B.5 and Equation B.6). This can be substituted into Equation B.4 to obtain:

$$\dot{m}_{in}^{gas} = \dot{V}_{in} \times C_{in}^{gas} \quad (\text{Equation B.5})$$

$$\dot{m}_{out}^{gas} = \dot{V}_{ex} \times C_{ex}^{gas} \quad (\text{Equation B.6})$$

where

C_{in}^{gas} = incoming gas concentration in absolute units ($\text{g m}_{\text{ma}}^{-3}$)

C_{ex}^{gas} = exhaust gas concentration in absolute units ($\text{g m}_{\text{ma}}^{-3}$)

It is important to discuss that absolute units (e.g. $\text{g m}_{\text{ma}}^{-3}$) is dependent on temperature and pressure and the volume in the denominator is determined at the conditions of the air stream in which the gas was sampled. Most gas analyzers e.g. INNOVA 1412 standardize absolute units by correcting directly for temperature and pressure (measured internally). For concentrations reported in volumetric concentration units e.g. $\text{mL}_{\text{gas}} \text{m}_{\text{ma}}^{-3}$, the volumetric concentration is at local conditions i.e. independent of temperature and pressure. Volumetric concentration cannot be applied directly to determine mass flow rate; therefore, volumetric concentration must be converted to absolute units by determining the density of the gas at the measurement conditions.

B.4 Volumetric Concentration Conversion

B.4.1 Method 1

Absolute units can be obtained by multiplying the volumetric concentration by the density of air at measurement (local) conditions (Equation B.7). The ideal gas law ($PV=nRT$) and molecular mass were used to represent the density of the gas as mass of the gas per volume of moist air at local conditions.

$$C^{gas} = \frac{c^{gas} \times M \times P_b}{R \times T} \quad (\text{Equation B.7})$$

where

C^{gas} = absolute units at local conditions (g m^{-3})

c^{gas} = volumetric concentration at local conditions (ppm_v)

M = molecular mass of gas (g mol^{-1})

P_b = local barometric pressure (Pa)

R = universal constant of ideal gases ($8.314; \text{m}^3 \text{Pa K}^{-1} \text{mol}^{-1}$)

T = local temperature (K)

Returning to the gas mass flow balance and substituting the absolute units (Equation B.7) into the mass flow in (Equation B.8) and out (Equation B.9) yields the mass flow in and out in terms of measurable parameters (Equation B.9 and Equation B.10).

$$\dot{m}_{in}^{gas} = \dot{V}_{in} \times c_{in}^{gas} \times \frac{M \times P_b}{R \times T_{in}} \times 10^{-6} \quad (\text{Equation B.8})$$

$$\dot{m}_{ex}^{gas} = \dot{V}_{ex} \times c_{ex}^{gas} \times \frac{M \times P_b}{R \times T_{ex}} \times 10^{-6} \quad (\text{Equation B.9})$$

B.4.2 Method 2

Rather than directly applying the ideal gas law at local conditions to determine density, Method 2 utilizes molar volume, which is derived from a manipulation of the ideal gas law at standard (STD) conditions (i.e. 0 °C and 101325 Pa). The result says that the volume occupied by one mole of a gas at a given temperature and pressure is equal to a constant (molar volume). Density of the gas at standard conditions can be expressed as the molecular mass divided by molar volume (Equation B.10), which is similar to previous section where gas density was molecular mass divided by volume at local conditions; therefore, additional corrections are required using molar volume because gas density at local conditions is required.

$$C^{gas} = \frac{c^{gas} \times M}{V_m^{STD}} \quad (\text{Equation B.10})$$

where

- C^{gas} = absolute units at local conditions (g m^{-3})
- c^{gas} = volumetric concentration at local conditions (ppm_v)
- M = molecular mass of gas (g mol^{-1})
- V_m^{STD} = molar volume at STD conditions ($0.022414, \text{m}^3 \text{mol}^{-1}$)

To reiterate, this equation cannot be directly used to calculate mass concentration because the molar volume is at standard conditions while the measured volumetric concentration is a local conditions, therefore a correction to volumetric concentration must be applied to Equation B.10 before implementation. The following derivation shows how the correction is introduced

and how the correction effects the denominator of ppm_v and in fact that this method retains absolute units derived using Method 1 are still at local conditions. First, volumetric concentration can be written as an expansion of the ideal gas law:

$$c^{gas} = \frac{V_{gas}}{V_{ma}} = \frac{P_b}{\underbrace{n \times R \times T}_{V_{ma}}} \times \frac{n \times R \times T}{\underbrace{P_b}_{V_{gas}}} \quad (\text{Equation B.11})$$

where

- c^{gas} = volumetric concentration at local conditions (ppm_v)
- V_{gas} = volume of the gas at local conditions (m³)
- V_{ma} = volume of moist air at local conditions (m³)

Similarly, molar volume at standard conditions can be written as the ideal gas law:

$$V_m^{STD} = \frac{M \times R \times T_{STD}}{P_{STD}} \quad (\text{Equation B.12})$$

where

- T_{STD} = standard temperature (273.15; K)
- P_{STD} = standard pressure (101325; Pa)

Substituting volumetric concentration (Equation B.11) and molar volume (Equation B.12) into the conversion for absolute units at local conditions (Equation B.10) shows that the terms do not cancel (Equation B.13); thus, we need a correction (applied in Equation B.14):

$$C^{gas} = \frac{P_b}{\underbrace{n \times R \times T}_{V_{ma}}} \times \frac{n \times R \times T}{\underbrace{P_b}_{V_{gas}}} \times \frac{P_{STD}}{\underbrace{M \times R \times T_{STD}}_{V_{STD}}} \quad (\text{Equation B.13})$$

Applying the correction, (please note the correction is for the V_{gas}, the numerator in ppm_v):

$$C^{gas} = \frac{P_b}{\underbrace{n \times R \times T}_{V_{ma}}} \times \frac{n \times R \times T}{\underbrace{P_b}_{V_{gas}}} \times \frac{T_{STD}}{\underbrace{T}_{V_{gas} \text{ correction}}} \times \frac{P_b}{\underbrace{P_{STD}}_{V_{STD}}} \times \frac{P_{STD}}{\underbrace{M \times R \times T_{STD}}_{V_{STD}}} \quad (\text{Equation B.14})$$

Now, the correction cancels the terms in the numerator of volumetric concentration and we are left with:

$$C^{gas} = \frac{P_b}{\underbrace{n \times R \times T}_{V_{ma}}} \times M \quad (\text{Equation B.15})$$

Hence, the correction must be applied in order to find mass concentration. In other words, after applying the correction we are left with mass concentration units at local conditions. We rewrite Equation with the correction:

$$C^{gas} = c_g \times \underbrace{\frac{T_{STD}}{T} \times \frac{P_b}{P_{STD}}}_{V_{gas} \text{ correction}} \times \underbrace{\frac{M}{V_m^{STD}}}_{V_{STD}} \quad (\text{Equation B.16})$$

Returning to the gas mass flow balance and substituting the result from Equation B.16, the following is obtained:

$$\dot{m}_{ex}^{gas} = \dot{V}_{ex} \times c_{ex}^{gas} \times \frac{T_{STD}}{T_{ex}} \times \frac{P_b}{P_{STD}} \times \frac{M}{V_m^{STD}} \times 10^{-6} \quad (\text{Equation B.17})$$

$$\dot{m}_{in}^{gas} = \dot{V}_{in} \times c_{in}^{gas} \times \frac{T_{STD}}{T_{in}} \times \frac{P_b}{P_{STD}} \times \frac{M}{V_m^{STD}} \times 10^{-6} \quad (\text{Equation B.18})$$

B.5 Combining for Emission Rate

The result obtained for the exhaust moist airflow (Section B.1.2) and exhaust gas mass flow (Section B.1.3) were combined to accomplish:

$$\dot{m}_{ex}^{gas} = \dot{V}_{in} \left(\frac{\rho_{in}^{ma}}{\rho_{ex}^{ma}} \right) \times \frac{c_{ex}^{gas}}{10^6} \times \frac{T_{STD}}{T_{ex}} \times \frac{P_b}{P_{STD}} \times \frac{M}{V_m^{STD}} \quad (\text{Equation B.19})$$

$$\dot{m}_{ex}^{gas} = \dot{V}_{in} \left(\frac{\rho_{in}^{ma}}{\rho_{ex}^{ma}} \right) \times \frac{c_{ex}^{gas}}{10^6} \times \frac{M \times P_b}{R \times T_{ex}} \quad (\text{Equation B.20})$$

Where Equation B.19 uses Method 1 and Equation B.20 is using Method 2. Now, substituting the exhaust gas mass flow (Equation B.19 or Equation B.20) and the incoming gas mass flow (Equation B.9 or Equation B.18) into the gas component mass flow balance and applying steady-state conditions, the exhaust gas mass flow equals chamber gas mass flow ($\dot{m}_{ex}^{gas} = \dot{m}_{ch}^{gas}$):

$$\dot{m}_{gen}^{gas} = \left(\dot{V}_{in} \left(\frac{\rho_{in}^{ma}}{\rho_{ch}^{ma}} \right) \times \frac{c_{ch}^{gas}}{10^6} \times \frac{T_{STD}}{T_{ch}} \times \frac{P_b}{P_{STD}} \times \frac{M}{V_m^{STD}} \right) - \left(\dot{V}_{in} \times \frac{c_{in}^{gas}}{10^6} \times \frac{T_{STD}}{T_{in}} \times \frac{P_b}{P_{STD}} \times \frac{M}{V_m^{STD}} \right) \quad (\text{Equation B.21})$$

$$\dot{m}_{gen}^{gas} = \left(\dot{V}_{in} \left(\frac{\rho_{in}^{ma}}{\rho_{ch}^{ma}} \right) \times \frac{c_{ch}^{gas}}{10^6} \times \frac{M \times P_b}{R \times T_{ex}} \right) - \left(\dot{V}_{in} \times \frac{c_{in}^{gas}}{10^6} \times \frac{M \times P_b}{R \times T_{in}} \right) \quad (\text{Equation B.22})$$

Again, where Equation B.21 uses Method 1 and Equation B.23 is using Method 2. After simplification and writing in terms of emission rate from the animal:

$$ER = \dot{m}_{gen}^{gas} = \dot{V}_{in} \times T_{STD} \times \frac{P_b}{P_{STD}} \times \frac{M}{V_m^{STD}} \left(\frac{\rho_{in}^{ma} c_{ch}^{gas}}{\rho_{ch}^{ma} T_{ch}} - \frac{c_{in}^{gas}}{T_{in}} \right) \times 10^{-6} \quad (\text{Equation B.23})$$

$$ER = \dot{m}_{gen}^{gas} = \dot{V}_{in} \left(\frac{\rho_{in}^{ma} c_{ch}^{gas}}{\rho_{ch}^{ma} T_{ch}} - \frac{c_{in}^{gas}}{T_{in}} \right) 10^{-6} \times \frac{M \times P_b}{R} \quad (\text{Equation B.24})$$

Again, where Equation B.24 uses Method 1 and Equation B.24 is using Method 2. Nevertheless, the results are equivalent and will yield approximately the same value for ER.

APPENDIX C: EMISSION RATE SENSITIVITY ANALYSIS

CODE

The following code was written in MATLAB R2013a and calculates the emission rate standard uncertainty associated with the REMS using simulated data (expected when monitoring an animal) as explained in the Section 4.2. Uncertainty analysis represented in this code was originally derived by Dr. Guilherme D.N. Maia. Eleven different emission rates are determined from the simulated data to determine the expected emission rate standard uncertainty (Scenario 1). The same simulated data used in Scenario 1 was subsequently utilized to perform a sensitivity analysis by adjusting the uncertainty associated with the gas analyzer (Scenario 2) and ventilation rate measurement (Scenario 3). The pseudo code is presented below:

1. Import simulated data
2. Check which scenario is being tested i.e. scenario 1,2, or 3
 - 2.1. If scenario 1, compute gas analyzer and ventilation rate uncertainty using simulated data
 - 2.2. If scenario 2 or 3, vary gas analyzer and ventilation rate uncertainty at 1%, 2.5%, 5%, 7.5%, and 10%
3. Create a loop to go through all the simulated data
4. Declare symbolic representation for variables in the emission rate equation
5. Create the emission rate equation and its associated standard uncertainty equation
6. Create the contributions of the each parameter to emission rate standard uncertainty
7. Use the simulated data and the uncertainty associated with each instrument to evaluate the emission rate equation and then the standard uncertainty.
8. Assess the contributions of each parameter

9. Save output to excel file and plot the results.

C.1 REMS_ER_STD_UNCERTAINTY.m

```
%% REMS ER STANDARD UNCERATINY & SENSITIVITY ANALYSIS
%   Brett C. Ramirez (01-20-2014)
%   Department of Agricultural and Biological Engineering
%   University of Illinois at Urbana-Champaign
%
%   Calculates ER and its associated standard uncertainty for
%   sensitivity analysis performed in Part I
%
%   INPUTS
%   name          = data file w/o extension (assumes '.xlsx' file type)
%   scenario      = 1 - no sensitivity analysis (baseline)
%                 2 - gas analyzer sensitivity analysis
%                 3 - ventilation rate sensitivity analysis
function REMS_ER_STD_UNCERTAINTY(name,scenario)
if scenario == 1
    sens = 1; % no sensitivity
else
% Scenario 2 and 3, use gas analyzer and ventilation rate uncertainty
% at these fixed values
    sens = [.01 .025 .05 .075 .1];
end
%% IMPORT DATA
% create file name
ext = '.xlsx';
filename = strcat(name, ext);

% read in simulation data from excel file
[T_ch,T_in,C_ch,C_in,~,RH_in,RH_ch] = importfile2(filename);
%% LOOPS
% loop through the five sensitivity values 1%, 2.5%, 5%, 7.5%, and 10%
for u=1:length(sens)
    % loop through the exhaust concentrations of 50-900 ppm
    for n=1:11
%% REMS ER STD UNCERTAINTY COMPUTATION
        % symbolic representation for each parameter
        syms Tch Tin Cch Cin Vdot_in din dch...
            R pb pstd Tstd % constants

        % symbolic representation for abs std uncertainty
        syms DTch DTin DCch DCin DVdot_in Ddin Ddch

        % symbolic representation for the contributions
        syms C_Tch C_Tin C_Cch C_Cin C_Vdot_in C_din C_dch

        % emission rate (ER) equation (g h^-1)
        ER = (Vdot_in*16.04*1E-6*pb/R*3600)*((din/dch)*(Cch/Tch)-(Cin/Tin));

        % individual parameter contribution (%)
        % chamber temperature
        C_Tch =(DTch*diff(ER,Tch))^2;
```

```

% incoming temperature
C_Tin = (DTin*diff(ER,Tin))^2;
% chamber concentration
C_Cch = (DCch*diff(ER,Cch))^2;
% incoming concentration
C_Cin = (DCin*diff(ER,Cin))^2;
% ventiatlion rate
C_Vdot_in = (DVdot_in*diff(ER,Vdot_in))^2;
% incoming moist air density
C_din = (Ddin*diff(ER,din))^2;
% chamber moist air density
C_dch = (Ddch*diff(ER,dch))^2;

% REMS ER std uncertainty
DER = (C_Tch+C_Tin+C_Cch+C_Cin+C_Vdot_in+C_din+C_dch)^0.5;

% constants
% barometric pressure (Pa) (ASHRAE 2013, Chp 1, Eqn 3)
pb = 98639.3086;
% standard temperature (K)
Tstd = 273.15;
% standard pressure (Pa)
pstd = 101325;
% universal gas constant (m^3 Pa mol^-1 K^-1)
R = 8.314;

% use values from excel file
% chamber temperature (K)
Tch = T_ch(n);
% chamber temperature std uncertainty (K)
DTch = 0.5;
% incoming temperature (K)
Tin = T_in(n);
% incoming temperature std uncertainty (K)
DTin = 0.5;

% incoming and chamber moist air density std uncertainty (kg m^-3)
[din,Ddin] = air density std uncertainty(T_in(n),RH_in(n));
[dch,Ddch] = air density std uncertainty(T_ch(n),RH_ch(n));

% ventilation rate and its std uncertainty
% use 1%, 2.5%, 5%, 7.5%, and 10% for sensitivity analysis
if scenario == 3
    % ventilation rate (m^3 s^-1)
    Vdot_in = 0.008333333333;
    % ventilation rate std uncertainty (m^3 s^-1)
    DVdot_in = sens(u)*Vdot_in;
else
    % ventilation rate (m^3 s^-1)
    Vdot_in = 0.008333333333;
    % ventilation rate std uncertainty (m^3 s^-1)
    DVdot_in = 0.00020533;
end
% chamber concentration (ppmv)
Cch = C_ch(n);
% incoming concentration (ppmv)

```



```

Cin = C_in(n);

% gas analyzer std uncertainty
% post calibration
rep_pc = (0.005*.42)^2;
% instrument repeatability
rep_insch = ((0.01*C_ch(n))/(3^0.5))^2;
rep_insin = ((0.01*C_in(n))/(3^0.5))^2;
% primary certified tolerance
pct = ((0.01*499.9)/(360.5))^2;
% range drift
rd_ch = ((0.025*C_ch(n))/(3^0.5))^2;
rd_in = ((0.025*C_in(n))/(3^0.5))^2;
%resolution
res = ((5*0.4)/(3^0.5))^2;

% use 1%, 2.5%, 5%, 7.5%, and 10% for sensitivity analysis
if scenario == 2
    % chamber concentration std uncertainty (ppmv)
    DCch = sens(u)*C_ch(n);
    % incoming concentration std uncertainty (ppmv)
    DCin = sens(u)*C_in(n);
else
    % chamber concentration std uncertainty (ppmv)
    DCch = sqrt(rep_pc+rep_insch+pct+rd_ch+res);
    % incoming concentration std uncertainty (ppmv)
    DCin = sqrt(rep_pc+rep_insin+pct+rd_in+res);
end

format long;

% evaluate ER and ER std uncertainty
ER = eval(subs(ER)); % subs is not needed
DER = eval(subs(DER));

% evaluate individual parameter contributions
Total = eval(subs(C_Tch+C_Tin+C_Cch+C_Cin+C_Vdot_in+C_din+C_dch));

Temperature_out = 100*(eval(subs(C_Tch)))/Total;

Temperature_in = 100*(eval(subs(C_Tin)))/Total;

Concentration_out = 100*(eval(subs(C_Cch)))/Total;

Concentration_in = 100*(eval(subs(C_Cin)))/Total;

Flowrate_orifice_meter = 100*(eval(subs(C_Vdot_in)))/Total;

Density_in = 100*(eval(subs(C_din)))/Total;

Density_out = 100*(eval(subs(C_dch)))/Total;

% relative ER std uncertainty
rel = 100*DER./ER;

```

```

% save variables
save 'var_out.mat'
%% OUTPUT FORMATTING
A = {Temperature_out;Temperature_in;Concentration_out;...
      Concentration_in;Flowrate_orifice_meter;Density_in;...
      Density_out;ER;DER;rel;Tch;Tin;Cch;Cin;Vdot_in*60000;din;...
      dch;pb;DTch; DTin; DCch; DCin; DVdot_in*60000;Ddin;Ddch};

alpha = 'BCDEFGHIJKLMNOPQRSTUVWXYZ';
Q = alpha(n);
col_start2 = strcat(Q, '1');
output = strcat(name, '_out', ext);

xlswrite(output,A,u,col_start2); % write to excel file
B = {'rel Temperature_out (%)';' rel Temperature_in (%)';...
      'rel Concentration_out (%)';'rel Concentration_in (%)';...
      'rel Flowrate_orifice_meter (%)';'rel Density_in (%)';...
      'rel Density_out (%)';'ER (g/h)';'abs DER (g/h)';...
      'rel ER (%)';'Tch (K)';'Tin (K)';'Cch (ppmv)';...
      'Cin (ppmv)'; 'Vdot_in (lpm)'; 'din (kg/m^3)';...
      'dch (kg/m^3)'; 'pb (Pa)';'DTch (K)'; 'DTin (K)';...
      'DCch (ppmv)'; 'DCin (ppmv)';'DVdot_in (lpm)';...
      'Ddin (kg/m^3)'; 'Ddch (kg/m^3)'};
xlswrite(output,B,1,'A1'); % write to excel file
%% ORGANIZATION FOR PLOTTING
if scenario ==2
    y_mat{1,u}(n) = rel*2; % expanded rel ER uncertainty
    x_mat(n) = ER;
end
if scenario == 3
    y_mat{1,u}(n) = rel*2; % expanded rel ER uncertainty
    x_mat(n) = ER;
end
end
end
end
%% PLOTT AND SAVE FIG
if scenario == 2
    REMS_ER_SA_PLOT(x_mat,y_mat,2,name)
end
if scenario == 3
    REMS_ER_SA_PLOT(x_mat,y_mat,3,name)
end
end
end

```

C.2 air_density_std_uncertainty.m

```

%% MOSIT AIR DENSITY STD UNCERTAINTY
%   Brett C. Ramirez (02-04-2014)
%   Department of Agricultural and Biological Engineering
%   University of Illinois at Urbana-Champaign
%
%   Adapted from Dr. Guilherme D.N. Maia
%
%   Calculates moist air density and its associated std uncertainty
%

```

```

%      INPUTS
%      Ti          = temperature (K)
%      RHi         = relative humidity (%)
%
%      OUTPUTS
%      density     = moist air density (kg m^-3)
%      Ddensity    = moist air density std uncertainty (kg m^-3)
%
function [density, Ddensity] = air_density_std_uncertainty (Ti, RHi)
% symbolic representation of parameters
syms T RH pws pw Tdew W K

% constants to calculate saturated water vapor partial pressure constants
% apply for temperature range: 0<T<200 deg C
A1 = -5.8002206E+03;    A2 = +1.3914993;        A3 = -48.640239E-03;
A4 = +41.764768E-06;   A5 = -14.452093E-09;     A6 = 0;
A7 = +6.5459673;

% barometric pressure (Pa) (ASHRAE 2013, Chp 1, Eqn 3)
pb = 98639.3086041447;
% universal gas constant for dry air (J kg_da^-1 K^-1)
Ra = 287.055;

% saturation water vapor partial pressure (Albright, 1990)
pws = exp((A1./(T))+A2+(A3.*(T))+(A4.*(T).^2)+(A5.*...
    ((T).^3)+(A6.*(T).^4)+(A7.*(log((T))))));

% water vapor partial pressure (Albright, 1990)
pw =(RH./100).*pws;

% moist air density (Albright, 1990)
d_air=((1+((0.62198*pw)/((pb-pw)))))/(((1/pb)*Ra*(T)*(1+(1.6078*...
    ((0.62198*pw)/((pb-pw))))));

% partial derivatives (air density)
dd_air_dT=diff(d_air,T);
dd_air_dRH=diff(d_air,RH);

delta_T=0.6;    % temperature accuracy (K)
delta_RH=3;     % relative humidity accuracy (%)

% root-sum square combined std uncertainty for moist air density
E_ms_d_air=sqrt(((dd_air_dT*delta_T).^2)+((dd_air_dRH*delta_RH).^2));

% use input parameters
T=Ti;
RH=RH;

% evaluate moist air density and its associated std uncertainty
Ddensity=eval(subs(E_ms_d_air));
density=eval(subs(d_air));
end

```

C.3 REMS_ER_SA_PLOT.m

```
%% REMS ER STANDARD UNCERATINY SENSITIVITY ANALYSIS PLOTTING FUNCTION
% Brett C. Ramirez (05-02-2014)
% Department of Agricultural and Biological Engineering
% University of Illinois at Urbana-Chmpaign
%
% Creates and saves plots of the sensitivity analysis
%
% INPUTS
% x = emission rate (g h^-1)
% y = ER relative std uncertainty (%)
% name = data file w/o extension (assumes '.xlsx' file type)
% scenario = 1 - no sensitivity analysis (baseline)
%           2 - gas analyzer sensitivity analysis
%           3 - ventialtion rate sensitivity analysis
%
function REMS_ER_SA_PLOT(x,y_mat,scenario,name)
% separate the five sensitivities and give them a unique line and marker
a = plot(x,y_mat{1,1},'-ro','LineWidth',1,'MarkerSize',7,...
'MarkerEdgeColor','k','MarkerFaceColor','w');
hold on
b = plot(x,y_mat{1,2},'-gd','LineWidth',1,'MarkerSize',7,...
'MarkerEdgeColor','k','MarkerFaceColor','w');
hold on
c = plot(x,y_mat{1,3},'-bs','LineWidth',1,'MarkerSize',7,...
'MarkerEdgeColor','k','MarkerFaceColor','w');
hold on
d = plot(x,y_mat{1,4},'-m^','LineWidth',1,'MarkerSize',7,...
'MarkerEdgeColor','k','MarkerFaceColor','w');
hold on
e = plot(x,y_mat{1,5},'-cv','LineWidth',1,'MarkerSize',7,...
'MarkerEdgeColor','k','MarkerFaceColor','w');
hold on

% create labels in plot
if scenario == 2
    set(text(450,26,'Gas analyzer uncertainty','Color','k',...
'FontSize',9,'FontWeight','bold'))
    k = 38;
end
if scenario == 3
    text(450,26,'Ventilation rate uncertainty','Color','k',...
'FontSize',9,'FontWeight','bold')
    k = 26;
end

% x and y axis labels
xname = xlabel('Methane ER (g h^-1)');
yname = ylabel('ER relative standard uncertainty (%)');
% create legend
hlegend = legend([a,b,c,d,e],'1%', '2.5%', '5%', '7.5%', '10%',...
'location','NorthEast');
% set fonts
set(xname,'FontName','Times New Roman','FontSize',14,...
'FontWeight','bold')
```

```

set(yname, 'FontName','Times New Roman','FontSize', 14,...
    'FontWeight' , 'bold')
set([hlegend], 'FontName','Times New Roman','FontSize',9 ,...
    'FontWeight' , 'bold')
% set axis limits
axis([0 18 0 k])
% more formatting for figure
set(gca, ...
    'Box'          , 'on'          , ...
    'TickDir'     , 'in'          , ...
    'TickLength'  , [.01 .01] , ...
    'XMinorTick'  , 'off'         , ...
    'YMinorTick'  , 'off'         , ...
    'YGrid'       , 'off'         , ...
    'XColor'      , 'k', ...
    'YColor'      , 'k', ...
    'XTick'       , 0:2:18, ...
    'YTick'       , 0:4:k, ...
    'LineWidth'   , 1, ...
    'FontWeight'  , 'bold');
% save figure as .png and 800 dpi resolution
fig_name=strcat(name, '_fig');
print('-dpng', '-r800', fig_name);
end

```

APPENDIX D: STEADY-STATE MASS RECOVERY

PERCENT DERVIATION

D.1 Introduction

The Steady-State Mass Recovery Percent (SSMRP) compares the amount of mass recovered by the REMS to the total mass injected by the reference shown by Equation D.1.

$$SSMRP = 100 \times \left(\frac{m^{rec}}{m^{inj}} \right) \quad (\text{Equation D.1})$$

where

- $SSMRP$ = steady-state mass recovery percent (%)
- m^{rec} = total tracer gas mass recovered by the REMS (g)
- m^{inj} = total tracer gas mass injected by the reference (g)

Mass recovered by the REMS requires a derivation similar to that presented in Appendix B with the addition of some parameters specific to a mass recovery test that are not included when determining the emission rate from the animal and there is the integration of mass flow to determine mass. Further, mass injected is derived from several measurements and is critical for establishing the reference value in which mass recovered is compared to (Equation D.1). Essentially, mass flow generated and mass flow recovered represent the same concept, which is the measurement of mass flow generated in the chamber.

D.2 Moist Air Mass Flow Balance

The moist air mass flow balance shows that incoming moist air mass flow must be equal to the exhaust moist air mass flow (Equation D.1). Moist air mass flow was determined volumetric flowrate and moist air density derived from the measurable parameters temperature, relative humidity and barometric pressure using psychrometric equations (Equation B.3). There is an

additional input due to the non-negligible mass contribution of the injected dry tracer gas mixture.

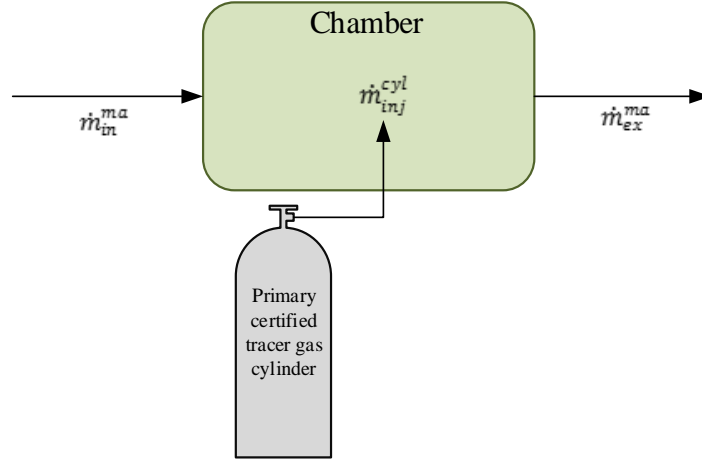


Figure D.1. Simplified moist air (ma) mass flow balance diagram. Total mass entering the chamber (control volume) must also exit the chamber with the addition of the air mass generated from injection of the tracer gas.

$$\dot{m}_{in}^{ma} + \dot{m}_{inj}^{cyl} = \dot{m}_{ex}^{ma} \quad (\text{Equation D.2})$$

$$\underbrace{\dot{V}_{in} \times \rho_{in}^{ma}}_{\dot{m}_{in}^{ma}} + \underbrace{\dot{V}_{inj} \times \rho_{inj}^{cyl}}_{\dot{m}_{inj}^{cyl}} = \underbrace{\dot{V}_{ex} \times \rho_{ex}^{ma}}_{\dot{m}_{ex}^{ma}} \quad (\text{Equation D.3})$$

$$\dot{V}_{ex} = \dot{V}_{in} \times \left(\frac{\rho_{in}^{ma}}{\rho_{ex}^{ma}} \right) + \dot{V}_{inj} \times \left(\frac{\rho_{inj}^{cyl}}{\rho_{ex}^{ma}} \right) \quad (\text{Equation D.4})$$

where

- \dot{V}_{ex} = exhaust volumetric flowrate leaking out of the chamber ($\text{m}^3 \text{s}^{-1}$)
- \dot{V}_{in} = incoming air flowrate ($\text{m}^3 \text{s}^{-1}$)
- ρ_{in}^{ma} = incoming moist air density (kg m^{-3})
- ρ_{ex}^{ma} = exhaust moist air density (kg m^{-3})
- \dot{V}_{inj} = the injected tracer gas flowrate ($\text{m}^3 \text{h}^{-1}$)
- ρ_{inj}^{cyl} = dry density of the cylinder at standard conditions (273.15 K and 101325 Pa) ($\text{kg}_{\text{dry mixture}} \text{m}_{\text{dry mixture volume}}^{-3}$)

The injected dry tracer gas mixture was treated as air for consistency of mass flow balance air properties. This assumption had negligible impact on the results because: (i) most of the gas

in the cylinder was N₂ (approximately 78% of air), (ii) specific gravity of the cylinder gas mixture was close to unity (actual was 0.983 with dry air as the reference), and (iii) the mass flow of dry gas from the cylinder was small and only 1% of the total air mass entering the chamber through ventilation. Density of the tracer gas mixture was determined as follows:

$$\rho_{inj}^{cyl} = y_{N_2} \times \rho_{N_2}^{std} + y_{SF_6} \times \rho_{SF_6}^{std} \quad (\text{Equation D.5})$$

where

- y_{N_2} = mole fraction of N₂ in the cylinder
- $\rho_{N_2}^{std}$ = dry densities of N₂ at standard conditions (1.25 kg_{dry mixture} m_{dry mixture volume}⁻³)
- y_{SF_6} = mole fraction of SF₆ in the cylinder
- $\rho_{SF_6}^{std}$ = dry densities of SF₆ at standard conditions (6.17 kg_{dry mixture} m_{dry mixture volume}⁻³)

D.3 Tracer Gas Component Mass Flow Balance

The same methodology as the moist air mass flow balance was applied to the gas component mass flow balance (Figure D.2). The difference between the chamber exhaust gas mass flow and incoming gas mass flow yields the tracer gas injection rate.

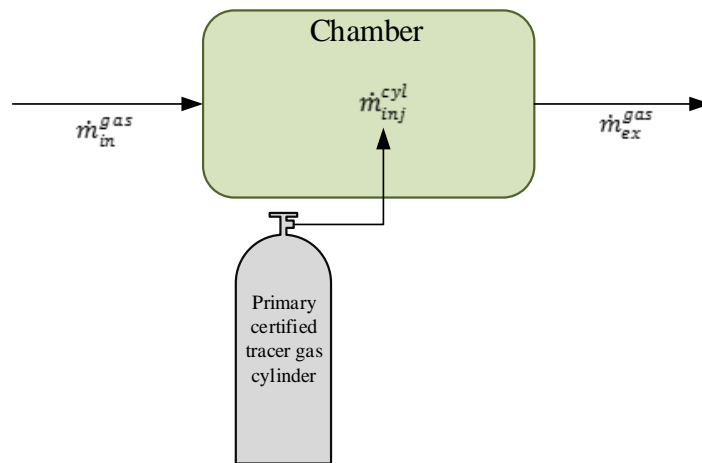


Figure D.2. Gas mass flow balance with injection of the tracer gas for evaluating the steady-state mass recovery test

$$\underbrace{\dot{m}_{in}^{gas} - \dot{m}_{ex}^{gas}}_{\dot{m}^{rec}} = \underbrace{\dot{m}_{inj}^{cyl}}_{\dot{m}^{inj}} \quad (\text{Equation D.6})$$

$$\dot{m}^{rec} = \left(\dot{V}_{ex} \times \frac{c_{ex}^{gas}}{10^6} \times \frac{M \times P_b}{R \times T_{ex}} \right) - \left(\dot{V}_{in} \times \frac{c_{in}^{gas}}{10^6} \times \frac{M \times P_b}{R \times T_{in}} \right) \quad (\text{Equation D.7})$$

where

- c_{ex}^{gas} = exhaust volumetric concentration (ppm_v)
- c_{in}^{gas} = incoming volumetric concentration (ppm_v)
- T_{ex} = exhaust temperature (K)
- T_{in} = incoming temperature (K)
- P_b = local barometric pressure (Pa)
- M = molecular mass of gas (g mol⁻¹)
- P_b = local barometric pressure (Pa)
- R = universal constant of ideal gases (8.314; unit: m³ Pa K⁻¹ mol⁻¹)

After substitution of the result from the moist air mass flow balance, the outcome is:

$$\dot{m}^{rec} = \left[\left(\dot{V}_{in} \frac{\rho_{in}^{ma}}{\rho_{ex}^{ma}} + \dot{V}_{inj} \frac{\rho_{inj}^{ma}}{\rho_{ex}^{ma}} \right) \frac{c_{ch}^{gas}}{T_{ch}} - \dot{V}_{in} \frac{c_{in}^{gas}}{T_{in}} \right] \frac{M \times P_b}{R} \times 10^{-6} \times 3600 \quad (\text{Equation D.8})$$

D.4 Mass Flow Injected

The reference consisted of a primary certified tracer gas cylinder and a mass flow controller. Further, the mass flow injected was calculated from the volumetric flowrate at standard conditions and the concentration of the tracer gas. Firstly, the volumetric flow injected was determined by applying the correction factor determined in Section A.1.3.1 expect that volumetric flow from the mass flow controller is reported at standard conditions:

$$\dot{V}_{inj} = \dot{V}_{inj}^{STD} \times \frac{T_{in}}{T_{STD}} \times \frac{P_{STD}}{P_b} \quad (\text{Equation D.9})$$

where

- \dot{V}_{inj} = injected volumetric flowrate (m³ s⁻¹)
- \dot{V}_{inj}^{STD} = injected volumetric flowrate at standard conditions (sm³ s⁻¹)
- T_{STD} = standard temperature (273.15 K)
- P_{STD} = standard pressure (101325 Pa)
- P_b = local barometric pressure (Pa)
- T_{in} = local temperature of the gas cylinder (K)

Combing with a similar methodology as described in Section for determining the mass flow of a gas, the following is obtained:

$$\dot{m}^{inj} = \dot{V}_{inj} \times c_{inj} \times \frac{M \times P_b}{R \times T_{in}} \times 10^{-6} \quad (\text{Equation D.10})$$

$$\dot{m}^{inj} = \dot{V}_{inj}^{STD} \times \frac{T_{in}}{T_{STD}} \times \frac{P_{STD}}{P_b} \times c_{inj} \times \frac{M \times P_b}{R \times T_{in}} \times 10^{-6} \quad (\text{Equation D.11})$$

$$\dot{m}^{inj} = \dot{V}_{inj}^{STD} \times c_{inj} \times \frac{M \times P_{STD}}{R \times T_{STD}} \times 10^{-6} \quad (\text{Equation D.12})$$

where

- \dot{m}^{inj} = mass flow injected (g h^{-1})
- C_{inj} = injected gas concentration (ppm_v)
- M = molecular mass of gas ($146.06; \text{g mol}^{-1}$)
- R = universal constant of ideal gases ($8.314; \text{m}^3 \text{Pa K}^{-1} \text{mol}^{-1}$)

APPENDIX E: STEADY-STATE MASS RECOVERY TEST

SOP

The following documentation on the standard operating procedures for conducting the Steady-State Mass Recovery Test (SSMRT) was adapted and modified from Appendix E in the Quality Assurance Project Plan for a Ruminant Emissions Measurement System by Sun (2013).

E.1 Scope and Applicability

Compare a known amount of injected mass from a reference to the total mass recovered by the REMS to assess whole system performance and systematic errors. In order to conduct this experiment, the user will need to setup the reference system, operate and understand all functions of the REMS, and either in Excel or MatLab, use the equations defined in Sections 5.2.3 to 5.2.6, to determine the Steady-State Mass Recovery Percent.

E.2 Personnel Qualifications

1. Access to Beef and Sheep Field Research Unit
2. Safe handling practices for compressed gas cylinders
3. Experience with compression fittings

E.3 Equipment and Supplies

1. PC with LabView installed and program Project(3).vi
2. Laptop with EnviroNics Series 4000 Instrument Control Software installed
3. EnviroNics 4040 Gas Dilution System (GDS)
4. Null-modem RS-232 cable (laptop to GDS)
5. Primary certified gas cylinder for the tracer gas (e.g. SF₆, CO₂, CH₄, etc.)

6. Two-stage pressure regulator specific to the aforementioned compressed gas cylinder
7. Circular Styrofoam board cut-out with 10 in² opening secured in a 15 in² plastic pipe
8. Crescent wrench and a variety of other wrench sizes for Swageloc compression fittings
9. 1 ½ in. wrench for two-stage pressure regulator
10. Teflon tape for reducing leakage from the two-stage pressure regulator to compressed gas cylinder
11. Duct tape
12. ~10 m of Teflon tubing (from Environics 4040 GDS to inside the chamber)
13. ~1 m of Teflon tubing (from two-stage pressure regulator to Environics 4040 GDS) with compression fittings on each end

E.4 Procedures

Simple Summary:

1. Assemble and connect the reference system to inject the gas into the cylinder
2. Initialize GDS software, initialize the REMS and record necessary data
3. Begin the experiment with the release of gas
4. Record sufficient number of measurements and complete the experiments

E.4.1 Injection Setup

1. Wrap the Teflon tape about seven times around the threaded piece of the two-stage pressure regulator and insert into the compressed gas cylinder
2. Use the 1 ½ in. wrench to tighten the two-stage pressure regulator to the gas cylinder
3. Connect the ~1 m Teflon tubing from the two-stage pressure regulator on the compressed gas cylinder to Port 1 of GDS

4. Locate the first chamber for analysis (it is recommended to begin with chamber 6 and work sequentially downward)
 - 4.1. As subsequent tests occur, there will be some accumulation of the tracer gas in the barn; thus, it will take longer for the gas to reach the ventilation inlet (near chamber 1)
5. Open the canvas hood located in the back of the chamber and insert the circular Styrofoam board cut-out with 10 in² opening secured in a 15 in² plastic pipe (Figure E.1)
 - 5.1. Use some small 10 gallon buckets flipped upside down to support the pipe (other objects will work too)
6. Connect the ~10 m Teflon tube to OUTPUT on the GDS
7. Lead the opposing end connected to the GDS through gap in the Styrofoam (circular pipe) and with the duct tape, secure to the underside of the metal diffuser (recirculation supply) such that the tip of the tube is directly under the ventilation inlet (Figure E.2).



Figure E.1. Hood blocked using Styrofoam board set within plastic tube.

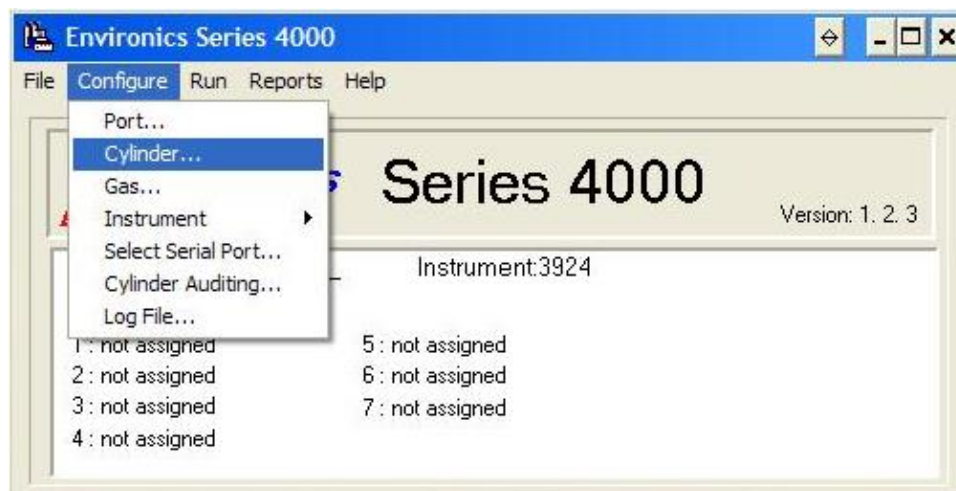


Figure E.2. Injection point taped next to ventilation inlet and recirculation return.

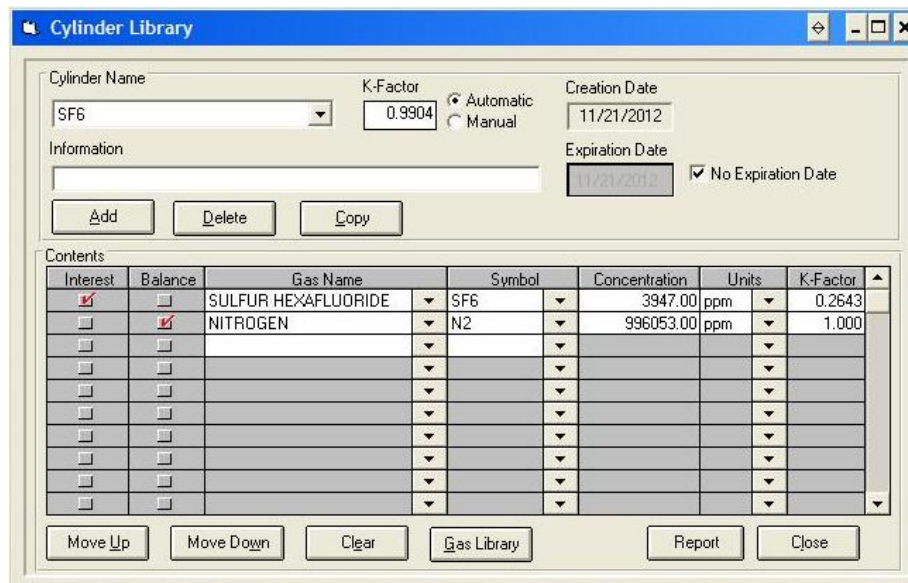
E.4.2 Initializing the Gas Dilution System Software

In the Enviroics Series 4000 Instrument Control Software:

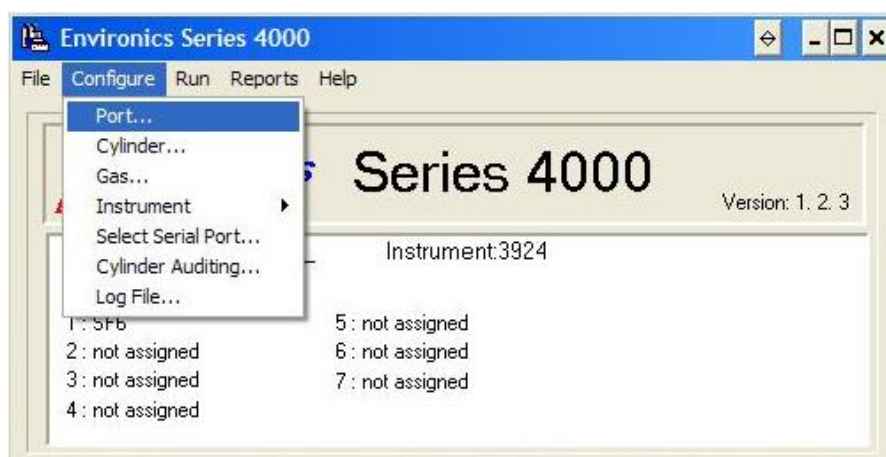
1. Pull down the **File** Menu. Click **New**.
2. Input file name for test (Recovery_test_MMDDYYYY). Instrument should be 3924.
Click **OK**.
3. Pull down the **Configuration** menu. Click **Cylinder**.



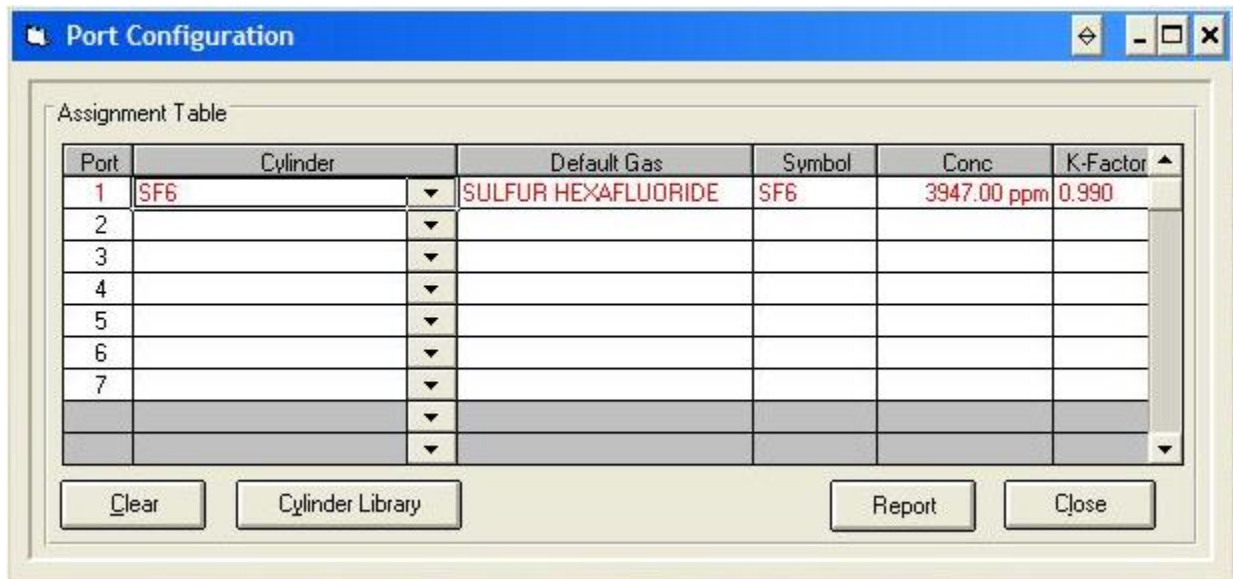
- Click **Add** and input Cylinder name (SF₆).



- Click **OK**.
- Choose the zero gas (N₂) as Balance, and SF₆ as Interest.
- Input concentration according to concentration on SF₆ cylinder (3947 ppm).
- Click **Close** and save changes.
- Pull down the **Configuration** menu. Click **Port**.

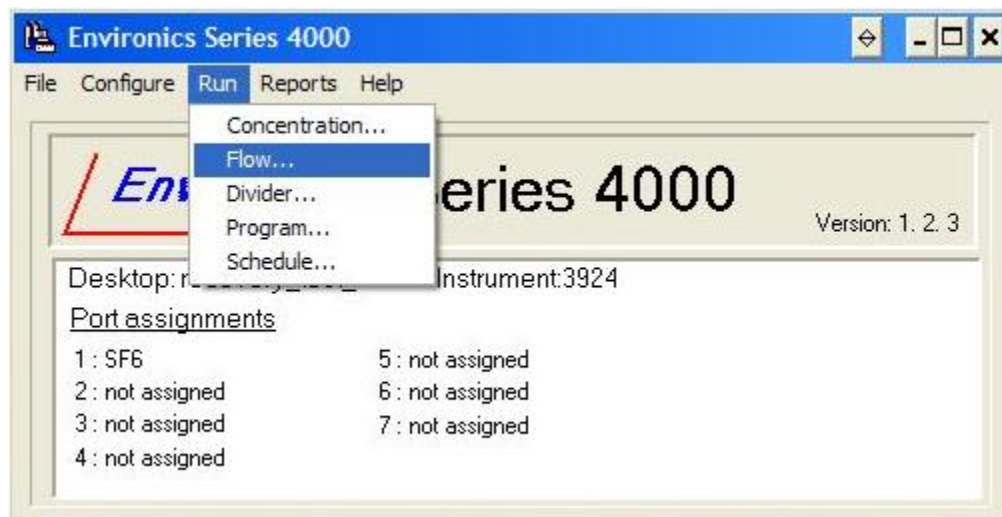


10. Choose Cylinder name (SF₆). Concentration for chosen gas should show up automatically.



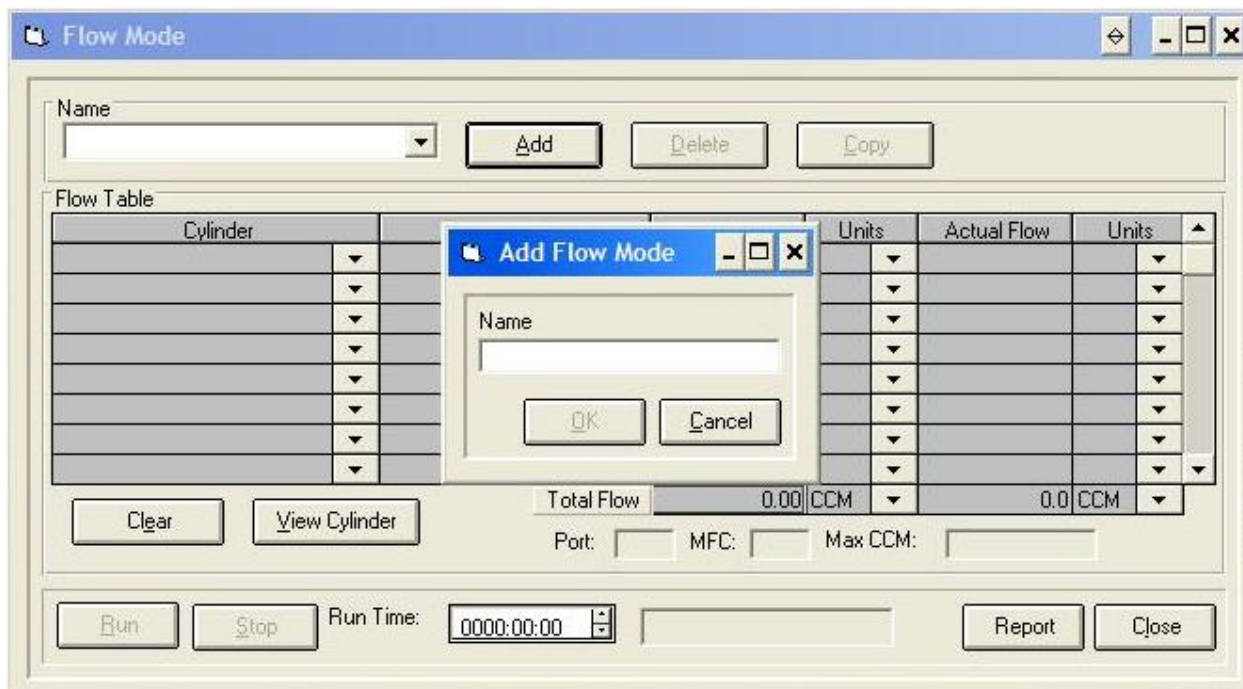
11. Click **Close** and save changes.

12. Pull down the **Run** menu. Click **Flow**.



13. Click **Add** and input Flow Mode (SF₆) then click **OK**.

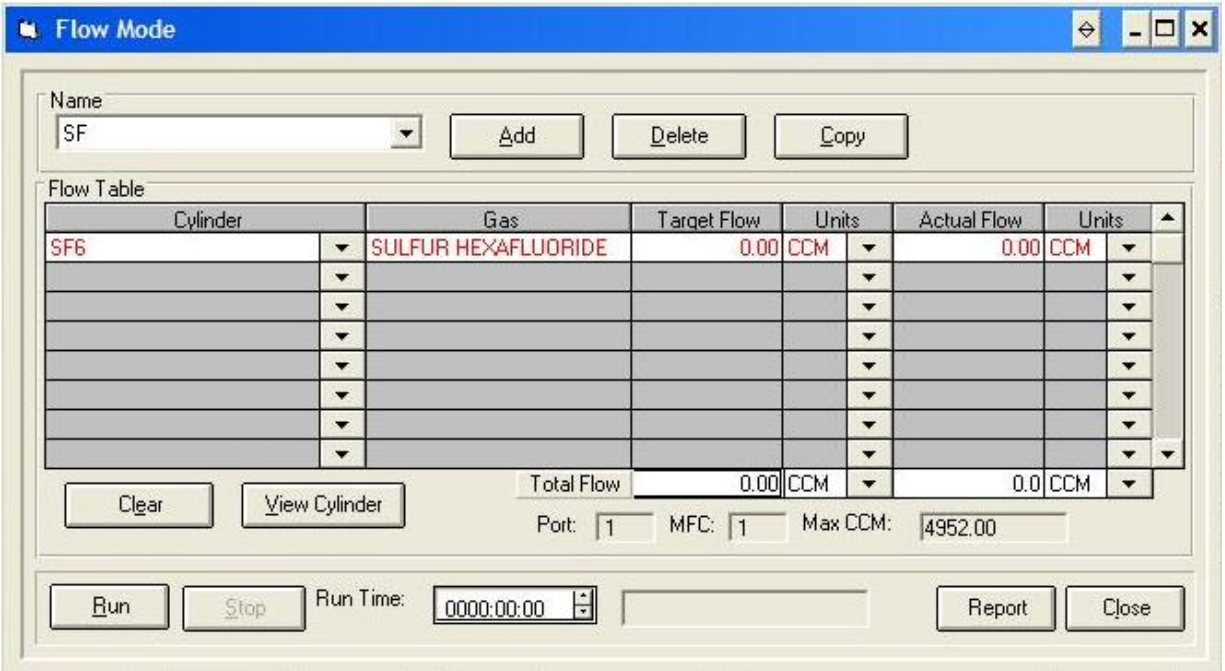
14. Pull down **Cylinder** and choose SF₆.



15. Change the units to LPM for both target and actual flow rates.

16. Enter a target flow of 4.025 lpm to achieve an actual flow of 4.00 lpm

17. Click **Run** when ready to inject gas.



E.4.3 Initialing the REMS and Measurements

1. Turn on the gas analyzer at least 30 min prior to beginning the first gas measurements
2. Locate the oil inclined-vertical manometer positioned to the left of the odd numbered chambers and to the right of the even numbered chambers
3. Record the pressure drop to two decimal places
4. Go to the PC with LabView installed and open Project(3).vi
 - 4.1. Go to the control tab
 - 4.2. Set VISA resource name: COM1
 - 4.3. Set Range: ± 10 V
 - 4.4. Set Innova Filter: Innova Filter #5
 - 4.5. AI Calibration should resemble $AI0a = 20$, $AI0b = -40$, $AI1a = 20$, and $AI1b = 0$
 - 4.5.1. This should repeat for each pair (e.g. AI8 (a and b) and AI9 (a and b))
 - 4.6. Go to Display tab

4.7. Under Select: choose appropriate chamber number

4.8. Note, the program samples as follows:

4.8.1. 10 background samples (solenoid 7, barn)

4.8.2. Automatically switches to 90 chamber samples (solenoid 1 – 6, chamber)

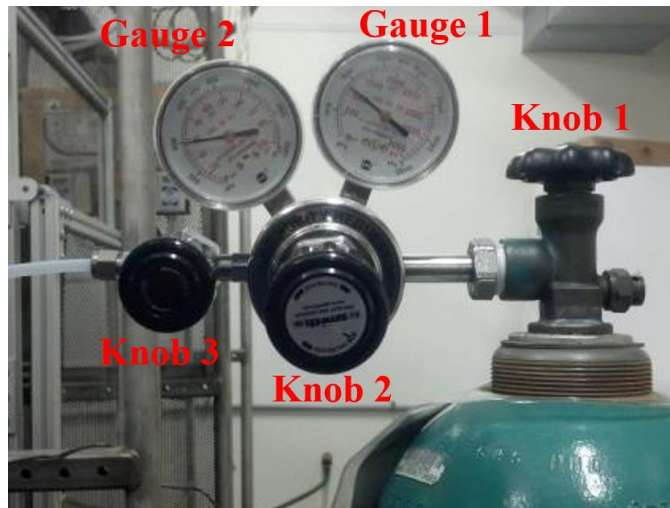
4.8.3. Repeats with 10 background samples and chamber samples etc.

4.9. We do not need 90 samples so click STOP when enough samples past the steady-state have been recorded

E.4.4 Conducting the Experiment

After the previous sections covered under procedures have been completed, it is time to being collecting gas samples and injecting the gas.

1. Start the LabView program Project(3).vi by clicking the white arrow facing the right in the toolbar
2. Allow for the collection of the 10 background samples
3. Go to the two-stage pressure regulator and compressed gas cylinder (Figure E.3):
 - 3.1. Make sure both Knob2 and Knob 3 and completely closed
 - 3.2. Open Knob 1 completely and if Gauge 1 shows < 500 psi do not use
 - 3.3. Open Knob 2 slowly until pressure Gauge 1 reads 30 psi
 - 3.4. Open Knob 3 completely
4. Further adjustments to Knob 2 might be required if pressure is lost over time



4.1. Check after the completion of each test and adjust such that 30 psi is always in Gauge

Figure E.3. Identification of the knobs and gauges for the two-stage pressure regulator and compressed gas cylinder.

5. Allow for the collection of 5 samples of the chamber
6. Click Run in the GDS software to begin the flow of gas into the chamber
7. Allow for 40 total (5 before injection and 35 post injection) samples to be collected from the chamber
8. Click Stop in the GDS software
9. Repeat Section E.4.1 for the next chamber, record the pressure for the inclined-vertical manometer
10. Select the next chamber in the Display tab and click start
11. The initial samples taken for the next chamber will be used to find the average concentration of the tracer gas during the previous test
12. That said, after the gas is turned off for the last chamber, return to the first chamber sampled in that series of tests

E.5 Data Management

The data management process includes retrieving the output data file, selecting the appropriate data, and organizing it in Excel so it can be processed in MatLab.

1. Open Microsoft Office Excel and save the file as SSMRT_raw_data.xlsx
2. Open Get External Data
3. Locate C:\User\Data (as of 05/02/2014 User = Gui)
4. Locate the appropriate text file
 - 4.1. Text files are organized by the date in which it was created and then in ascending alphabetical order
 - 4.2. In addition, solenoid location # is used to differentiate the chambers
5. Follow the Text Import Wizard
6. Insert the data from each text file on the same sheet, one after another
7. Complete for all six chambers
 - 7.1. Name the sheet as the date of the SSMRT
 - 7.2. This file (SSMRT_raw_data) can be used to store all the raw SSMRT data
8. Concatenate the date and the time for all the data by e.g. =A1+B1
9. Adjust the format of the newly created column to mm/dd/yyyy hh:mm
10. Copy and paste while preserving formats and values in a new column adjacent to that one
11. Delete the other two columns to the left
 - 11.1. The date time column should resemble column one in Table E.1
12. Open a new Excel file, create six sheets (i.e. one for each chamber), and save it as SSMRT_date.xlsx
 - 12.1. The sheets do not need to be named

13. Copy and paste the header row in Table E.1 into each of the sheets
14. For each chamber copy and paste its last 12 data points for the columns highlighted in grey in Table E.1
15. Calculate the mean background concentration by taking the average of the five measurements before the gas was injected and of the last five measurements of ten measurements following the switching of the solenoids (i.e. next chamber)
16. For the last three columns of Table E.1, input their respective values in row one and drag them down (they are constant during the test)
17. Repeat for each chamber on its respective sheet (i.e. Chamber ID 3 should go on Sheet3)
18. Save both files and now the SSMRT_”data”.xlsx file is now ready to be processed by the program located in Appendix F

Table E.1. Steady-state data organization for Chamber ID 1 for processing to determine the steady-state mass recovery percent.

date time	Solenoid Loc#	Cch SF6, ppm	Tch, C	RHch, %	T7, C	RH7, %	Cin SF6, ppm	dP, in wc	Ccyl, ppm	Qinj, lpm
5/9/2013 16:55	1	32	21.15	52.34	20.39	71.45	-0.085	1.51	3947	4
5/9/2013 16:56	1	32	21.19	52.56	20.35	71.41	-0.085	1.51	3947	4
5/9/2013 16:56	1	31.9	21.06	53.21	20.33	71.52	-0.085	1.51	3947	4
5/9/2013 16:57	1	32	20.86	53.8	20.31	71.55	-0.085	1.51	3947	4
5/9/2013 16:58	1	31.9	20.81	54.21	20.33	71.55	-0.085	1.51	3947	4
5/9/2013 16:59	1	31.8	20.93	54.14	20.28	71.66	-0.085	1.51	3947	4
5/9/2013 16:59	1	32	20.96	53.45	20.29	71.78	-0.085	1.51	3947	4
5/9/2013 17:00	1	31.9	21.04	52.87	20.25	71.81	-0.085	1.51	3947	4
5/9/2013 17:01	1	32	21.07	52.23	20.29	71.88	-0.085	1.51	3947	4
5/9/2013 17:01	1	31.9	21.09	51.89	20.24	71.94	-0.085	1.51	3947	4
5/9/2013 17:02	1	32	20.79	52.06	20.24	71.9	-0.085	1.51	3947	4
5/9/2013 17:03	1	32	20.92	52.75	20.27	71.86	-0.085	1.51	3947	4

APPENDIX F: STEADY-STATE MASS RECOVERY TEST DATA

The following data were collected periodically over one year and a summary of all the measurements and recorded parameters during a steady-state mass recovery test is documented in Table F.1. For all tests barometric pressure was assumed a constant 98639.3086 Pa (Chapter 1, Equation 3, ASHRAE, 2013), the damper on the TECS supply was 100% open, the TECS recirculation was on, the six holes in the bottom of the chambers were sealed with duct tape, the feed bin was in the chamber, and the injection location was where the TECS supply and FASMS mixed in the top of the chamber (Figure E.3).

Table F.1. Summary of all data collected for steady-state mass recovery tests. This data were collected periodically over one year and used as inputs to calculations the program described Appendix G.

Date and time (m/d/yyyy hh:mm)	Chamber ID	SF ₆ Steady-state concentration (ppm _v)		Temperature (°C)		Relative humidity (%)		Differential pressure (in. H ₂ O)	Gas cylinder concentration (ppm _v)	Injected flowrate (lpm)
		Chamber	Background	Chamber	Background	Chamber	Background			
5/9/2013 16:55	1	32	-0.09	21.15	20.39	52.34	71.45	1.51	3947	4
5/9/2013 16:56	1	32	-0.09	21.19	20.35	52.56	71.41	1.51	3947	4
5/9/2013 16:56	1	31.9	-0.09	21.06	20.33	53.21	71.52	1.51	3947	4
5/9/2013 16:57	1	32	-0.09	20.86	20.31	53.8	71.55	1.51	3947	4
5/9/2013 16:58	1	31.9	-0.09	20.81	20.33	54.21	71.55	1.51	3947	4
5/9/2013 16:59	1	31.8	-0.09	20.93	20.28	54.14	71.66	1.51	3947	4
5/9/2013 16:59	1	32	-0.09	20.96	20.29	53.45	71.78	1.51	3947	4
5/9/2013 17:00	1	31.9	-0.09	21.04	20.25	52.87	71.81	1.51	3947	4
5/9/2013 17:01	1	32	-0.09	21.07	20.29	52.23	71.88	1.51	3947	4
5/9/2013 17:01	1	31.9	-0.09	21.09	20.24	51.89	71.94	1.51	3947	4
5/9/2013 17:02	1	32	-0.09	20.79	20.24	52.06	71.9	1.51	3947	4
5/9/2013 17:03	1	32	-0.09	20.92	20.27	52.75	71.86	1.51	3947	4

Table F.1 (cont.)

5/9/2013 13:35	2	32.8	-0.07	21.4	21.14	57.64	70.62	1.38	3947	4
5/9/2013 13:36	2	32.7	-0.07	21.28	21.14	57.51	70.6	1.38	3947	4
5/9/2013 13:36	2	32.7	-0.07	21.11	21.11	57.55	70.47	1.38	3947	4
5/9/2013 13:37	2	32.8	-0.07	21.04	21.15	57.47	70.75	1.38	3947	4
5/9/2013 13:38	2	32.8	-0.07	20.97	21.08	57.12	70.42	1.38	3947	4
5/9/2013 13:38	2	32.7	-0.07	21.17	21.13	56.68	71.37	1.38	3947	4
5/9/2013 13:39	2	33	-0.07	21.3	21.05	56.45	71.41	1.38	3947	4
5/9/2013 13:40	2	32.9	-0.07	21.34	21.1	56.54	70.86	1.38	3947	4
5/9/2013 13:41	2	32.9	-0.07	21.29	21.11	56.99	71.17	1.38	3947	4
5/9/2013 13:41	2	32.8	-0.07	21.19	21.04	57.87	71.12	1.38	3947	4
5/9/2013 13:42	2	32.9	-0.07	21.11	21.05	58.39	71.15	1.38	3947	4
5/9/2013 13:43	2	32.9	-0.07	21.1	21.07	58.52	70.69	1.38	3947	4
5/9/2013 14:13	3	31.1	0.20	20.89	20.84	54.35	71.56	1.44	3947	4
5/9/2013 14:14	3	31.1	0.20	20.89	20.79	55.02	71.17	1.44	3947	4
5/9/2013 14:14	3	31	0.20	20.78	20.78	55.4	71.32	1.44	3947	4
5/9/2013 14:15	3	31.1	0.20	20.69	20.83	55.51	71.34	1.44	3947	4
5/9/2013 14:16	3	31.2	0.20	20.63	20.84	55.43	71.36	1.44	3947	4
5/9/2013 14:17	3	31	0.20	20.55	20.8	55.11	71.45	1.44	3947	4
5/9/2013 14:17	3	31	0.20	20.6	20.82	54.44	71.37	1.44	3947	4
5/9/2013 14:18	3	31.1	0.20	20.68	20.76	53.68	71.25	1.44	3947	4
5/9/2013 14:19	3	31	0.20	20.74	20.73	53.09	70.87	1.44	3947	4
5/9/2013 14:20	3	31.1	0.20	20.73	20.8	53.16	70.67	1.44	3947	4
5/9/2013 14:20	3	31.3	0.20	20.68	20.78	53.64	70.66	1.44	3947	4
5/9/2013 14:21	3	31	0.20	20.68	20.73	54.53	70.58	1.44	3947	4

Table F.1 (cont.)

5/9/2013 14:52	4	30.2	0.08	20.66	20.35	53.55	71.32	1.29	3947	4
5/9/2013 14:53	4	30.2	0.08	20.63	20.43	53.98	71.24	1.29	3947	4
5/9/2013 14:53	4	30.1	0.08	20.71	20.35	54.27	71.25	1.29	3947	4
5/9/2013 14:54	4	30.2	0.08	20.86	20.44	54.47	71.14	1.29	3947	4
5/9/2013 14:55	4	30.1	0.08	20.93	20.33	54.69	71.31	1.29	3947	4
5/9/2013 14:56	4	30.4	0.08	20.89	20.33	54.8	71.3	1.29	3947	4
5/9/2013 14:56	4	30.2	0.08	20.8	20.41	54.76	71.3	1.29	3947	4
5/9/2013 14:57	4	30.3	0.08	20.66	20.45	54.78	71.15	1.29	3947	4
5/9/2013 14:58	4	30.7	0.08	20.59	20.38	54.66	71.23	1.29	3947	4
5/9/2013 14:58	4	30.4	0.08	20.61	20.42	54.22	71.22	1.29	3947	4
5/9/2013 14:59	4	30.3	0.08	20.74	20.46	53.44	71.39	1.29	3947	4
5/9/2013 15:00	4	30.3	0.08	20.78	20.45	53.16	71.34	1.29	3947	4
5/9/2013 15:29	5	32.4	0.06	20.72	20.3	55.02	72.61	1.45	3947	4
5/9/2013 15:30	5	32.4	0.06	20.77	20.26	54.24	72.87	1.45	3947	4
5/9/2013 15:31	5	32.7	0.06	20.7	20.18	53.94	72.97	1.45	3947	4
5/9/2013 15:32	5	32.5	0.06	20.57	20.22	53.92	73.11	1.45	3947	4
5/9/2013 15:32	5	32.6	0.06	20.5	20.28	53.92	72.92	1.45	3947	4
5/9/2013 15:33	5	32.5	0.06	20.48	20.29	54.02	72.84	1.45	3947	4
5/9/2013 15:34	5	32.5	0.06	20.49	20.27	54.1	72.82	1.45	3947	4
5/9/2013 15:34	5	32.5	0.06	20.83	20.22	54.3	72.91	1.45	3947	4
5/9/2013 15:35	5	32.6	0.06	20.85	20.27	54.93	73.1	1.45	3947	4
5/9/2013 15:36	5	32.6	0.06	20.64	20.22	55.62	73.29	1.45	3947	4
5/9/2013 15:37	5	32.5	0.06	20.54	20.17	55.78	73.23	1.45	3947	4
5/9/2013 15:37	5	32.4	0.06	20.53	20.22	55.76	73.2	1.45	3947	4

Table F.1 (cont.)

5/9/2013 16:07	6	35	0.06	20.23	20.41	54.41	73.13	1.51	3947	4
5/9/2013 16:07	6	34.7	0.06	20.22	20.48	55.02	73.27	1.51	3947	4
5/9/2013 16:08	6	35.1	0.06	20.28	20.41	55.44	73.27	1.51	3947	4
5/9/2013 16:09	6	35	0.06	20.32	20.49	55.33	73.33	1.51	3947	4
5/9/2013 16:10	6	34.9	0.06	20.45	20.39	55.07	73.44	1.51	3947	4
5/9/2013 16:10	6	35.2	0.06	20.31	20.5	54.86	73.28	1.51	3947	4
5/9/2013 16:11	6	34.9	0.06	20.19	20.49	54.66	73.25	1.51	3947	4
5/9/2013 16:12	6	35	0.06	20.19	20.49	54.28	73.38	1.51	3947	4
5/9/2013 16:13	6	35.1	0.06	20.05	20.48	53.94	73.26	1.51	3947	4
5/9/2013 16:13	6	34.8	0.06	20.27	20.47	53.52	73.46	1.51	3947	4
5/9/2013 16:14	6	34.9	0.06	20.36	20.54	53.7	73.46	1.51	3947	4
5/9/2013 16:15	6	35.1	0.06	20.19	20.46	54.09	73.32	1.51	3947	4
5/13/2013 9:20	1	30.9	0.32	18.2	14.96	32.28	38.1	1.59	3947	4
5/13/2013 9:20	1	30.7	0.32	18.31	14.94	32.18	37.9	1.59	3947	4
5/13/2013 9:21	1	31	0.32	18.54	15.03	31.81	37.85	1.59	3947	4
5/13/2013 9:22	1	30.9	0.32	18.64	15.04	31.56	37.76	1.59	3947	4
5/13/2013 9:23	1	31	0.32	18.61	15.1	31.65	37.56	1.59	3947	4
5/13/2013 9:23	1	31	0.32	18.5	14.94	31.57	37.02	1.59	3947	4
5/13/2013 9:24	1	30.9	0.32	18.48	15.04	31.6	36.94	1.59	3947	4
5/13/2013 9:25	1	30.9	0.32	18.42	15.07	31.68	36.76	1.59	3947	4
5/13/2013 9:26	1	30.7	0.32	18.46	15.05	31.43	36.35	1.59	3947	4
5/13/2013 9:26	1	30.9	0.32	18.36	15.08	31.13	35.93	1.59	3947	4
5/13/2013 9:27	1	31	0.32	18.59	15.13	30.71	35.44	1.59	3947	4
5/13/2013 9:28	1	30.8	0.32	18.64	15.05	30.49	35.22	1.59	3947	4

Table F.1 (cont.)

5/13/2013 9:56	2	31.2	0.31	19.09	15.93	26.42	30.96	1.4	3947	4
5/13/2013 9:56	2	31.3	0.31	19.2	15.91	26.27	30.52	1.4	3947	4
5/13/2013 9:57	2	31.3	0.31	19.06	15.94	26.04	30.43	1.4	3947	4
5/13/2013 9:58	2	31.3	0.31	18.98	15.96	26.26	30.43	1.4	3947	4
5/13/2013 9:59	2	31.2	0.31	18.94	16.01	26.1	30.35	1.4	3947	4
5/13/2013 9:59	2	31.3	0.31	18.77	16.01	26.1	30.38	1.4	3947	4
5/13/2013 10:00	2	31.2	0.31	19.09	16.08	26.06	30.33	1.4	3947	4
5/13/2013 10:01	2	31.3	0.31	19.19	16.12	25.67	30.16	1.4	3947	4
5/13/2013 10:02	2	31.2	0.31	19.28	16.1	25.73	30.37	1.4	3947	4
5/13/2013 10:02	2	31.4	0.31	19.22	16.11	25.6	30.24	1.4	3947	4
5/13/2013 10:03	2	31.3	0.31	18.95	16.13	25.67	30.27	1.4	3947	4
5/13/2013 10:04	2	31.2	0.31	19	16.04	25.9	30.17	1.4	3947	4
5/13/2013 10:32	3	30.2	0.19	18.78	16.63	25.32	28.45	1.49	3947	4
5/13/2013 10:32	3	30.1	0.19	18.72	16.59	25.48	28.37	1.49	3947	4
5/13/2013 10:33	3	30.2	0.19	18.67	16.6	25.48	28.17	1.49	3947	4
5/13/2013 10:34	3	30.2	0.19	18.65	16.68	25.46	28.21	1.49	3947	4
5/13/2013 10:35	3	30.3	0.19	18.69	16.68	25.31	28.25	1.49	3947	4
5/13/2013 10:35	3	30.4	0.19	18.75	16.64	25.21	28.86	1.49	3947	4
5/13/2013 10:36	3	30.3	0.19	18.78	16.68	25.24	29.13	1.49	3947	4
5/13/2013 10:37	3	30.4	0.19	18.72	16.73	25.4	29.34	1.49	3947	4
5/13/2013 10:37	3	30.1	0.19	18.69	16.71	25.67	29.46	1.49	3947	4
5/13/2013 10:38	3	30.1	0.19	18.61	16.75	26	29.41	1.49	3947	4
5/13/2013 10:39	3	30.3	0.19	18.67	16.88	26.16	29.3	1.49	3947	4
5/13/2013 10:40	3	30.2	0.19	18.75	16.87	26.16	29.48	1.49	3947	4

Table F.1 (cont.)

5/13/2013 11:08	4	29.9	0.16	19.19	17.46	25.49	29.02	1.31	3947	4
5/13/2013 11:09	4	29.9	0.16	19.26	17.48	25.51	29.19	1.31	3947	4
5/13/2013 11:10	4	30	0.16	19.24	17.53	25.78	29.22	1.31	3947	4
5/13/2013 11:10	4	29.9	0.16	19.11	17.53	26.16	29.35	1.31	3947	4
5/13/2013 11:11	4	30	0.16	19.11	17.59	26.45	29.13	1.31	3947	4
5/13/2013 11:12	4	29.8	0.16	19.11	17.63	26.51	29.2	1.31	3947	4
5/13/2013 11:13	4	29.8	0.16	19.27	17.65	26.51	29.35	1.31	3947	4
5/13/2013 11:13	4	30	0.16	19.36	17.62	26.34	29.15	1.31	3947	4
5/13/2013 11:14	4	30	0.16	19.36	17.6	26.26	28.91	1.31	3947	4
5/13/2013 11:15	4	30.2	0.16	19.25	17.6	26.34	28.54	1.31	3947	4
5/13/2013 11:16	4	29.9	0.16	19.12	17.63	26.38	28.36	1.31	3947	4
5/13/2013 11:16	4	30.1	0.16	19.06	17.65	26.42	28.44	1.31	3947	4
5/13/2013 11:42	5	30.8	0.14	19.36	18.11	25.87	27.92	1.5	3947	4
5/13/2013 11:43	5	30.9	0.14	19.56	18.04	25.81	27.84	1.5	3947	4
5/13/2013 11:44	5	31	0.14	19.69	18.06	25.74	27.79	1.5	3947	4
5/13/2013 11:45	5	30.9	0.14	19.74	18.2	25.73	27.64	1.5	3947	4
5/13/2013 11:45	5	31	0.14	19.51	18.2	25.65	27.58	1.5	3947	4
5/13/2013 11:46	5	31	0.14	19.47	18.25	25.85	27.46	1.5	3947	4
5/13/2013 11:47	5	30.9	0.14	19.3	18.28	25.85	27.11	1.5	3947	4
5/13/2013 11:47	5	31.1	0.14	19.36	18.23	25.82	27.08	1.5	3947	4
5/13/2013 11:48	5	31.1	0.14	19.44	18.29	25.62	27.22	1.5	3947	4
5/13/2013 11:49	5	31.1	0.14	19.48	18.26	25.71	27.43	1.5	3947	4
5/13/2013 11:50	5	30.9	0.14	19.63	18.28	25.58	27.67	1.5	3947	4
5/13/2013 11:50	5	30.9	0.14	19.53	18.29	25.61	27.67	1.5	3947	4

Table F.1 (cont.)

5/13/2013 12:20	6	33.6	0.17	19.11	18.56	24.55	26.35	1.52	3947	4
5/13/2013 12:20	6	33.7	0.17	19.11	18.51	24.54	26.31	1.52	3947	4
5/13/2013 12:21	6	34	0.17	19.05	18.57	24.73	26.45	1.52	3947	4
5/13/2013 12:22	6	33.8	0.17	19.2	18.6	24.68	26.5	1.52	3947	4
5/13/2013 12:23	6	33.8	0.17	19.37	18.58	24.55	26.71	1.52	3947	4
5/13/2013 12:23	6	33.7	0.17	19.39	18.56	24.58	26.46	1.52	3947	4
5/13/2013 12:24	6	34	0.17	19.32	18.64	24.57	25.87	1.52	3947	4
5/13/2013 12:25	6	34	0.17	19.2	18.63	24.64	25.88	1.52	3947	4
5/13/2013 12:25	6	33.7	0.17	18.97	18.64	24.65	25.24	1.52	3947	4
5/13/2013 12:26	6	33.8	0.17	19.15	18.61	24.48	25.16	1.52	3947	4
5/13/2013 12:27	6	33.8	0.17	18.98	18.58	24.38	25.68	1.52	3947	4
5/13/2013 12:28	6	34.1	0.17	19.3	18.56	24.16	25.89	1.52	3947	4
5/16/2013 11:07	1	30.9	0.00	20.78	19.42	47.86	43.33	1.52	3947	4
5/16/2013 11:08	1	30.8	0.00	20.71	19.41	47.56	43.4	1.52	3947	4
5/16/2013 11:09	1	30.9	0.00	20.69	19.33	46.8	43.29	1.52	3947	4
5/16/2013 11:09	1	30.8	0.00	20.95	19.37	46.2	43.3	1.52	3947	4
5/16/2013 11:10	1	31	0.00	20.71	19.4	45.61	43.23	1.52	3947	4
5/16/2013 11:11	1	31	0.00	20.74	19.32	45.54	43.43	1.52	3947	4
5/16/2013 11:11	1	30.9	0.00	20.51	19.35	45.98	43.54	1.52	3947	4
5/16/2013 11:12	1	30.7	0.00	20.67	19.5	46.42	43.06	1.52	3947	4
5/16/2013 11:13	1	30.8	0.00	20.78	19.55	46.55	42.57	1.52	3947	4
5/16/2013 11:14	1	30.8	0.00	20.95	19.5	46.84	42.18	1.52	3947	4
5/16/2013 11:14	1	31	0.00	20.98	19.42	46.9	42.19	1.52	3947	4
5/16/2013 11:15	1	30.9	0.00	20.97	19.4	46.89	42.17	1.52	3947	4

Table F.1 (cont.)

5/16/2013 11:42	2	31.6	0.07	21.06	19.08	48	42.86	1.39	3947	4
5/16/2013 11:43	2	31.7	0.07	21.02	19.01	47.78	42.79	1.39	3947	4
5/16/2013 11:44	2	31.9	0.07	20.91	19.06	47.89	42.86	1.39	3947	4
5/16/2013 11:45	2	31.9	0.07	20.86	19.06	48.27	42.61	1.39	3947	4
5/16/2013 11:45	2	31.5	0.07	20.88	19.11	48.54	42.41	1.39	3947	4
5/16/2013 11:46	2	31.8	0.07	21.01	19.02	48.63	42.11	1.39	3947	4
5/16/2013 11:47	2	31.7	0.07	20.98	19.09	48.65	41.9	1.39	3947	4
5/16/2013 11:47	2	31.6	0.07	21.11	19.07	48.57	41.79	1.39	3947	4
5/16/2013 11:48	2	31.9	0.07	20.95	19.05	48.6	41.52	1.39	3947	4
5/16/2013 11:49	2	31.6	0.07	20.87	19.05	48.6	41.41	1.39	3947	4
5/16/2013 11:50	2	31.7	0.07	20.78	19.09	48.43	41.3	1.39	3947	4
5/16/2013 11:50	2	31.8	0.07	20.83	19.02	48.11	41.29	1.39	3947	4
5/16/2013 12:21	3	29.9	0.04	20.61	18.84	45.41	40.08	1.42	3947	4
5/16/2013 12:22	3	30.1	0.04	20.66	18.91	44.64	39.9	1.42	3947	4
5/16/2013 12:23	3	30.2	0.04	20.71	18.98	43.96	39.83	1.42	3947	4
5/16/2013 12:23	3	30.1	0.04	20.66	19.03	43.76	39.72	1.42	3947	4
5/16/2013 12:24	3	30.1	0.04	20.63	19.07	43.9	39.7	1.42	3947	4
5/16/2013 12:25	3	30	0.04	20.61	18.95	44.45	39.69	1.42	3947	4
5/16/2013 12:26	3	30	0.04	20.52	18.9	45.09	39.82	1.42	3947	4
5/16/2013 12:26	3	30.1	0.04	20.59	18.9	45.54	39.78	1.42	3947	4
5/16/2013 12:27	3	30.2	0.04	20.71	19.03	45.69	39.85	1.42	3947	4
5/16/2013 12:28	3	30.2	0.04	20.74	19.03	45.65	39.87	1.42	3947	4
5/16/2013 12:28	3	30	0.04	20.79	19.06	45.42	39.83	1.42	3947	4
5/16/2013 12:29	3	30	0.04	20.73	19.05	45.01	39.84	1.42	3947	4

Table F.1 (cont.)

5/16/2013 13:12	4	30.1	0.03	20.54	18.89	48.86	55.82	1.3	3947	4
5/16/2013 13:13	4	30.3	0.03	20.41	18.8	48.94	55.36	1.3	3947	4
5/16/2013 13:13	4	30.1	0.03	20.45	18.81	49.07	55.4	1.3	3947	4
5/16/2013 13:14	4	30.1	0.03	20.62	18.82	49.17	55.29	1.3	3947	4
5/16/2013 13:15	4	30.3	0.03	20.68	18.81	49.32	55.27	1.3	3947	4
5/16/2013 13:15	4	30.3	0.03	20.68	18.8	49.73	55.32	1.3	3947	4
5/16/2013 13:16	4	30.2	0.03	20.54	18.86	50.18	55.44	1.3	3947	4
5/16/2013 13:17	4	30.3	0.03	20.46	18.76	50.39	55.34	1.3	3947	4
5/16/2013 13:18	4	30	0.03	20.34	18.78	50.31	55.27	1.3	3947	4
5/16/2013 13:18	4	30.1	0.03	20.4	18.91	49.93	55.16	1.3	3947	4
5/16/2013 13:19	4	30	0.03	20.47	19.01	49.08	55.3	1.3	3947	4
5/16/2013 13:20	4	30.3	0.03	20.52	18.97	48.52	55.37	1.3	3947	4
5/16/2013 13:44	5	31.1	0.04	20.59	20.63	49.11	51.69	1.49	3947	4
5/16/2013 13:45	5	31.2	0.04	20.42	20.53	49.09	52.12	1.49	3947	4
5/16/2013 13:46	5	31.2	0.04	20.6	20.32	49.44	52.64	1.49	3947	4
5/16/2013 13:46	5	31.2	0.04	20.75	20.1	49.35	53.17	1.49	3947	4
5/16/2013 13:47	5	31.3	0.04	20.75	19.94	49.6	53.64	1.49	3947	4
5/16/2013 13:48	5	31.4	0.04	20.77	19.75	50.07	54.33	1.49	3947	4
5/16/2013 13:49	5	31.2	0.04	20.74	19.76	50.43	54.92	1.49	3947	4
5/16/2013 13:49	5	31.3	0.04	20.6	19.67	50.68	55.45	1.49	3947	4
5/16/2013 13:50	5	31.4	0.04	20.6	19.67	50.86	56.1	1.49	3947	4
5/16/2013 13:51	5	31.5	0.04	20.58	19.53	50.53	56.3	1.49	3947	4
5/16/2013 13:51	5	31.3	0.04	20.46	19.46	49.94	56.37	1.49	3947	4
5/16/2013 13:52	5	31.3	0.04	20.63	19.47	49.3	56.38	1.49	3947	4

Table F.1 (cont.)

5/16/2013 14:20	6	34.3	0.04	20.21	18.76	50.74	57.28	1.52	3947	4
5/16/2013 14:21	6	34.2	0.04	20.11	18.78	51.3	57.42	1.52	3947	4
5/16/2013 14:22	6	34.1	0.04	20.02	18.8	51.39	57.39	1.52	3947	4
5/16/2013 14:22	6	34.1	0.04	19.97	18.73	51.41	57.51	1.52	3947	4
5/16/2013 14:23	6	34.1	0.04	19.95	18.69	51.09	57.46	1.52	3947	4
5/16/2013 14:24	6	34.6	0.04	20	18.72	50.38	57.44	1.52	3947	4
5/16/2013 14:25	6	34.1	0.04	20.06	18.71	49.57	57.5	1.52	3947	4
5/16/2013 14:25	6	34.4	0.04	20.05	18.71	49.61	57.75	1.52	3947	4
5/16/2013 14:26	6	34.2	0.04	20	18.7	49.8	57.94	1.52	3947	4
5/16/2013 14:27	6	34.3	0.04	19.99	18.69	50.41	58.12	1.52	3947	4
5/16/2013 14:27	6	34.3	0.04	19.95	18.64	51.06	58.03	1.52	3947	4
5/16/2013 14:28	6	34.4	0.04	20.03	18.66	51.32	57.97	1.52	3947	4
5/23/2013 13:12	1	32	0.15	19.94	18.29	51.72	63.13	1.52	3947	4
5/23/2013 13:12	1	32.2	0.15	19.97	18.24	52.26	63.05	1.52	3947	4
5/23/2013 13:13	1	31.9	0.15	20.03	18.29	52.52	62.67	1.52	3947	4
5/23/2013 13:14	1	32.1	0.15	20.2	18.25	52.33	62.67	1.52	3947	4
5/23/2013 13:15	1	32.1	0.15	20.22	18.2	52.11	62.6	1.52	3947	4
5/23/2013 13:15	1	32	0.15	20.19	18.15	51.65	62.54	1.52	3947	4
5/23/2013 13:16	1	32	0.15	20	18.15	51.28	62.63	1.52	3947	4
5/23/2013 13:17	1	32.1	0.15	19.75	18.21	51.14	62.54	1.52	3947	4
5/23/2013 13:17	1	32.2	0.15	19.92	18.11	51.18	62.45	1.52	3947	4
5/23/2013 13:18	1	32	0.15	20.01	18.12	51.18	62.37	1.52	3947	4
5/23/2013 13:19	1	32.2	0.15	20.13	18.07	50.99	62.41	1.52	3947	4
5/23/2013 13:20	1	32.2	0.15	20.13	18.1	50.92	62.41	1.52	3947	4

Table F.1 (cont.)

5/23/2013 12:31	2	32	0.09	20.08	18.12	57.03	69.65	1.38	3947	4
5/23/2013 12:32	2	32	0.09	20.11	18.2	56.97	69.57	1.38	3947	4
5/23/2013 12:33	2	31.8	0.09	20.16	18.15	57.18	69.51	1.38	3947	4
5/23/2013 12:34	2	31.9	0.09	20.02	18.12	57.64	69.45	1.38	3947	4
5/23/2013 12:34	2	31.7	0.09	19.84	18.06	58.31	69.31	1.38	3947	4
5/23/2013 12:35	2	31.7	0.09	19.99	18.03	58.53	68.95	1.38	3947	4
5/23/2013 12:36	2	31.9	0.09	19.86	18.01	58.23	68.88	1.38	3947	4
5/23/2013 12:36	2	32	0.09	19.96	18.04	57.48	68.9	1.38	3947	4
5/23/2013 12:37	2	31.8	0.09	20.13	18.04	56.88	68.71	1.38	3947	4
5/23/2013 12:38	2	31.8	0.09	19.92	17.97	56.51	68.71	1.38	3947	4
5/23/2013 12:39	2	31.7	0.09	19.83	18.1	56.43	68.68	1.38	3947	4
5/23/2013 12:39	2	32	0.09	19.94	18.06	56.79	68.65	1.38	3947	4
5/23/2013 11:56	3	30.1	0.04	20.16	18.53	54	70.18	1.43	3947	4
5/23/2013 11:57	3	30.1	0.04	20.02	18.53	53.75	70.31	1.43	3947	4
5/23/2013 11:58	3	30.2	0.04	19.95	18.53	53.53	70.35	1.43	3947	4
5/23/2013 11:58	3	30	0.04	19.86	18.55	53.12	70.25	1.43	3947	4
5/23/2013 11:59	3	30.2	0.04	19.91	18.51	52.99	70.08	1.43	3947	4
5/23/2013 12:00	3	30	0.04	20.08	18.53	52.89	69.82	1.43	3947	4
5/23/2013 12:00	3	30.1	0.04	20.1	18.44	52.9	69.59	1.43	3947	4
5/23/2013 12:01	3	30.1	0.04	20.16	18.44	53.11	69.41	1.43	3947	4
5/23/2013 12:02	3	30	0.04	20.13	18.35	53.78	69.12	1.43	3947	4
5/23/2013 12:03	3	30.1	0.04	20.04	18.39	54.21	69.07	1.43	3947	4
5/23/2013 12:03	3	30	0.04	19.97	18.4	54.26	68.84	1.43	3947	4
5/23/2013 12:04	3	30.2	0.04	19.89	18.36	54.08	68.77	1.43	3947	4

Table F.1 (cont.)

5/23/2013 11:22	4	30.5	0.01	20.24	18.79	54.28	72.78	1.3	3947	4
5/23/2013 11:22	4	30.6	0.01	20.19	18.81	54.93	72.86	1.3	3947	4
5/23/2013 11:23	4	30.4	0.01	20.1	18.79	55.85	72.94	1.3	3947	4
5/23/2013 11:24	4	30.3	0.01	20.03	18.81	56.18	72.75	1.3	3947	4
5/23/2013 11:24	4	30.6	0.01	20.05	18.83	55.89	72.27	1.3	3947	4
5/23/2013 11:25	4	30.5	0.01	20.12	18.78	55.13	71.86	1.3	3947	4
5/23/2013 11:26	4	30.4	0.01	20.18	18.82	54.19	71.5	1.3	3947	4
5/23/2013 11:27	4	30.6	0.01	20.17	18.8	53.56	71.43	1.3	3947	4
5/23/2013 11:27	4	30.5	0.01	20.1	18.83	53.45	71.17	1.3	3947	4
5/23/2013 11:28	4	30.7	0.01	20.01	18.84	53.77	71.05	1.3	3947	4
5/23/2013 11:29	4	30.4	0.01	20.02	18.8	54.32	70.76	1.3	3947	4
5/23/2013 11:29	4	30.5	0.01	20.11	18.84	54.58	70.4	1.3	3947	4
5/23/2013 10:47	5	31.3	0.01	19.92	18.51	54.04	70.25	1.48	3947	4
5/23/2013 10:48	5	31.4	0.01	19.99	18.56	53.45	70.14	1.48	3947	4
5/23/2013 10:48	5	31.2	0.01	20.03	18.57	53.29	69.87	1.48	3947	4
5/23/2013 10:49	5	31.3	0.01	20.16	18.54	53.27	69.77	1.48	3947	4
5/23/2013 10:50	5	31.3	0.01	20.28	18.55	53.36	69.78	1.48	3947	4
5/23/2013 10:51	5	31.3	0.01	20.17	18.56	54.03	69.6	1.48	3947	4
5/23/2013 10:51	5	31.3	0.01	20.04	18.58	54.88	69.84	1.48	3947	4
5/23/2013 10:52	5	31.4	0.01	20.03	18.56	55.4	70.1	1.48	3947	4
5/23/2013 10:53	5	31.2	0.01	20.02	18.63	55.22	70.44	1.48	3947	4
5/23/2013 10:53	5	31.2	0.01	20.06	18.53	54.47	70.39	1.48	3947	4
5/23/2013 10:54	5	31.3	0.01	20.02	18.54	53.59	70.8	1.48	3947	4
5/23/2013 10:55	5	31.4	0.01	20.22	18.53	53.12	70.84	1.48	3947	4

Table F.1 (cont.)

5/23/2013 10:12	6	34.2	-0.03	19.88	17.89	55.09	75.93	1.51	3947	4
5/23/2013 10:13	6	34	-0.03	19.74	17.87	55.15	75.69	1.51	3947	4
5/23/2013 10:14	6	34.2	-0.03	19.72	17.91	55.21	75.75	1.51	3947	4
5/23/2013 10:15	6	34.1	-0.03	19.68	17.93	54.99	75.57	1.51	3947	4
5/23/2013 10:15	6	34.3	-0.03	19.71	17.92	54.24	75.36	1.51	3947	4
5/23/2013 10:16	6	34.3	-0.03	19.77	17.89	53.45	75.19	1.51	3947	4
5/23/2013 10:17	6	34.1	-0.03	19.7	17.95	53.22	75.11	1.51	3947	4
5/23/2013 10:17	6	34	-0.03	19.68	17.89	53.61	75.1	1.51	3947	4
5/23/2013 10:18	6	34.1	-0.03	19.52	17.93	54.21	74.99	1.51	3947	4
5/23/2013 10:19	6	34.2	-0.03	19.7	17.94	54.85	75.02	1.51	3947	4
5/23/2013 10:20	6	34	-0.03	19.65	17.93	55.04	74.49	1.51	3947	4
5/23/2013 10:20	6	34	-0.03	19.85	17.97	55.27	74.26	1.51	3947	4
11/4/2013 12:04	1	31.4	0.25	19.17	16.36	33.54	39.51	1.54	3929	4
11/4/2013 12:05	1	31.5	0.25	19.23	16.34	33.59	39.52	1.54	3929	4
11/4/2013 12:06	1	31.5	0.25	19.12	16.32	33.63	39.47	1.54	3929	4
11/4/2013 12:07	1	31.5	0.25	19.1	16.33	33.84	39.48	1.54	3929	4
11/4/2013 12:08	1	31.5	0.25	19.06	16.41	33.65	39.44	1.54	3929	4
11/4/2013 12:09	1	31.7	0.25	19.17	16.44	33.51	39.48	1.54	3929	4
11/4/2013 12:10	1	31.6	0.25	19.25	16.4	33.51	39.45	1.54	3929	4
11/4/2013 12:11	1	31.6	0.25	19.17	16.48	33.68	39.11	1.54	3929	4
11/4/2013 12:12	1	31.7	0.25	19.12	16.45	33.67	39.2	1.54	3929	4
11/4/2013 12:13	1	31.7	0.25	19.18	16.45	33.72	39.22	1.54	3929	4
11/4/2013 12:14	1	31.5	0.25	19.26	16.49	33.48	39.17	1.54	3929	4
11/4/2013 12:15	1	31.6	0.25	19.25	16.43	33.44	39.2	1.54	3929	4

Table F.1 (cont.)

11/6/2013 8:28	2	31.8	0.05	19.35	15.93	54.48	68.3	1.36	3929	4
11/6/2013 8:29	2	31.7	0.05	19.37	15.84	54.63	68.26	1.36	3929	4
11/6/2013 8:30	2	31.8	0.05	19.28	15.92	55.04	68.28	1.36	3929	4
11/6/2013 8:31	2	31.9	0.05	19.19	15.86	55.5	68.16	1.36	3929	4
11/6/2013 8:32	2	31.8	0.05	19.11	16.05	55.21	67.9	1.36	3929	4
11/6/2013 8:33	2	31.9	0.05	19.19	15.98	54.26	68.01	1.36	3929	4
11/6/2013 8:34	2	31.9	0.05	19.37	15.85	53.82	68.24	1.36	3929	4
11/6/2013 8:35	2	31.9	0.05	19.28	15.82	54	68.4	1.36	3929	4
11/6/2013 8:36	2	32	0.05	19.22	15.86	54.74	68.3	1.36	3929	4
11/6/2013 8:36	2	31.8	0.05	19.17	15.85	55.18	68.36	1.36	3929	4
11/6/2013 8:37	2	31.8	0.05	19.42	15.85	55.11	68.55	1.36	3929	4
11/6/2013 8:38	2	31.9	0.05	19.5	15.84	54.66	68.6	1.36	3929	4
11/4/2013 10:45	3	29.2	0.09	18.91	15.77	34.61	41.29	1.48	3929	4
11/4/2013 10:46	3	29.4	0.09	18.8	15.81	35	41.06	1.48	3929	4
11/4/2013 10:47	3	29.5	0.09	18.83	15.8	34.95	40.88	1.48	3929	4
11/4/2013 10:48	3	29.1	0.09	18.94	15.91	34.65	40.8	1.48	3929	4
11/4/2013 10:49	3	29.2	0.09	18.94	15.93	34.43	40.72	1.48	3929	4
11/4/2013 10:50	3	29.4	0.09	18.81	15.9	34.49	40.63	1.48	3929	4
11/4/2013 10:51	3	29.5	0.09	18.78	15.87	34.75	40.64	1.48	3929	4
11/4/2013 10:52	3	29.3	0.09	18.78	15.88	34.88	40.59	1.48	3929	4
11/4/2013 10:53	3	29.4	0.09	18.99	15.87	34.55	40.59	1.48	3929	4
11/4/2013 10:54	3	29.7	0.09	19.08	15.86	34.46	40.61	1.48	3929	4
11/4/2013 10:55	3	29.5	0.09	19.03	15.88	34.36	40.65	1.48	3929	4
11/4/2013 10:56	3	29.1	0.09	18.89	15.93	34.48	40.6	1.48	3929	4

Table F.1 (cont.)

11/4/2013 10:06	4	30.3	0.17	19.03	15.82	34.62	41.41	1.31	3929	4
11/4/2013 10:07	4	30.4	0.17	18.97	15.83	34.83	41.67	1.31	3929	4
11/4/2013 10:08	4	30.4	0.17	18.87	15.73	35.02	41.71	1.31	3929	4
11/4/2013 10:09	4	30.5	0.17	18.89	15.67	35	41.77	1.31	3929	4
11/4/2013 10:10	4	30.5	0.17	19.05	15.63	34.77	41.96	1.31	3929	4
11/4/2013 10:10	4	30.6	0.17	19.03	15.62	34.59	42.11	1.31	3929	4
11/4/2013 10:11	4	30.4	0.17	18.85	15.56	34.81	41.94	1.31	3929	4
11/4/2013 10:12	4	30.2	0.17	18.8	15.56	35.06	41.86	1.31	3929	4
11/4/2013 10:13	4	30.6	0.17	18.89	15.61	34.95	41.83	1.31	3929	4
11/4/2013 10:14	4	30.7	0.17	19.03	15.63	34.77	41.9	1.31	3929	4
11/4/2013 10:15	4	30.4	0.17	19.05	15.62	34.72	42.14	1.31	3929	4
11/4/2013 10:16	4	30.5	0.17	18.89	15.49	34.89	42.22	1.31	3929	4
11/4/2013 9:26	5	31.5	0.08	19.21	15.21	33.72	42.1	1.51	3929	4
11/4/2013 9:27	5	31.4	0.08	19	15.15	34	42.37	1.51	3929	4
11/4/2013 9:28	5	31.5	0.08	19.19	15.03	34.03	42.52	1.51	3929	4
11/4/2013 9:29	5	31.5	0.08	19.31	15	33.78	42.63	1.51	3929	4
11/4/2013 9:30	5	31.5	0.08	19.39	15.05	33.53	42.8	1.51	3929	4
11/4/2013 9:31	5	31.6	0.08	19.25	15.02	33.86	43.04	1.51	3929	4
11/4/2013 9:32	5	31.6	0.08	19.03	14.9	34.22	43.27	1.51	3929	4
11/4/2013 9:33	5	31.3	0.08	18.95	14.97	34.27	43.23	1.51	3929	4
11/4/2013 9:34	5	31.5	0.08	19.03	15.36	34.41	42.22	1.51	3929	4
11/4/2013 9:35	5	31.5	0.08	19.1	15.8	34.12	41.17	1.51	3929	4
11/4/2013 9:36	5	31.5	0.08	19.4	16.08	33.86	40.37	1.51	3929	4
11/4/2013 9:37	5	31.3	0.08	19.27	16.27	33.98	40.15	1.51	3929	4

Table F.1 (cont.)

11/4/2013 8:47	6	33.9	0.06	18.78	16.2	33.16	39.39	1.55	3929	4
11/4/2013 8:48	6	33.9	0.06	18.64	16.32	33.37	39.11	1.55	3929	4
11/4/2013 8:49	6	33.7	0.06	18.59	16.37	33.44	38.89	1.55	3929	4
11/4/2013 8:50	6	33.9	0.06	18.86	16.42	33.23	38.65	1.55	3929	4
11/4/2013 8:51	6	34	0.06	18.89	16.48	32.85	38.57	1.55	3929	4
11/4/2013 8:52	6	34.1	0.06	18.86	16.52	33.05	38.35	1.55	3929	4
11/4/2013 8:53	6	33.9	0.06	18.7	16.46	33.35	38.74	1.55	3929	4
11/4/2013 8:54	6	33.9	0.06	18.76	16.15	33.18	39.29	1.55	3929	4
11/4/2013 8:55	6	34.3	0.06	18.76	15.92	33.02	40.03	1.55	3929	4
11/4/2013 8:56	6	34	0.06	18.95	15.68	32.95	40.3	1.55	3929	4
11/4/2013 8:57	6	34.3	0.06	18.81	15.59	33.12	40.72	1.55	3929	4
11/4/2013 8:58	6	34	0.06	18.65	15.3	33.18	41.13	1.55	3929	4
11/16/2013 16:34	1	31.1	0.11	19.63	17.54	52.64	66.89	1.52	3929	4
11/16/2013 16:35	1	31.3	0.11	19.55	17.51	52.71	67.07	1.52	3929	4
11/16/2013 16:35	1	31.8	0.11	19.53	17.52	52.63	66.9	1.52	3929	4
11/16/2013 16:36	1	31.8	0.11	19.49	17.57	52.55	67.03	1.52	3929	4
11/16/2013 16:37	1	32.1	0.11	19.42	17.53	52.23	66.97	1.52	3929	4
11/16/2013 16:37	1	32.1	0.11	19.36	17.49	51.82	66.77	1.52	3929	4
11/16/2013 16:38	1	32.2	0.11	19.32	17.56	51.41	66.72	1.52	3929	4
11/16/2013 16:39	1	32.2	0.11	19.54	17.62	51.45	66.56	1.52	3929	4
11/16/2013 16:40	1	32.4	0.11	19.61	17.64	51.45	66.5	1.52	3929	4
11/16/2013 16:40	1	32.3	0.11	19.65	17.62	51.65	66.43	1.52	3929	4
11/16/2013 16:41	1	32.3	0.11	19.59	17.59	52.58	66.41	1.52	3929	4
11/16/2013 16:42	1	32.3	0.11	19.42	17.57	53.02	66.35	1.52	3929	4

Table F.1 (cont.)

11/16/2013 15:21	2	32	0.20	19.2	17.8	55.73	65.49	1.39	3929	4
11/16/2013 15:22	2	32.4	0.20	19.28	17.81	55.1	65.16	1.39	3929	4
11/16/2013 15:23	2	32.2	0.20	19.34	17.81	54.98	64.87	1.39	3929	4
11/16/2013 15:23	2	32.5	0.20	19.23	17.75	55.29	65.25	1.39	3929	4
11/16/2013 15:24	2	32.5	0.20	19.16	17.84	55.83	65.14	1.39	3929	4
11/16/2013 15:25	2	32.6	0.20	19.21	17.85	56.35	65	1.39	3929	4
11/16/2013 15:25	2	32.4	0.20	19.19	17.75	56.67	65.39	1.39	3929	4
11/16/2013 15:26	2	32.5	0.20	19.35	17.77	56.57	64.89	1.39	3929	4
11/16/2013 15:27	2	32.6	0.20	19.47	17.84	56.16	65.17	1.39	3929	4
11/16/2013 15:28	2	32.6	0.20	19.48	17.75	55.8	66.05	1.39	3929	4
11/16/2013 15:28	2	32.5	0.20	19.26	17.76	55.43	65.67	1.39	3929	4
11/16/2013 15:29	7	32.6	0.20	19.19	17.79	55.44	65.77	1.39	3929	4
11/16/2013 14:51	3	30.4	0.15	18.67	17.66	53.45	68.06	1.5	3929	4
11/16/2013 14:52	3	30.6	0.15	18.59	17.65	53.68	68.01	1.5	3929	4
11/16/2013 14:52	3	30.6	0.15	18.57	17.68	54.05	67.62	1.5	3929	4
11/16/2013 14:53	3	30.8	0.15	18.68	17.65	54.19	66.64	1.5	3929	4
11/16/2013 14:54	3	30.9	0.15	18.81	17.73	54.32	67.91	1.5	3929	4
11/16/2013 14:54	3	31.1	0.15	18.91	17.66	54.6	67.8	1.5	3929	4
11/16/2013 14:55	3	31	0.15	18.92	17.69	54.85	67.21	1.5	3929	4
11/16/2013 14:56	3	31	0.15	18.87	17.67	54.73	67.45	1.5	3929	4
11/16/2013 14:57	3	30.9	0.15	18.8	17.66	54.55	67.91	1.5	3929	4
11/16/2013 14:57	3	31.2	0.15	18.74	17.75	54.28	67.19	1.5	3929	4
11/16/2013 14:58	3	31	0.15	18.7	17.71	53.83	67.9	1.5	3929	4
11/16/2013 14:59	3	31.2	0.15	18.66	17.65	53.52	68.51	1.5	3929	4

Table F.1 (cont.)

11/16/2013 15:52	4	31	0.12	19.21	17.7	52.5	65.06	1.3	3929	4
11/16/2013 15:53	4	31	0.12	19.31	17.68	52.25	65.16	1.3	3929	4
11/16/2013 15:54	4	31.2	0.12	19.28	17.73	52.44	65.11	1.3	3929	4
11/16/2013 15:54	4	31.2	0.12	19.24	17.8	52.83	65.35	1.3	3929	4
11/16/2013 15:55	4	31.2	0.12	19.17	17.65	53.71	65.33	1.3	3929	4
11/16/2013 15:56	4	31.1	0.12	19.15	17.63	54.21	65.23	1.3	3929	4
11/16/2013 15:56	4	31.5	0.12	19.24	17.64	54.39	65.25	1.3	3929	4
11/16/2013 15:57	4	31.3	0.12	19.36	17.64	53.83	65.17	1.3	3929	4
11/16/2013 15:58	4	31.4	0.12	19.34	17.76	53.02	65.17	1.3	3929	4
11/16/2013 15:59	4	31.3	0.12	19.31	17.65	52.63	65.35	1.3	3929	4
11/16/2013 15:59	4	31.5	0.12	19.14	17.57	52.4	65.42	1.3	3929	4
11/16/2013 16:00	4	31.3	0.12	19.06	17.57	52.54	65.7	1.3	3929	4
11/16/2013 13:53	5	29.9	0.10	19.01	17.67	53.39	65.84	1.45	3929	4
11/16/2013 13:53	5	30.4	0.10	18.9	17.74	54.04	64.94	1.45	3929	4
11/16/2013 13:54	5	30.7	0.10	18.77	17.74	54.45	65	1.45	3929	4
11/16/2013 13:55	5	31.1	0.10	18.76	17.73	55.11	65.2	1.45	3929	4
11/16/2013 13:55	5	31	0.10	18.93	17.73	54.91	65.03	1.45	3929	4
11/16/2013 13:56	5	31.3	0.10	18.94	17.75	54.37	65.8	1.45	3929	4
11/16/2013 13:57	5	31.3	0.10	18.92	17.74	53.52	66.03	1.45	3929	4
11/16/2013 13:58	5	31.4	0.10	18.92	17.71	52.75	65.84	1.45	3929	4
11/16/2013 13:58	5	31.7	0.10	18.89	17.67	52.58	65.91	1.45	3929	4
11/16/2013 13:59	5	31.5	0.10	18.97	17.72	52.95	67.44	1.45	3929	4
11/16/2013 14:00	5	31.6	0.10	18.8	17.58	53.29	66.27	1.45	3929	4
11/16/2013 14:01	5	31.7	0.10	18.8	17.59	53.75	66.93	1.45	3929	4

Table F.1 (cont.)

11/16/2013 13:27	6	33.7	0.07	18.41	17.39	53.91	66.17	1.51	3929	4
11/16/2013 13:27	6	34	0.07	18.4	17.4	53.85	66	1.51	3929	4
11/16/2013 13:28	6	34.3	0.07	18.45	17.5	53.74	65.69	1.51	3929	4
11/16/2013 13:29	6	34.4	0.07	18.54	17.54	53.59	65.41	1.51	3929	4
11/16/2013 13:30	6	34.5	0.07	18.53	17.54	53.61	65.33	1.51	3929	4
11/16/2013 13:30	6	34.2	0.07	18.65	17.58	53.97	65.47	1.51	3929	4
11/16/2013 13:31	6	34.6	0.07	18.61	17.59	54.47	66.09	1.51	3929	4
11/16/2013 13:32	6	34.6	0.07	18.61	17.54	55.15	67.47	1.51	3929	4
11/16/2013 13:32	6	34.7	0.07	18.4	17.47	55.26	66.52	1.51	3929	4
11/16/2013 13:33	6	34.4	0.07	18.58	17.51	54.82	66.15	1.51	3929	4
11/16/2013 13:34	6	34.7	0.07	18.61	17.51	53.85	66.12	1.51	3929	4
11/16/2013 13:35	6	34.7	0.07	18.47	17.5	52.91	66.34	1.51	3929	4
2/18/2014 18:15	1	32.8	0.21	18.57	14.64	25.68	34.01	1.5	3929	4
2/18/2014 18:16	1	32.6	0.21	18.66	14.85	25.59	33.61	1.5	3929	4
2/18/2014 18:17	1	32.8	0.21	18.56	15.1	25.65	32.96	1.5	3929	4
2/18/2014 18:17	1	32.7	0.21	18.48	15.47	25.76	32.19	1.5	3929	4
2/18/2014 18:18	1	32.9	0.21	18.52	15.99	25.81	31.05	1.5	3929	4
2/18/2014 18:19	1	32.9	0.21	18.38	16.27	25.7	30.18	1.5	3929	4
2/18/2014 18:20	1	32.6	0.21	18.52	16.51	25.6	29.53	1.5	3929	4
2/18/2014 18:20	1	32.8	0.21	18.71	16.6	25.44	29.47	1.5	3929	4
2/18/2014 18:21	1	32.9	0.21	18.81	16.46	25.16	29.61	1.5	3929	4
2/18/2014 18:22	1	32.9	0.21	18.75	16.5	25.36	29.67	1.5	3929	4
2/18/2014 18:22	1	32.8	0.21	18.66	16.37	25.5	30.16	1.5	3929	4
2/18/2014 18:23	1	33	0.21	18.54	16.07	25.37	30.6	1.5	3929	4

Table F.1 (cont.)

2/18/2014 17:08	2	32.6	0.24	18.77	16.34	24.68	29.69	1.35	3929	4
2/18/2014 17:09	2	32.7	0.24	18.91	16.16	24.84	30.24	1.35	3929	4
2/18/2014 17:10	2	32.9	0.24	19.04	15.86	24.57	31.15	1.35	3929	4
2/18/2014 17:10	2	32.9	0.24	19.11	15.7	24.4	31.16	1.35	3929	4
2/18/2014 17:11	2	32.8	0.24	19.17	15.41	24.5	31.4	1.35	3929	4
2/18/2014 17:12	2	33	0.24	19	15.35	24.37	31.63	1.35	3929	4
2/18/2014 17:13	2	33	0.24	18.81	15.17	24.69	31.8	1.35	3929	4
2/18/2014 17:13	2	33.1	0.24	18.94	15.04	24.82	31.96	1.35	3929	4
2/18/2014 17:14	2	33.3	0.24	18.94	14.92	24.82	32.23	1.35	3929	4
2/18/2014 17:15	2	33.1	0.24	18.83	14.76	24.6	32.63	1.35	3929	4
2/18/2014 17:16	2	33.3	0.24	19.03	14.58	24.71	33.06	1.35	3929	4
2/18/2014 17:16	2	33.3	0.24	18.85	14.44	24.66	33.37	1.35	3929	4
2/18/2014 16:02	3	31.7	0.16	18.45	15.49	24.96	30.9	1.4	3929	4
2/18/2014 16:03	3	31.8	0.16	18.33	15.35	25.02	31.11	1.4	3929	4
2/18/2014 16:04	3	31.9	0.16	18.42	15.27	25.07	31.18	1.4	3929	4
2/18/2014 16:04	3	31.9	0.16	18.41	15.17	25.01	31.28	1.4	3929	4
2/18/2014 16:05	3	31.9	0.16	18.53	15.01	24.98	31.54	1.4	3929	4
2/18/2014 16:06	3	31.7	0.16	18.59	14.87	24.93	31.95	1.4	3929	4
2/18/2014 16:06	3	31.9	0.16	18.58	14.74	24.86	32.29	1.4	3929	4
2/18/2014 16:07	3	31.7	0.16	18.5	14.47	24.93	32.54	1.4	3929	4
2/18/2014 16:08	3	31.9	0.16	18.44	14.4	25.05	32.87	1.4	3929	4
2/18/2014 16:09	3	31.8	0.16	18.43	14.3	25.16	33.12	1.4	3929	4
2/18/2014 16:09	3	31.7	0.16	18.41	14.41	25.12	33.33	1.4	3929	4
2/18/2014 16:10	3	31.7	0.16	18.42	14.46	25.07	33.31	1.4	3929	4

Table F.1 (cont.)

2/18/2014 15:25	4	32.4	0.16	18.54	14.49	23.95	31.56	1.28	3929	4
2/18/2014 15:25	4	32.5	0.16	18.52	14.6	23.89	31.41	1.28	3929	4
2/18/2014 15:26	4	32.3	0.16	18.53	14.72	23.87	31.37	1.28	3929	4
2/18/2014 15:27	4	32.1	0.16	18.65	14.75	23.96	31.32	1.28	3929	4
2/18/2014 15:28	4	32.4	0.16	18.57	14.93	24.1	31.24	1.28	3929	4
2/18/2014 15:28	4	32	0.16	18.59	15.19	24.23	30.77	1.28	3929	4
2/18/2014 15:29	4	32.3	0.16	18.52	15.44	24.27	30.2	1.28	3929	4
2/18/2014 15:30	4	32.4	0.16	18.62	15.7	24.12	29.54	1.28	3929	4
2/18/2014 15:30	4	32	0.16	18.69	16.16	24.01	28.97	1.28	3929	4
2/18/2014 15:31	4	32.2	0.16	18.7	16.41	23.96	28.26	1.28	3929	4
2/18/2014 15:32	4	32.3	0.16	18.61	16.53	24.1	27.84	1.28	3929	4
2/18/2014 15:33	4	32.7	0.16	18.47	16.38	24.11	28.25	1.28	3929	4
2/18/2014 14:51	5	32.3	0.16	18.64	14.74	23.67	31.13	1.41	3929	4
2/18/2014 14:52	5	32.2	0.16	18.72	14.69	23.66	31.08	1.41	3929	4
2/18/2014 14:52	5	32.3	0.16	18.58	14.79	23.8	30.85	1.41	3929	4
2/18/2014 14:53	5	32.3	0.16	18.51	14.93	23.87	30.68	1.41	3929	4
2/18/2014 14:54	5	32.4	0.16	18.44	14.9	23.82	30.71	1.41	3929	4
2/18/2014 14:54	5	32.3	0.16	18.39	15.04	23.95	30.73	1.41	3929	4
2/18/2014 14:55	5	32.5	0.16	18.49	15.15	23.82	30.53	1.41	3929	4
2/18/2014 14:56	5	32.3	0.16	18.63	15.51	23.86	29.96	1.41	3929	4
2/18/2014 14:57	5	32.3	0.16	18.7	15.87	23.72	29.27	1.41	3929	4
2/18/2014 14:57	5	32.4	0.16	18.67	16.44	23.69	28.14	1.41	3929	4
2/18/2014 14:58	5	32.3	0.16	18.64	16.75	23.71	27.55	1.41	3929	4
2/18/2014 14:59	5	32.3	0.16	18.66	16.71	23.8	27.47	1.41	3929	4

Table F.1 (cont.)

2/18/2014 14:10	6	35.1	0.09	18.19	15.44	23.5	30.43	1.51	3929	4
2/18/2014 14:11	6	35.1	0.09	18.07	15.91	23.75	29.57	1.51	3929	4
2/18/2014 14:11	6	35.4	0.09	18.01	16.3	23.74	28.46	1.51	3929	4
2/18/2014 14:12	6	35.2	0.09	18.03	16.57	23.76	27.75	1.51	3929	4
2/18/2014 14:13	6	35.4	0.09	18.28	16.73	23.58	27.64	1.51	3929	4
2/18/2014 14:13	6	35.4	0.09	18.34	16.74	23.52	27.53	1.51	3929	4
2/18/2014 14:14	6	35.3	0.09	18.29	16.65	23.52	27.58	1.51	3929	4
2/18/2014 14:15	6	35.4	0.09	18.17	16.6	23.49	27.68	1.51	3929	4
2/18/2014 14:16	6	35.5	0.09	18.11	16.19	23.54	28.3	1.51	3929	4
2/18/2014 14:16	6	35.2	0.09	18.07	15.91	23.69	28.8	1.51	3929	4
2/18/2014 14:17	6	35.6	0.09	18.31	15.65	23.55	29.16	1.51	3929	4
2/18/2014 14:18	6	35.4	0.09	18.33	15.49	23.52	29.7	1.51	3929	4
2/27/2014 11:09	1	31.7	0.78	18.06	15.29	13.22	14.22	1.51	3942	4
2/27/2014 11:09	1	31.7	0.78	18.11	15.41	13.09	14.14	1.51	3942	4
2/27/2014 11:10	1	31.6	0.78	17.95	15.69	13.13	11.47	1.51	3942	4
2/27/2014 11:11	1	31.6	0.78	18.06	15.86	13.13	11.19	1.51	3942	4
2/27/2014 11:12	1	31.9	0.78	18.04	15.86	13.09	11.38	1.51	3942	4
2/27/2014 11:12	1	32	0.78	18.02	15.77	13.02	11.4	1.51	3942	4
2/27/2014 11:13	1	31.6	0.78	18.2	15.83	12.95	11.11	1.51	3942	4
2/27/2014 11:14	1	32	0.78	18.26	15.92	12.86	11.4	1.51	3942	4
2/27/2014 11:14	1	31.8	0.78	18.12	15.8	12.71	11.84	1.51	3942	4
2/27/2014 11:15	1	31.8	0.78	18.31	15.92	12.77	11.28	1.51	3942	4
2/27/2014 11:16	1	31.9	0.78	18.28	16.13	12.59	10.86	1.51	3942	4
2/27/2014 11:17	1	31.8	0.78	18.17	16.24	12.63	10.46	1.51	3942	4

Table F.1 (cont.)

2/28/2014 8:32	2	31.4	0.14	18.09	15.1	11.35	13.83	1.4	3942	4
2/28/2014 8:33	2	31.3	0.14	18.18	15.19	11.29	13.42	1.4	3942	4
2/28/2014 8:33	2	31.6	0.14	18.29	15.27	11.28	13.46	1.4	3942	4
2/28/2014 8:34	2	31.3	0.14	18.15	15.22	11.1	13.7	1.4	3942	4
2/28/2014 8:35	2	31.1	0.14	18.09	15.03	11.25	13.96	1.4	3942	4
2/28/2014 8:35	2	31.6	0.14	18.17	15.16	11.35	14	1.4	3942	4
2/28/2014 8:36	2	31.3	0.14	18.26	15.38	11.39	13.81	1.4	3942	4
2/28/2014 8:37	2	31.4	0.14	18.22	15.71	11.32	13.5	1.4	3942	4
2/28/2014 8:38	2	31.4	0.14	18.36	15.77	11.28	13.13	1.4	3942	4
2/28/2014 8:38	2	32.1	0.14	18.29	15.78	11.23	13.02	1.4	3942	4
2/28/2014 8:39	2	31.6	0.14	18.14	15.71	11.29	13.08	1.4	3942	4
2/28/2014 8:40	1	31.4	0.14	18.17	15.62	11.3	13.7	1.4	3942	4
2/27/2014 9:49	3	30.7	0.22	17.82	15.76	11.61	12.78	1.48	3942	4
2/27/2014 9:50	3	31.3	0.22	17.81	15.43	11.63	13.36	1.48	3942	4
2/27/2014 9:50	3	30.9	0.22	17.77	14.94	11.75	21.2	1.48	3942	4
2/27/2014 9:51	3	31	0.22	17.7	14.49	12.17	17.48	1.48	3942	4
2/27/2014 9:52	3	31	0.22	17.71	14.06	12.4	16.79	1.48	3942	4
2/27/2014 9:52	3	30.8	0.22	17.69	13.63	12.55	17.03	1.48	3942	4
2/27/2014 9:53	3	30.7	0.22	17.78	13.16	12.71	17.24	1.48	3942	4
2/27/2014 9:54	3	30.5	0.22	17.83	12.7	12.74	17.48	1.48	3942	4
2/27/2014 9:55	3	30.8	0.22	17.9	12.23	12.76	17.98	1.48	3942	4
2/27/2014 9:55	3	30.8	0.22	17.82	11.82	12.78	18.62	1.48	3942	4
2/27/2014 9:56	3	30.5	0.22	17.68	11.56	12.97	19.15	1.48	3942	4
2/27/2014 9:57	3	31	0.22	17.52	11.24	13.16	19.76	1.48	3942	4

Table F.1 (cont.)

2/27/2014 9:11	4	32.5	0.15	17.93	16.15	15.24	11.35	1.3	3942	4
2/27/2014 9:12	4	33.1	0.15	17.92	16.24	15.13	11.08	1.3	3942	4
2/27/2014 9:13	4	32.9	0.15	17.82	16.2	15.19	11.83	1.3	3942	4
2/27/2014 9:14	4	32.9	0.15	17.82	16.14	15.39	12.06	1.3	3942	4
2/27/2014 9:14	4	32.9	0.15	17.82	16.03	15.45	11.98	1.3	3942	4
2/27/2014 9:15	4	33.1	0.15	17.95	15.94	15.36	11.5	1.3	3942	4
2/27/2014 9:16	4	32.6	0.15	18.04	16.04	15.24	11.44	1.3	3942	4
2/27/2014 9:16	4	32.9	0.15	18.14	16.02	15.14	12.24	1.3	3942	4
2/27/2014 9:17	4	32.5	0.15	18.07	15.85	15.19	12.1	1.3	3942	4
2/27/2014 9:18	4	32.5	0.15	18.01	15.37	15.26	12.92	1.3	3942	4
2/27/2014 9:19	4	32.9	0.15	17.97	15.01	15.41	13.69	1.3	3942	4
2/27/2014 9:19	4	33.1	0.15	17.93	14.48	15.48	14.66	1.3	3942	4
2/26/2014 12:41	5	32.1	0.22	18.21	14.61	19.93	29.06	1.4	3929	4
2/26/2014 12:41	5	31.9	0.22	18.17	14.61	19.47	23.28	1.4	3929	4
2/26/2014 12:42	5	31.9	0.22	18.13	14.8	18.98	26.56	1.4	3929	4
2/26/2014 12:43	5	31.9	0.22	18.06	14.79	18.13	25.09	1.4	3929	4
2/26/2014 12:43	5	31.9	0.22	18.34	14.72	17.46	30.22	1.4	3929	4
2/26/2014 12:44	5	31.9	0.22	18.2	15.21	17.14	20.68	1.4	3929	4
2/26/2014 12:45	5	32.1	0.22	18.31	15.5	16.63	18.13	1.4	3929	4
2/26/2014 12:46	5	32.1	0.22	18.17	15.71	16.44	19.89	1.4	3929	4
2/26/2014 12:46	5	32.1	0.22	18.22	15.8	16.36	19.78	1.4	3929	4
2/26/2014 12:47	5	32	0.22	18.13	15.73	16	19.17	1.4	3929	4
2/26/2014 12:48	5	32.2	0.22	18.17	15.66	15.88	19.42	1.4	3929	4
2/26/2014 12:48	5	32.1	0.22	18.14	15.73	15.75	20.34	1.4	3929	4

Table F.1 (cont.)

2/26/2014 12:05	6	34.7	0.18	18.31	16.16	16.86	25.98	1.5	3929	4
2/26/2014 12:06	6	34.8	0.18	18.01	15.99	17.05	32.57	1.5	3929	4
2/26/2014 12:07	6	34.8	0.18	18.04	16.01	17.35	21.39	1.5	3929	4
2/26/2014 12:07	6	34.9	0.18	18.07	16.12	17.38	29.74	1.5	3929	4
2/26/2014 12:08	6	34.6	0.18	18.07	16.13	17.29	20.99	1.5	3929	4
2/26/2014 12:09	6	34.9	0.18	18.26	16.35	16.97	18.3	1.5	3929	4
2/26/2014 12:10	6	34.8	0.18	18.3	16.28	16.62	21.17	1.5	3929	4
2/26/2014 12:10	6	34.6	0.18	18.32	16.26	16.47	22.53	1.5	3929	4
2/26/2014 12:11	6	34.5	0.18	18.14	16.33	16.4	22.88	1.5	3929	4
2/26/2014 12:12	6	34.8	0.18	18.15	16.29	16.37	21.42	1.5	3929	4
2/26/2014 12:13	6	34.6	0.18	18.17	16.13	16.35	22.97	1.5	3929	4
2/26/2014 12:13	6	34.7	0.18	18.27	16.22	16.52	19.22	1.5	3929	4

APPENDIX G: STEADY-STATE MASS RECOVERY

PERCENT ANALYSIS AND STANDARD UNCERTAINTY

CODE

The following code was written in MATLAB R2013a and used to generate the results in Section 5.3.4. Corresponding input data is located in Appendix F. The program calculates the steady-state mass recovery percent following a mass recovery test and the associated standard uncertainty with steady-state mass recovery percent. In addition, individual parameter contributions to mass flow recovered and injected standard uncertainty are computed. The uncertainty analysis presented here was initially developed by Dr. Guilherme D.N. Maia and specific to the REMS. Prior to running the program, the data file must be formatted correctly as described in Appendix E.5. The pseudo code is as follows:

1. Loop throughout each chamber and import the data file into a matrix
2. Separate data into its respective variables
3. Declare symbolic representation for the parameters in the steady-state mass recovery percent equation, mass flow recovered equation, and mass flow injected equation
4. Declare the individual parameter's contribution to the standard uncertainty associated with the three aforementioned equations
5. Express the standard uncertainty associated with the three aforementioned equations as the sum of the individual parameter contributions

G.1 MR_std_uncertainty.m

```
%% STEADY-STATE MASS RECOVERY TEST ANALYSIS AND STD UNCERTAINTY
%   Brett C. Ramirez (05-02-2014)
%   Department of Agricultural and Biological Engineering
%   University of Illinois at Urbana-Champaign
```

```

%
%     Calculates SSMRP and its associated std uncertainty
%
%     INPUTS
%     name      = data file w/o extension (assumes '.xlsx' file type)
%
function MR_std_uncertainty(name)
% file naming and deleting of old files and matlab data
ext = '.xlsx';
output = strcat(name, '_out', ext);
delete(output);
warning('off', 'all');
% loop for chambers one thru six corresponding to Sheet1 thru Sheet6
in
% excel file; thus, j=1:6
for j=1:6
    %% Data input
    % Reads columns of data from excel file and stores them in a
matrix
    % which is then arranged into its appropriate variables

    % read data from mass recovery test
    data_mat = MR_importfile(name, j);

    % convert datenum to h
    dt = [0 cumsum(diff(data_mat(:,1).*24))'];
    % chamber concentration at steady-state (ppmv)
    C_ch = data_mat(:,3);
    % chamber temperature (deg C)
    T_ch = data_mat(:,4);
    % chamber relative humidity (%)
    RH_ch = data_mat(:,5);
    % incoming temperature (deg C)
    T_in = data_mat(:,6);
    % incoming relative humidity (%)
    RH_in = data_mat(:,7);
    % mean incoming concentration before and after steady-state (ppmv)
    C_in = data_mat(:,8);
    % orifice meter differential pressure (in wc)
    dP = data_mat(:,9);
    % gas cylinder concentration (ppmv)
    C_cyl = data_mat(:,10);
    % injected gas flow rate (lpm -> m^3 s^-1)
    Q_inj = data_mat(:,11)./60000;

    chamber = strcat('Chamber', ' ', num2str(j), ' successfully
imported');
    disp(chamber);
    %%
    % loop for every row in the Sheet[j] i.e. for each steady-state
data

```

```

% point
for i=1:length(dt)
    %% SYMBOLIC REPRESENTATION
    % Prefix guide
    % D = absolute std uncertainty
    % C_ = contribution

    % chamber concentration
    syms Cch DCch Crec_Cch
    % incoming (backgorund) concentration
    syms Cin DCin Crec_Cin
    % chamber temperature
    syms Tch DTch Crec_Tch Cinj_Tch
    % incoming temperature
    syms Tin DTin Crec_Tin
    % ventilation rate
    syms Qin DQin Crec_Qin
    % injected voluemtric flowrate
    syms Qinj DQinj Crec_Qinj Cinj_Qinj
    % chamber moist air density
    syms rhoch Drhoch Crec_rhoch
    % incoming moist air density
    syms rhoin Drhoin Crec_rhoin
    % injected dry gas cylinder mixture density
    syms rhoinj Drhoinj Cinj_rhoinj
    % Constant: barometric pressure
    syms pb
    % Constant: molecular weight
    syms M
    % Constant: universal gas constant
    syms R
    % std temperature and pressure
    syms Tstd pstd
    % injected gas cylinder concentration
    syms Ccyl DCcyl Cinj_Ccyl
    % mass flow injected
    syms m_inj Dm_inj
    % mass injected
    syms m_inj_int Dm_inj_int Cmrp_minj_int
    % mass flow recovered
    syms m_rec Dm_rec
    % mass recoved
    syms m_rec_int Dm_rec_int Cmrp_mrec_int
    % steady-state mass recovery percent
    syms MRP DMRP rep
    %% EQUATION FOR MR ANALYSIS

    % injected gas mass flow equation (g h^-1)
    m_inj=Qinj*((Tin+273.15)/Tstd)*(pstd/pb)*3600*Ccyl*1E-
6*(M*pb)...
    /(R*(Tin+273.15));

```

```

% recovered gas mass flow equation (g h^-1)
m_rec=(M*3600*pb*1E-6/R)*(((Qin*(rhoin/rhoch)+Qinj*...
    (rhoinj/rhoch))*(Cch/(Tch+273.15)))-
(Qin*(Cin/(Tin+273.15))));

% steady-state mass recovery percent (%)
MRP=100*(m_rec_int/m_inj_int);

%% PARAMETER INDIVIDUAL CONTRIBUTION

% injected mass flow std uncertainty parameter contributions
Cinj_Qinj=(DQinj*diff(m_inj,Qinj))^2;
Cinj_Ccyl=(DCcyl*diff(m_inj,Ccyl))^2;
Cinj_Tch=(DTin*diff(m_inj,Tin))^2;

% recovered mass flow std uncertainty parameter contributions
Crec_Tch=(DTch*diff(m_rec,Tch))^2;
Crec_Tin=(DTin*diff(m_rec,Tin))^2;
Crec_Cch=(DCch*diff(m_rec,Cch))^2;
Crec_Cin=(DCin*diff(m_rec,Cin))^2;
Crec_Qinj=(DQinj*diff(m_rec,Qinj))^2;
Crec_Qin=(DQin*diff(m_rec,Qin))^2;
Crec_rhoin=(Drhoin*diff(m_rec,rhoin))^2;
Crec_rhoch=(Drhoch*diff(m_rec,rhoch))^2;
Crec_rhoinj=(Drhoinj*diff(m_rec,rhoinj))^2;

% indivual contributions to mass recovery percent std
% uncertaintny after integration over steady-state
Cmrp_mrec_int=(Dm_rec_int*diff(MRP,m_rec_int))^2;
Cmrp_minj_int=(Dm_inj_int*diff(MRP,m_inj_int))^2;
Cmrp_rep=rep^2;

%% STD UNCERTAINTY EQNS

% std uncertainty of injected gas mass flow
Dm_inj=sqrt(Cinj_Ccyl+Cinj_Tch+Cinj_Qinj);

% std uncertainty of recovered gas mass flow
Dm_rec=sqrt(Crec_Tch+Crec_Tin+Crec_Cch+Crec_Cin+Crec_Qinj...
    +Crec_Qin+Crec_rhoin+Crec_rhoch+Crec_rhoinj);

% std uncertainty of ss mass recovery percent
DMRP=sqrt(Cmrp_mrec_int+Cmrp_minj_int+Cmrp_rep);
%DMRP=sqrt(Cmrp_mrec_int+Cmrp_minj_int);

%% DETERMINATION OF STD UNCERTAINTY FOR EACH PARAMETER

% store data corresponding to row[i] into symbolic variable
for

```

```

% evaultion later
Tch=T_ch(i);
Tin=T_in(i);
Cch=C_ch(i);
Cin=C_in(i);
Qinj=Q_inj(i);
Ccyl=C_cyl(i);

% define constants with assumed negligible contribution to
% std uncertainty
% barometric pressure (Pa) (ASHRAE 2013, Chp 1, Eqn 3)
pb=98639.3086;
% std temperature (K)
Tstd=273.15;
% std pressure (Pa)
pstd=101325;
% ideal gas constant (m^3 Pa K^-1 mol^-1)
R=8.314;
% molecular mass of SF6 (g mol^-1)
M=146.06;

% injected gas density std uncertainty function
% input 0 to use 1% injected gas conc. uncertainty
[rhoinj, Drhoinj]=std_uncertainty_rho_inj(C_cyl(i));

% injected gas MWavg std uncertainty function
%[MWavg, DMWavg]=std_uncertainty_MWavg_inj(C_cyl(i));

% moist air density std uncertainty function

[rhoin,Drhoin]=air_density_std_uncertainty(T_in(i)+273.15,RH_in(i));

[rhoch,Drhoch]=air_density_std_uncertainty(T_ch(i)+273.15,RH_ch(i));

% ventiation rate std uncertainty function
[Qin, DQin]=std_uncertainty_om(dP(i),j,T_in(i),RH_in(i));

% temperature uncertainty
DTch=.5;
DTin=.5;

% primary certified gas cylinder concentration std
uncertainty
DCcyl=sqrt((.01*C_cyl(i))/sqrt(3)+((.01*C_cyl(i))/sqrt(3)));

% inject gas flow std uncertainty
DQinj=3.63326E-07;

% individual components of gas analyzer std uncertainty
% post calibration repeatability
rep_pc=(0.005*.016)^2;

```

```

% instrument repeatability
rep_insch=((0.01*C_ch(i))/(3^0.5))^2;
rep_insic=((0.01*C_in(i))/(3^0.5))^2;
% primary certified tolerance
pct=((0.01*40)/(3^0.5))^2;
% range drift
rd_ch=((0.025*C_ch(i))/(3^0.5))^2;
rd_in=((0.025*C_in(i))/(3^0.5))^2;
% resolution
res=((5*0.006)/(3^0.5))^2;

% propagation of gas analyzer std uncertainty
DCch=sqrt(rep_pc+rep_insch+pct+rd_ch+res);
DCin=sqrt(rep_pc+rep_insic+pct+rd_in+res);

% reproducibility determined as std dev of SSMRP
MR_rep=[1.7114 1.6135 2.1768 3.2204 1.2861 1.4367];
rep=MR_rep(j);

%% EVALUATE EQUATIONS

format long;

% calculate gas mass flow recovered
m_recs(i)=eval(m_rec);
% calculate gas mass flow recovered std uncertainty
Dm_recs(i)=eval(Dm_rec);
% calculate gas mass flow injected
m_injs(i)=eval(m_inj);
% calculate gas mass flow injected std uncertainty
Dm_injs(i)=eval(Dm_inj);

%% PREPARE OUTPUT MATRICES

% collect parameter value used in calculations
value(1,i)=Tch;
value(2,i)=Tin;
value(3,i)=Cch;
value(4,i)=Cin;
value(5,i)=Qin*60000;
value(6,i)=Qinj*60000;
value(7,i)=rhoin;
value(8,i)=rhoch;
value(9,i)=rhoinj;
value(10,i)=m_recs(i);

value(11,i)=Tin;
value(12,i)=Ccyl;
value(13,i)=Qinj*60000;
value(14,i)=m_injs(i);

```

```

% collect parameter absolute std uncertainty
u_abs(1,i)=DTch;
u_abs(2,i)=DTin;
u_abs(3,i)=DCch;
u_abs(4,i)=DCin;
u_abs(5,i)=DQin*60000;
u_abs(6,i)=DQinj*60000;
u_abs(7,i)=Drhoin;
u_abs(8,i)=Drhoch;
u_abs(9,i)=Drhoinj;
u_abs(10,i)=Dm_recs(i);

u_abs(11,i)=DTch;
u_abs(12,i)=DCcyl;
u_abs(13,i)=DQinj*60000;
u_abs(14,i)=Dm_injs(i);

% contributions to recovered mass flow std uncertainty

m_rec_total=eval(Crec_Tch+Crec_Tin+Crec_Cch+Crec_Cin+Crec_Qinj+...
    Crec_Qin+Crec_rhoin+Crec_rhoch+Crec_rhoinj);

% evaluate individual contributions
contribution(1,i)=100*eval(Crec_Tch)/m_rec_total;
contribution(2,i)=100*eval(Crec_Tin)/m_rec_total;
contribution(3,i)=100*eval(Crec_Cch)/m_rec_total;
contribution(4,i)=100*eval(Crec_Cin)/m_rec_total;
contribution(5,i)=100*eval(Crec_Qin)/m_rec_total;
contribution(6,i)=100*eval(Crec_Qinj)/m_rec_total;
contribution(7,i)=100*eval(Crec_rhoin)/m_rec_total;
contribution(8,i)=100*eval(Crec_rhoch)/m_rec_total;
contribution(9,i)=100*eval(Crec_rhoinj)/m_rec_total;
% mass flow recovered std uncertainty
contribution(10,i)=100*Dm_recs(i)/m_recs(i);

% contributions to injected mass flow std uncertainty
m_inj_total=eval(Cinj_Qinj+Cinj_Ccyl+Cinj_Tch);

% evaluate individual contributions
contribution(11,i)=100*eval(Cinj_Tch)/m_inj_total;
contribution(12,i)=100*eval(Cinj_Ccyl)/m_inj_total;
contribution(13,i)=100*eval(Cinj_Qinj)/m_inj_total;
% mass flow injected std uncertainty
contribution(14,i)=100*Dm_injs(i)/m_injs(i);
end
%% SSMRP ANALYSIS AND STD UNCERTAINTY ANALYSIS

% calculate total mass recovered by integrating of SS period
m_rec_int=trapz(dt,m_recs);
m_inj_int=trapz(dt,m_injs);

```

```

% calculate total mass recovered std uncertainty assume root-sum
% square
for h=1:length(dt)-1
Dmrec_temp1=(0.5*Dm_recs(h)*dt(h))^2;
Dmrec_temp2=(0.5*Dm_recs(h)*dt(h+1))^2;
Dmrec_temp3=(0.5*Dm_recs(h+1)*dt(h))^2;
Dmrec_temp4=(0.5*Dm_recs(h+1)*dt(h+1))^2;
Dm_rec_temp(h)=Dmrec_temp1+Dmrec_temp2+Dmrec_temp3+Dmrec_temp4;

Dminj_temp1=(0.5*Dm_injs(h)*dt(h))^2;
Dminj_temp2=(0.5*Dm_injs(h)*dt(h+1))^2;
Dminj_temp3=(0.5*Dm_injs(h+1)*dt(h))^2;
Dminj_temp4=(0.5*Dm_injs(h+1)*dt(h+1))^2;
Dm_inj_temp(h)=Dminj_temp1+Dminj_temp2+Dminj_temp3+Dminj_temp4;

end
% mass recovered std uncertainty
Dm_rec_int=sqrt(sum(Dm_rec_temp));
% mass injected std uncertainty
Dm_inj_int=sqrt(sum(Dm_inj_temp));

% evaluate
MRP=eval(MRP);
DMRP=eval(DMRP);

% preparing for output to excel
% before computing reproducibility uncomment the following line
%mrp_total=eval(Cmrp_mrec_int+Cmrp_minj_int);
mrp_total=eval(Cmrp_mrec_int+Cmrp_minj_int+Cmrp_rep);
mrp_contribution(1,1)=m_rec_int;
mrp_contribution(2,1)=Dm_rec_int;
mrp_contribution(3,1)=100*eval(Cmrp_mrec_int)/mrp_total;
mrp_contribution(4,1)=m_inj_int;
mrp_contribution(5,1)=Dm_inj_int;
mrp_contribution(6,1)=100*eval(Cmrp_minj_int)/mrp_total;
mrp_contribution(7,1)=MRP;
mrp_contribution(8,1)=DMRP;
mrp_contribution(9,1)=(DMRP/MRP)*100;
mrp_contribution(10,1)=100*eval(Cmrp_rep)/mrp_total;
func_out(1,j)=MRP;
func_out(2,j)=DMRP;
%% FORMATING FOR OUTPUT

A={'Values'; 'Temperature chamber (C)'; 'Temperature incoming
(C)'; ...
'Concentration chamber (ppmv)'; 'Concentration incoming
(ppmv)'; ...
'Flow incoming (lpm)'; 'Flow injected (lpm)'; ...
'Density incoming (kg m^-3)'; 'Density chamber (kg m^-3)'; ...
'Density injected (kg m^-3)'; 'Mass flow recovered (g h^-
1)'; ...

```



```

        'Temperature incoming (C)'; 'Concentration injected (ppmv)'; ...
        'Flow injected (lpm)'; 'Mass flow injected (g h^-1)'};

    xlswrite(output,A,j,'A1');
    xlswrite(output,value,j,'B2');

    B={'Absolute standard uncertainty'; 'u(Temperature chamber)
(C)'; ...
      'u(Temperature incoming (C))'; 'u(Concentration chamber
(ppmv))'; ...
      'u(Concentration incoming (ppmv))'; 'u(Flow incoming
(lpm))'; ...
      'u(Flow injected (lpm))'; 'u(Density incoming (kg m^-3))'; ...
      'u(Density chamber (kg m^-3))'; 'u(Density injected (kg m^-
3))'; ...
      'u(Mass flow recovered (g h^-1))'; ...
      'u(Temperature incoming (C))'; 'u(Concentration injected
(ppmv))'; ...
      'u(Flow injected (lpm))'; 'u(Mass flow injected (g h^-1))'};

    q=strcat('A',num2str(length(A)+2));
    w=strcat('B',num2str(length(A)+3));
    xlswrite(output,B,j,q);
    xlswrite(output,u_abs,j,w);

    C={'Relative contributions'; 'u(Temperature chamber) (%)'; ...
      'u(Temperature incoming) (%)'; 'u(Concentration chamber
(%))'; ...
      'u(Concentration incoming) (%)'; 'u(Flow incoming) (%)'; ...
      'u(Flow injected) (%)'; 'u(Density incoming) (%)'; ...
      'u(Density chamber) (%)'; 'u(Density injected) (%)'; ...
      'Rel std u(Mass flow recovered) (%)'; ...
      'u(Temperature incoming) (%)'; 'u(Concentration injected
(%))'; ...
      'u(Flow injected) (%)'; 'Rel std u(Mass flow injected) (%)'};

    e=strcat('A',num2str(length(A)+length(B)+3));
    s=strcat('B',num2str(length(A)+length(B)+4));
    xlswrite(output,C,j,e);
    xlswrite(output,contribution,j,s);

    D={'Mass recovery'; 'Mass recovered (g)'; 'u(Mass recovered
(g))'; ...
      'Mass recovered contribution (%)'; 'Mass injected (g)'; ...
      'u(Mass injected(g))'; 'Mass injected contribution (%)'; ...
      'Mass recovery percent (%)'; 'u(Mass recovery percent)
(%)'; ...
      'Rel std uncertainty (%)'; 'Contribution u(Rep)'};

    v=strcat('A',num2str(length(A)+length(B)+length(C)+4));
    h=strcat('B',num2str(length(A)+length(B)+length(C)+5));

```

```

    xlswrite(output,D,j,v);
    xlswrite(output,mrp_contribution,j,h);

    % variables
    save(strcat(output, '.mat'));
end
end

```

G.2 std_uncertainty_rho_inj.m

```

%% INJECTED TRACER GAS DENSITY STD UNCERTAINTY
%   Brett C. Ramirez (05-02-2014)
%   Department of Agricultural and Biological Engineering
%   University of Illinois at Urbana-Champaign
%
%   Calculates the gas cyldiner mixture density and its associated
std
uncertainty
%
%   INPUTS
%   y_SF6      = mole fraction of SF6 in gas cylinder
%
function [dcyl, Ddcyl] = std_uncertainty_rho_inj (y_SF6)
% Prefix guide
% D = abosolute std uncertainty
% C_ = contribution

% mole fraction (y) of N2
syms yN2 DyN2 C_yN2
% mole fraction (y) SF6
syms ySF6 DySF6 C_ySF6
% density at std conditions
syms dN2 dSF6
% gas cylinder mixture density and its associated uncertainty
syms dcyl Ddcyl

% injected gas mixture density (g /m^-3)
dcyl=yN2*dN2+ySF6*dSF6;

% individual contributions to injected gas mixture density std
uncertainty
C_yN2=(DyN2*diff(dcyl,yN2))^2;
C_ySF6=(DySF6*diff(dcyl,ySF6))^2;

% injected gas mixture density std uncertainty
Ddcyl=(C_yN2+C_ySF6)^0.5;

% mole fraction of bi-component mixture
ySF6=y_SF6/1E6;
yN2=1-(y_SF6/1E6);

```

```

% density of components (g /m^-3)
dN2=1.250;
dSF6=6.516;

% primary certified gas cylinder has 1% error

    DyN2=0.01*yN2;
    DySF6=0.01*ySF6;

% calculate injected gas mixture density
dcyl=eval(dcyl);
% calculate injected gas mixture density std uncertainty
Ddcyl=eval(Ddcyl);
end

```

G.3 std_uncertainty_om.m

```

%% VENTILATION RATE STD UNCERTAINTY
%   Brett C. Ramirez (05-02-2014)
%   Department of Agricultural and Biological Engineering
%   University of Illinois at Urbana-Champaign
%
%   Calculates ventilation rate and associated standard
uncertainty
%
%   INPUTS
%   d_P   = differential pressure (in wc)
%   j     = chamber ID
%   Tino  = incoming temperature (C)
%   RHino = incoming relative humidity (%)
%
%   OUTPUTS
%   Vin   = ventilation rate (m^3 s^-1)
%   DVin  = ventilation rate std uncertainty (m^3 s^-1)
%
function [Vin, DVin] = std_uncertainty_om (d_P,j,Tino,RHino)

% orifice meter regression coefficient
om_c = [1.0199 0.9650 0.9735 0.9244 0.9865 1.0699];

% std error for orifice meter regression coefficient
Dom_c = [0.00162 0.00159 0.00157 0.00248 0.00271 0.00250];

% calibration regression std error (dependent variable)
DCRSEx = [0.1068 0.1035 0.1024 0.1604 0.1730 0.1629]./60./1000;

% Prefix guide
% D = absolute std uncertainty
% C_ = contribution

```

```

% orifice diameter
syms d
% pipe diameter
syms D
% differential pressure
syms dP DdP C_dP
% calibration reference std error (x-axis)
syms CRSEx
% slope unique to each orifice meter
syms c Dc C_c
% incoming moist air density
syms din Ddin C_din
% ventilation rate and its associated std uncertainty
syms Vin DVin

% ventilation rate measured by the orifice meter (m^3 s^-1)
Vin = ((pi*d^2)/(4*c))*(((2*dP)/(din*(1-((d/D)^4))))^0.5);

% individual contributions to ventilation rate std uncertainty
C_din = (Ddin*diff(Vin,din))^2;
C_dP = (DdP*diff(Vin,dP))^2;
C_c = (Dc*diff(Vin,c))^2;

% ventilation std uncertainty
DVin = ((CRSEx^2)+C_c+C_din+C_dP)^0.5;

% moist air density std uncertainty function
[din,Ddin] = air_density_std_uncertainty(Tino+273.15,RHino);

% convert manometer differential pressure to Pa
dP = d_P*249.089;

% constants
% orifice diameter (m)
d = 0.0206;
% pipe diameter (m)
D = 0.0508;

% differential pressure std uncertainty
DdP = 14.85082068;

% get correct constants for the individual orifice meter ID[j]
c = om_c(j);
Dc = Dom_c(j);
CRSEx = DCRSEx(j);

% evaluate ventilation rate (m^3 s^-1)
Vin = eval(Vin);
% evaluate ventilation rate std uncertainty (m^3 s^-1)
DVin = eval(DVin);

```

end

G.4 MR_importfile.m

```
function data = MR_importfile(workbookFile, sheetName, range)
%Import numeric data from a spreadsheet
% DATA = IMPORTFILE2(FILE) reads all numeric data from the first
% worksheet in the Microsoft Excel spreadsheet file named FILE and
% returns the numeric data.
%
% DATA = IMPORTFILE2(FILE,SHEET) reads from the specified worksheet.
%
% DATA = IMPORTFILE2(FILE,SHEET,RANGE) reads from the specified
worksheet
% and from the specified RANGE. Specify RANGE using the syntax
% 'C1:C2',where C1 and C2 are opposing corners of the region.
%
% Date formatted cells are converted to MATLAB datenum format.
% Rows with non-numeric cells are excluded.
%
% Example:
% untitled = importfile2('test_1.xlsx','Sheet1','A2:AH12');
%
% See also XLSREAD.

% Auto-generated by MATLAB on 2013/11/07 14:11:49

%% Input handling

% If no sheet is specified, read first sheet
if nargin == 1 || isempty(sheetName)
    sheetName = 1;
end

% If no range is specified, read all data
if nargin <= 2 || isempty(range)
    range = '';
end

%% Import the data, extracting spreadsheet dates in MATLAB datenum
format
[~, ~, raw, dateNums] = xlsread(workbookFile, sheetName, range, '',
@convertSpreadsheetDates);

%% Replace date strings by MATLAB datenums
R = ~cellfun(@isequalwiththequalnans,dateNums,raw) &
cellfun('isclass',raw,'char'); % Find Excel dates
raw(R) = dateNums(R);

%% Exclude rows with non-numeric cells
```

```
J = ~all(cellfun(@(x) isnumeric(x) && ~isnan(x),raw),2); % Find rows
with non-numeric cells
raw(J,:) = [];

%% Create output variable
data = cell2mat(raw);
```

APPENDIX H: ANIMAL DAILY EMISSION PROGRAM

The following program was written in MATLAB R2013a and used to process greenhouse gas emissions data collected by the REMS. The program computes the emission rate each measurement and then finds daily emissions after integrating the ERs and normalization. In addition, the daily emissions are computed with several different estimation types including, trapezoidal, left Riemann sums, and one commonly used in practice that multiplies the sum of the total emission rates in the measurement cycle and multiplies it by the sampling frequency. Further, the program includes the subsampling to evaluate if data were only conducted for the e.g. first 4 h of the animal being the chamber is representative of the daily emissions determine from the data collected in the measurement cycle. The percent difference is calculated to compare the different integration methods and 24 h representation. The pseudo code is as follows:

1. Define constants and import animal emissions data from preformatted data file
2. Linear interpolate the background gas concentration and calculate the emission rate
3. Calculate the daily emissions for the different integration methods
4. Loop through the different periods for the 24 h representation
5. Calculate the percent difference between e.g. the first 4 h daily emissions and the daily emission from the data
6. Calculate the percent difference amongst the different integration methods
7. Write data to excel file

H.1 REMS_ER_calc_28.m

```
%% [data_out]=REMS_ER_calc_28(name,graph)
%     Brett C. Ramirez (05-02-2014)
%     Department of Agricultural and Biological Engineering
```

```

%      University of Illinois at Urbana-Champaign
%
%      Calculates daily GHG emissions and perform subsampling for 24
h
%      sampling representation
%
%      OUTPUTS
%      data_out      = has daily E and u(E) in matrix in matlab
%
%      INPUTS*
%      name          = data filename w/o extension in a cell (.xlsx)
%      graph         = controls plotting: 1-on; 0-off
% * data is from LabView Project(4) and must be preformatted
%%
function [data_out]=REMS_ER_calc_28(name,graph)
%% Initializing
% close open figures
close all;
% disable warning messages
warning('off','all')
% define data file extesnsion
ext = '.xlsx';
% convert file name to matrix string
name = cell2mat(name);
% create output file name (appends '_out')
output = strcat(name, '_out',ext);
% delete existing output file
delete(output)
% delete exisiting variables
delete(name)
%% ER Uncertainty [u(ER)]
% symbolic representaton for each parameter for ER uncertainty
syms Tch Tin Cch Cin Vdot_in din dch...
    R pb pstd Tstd % constants
% symbolic representation for abs std uncertainty
syms DTch DTin DCch DCin DVdot_in Ddin Ddch
% symbolic representation for the contributions
syms C_Tch C_Tin C_Cch C_Cin C_Vdot_in C_din C_dch
% emission rate (ER) equation (g h^-1)
ER1 = (Vdot_in*0.01604*1000*((1E-
6*pb)/R))*((din/dch)*(Cch/(Tch+273.15))...
    -(Cin/(Tin+273.15)));
% individual parameter contribution (%)
% chamber temperature
C_Tch =(DTch*diff(ER1,Tch))^2;
% incoming temperature
C_Tin =(DTin*diff(ER1,Tin))^2;
% chamber concentration
C_Cch =(DCch*diff(ER1,Cch))^2;
% incoming concentration
C_Cin =(DCin*diff(ER1,Cin))^2;
% ventiatlion rate

```



```

C_Vdot_in =(DVdot_in*diff(ER1,Vdot_in))^2;
% incoming moist air density
C_din =(Ddin*diff(ER1,din))^2;
% chamber moist air density
C_dch =(Ddch*diff(ER1,dch))^2;
% REMS ER std uncertainty
DER =(C_Tch+C_Tin+C_Cch+C_Cin+C_Vdot_in+C_din+C_dch)^0.5;
%% Constants
% barometric pressure(Pa) (ASHRAE 2013, Chp1, Eqn 3)
pb = 98639.3086;
% ideal gas constant (m^3 Pa mol^-1 K)
R = 8.3144621;
% constant (K) for ER eqn
K =(pb*1E-6)/R;
% molar mass of GHG (kg mol^-1)
%   CH4   CO2   NH3   N2O   SF6
MM =[0.01604 0.04401 0.044013 0.017031 0.14606];
% time interval (s) to compare to the daily emissions
rep = [1:1:22]*3600;
% row header for data organization
row_head = {'Chamber 1', 'Chamber 2', 'Chamber 3', 'Chamber 4',...
            'Chamber 5', 'Chamber 6' };
%% Import Data
% loop thru 7 sheets {CH1,...,CH6,bckgnd} and store data in cells
for chamber = 1:7
    % import data for one chamber
    data_mat = importfile2(name,chamber);
    % convert dd/mm/yyyy hh:mm:ss to do cumulative sum
    time_mat{1,chamber} = [0 cumsum(diff(data_mat(:,1).*24*3600))'];
    % store vecotors of GHG conc data in cell rows (ppmv)
    for ii = 1:5
        C_mat{ii,chamber} = data_mat(:,ii+2);
    end
    % none of the following data is for bckgnd (chambers only)
    if chamber ~= 7
        % mean incoming temperature (deg C)
        T_in_mat{1,chamber} = data_mat(:,9);
        % mean chamebr temperature (deg C)
        T_ch_mat{1,chamber} = data_mat(:,8);
        % mean incoming moist air density (kg m^-3)
        rho_in_mat{1,chamber} = data_mat(:,10);
        % mean chamber moist air density (kg m^-3)
        rho_ch_mat{1,chamber} = data_mat(:,11);
        % mean incoming ventilation rate (m^3 s^-1)
        vent_mat{1,chamber} = data_mat(:,12)./60./1000;
        % mean chamber relative humidity (%)
        RH_ch_mat{1,chamber} = data_mat(:,13);
        % mean incoming relative humidity (%)
        RH_in_mat{1,chamber} = data_mat(:,14);
    end
end
end
%% ER & Associated Uncertainty Calculation

```

```

% loop thru {CH1,...,CH6}
for chamber = 1:6
    % loop for every row (h) of data
    for h = 1:length(time_mat{1,chamber})
        % loop thru 5 GHGs (ii)
        for ii = 1:5
            % linear interpolation for background gas concentration
            C_i{ii,chamber}(h) = interp1(time_mat{1,7},C_mat{ii,7},...
                time_mat{1,chamber}(h));
            % GHG ER (g s^-1)
            ER{ii,chamber}(h) =
1000*vent_mat{1,chamber}(h)*MM(ii)*K*...

((rho_in_mat{1,chamber}(h)/rho_ch_mat{1,chamber}(h))...
    *(C_mat{ii,chamber}(h)/...
    (T_ch_mat{1,chamber}(h)+273.15))-
(C_i{ii,chamber}(h)/...
    (T_in_mat{1,chamber}(h)+273.15)));
        % calculate u(ER) for CH4 only (ii=1)
        if ii == 1
            % sub in values in ER calculation into symbolic
parameters
            Vdot_in = vent_mat{1,chamber}(h);
            din = rho_in_mat{1,chamber}(h);
            dch = rho_ch_mat{1,chamber}(h);
            Cch = C_mat{ii,chamber}(h);
            Tch = T_ch_mat{1,chamber}(h);
            RHch = RH_ch_mat{1,chamber}(h);
            Cin = C_i{ii,chamber}(h);
            Tin = T_in_mat{1,chamber}(h);
            RHin = RH_in_mat{1,chamber}(h);
            % u(incoming ventilation rate)
            [~, DVdot_in] = std_uncertainty_om_ER
(chamber,Tin,RHin);
            % u(incoming moist air density)
            [~, Ddin] =
air_density_std_uncertainty(Tin+273.15,RHin);
            % u(chamber moist air density)
            [~, Ddch] =
air_density_std_uncertainty(Tch+273.15,RHch);

            % u(gas concentration measurement)
            % post calibration
            rep_pc = (0.005*.42)^2;
            % instrument repeatability
            rep_insch = ((0.01*Cch)/(3^0.5))^2;
            rep_insin = ((0.01*Cin)/(3^0.5))^2;
            % primary certified tolerance
            pct = ((0.01*499.9)/(3^0.5))^2;
            % range drift
            rd_ch = ((0.025*Cch)/(3^0.5))^2;

```

```

        rd_in = ((0.025*Cin)/(3^0.5))^2;
        %resolution
        res = ((5*0.4)/(3^0.5))^2;
        % u(chamber concentration)
        DCch = sqrt(rep_pc+rep_insch+pct+rd_ch+res);
        % u(incoming concentration)
        DCin = sqrt(rep_pc+rep_insin+pct+rd_in+res);
        % u(chamber temperature)
        DTch = 0.5;
        % u(incoming temperature)
        DTin = 0.5;
        % evaluate ER (as a check)
        ER1_mat(h,chamber) = eval(ER1);
        % evalute u(ER)= DER
        DER_mat(h,chamber) = eval(DER);
        % evalute u(ER) = DER = DER_ERabs
        DER_ER_abs(h,chamber) =
eval(C_Tch+C_Tin+C_Cch+C_Cin+...
        C_Vdot_in+C_din+C_dch)^0.5;
        % evalute relative u(ER) (%)
        DER_ER_rel(h,chamber) = 100*(DER_ER_abs(h,chamber)/...
        ER{ii,chamber}(h));
    end
end
end
end
% initialize empty vectors
int_meth = [];
data_out = [];
for chamber = 1:6
    %% Integration Methods Analysis
    % redefine cumsum of time as x
    x = time_mat{1,chamber};
    % redefine ER as y (only CH4)
    y = ER{1,chamber};
    % absolute CH4 u(ER) vector
    dER = DER_ER_abs(:,chamber);
    % estimation of sampling interval
    interval_out = 50.3*60;
    % calculate ER for each of the different integration methods
    [int_meth_rtrn,int_meth_str_rtrn] =
daily_E_std_uncertainty(x,y,dER);
    % append all integration methods for all chambers together in one
mat
    data_out=[data_out int_meth_rtrn];
    % determine how many methods were used
    [no_int_meth,~] = size(int_meth_rtrn);
    % int_meth(n,m)=n=integration methods; m=chambers
    int_meth = [int_meth int_meth_rtrn];
    % store the inetrgration method label
    int_meth_str = int_meth_str_rtrn;

```

```

%% 24 h Representation
rep_count = 1;
for m = 1:length(rep)
    % find index in time vector less than e.g. 1 h
    interval_ind = find(x<rep(m));
    % create new x vector for smaller interval
    x_interval = x(1:length(interval_ind));
    % create new y vector for smaller interval
    y_interval = y(1:length(interval_ind));
    % NOTE: new interval will not be exactly from {0,...1} h,
    % probably {0,...,0.98} h so the corresponding ER must be
    % determined to obtain an exactly 1 h interval

    % linear interpolate to find ER at interval time
    ER_lin = interp1(x,y,rep(m));
    % add that value to the new y vector
    ER_interval = [y_interval ER_lin];
    % add the corresponding x value
    time_interval = [x_interval rep(m)];

    % calculate ER for each of the different integration methods
for
    % the subsample representation
    [int_meth_rtrn,int_meth_str_rtrn]...
        = subsamp_ER_integration(time_interval,ER_interval);

    % add a label to identify the data
    int_meth_rep_out{rep_count,1}...
        = strcat('First ',num2str(rep(m)/3600),' h subsample');
    p_diff_rep_out{rep_count,1}...
        = strcat('First ',num2str(rep(m)/3600),' h subsample');
    [no_int_meth_rep,~] = size(int_meth_rtrn);

    % data organization
    for j = 1:no_int_meth_rep
        % calculate the percent difference
        p_diff_rep_out{rep_count+1,chamber+1}...
            = P_diff_func(int_meth(j,chamber),int_meth_rtrn(j,1));

        p_diff_rep_out{rep_count+1,1} = int_meth_str_rtrn{j,1};

        int_meth_rep_out{rep_count+1,1} = int_meth_str_rtrn{j,1};

        int_meth_rep_out{rep_count+1,chamber+1} =
int_meth_rtrn(j,1);
        rep_count = rep_count+1;
    end

    rep_count = rep_count+1;
    % add the row heading

```

```

int_meth_rep_out{1,chamber+1} = row_head{1,chamber};

% clear vector data for next iteration
time_interval = [];
ER_interval = [];
x_interval = [];
y_interval = [];
end

% plot data
if graph == 1

ER_plot(time_mat{1,chamber}./3600,ER{1,chamber}.*3600,chamber,name);
end
% clear vector data for next iteration
y = [];
x = [];
end
%% Preparing Output
% if no_int_meth=5 then:
% int_meth_perm{1,1}=[2 3 4 5],int_meth_perm{1,2}=[1 3 4 5],...
for int_meth_i = 1:no_int_meth-1
    int_array_temp = 1:1:no_int_meth-1;
    int_array_temp(int_meth_i) = [];
    int_meth_perm{1,int_meth_i} = int_array_temp;
end

for j = 1:no_int_meth-1
    % loop thru each of the integration methods to calculate the
    % percent difference wrt to the other methods
    p_diff{1,j}{1,1}...
        = strcat('Percent difference wrt to ',int_meth_str{j,1});
    for int_meth_i = 1:no_int_meth-2
        for chamber = 1:6
            p_diff{1,j}{int_meth_i+1,chamber+1}...
                = P_diff_func(int_meth(j,chamber),...
                    int_meth(int_meth_perm{1,j}(int_meth_i),chamber));
            % add chamber labels to data
            p_diff{1,j}{1,chamber+1} = row_head{1,chamber};
        end
        % add integration method label
        p_diff{1,j}{int_meth_i+1,1}...
            =
cell2mat(int_meth_str(int_meth_perm{1,j}(int_meth_i),1));
    end
end
% add column and row headings the computed integration methods for
output
for j = 1:no_int_meth
    for chamber = 1:6
        int_meth_out{1,chamber+1} = row_head{1,chamber};
    end
end

```

```

        int_meth_out{j+1,chamber+1} = int_meth(j,chamber);
        int_meth_out{j+1,1} = int_meth_str{j,1};
    end
end
%% Write to Excel File
xlswrite(output,int_meth_out,1,'A1')
xlswrite(output,int_meth_rep_out,1,'A8')
xlswrite(output,p_diff_rep_out,2,'A1')

range_count = 1;
for j = 1:no_int_meth-1
    range_str = strcat('A',num2str(range_count));
    xlswrite(output,p_diff{1,j},3,range_str)
    range_count = range_count+no_int_meth+1;
end
% save variables
save(name)
end

```

H.2 daily_E_std_uncertainty.m

```

%% [int, int_str] = daily_E_std_uncertainty(x,y,DER)
%     Brett C. Ramirez (05-02-2014)
%     Department of Agricultural and Biological Engineering
%     University of Illinois at Urbana-Champaign
%
%     INPUTS
%     x           = cumulative sum of time in seconds
%     y           = ER (g s^-1)
%     DER         = u(ER) (g s^-1)
%
%     OUTPUTS
%     int         = integration cell hold the different
approximation
%                 methods
%     int_str     = holds the strings corresponding to the
integration
%                 method
%%
function [int,int_str] = daily_E_std_uncertainty(x,y,DER,chamber)

syms E_corr dE_corr E C_E dE
syms avg_SSMRP davg_SSMRP C_avgSSMRP

E_corr = E*(100/avg_SSMRP);

C_E = (dE*diff(E_corr,E))^2;
C_avgSSMRP = (davg_SSMRP*diff(E_corr,avg_SSMRP))^2;

dE_corr = sqrt(C_E+C_avgSSMRP);

```

```

% trapezoidal integration (g d^-1)
int_str{1,1} = 'E_Trapezoidal (g/d)';
int(1,1)=trapz(x,y)*(86400/x(end));

% Left Riemann Sum (LRS) (g d^-1)
int_str{2,1} = 'E_Left Riemann Sum (g/d)';
int(2,1)=leftsum(x,y)*(86400/x(end));

% approximation data (g d^-1)
% x(2) is the sampling interval
int_str{3,1} = 'E_Approximation (g/d)';
int(3,1)=(x(2)*sum(y))*(86400/(x(2)*length(x)));

% trapezoidal integration of u(ER) to get u(E) or the std uncertainty
of
% daily emissions (g d^-1)
int_str{4,1} = 'u(E) (g/d)';
for h=1:length(x)-1
    DER_temp1=(0.5*DER(h)*x(h))^2;
    DER_temp2=(0.5*DER(h)*x(h+1))^2;
    DER_temp3=(0.5*DER(h+1)*x(h))^2;
    DER_temp4=(0.5*DER(h+1)*x(h+1))^2;
    DE_temp(h)=DER_temp1+DER_temp2+DER_temp3+DER_temp4;
end
% combine everything
int(4,1)=sqrt(sum(DE_temp))*(86400/x(end));

% uncertainty with bias correction (05/02/2014)
davg_SSMRP_v = [1.87 1.97 1.94 2.23 1.88 1.89];
avg_SSMRP_v = [93.24 94.94 92.01 92.83 94.30 96.59];

avg_SSMRP = avg_SSMRP_v(chamber);
davg_SSMRP = davg_SSMRP_v(chamber);

E = int(1,1);
dE = int(4,1);

int(5,1)=eval(E_corr);
int(6,1)=eval(dE_corr);

end

```

H.3 subsamp_ER_integration.m

```

% [int,int_str] = subsamp_ER_integration(x,y,k,j,uER)
% Brett C. Ramirez (05-02-2014)
% Department of Agricultural and Biological Engineering
% University of Illinois at Urbana-Champaign

```

```

%
%     INPUTS
%     x           = cumulative sum of time in seconds
%     y           = ER (g s^-1)
%
%     OUTPUTS
%     int         = integration cell hold the different
approximation
%                 methods
%     int_str     = cell holding the string for the name of
integration
%                 performed
%%
function [int,int_str] = subsamp_ER_integration(x,y)

% trapezoidal integration (g d^-1)
int_str{1,1} = 'E_Trapezoidal (g/d)';
int(1,1)=trapz(x,y)*(86400/x(end));

% Left Riemann Sum (LRS) (g d^-1)
int_str{2,1} = 'E_Left Riemann Sum (g/d)';
int(2,1)=leftsum(x,y)*(86400/x(end));

end

```

H.4 P_diff_func.m

```

%% P = P_diff_func(x1,x2)
%     Brett C. Ramirez (05-02-2014)
%     Department of Agricultural and Biological Engineering
%     University of Illinois at Urbana-Champaign
%
%     calculates the percent difference between value 1 and value 2
%
%     INPUTS
%     x1         = value 1
%     y2         = value 2
%
%     OUTPUTS
%     P         = percent difference (%)
%%
function P = P_diff_func(x1,x2)

P=((x1-x2)/((x1+x2)/2))*100;

end

```

H.5 std_uncertainty_om_ER.m

```

%% VENTILATION RATE STD UNCERTAINTY
%     Brett C. Ramirez (05-02-2014)
%     Department of Agricultural and Biological Engineering

```



```

%      University of Illinois at Urbana-Champaign
%
%      Calculates ventilation rate std uncertainty
%
%      uncertainty
%
%      INPUTS
%      d_P      = differential pressure (in wc)
%      j        = chamber ID
%      Tino     = incoming temperature (C)
%      RHino    = incoming relative humidity (%)
%
%      OUTPUTS
%      Vin      = ventilation rate (m^3 s^-1)
%      DVin     = ventilation rate std uncertainty (m^3 s^-1)
%
function [Vin, DVin] = std_uncertainty_om_ER (j,Tino,RHino)
d_P=1;
% orifice meter regression coefficient
om_c = [1.0199 0.9650 0.9735 0.9244 0.9865 1.0699];

% std error for orifice meter regression coefficient
Dom_c = [0.00162 0.00159 0.00157 0.00248 0.00271 0.00250];

% calibration regression std error (dependent variable)
DCRSEx = [0.1068 0.1035 0.1024 0.1604 0.1730 0.1629]./60./1000;

% Prefix guide
% D = absolute std uncertainty
% C_ = contribution

% orifice diameter
syms d
% pipe diameter
syms D
% differential pressure
syms dP DdP C_dP
% calibration reference std error (x-axis)
syms CRSEx
% slope unique to each orifice meter
syms c Dc C_c
% incoming moist air density
syms din Ddin C_din
% ventilation rate and its associated std uncertainty
syms Vin DVin

% ventilation rate measured by the orifice meter (m^3 s^-1)
Vin = ((pi*d^2)/(4*c))*(((2*dP)/(din*(1-((d/D)^4))))^0.5);

% individual contributions to ventilation rate std uncertainty
C_din = (Ddin*diff(Vin,din))^2;

```

```

C_dP = (DdP*diff(Vin,dP))^2;
C_c = (Dc*diff(Vin,c))^2;

% ventilation std uncertainty
DVin = ((CRSEx^2)+C_c+C_din+C_dP)^0.5;

% moist air density std uncertainty function
[din,Ddin] = air_density_std_uncertainty(Tino+273.15,RHino);

% convert manometer differential pressure to Pa
dP = d_P*249.089;

% constants
% orifice diameter (m)
d = 0.0206;
% pipe diameter (m)
D = 0.0508;

% differential pressure std uncertainty
DdP = 14.85082068;

% get correct constants for the individual orifice meter ID[j]
c = om_c(j);
Dc = Dom_c(j);
CRSEx =DCRSEx(j);

% evaluate ventilation rate (m^3 s^-1)
Vin = eval(Vin);
% evaluate ventilation rate std uncertainty (m^3 s^-1)
DVin = eval(DVin);
End

```

H.6 leftsum.m

```

%% L = leftsum(x,y)
%   Brett C. Ramirez (05-02-2014)
%   Department of Agricultural and Biological Engineering
%   University of Illinois at Urbana-Champaign
%
%   Calculates left riemann sum
%
%   INPUTS
%   x   = independent data vector
%   y   = dependent data vector
%
%   OUTPUT
%   L   = left Riemann sum of x and y
%
function L = leftsum(x,y)

n = max(size(x)); % safe for column or row vectors

```

```

L = 0;
for i = 1:n-1
L = L + y(i)*(x(i+1) - x(i));
end

```

H.7 ER_plot.m

```

%% ER_plot(x_plot,y_plot,j,name)
%       Brett C. Ramirez (05-02-2014)
%       Department of Agricultural and Biological Engineering
%       University of Illinois at Urbana-Champaign
%
%       Creates plots of the different methods and data
%
%       INPUTS
%       x_plot      = dependent data vector
%       y_plot      = independent data vector
%       j           = chamber number
%       name        = filename to save figures
%%
function ER_plot(x_plot,y_plot,j,name)

x_length=length(x_plot);

% right riemann rectangles
for m=1:x_length-1
    x_bars=[x_plot(m) x_plot(m) x_plot(m+1) x_plot(m+1)];
    y_bars=[0 y_plot(m) y_plot(m) 0];
    figure(j);
    hrect=plot(x_bars, y_bars, 'r', 'LineWidth',1.5);
    hold on
end

% midpoint rectangles
for m=1:x_length-1
    avg_y(m)=(y_plot(m)+y_plot(m+1))/2;
    avg_x(m)=(x_plot(m)+x_plot(m+1))/2;
    x_bars=[x_plot(m) x_plot(m) x_plot(m+1) x_plot(m+1)];
    y_bars=[0 avg_y(m) avg_y(m) 0];
    figure(j);
    hmid=plot(x_bars, y_bars, 'b', 'LineWidth',1);
    hold on
end

% figure(j);
% hmidscat=scatter(avg_x,avg_y,'MarkerEdgeColor','b',...
%     'MarkerFaceColor','c',...
%     'LineWidth',1);

figure(j);
hscat=scatter(x_plot,y_plot,'MarkerEdgeColor','r',...
    'MarkerFaceColor','y',...
    'LineWidth',1);

```

```

htrap=plot(x_plot,y_plot,'--g','LineWidth',1.5);

x_axis=xlabel('Cumulative Time (h)');
y_axis=ylabel('CH_4 Emission Rate (g h^-^1)');

title(strcat('Chamber', ' ',num2str(j),' - ',num2str(length(x_plot)),...
    ' Composite Samples per Period'),'FontName','Times New Roman',...
    'FontSize', 16,'FontWeight','bold');

axis([0 24 0 20]);

hlegend=legend([hscat,hrect,hmid,htrap],'Composite Sample',...
    'Left Riemann Sum','Midpoint Sum','Trapezoidal',...
    'location','NorthEast' );

set(x_axis, 'FontName','Times New Roman','FontSize', 14,...
    'FontWeight','bold')
set(y_axis, 'FontName','Times New Roman','FontSize', 14,...
    'FontWeight','bold')

set([hlegend], 'FontName','Times New Roman','FontSize', 9)

set(gca, ...
    'Box'          , 'on'          , ...
    'TickDir'      , 'in'          , ...
    'TickLength'   , [.01 .01] , ...
    'XMinorTick'   , 'off'         , ...
    'YMinorTick'   , 'off'         , ...
    'YGrid'        , 'off'         , ...
    'XTick'        , 0:2:24, ...
    'YTick'        , 0:1:20,...
    'XColor'       , 'k', ...
    'YColor'       , 'k', ...
    'LineWidth'    , 1           );

fig_name=strcat(name,'_fig_',num2str(j));
print('-dpng','-r800',fig_name);

end

```

H.8 importfile2.m

```

function data = importfile2(workbookFile, sheetName, range)
%IMPORTFILE2 Import numeric data from a spreadsheet
% DATA = IMPORTFILE2(FILE) reads all numeric data from the first
% worksheet in the Microsoft Excel spreadsheet file named FILE and
% returns the numeric data.
%
% DATA = IMPORTFILE2(FILE,SHEET) reads from the specified worksheet.
%

```

```

% DATA = IMPORTFILE2(FILE,SHEET,RANGE) reads from the specified
worksheet
% and from the specified RANGE. Specify RANGE using the syntax
% 'C1:C2', where C1 and C2 are opposing corners of the region.
%
% Date formatted cells are converted to MATLAB datenum format.
% Rows with non-numeric cells are excluded.
%
% Example:
% untitled = importfile2('test_1.xlsx','Sheet1','A2:AH12');
%
% See also XLSREAD.

% Auto-generated by MATLAB on 2013/11/07 14:11:49

%% Input handling

% If no sheet is specified, read first sheet
if nargin == 1 || isempty(sheetName)
    sheetName = 1;
end

% If no range is specified, read all data
if nargin <= 2 || isempty(range)
    range = '';
end

%% Import the data, extracting spreadsheet dates in MATLAB datenum
format
[~, ~, raw, dateNums] = xlsread(workbookFile, sheetName, range, '',
@convertSpreadsheetDates);

%% Replace date strings by MATLAB datenums
R = ~cellfun(@isequalwiththequalnans,dateNums,raw) &
cellfun('isclass',raw,'char'); % Find Excel dates
raw(R) = dateNums(R);

%% Exclude rows with non-numeric cells
J = ~all(cellfun(@(x) isnumeric(x) && ~isnan(x),raw),2); % Find rows
with non-numeric cells
raw(J,:) = [];

%% Create output variable
data = cell2mat(raw);

```

APPENDIX I: TESTING FOR CHAMBER BIAS

A series of eight ($n = 8$) Steady-State Mass Recovery Tests (SSMRTs) were conducted in each of the six chambers over a year to determine if there is a bias in the recovery of mass for each chamber. A bias is determined to be significant if mean Steady-State Mass Recovery Percent (SSMRP) for a given chamber is significantly different from 100%. Future use of the chambers requires completion of Steady-State Mass Recovery Tests (SSMRTs) before and after an animal is placed inside the chamber. Data obtained from future SSMRTs should be incorporated to expand to the existing SSMRP data to ensure no substantial changes in the mean SSMRP for a chamber have occurred. The standard uncertainty of SSMRP from all previous tests must be included in the bias significance testing and the reproducibility (standard deviation of SSMRP for an individual chamber) should be updated with each subsequent SSMRT.

The summary of the equations (previously defined in Section 5.2.3 through Section 5.2.6) to calculate SSMRP, mean SSMRP, and reproducibility are as follows:

$$SSMRP_{c,r} = 100 \times \frac{m_{c,r}^{rec}}{m_{c,r}^{inj}} \quad \text{(Equation I.1)}$$

where

- c = chamber: 1, 2, 3, 4, 5, 6
- r = replicate: 1, 2, 3, 4, 5, 6, 7, 8 ($n = 8$)
- $SSMRP_{c,r}$ = Steady-State Mass Recovery Percent (SSMRP) for chamber (c) and replicate (r) over time (%)
- $m_{c,r}^{rec}$ = mass recovered by the REMS (g)
- $m_{c,r}^{inj}$ = reference mass injected (g)

$$\overline{SSMRP}_c = \frac{1}{n} \sum_{r=1}^n SSMRP_{c,r} \quad \text{(Equation I.2)}$$

where

- \overline{SSMRP}_c = mean Steady-State Mass Recovery Percent for each chamber (%)

$$Rep_c = \sqrt{\frac{1}{n-1} \sum_{r=1}^n (SSMRP_{c,r} - \overline{SSMRP}_c)^2} \quad (\text{Equation I.3})$$

where

Rep_c = reproducibility for each chamber (%)

Next, the standard uncertainty of SSMRP for each chamber and replicate is:

$$\Delta SSMRP_{c,r} = \sqrt{\left(\frac{\partial SSMRP_{c,r}}{\partial m_{c,r}^{inj}} m_{c,r}^{inj}\right)^2 + \left(\frac{\partial SSMRP_{c,r}}{\partial m_{c,r}^{rec}} \Delta m_{c,r}^{rec}\right)^2 + (Rep_c)^2} \quad (\text{Equation I.4})$$

where

$\Delta SSMRP_{c,r}$ = standard uncertainty of SSMRP (%)

Combining the standard uncertainty of SSMRP for each chamber and replicates results in mean standard uncertainty of SSMRP for a given chamber:

$$\overline{\Delta SSMRP}_c = \frac{1}{n} \sqrt{\sum_{r=1}^n (\Delta SSMRP_{c,r})^2} \quad (\text{Equation I.5})$$

where

$\overline{\Delta SSMRP}_c$ = standard uncertainty of mean SSMRP (%)

Note that reproducibility is included in Equation I.4; thus, as additional repetitions are conducted over time, this term will continue to be used to represent the chamber's control precision.

In some instances, it may be simpler to add reproducibility when combining the standard uncertainty of associated with SSMRP for each replicate (Equation I.7 as opposed to Equation I.4). The code in Appendix G requires the user to calculate the mean SSMRP and reproducibility for each chamber first, then add the reproducibility into the code, and finally, re-run the code to obtain the standard uncertainty associated with mean SSMRP. With minor modifications to Appendix G, the user could implement Equation I.7; thus, the code would only need to be run

once. Expansion of the Equation I.7 and Equation I.5 result in the same algebraic expression for the standard uncertainty of mean SSMRP.

$$\Delta SSMRP_{c,r} = \sqrt{\left(\frac{\partial SSMRP_{c,r}}{\partial m_{c,r}^{inj}} m_{c,r}^{inj}\right)^2 + \left(\frac{\partial SSMRP_{c,r}}{\partial m_{c,r}^{rec}} \Delta m_{c,r}^{rec}\right)^2} \quad (\text{Equation I.6})$$

$$\overline{\Delta SSMRP}_c = \frac{1}{n} \sqrt{\left[\sum_{r=1}^n (\Delta SSMRP_{c,r})^2\right] + (n \times Rep_c)^2} \quad (\text{Equation I.7})$$

With the previous equations defined, the next step is to perform the inference testing for each chamber to determine if a significant bias exists. Let \overline{SSMRP}_c be independent normal random variables with $\mu = \text{unknown}$ and $\sigma^2 = \overline{\Delta SSMRP}_c^2$. The \overline{SSMRP}_c is our best estimate of the population mean ($\mu_{\bar{x}} = \mu$) with variance of the mean ($\sigma_{\bar{x}}^2 = \frac{1}{n^2} \sum_{i=1}^n \sigma^2 = \frac{\sigma^2}{n}$) estimated by the combining of the standard uncertainties of SSMRP associated with each SSMRT replicate (Equation I.5 or I.7), which is $\overline{\Delta SSMRP}_c^2$. The ideal mean of the population is 100%; that is, all the reference mass injected is measured by the REMS. Use of $\overline{\Delta SSMRP}_c$ (Equation I.7) and the mean value \overline{SSMRP}_c (Equation I.2) allows for developing confidence intervals or conducting inference testing on each chamber. The following criteria, reject H_0 for $|t_{calc}| \geq t_{\frac{(1-\alpha)}{2}, v}$ was established for the inference testing where, t_{calc} = calculated t value, $\alpha = 0.05$ (95% confidence level), and v = degrees of freedom ($n - 1 = 7$). For a two-tailed test, with $\alpha = 0.05$ and $v = 7$, the critical t value is 2.365.

The following equation (Equation I.10), shows the standard uncertainty of the mean SSMRP as the best estimate of the standard error of the mean and the mean SSMRP to calculate the t value.

$$t_{calc} = \frac{\overline{SSMRP}_c - 100}{\Delta \overline{SSMRP}_c} \quad (\text{Equation I.10})$$

Note in the typical t test, the standard deviation is divided by the square root of n, to determine the SE of the mean. As previously discussed, the standard uncertainty of the mean SSMRP is an estimate of the variance of the mean SSMRP; thus, it already represents a measure of the SE of the mean. The SSMRP for each chamber and replicate are summarized in Table I.1 and the results of the inference testing with the decision of Type I errors is summarized in Table I.2.

Table I.1. Summary of SSMRPs for the six chambers and eight replicates collected periodically over one year.

Replicate	<i>SSMRP_c</i> (%)					
	Chamber	Chamber 2	Chamber 3	Chamber 4	Chamber 5	Chamber 6
1	93.59	97.01	92.24	89.98	96.11	97.23
2	92.45	92.67	91.83	89.80	93.09	94.31
3	90.70	94.08	89.44	90.41	93.86	95.93
4	93.98	94.15	89.79	91.43	93.84	95.57
5	93.43	94.38	89.79	92.06	96.06	96.87
6	94.42	96.48	94.65	93.99	92.79	96.62
7	96.00	96.85	94.52	96.48	95.05	99.26
8	91.32	93.90	93.84	98.50	93.59	96.96
\overline{SSMRP}_c (%)	93.24	94.94	92.01	92.83	94.30	96.59
<i>Rep_c</i> (%)	1.71	1.61	2.18	3.22	1.29	1.44

Table I.2. Summary of Δ SSMRPs for the six chambers and eight replicates collected periodically over one year. A bias was found to be significantly different from 100% ($P < 0.05$) for chambers 1 through 5. Chamber 6 was found not to be significant ($P > 0.05$).

Replicate	Δ SSMRP _{c,r} (%)					
	Chamber 1	Chamber 2	Chamber 3	Chamber 4	Chamber 5	Chamber 6
1	5.29	5.67	5.54	6.20	5.42	5.35
2	5.16	5.44	5.44	6.16	5.20	5.22
3	5.16	5.50	5.43	6.19	5.26	5.29
4	5.31	5.53	5.43	6.24	5.27	5.27
5	5.27	5.58	5.39	6.26	5.33	5.31
6	5.36	5.63	5.58	6.38	5.31	5.35
7	5.43	5.75	5.70	6.52	5.43	5.46
8	5.24	5.50	5.56	6.55	5.40	5.36
\overline{SSMRP}_c (%)	93.24	94.94	92.01	92.83	94.30	96.59
$\Delta\overline{SSMRP}_c$ (%)	1.87	1.97	1.95	2.23	1.88	1.88
t_{calc} (Equation I.10)	3.62	2.57	4.1	3.21	3.03	1.81
P value	0.009	0.037	0.005	0.015	0.019	0.113
Decision	Reject H ₀	Reject H ₀	Reject H ₀	Reject H ₀	Reject H ₀	Cannot reject H ₀
Power	1.00	1.00	1.00	1.00	1.00	0.95

A bias correction is recommended for chambers 1 through 5 as outlined in Section 5.3.5 and no correction is recommended for chamber 6. A post-hoc statistical power test was conducted (Table I.2), to assess the probability that the null hypothesis (H₀) was correctly rejected. The power was found to be > 0.95 for all chambers; thus, the effect exists and was detectable.

A comparison between the traditional t test, where SE of the mean is estimated by the standard deviation over the square root of sample size or, in this case as $\frac{Rep_c}{\sqrt{n}}$, and the previous method was also evaluated. This method yields the following equation (Equation I.11), for calculating the inference testing using the reproducibility (Equation I.9):

$$t_{calc} = \frac{\overline{SSMRP}_c - 100}{\frac{Rep_c}{\sqrt{n}}} \quad \text{(Equation I.11)}$$

Recall, reproducibility was obtained for the group of n , SSMRPs. The criteria for rejecting H_0 , $|t_{calc}| \geq t_{\frac{(1-\alpha)}{2}, \nu}$ is the same. The results are summarized in Table I.3.

Table I.3. Summary of inference testing using reproducibility in estimating the SE of the mean SSMRP. A bias was found to be significantly different from 100% ($P < 0.05$) for all chambers.

Parameter	Chamber 1	Chamber 2	Chamber 3	Chamber 4	Chamber 5	Chamber 6
\overline{SSMRP}_c (%)	93.24	94.94	92.01	92.83	94.30	96.59
Rep_c (%)	1.71	1.61	2.18	3.22	1.29	1.44
t_{calc} (Equation I.11)	11.19	8.89	10.36	6.3	12.5	6.69
P value	1.01E-05	4.62E-05	1.69E-05	4.04E-04	4.83E-06	2.80E-04
Decision	Reject H_0	Reject H_0	Reject H_0	Reject H_0	Reject H_0	Reject H_0

Using only reproducibility to estimate variance, leads to the conclusion that all chambers are significantly ($P < 0.05$) different from 100% and a correction factor should be implemented to account for the bias (Table I.3). A bias correction is recommended for chamber 6. This differs from the result obtained using the previous method (Table I.2). A visual comparison of the two methods is shown in Figure I.1. Use of reproducibility in estimating the SE of the mean is not advised, as it does not account for the random error in the instruments and propagation of uncertainty in calculating SSMRP. It is shown here for comparison.

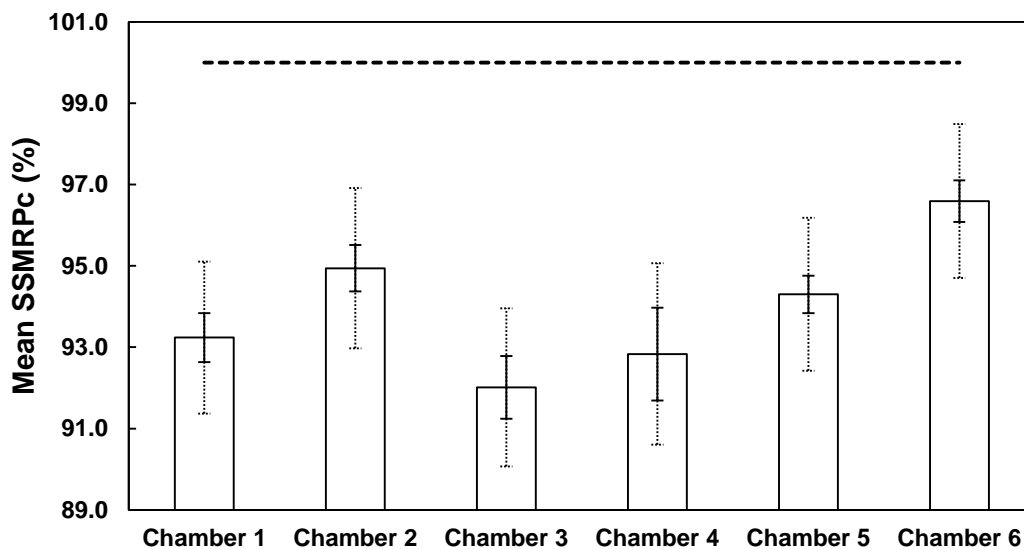


Figure I.1. Summary of mean SSMRPs ($n=8$) for the six chambers. Solid error bars represent SE ($Rep_c n^{-1/2}$) calculated from reproducibility and dashed error bars represent $\Delta SSMRP_c$. The ideal mean (100%) is indicated by the dashed line.

An additional method, referred to as the Weighted Averages (WAV) method, is described to provide an alternative method for calculating $\overline{\Delta SSMRP}_c$. The WAV method uses weights calculated from the $\Delta SSMRP_{c,r}$ to determine the WAV of \overline{SSMRP}_c and $\overline{\Delta SSMRP}_c$. It has been added for discussion and in the event that there is an uneven number of SSMRT replicates across chambers. This may occur if several chambers are removed to accommodate additional animals in a traditional metabolism trial; thus, less chambers are available for emissions research, or, an emissions trial is designed with fewer than six chambers implemented and SSMRTs are conducted for only those chambers used.

The first step is to calculate the weights from the $\Delta SSMRP_{c,r}$ obtained from each replicate.

$$w_{c,r} = \frac{1}{(\Delta SSMRP_{c,r})^2} \quad \text{(Equation I.12)}$$

where

$w_{c,r}$ = weight

These weights are used to determine the WAV of the mean SSMRP:

$$\overline{SSMRP}_c^{WAV} = \frac{\sum_{r=1}^n w_{c,r} \times SSMRP_{c,r}}{\sum_{r=1}^n w_{c,r}} \quad \text{(Equation I.13)}$$

where

\overline{SSMRP}_c^{WAV} = weighted average of the mean SSMRP

In addition, the weights are used to calculate the WAV of the mean SSMRP standard uncertainty:

$$\overline{\Delta SSMRP}_c^{WAV} = \frac{1}{\sqrt{\sum_{r=1}^n w_{c,r}}} \quad \text{(Equation I.14)}$$

where

$\overline{\Delta SSMRP}_c^{WAV}$ = weighted average of the mean standard uncertainty of SSMRP

Finally, the inference test with the criteria for rejecting H_0 , $|t_{calc}| \geq t_{\frac{(1-\alpha)}{2}, \nu}$ the same as the previously discussed methods:

$$t_{calc} = \frac{\overline{SSMRP}_c^{WAV} - 100}{\Delta \overline{SSMRP}_c^{WAV}} \quad (\text{Equation I.15})$$

Results using the WAV method are summarized in Table I.4.

Table I.4. Summary of results from using Weighted Averages (WAV). A bias was found to be significantly different from 100% ($P < 0.05$) for chambers 1 through 5. Chamber 6 was found not to be significant ($P > 0.05$).

Parameter	Weighted average method (Equation I.6 - I.8)					
	Chamber 1	Chamber 2	Chamber 3	Chamber 4	Chamber 5	Chamber 6
\overline{SSMRP}_c^{WAV} (%)	93.19	94.89	91.95	92.70	94.28	96.56
$\Delta \overline{SSMRP}_c^{WAV}$ (%)	1.86	1.97	1.95	2.23	1.88	1.88
t_{calc} (Equation I.14)	3.65	2.59	4.14	3.27	3.04	1.83
P value	0.008	0.036	0.004	0.014	0.019	0.11
Decision	Reject H_0	Reject H_0	Reject H_0	Reject H_0	Reject H_0	Cannot reject H_0

In this case, the conclusions from the WAV method and the first method are the identical.

This is because $\Delta \overline{SSMRP}_c^{WAV} = \Delta \overline{SSMRP}_c$ given equal replicates (n) for each chamber as shown in Table I.2.